The University Of Sheffield.

Phosphorylation of C_4 And Non-C_4 Phosphoenolpyruvate Carboxylase from Panicum and the Kinetic Behaviour of Phosphorylated and Non-Phosphorylated PEPC

By:

Dhiya Dalila Zawawi

A thesis submitted in partial fulfilment of the requirements for the degree of Doctor of Philosophy

The University of Sheffield

Faculty of Science

Department of Chemistry

Submission Date:

November 2019

Dedicated to the memory of my grandmother (Halimah Ismail) and my uncle (Rahim Mustafar), who believed in my ability to be successful in the academic arena. You were gone but your belief in me has made this journey possible

DECLARATION

The works presented in this thesis is, to the best of my knowledge and belief, original, except as acknowledgment in the text, and has not been submitted in whole or in part, for a degree at this or any other institution.

Dhiya Dalila Zawawi

November 2019

ACKNOWLEDGEMENTS

I would like to thanks my supervisor, Dr. Jim Reid for his guidance and support throughout my PhD journey at the University of Sheffield. I am lucky to have Jim as my supervisor as my supervisor as he always encourages me with his ideas and positive words.

My thanks is also extended to the members of Reid group, Dr. Chatchawwal, Antonia and Nick who helped me with my research throughout their knowledge, time and guidance.

A special thanks to the awesome staff and other post-graduate in Chemistry Department, especially Chemical Biological cluster. The experinces I got during my PhD journey were excellent.

Thank you also to my family, especially to my parents, Mr. Zawawi Mohammed and Mrs Rahimah Mustafar for the love, support, understanding throughout my PhD journey. Without all of you, I would not have been able to completet my PhD journey. Thank you, Allah, for all the achievements I have received in my whole life.

Finally, thank you to the Ministry of Higher Education Malaysia and Universiti Sultan Zainal Abidin for the opportunity and finaciall support for me to pursue my PhD.

TABLE OF CONTENTS

LIST OF FIGURES

LIST OF TABLES

ABBREVIATION

CAM	Crassulacean Acid Metabolism
F-6-P	fructose-6-phosphate
G-3-P	glyceraldehyde-3-phosphate
IPTG	isopropyl-1-thio-β-D-galactopyranoside
kDa	kilo Dalton
LB	Luria-Bertani
NAD-ME	NAD-malic enzyme
NADP-ME	NADP-malic enzyme
Ni	nickel
OAA	oxaloacetate
PEP	phosphoenolpyruvate
PEPC	phosphoenolpyruvate carboxylase
PEPCK	phosphoenolpyruvate carboxylase kinase
PCK subtype	phosphoenolpyruvate carboxylase kinase subtype
PCR	polymerase chain reaction
PP2A	protein phosphatase 2A
ppm	part per million
Rubisco	ribulose-1,5-bisphosphate carboxylase
RuBP	ribulose-1,5-bisphosphate
TAE	tris-acetate-EDTA

ABSTRACT

The C_4 photosynthesis pathway is more efficient than C_3 photosynthesis due to the capability of phosphoenolpyruvate carboxylase (PEPC) that provides a CO_2 high concentration at Rubisco, thus reducing the photorespiration rate. PEPC is regulated by internal metabolite with malate or aspartate as its inhibitors, and glucose-6-phosphate (G-6-P) as its activator. Besides, PEPC also regulated by reversible phosphorylation by protein kinase known as phosphoenolpyruvate carboxylase kinase (PEPCK), that leads to an activation of the enzyme by G-6-P and decrease the sensitivity to malate or aspartate. PEPCK shows a high specificity towards PEPC and the reaction has been reported to be light controlled, but the details of mechanisms of PEPC phosphorylation are still unknown.

In this study, comparative analysis was performed between phosphorylated PEPCs from C_3 *Panicum pygmaeum* and C4 *Panicum queenslandicum* produced either by PEPCK or Protein Kinase A (PKA). Over-expression of PEPCK with solubility tag NusA had produces soluble protein but in small amounts, and was insufficient for further analysis. Purifying PEPCK without the NusA tag, was unsuccessful because it exists as an insoluble protein. Thus, PKA was applied since it is known to phosphorylate PEPC.

The phosphorylation of PEPC by PKA has been confirmed with fluorescence detection, by combining Pro-Q Diamond and SYPRO Ruby gel stain in SDS-PAGE gel. The phosphate affinity Phos-Tag™ was performed subsequently to ensure all PEPCs present were fully phosphorylated. Peptides resulting from the trypsin digestion of Phos-Tag™ SDS-PAGE gels were analysed by mass spectrometry to identify phosphorylation site on PEPC. Two phosphopeptides were detected in the PEPC from *P. queenslandicum* and six from the *P. pygmaeum* enzyme.

Phosphorylation of PEPC changed the pattern of kinetic enzyme activity, as well as the malate and aspartate sensitivity when compared to the nonphosphorylated form. The enzyme activity (V_{max}) of PEPC from the C_4 species *P. queenslandicum* increased once phosphorylated, but this was not observed in the PEPC from the C_3 species *P. Pygmaeum.* In terms of PEP K_m, the phosphorylated *P. queenslandicum* PEPC, had a lower K_m value when compared to the nonphosphorylated one. In the *P. Pygmeaum* PEPC, phosphorylation did not change the K_m (PEP) value or the specific activity. Phosphorylation increased the specificity of PEPC to bicarbonate in the enzymes from both *P. queenslandicum* and *P. pygmaeum* at pH 8. Phosphorylated PEPC from *P. queenslandicum* becomes less sensitive to malate and aspartate inhibition at limiting PEP. In *P. pygmaeum*, phosphorylation of PEPC made it less sensitive to aspartate at limited PEP and to malate at both limited and saturated PEP.

Together, these results lead to understanding how the phosphorylation influence the catalytic activity of PEPC in C_3 and C_4 plant species differently and protect the PEPCs against malate and aspartate inhibition.

CHAPTER 1

INTRODUCTION

During the evolution of C_4 photosynthesis, photosynthetic phosphoenolpyruvate carboxylases (PEPC) develop distinguishable characteristics that can set them apart easily from other higher plant PEPCs. C_4 species can be evolved into a division of labour between mesophyll cells, where the C_4 cycle occurs primarily. The Rubisco and the C_3 cycle reactions are localised in the bundle sheath cells. C_4 photosynthesis is a carbon concentration system that increases the concentration of carbon dioxide (CO_2) in the bundle sheath cells where the Rubisco locates and to overcome the competitive inhibition by the high concentration of oxygen (O_2). The primary substrate of PEPC in mesophyll cells is the bicarbonate ion (HCO_3^-) which is not inhibited by O_2. Such mechanism decreases photorespiration and increases the carboxylation capacity of Rubisco significantly.

The C_4 photosynthesis initially starts with the conversion of the atmospheric CO_2 into HCO_3^- by carbonic anhydrase (CA). PEPC catalyses the carboxylation of phosphoenolpyruvate (PEP) with HCO_3^- to produce oxaloacetate (OAA) and inorganic phosphate. OAA is then transformed into a more stable four carbon acid, malate in the NADP-ME subtype, aspartate in the NAD-ME subtype, or a combination of both malate and aspartate in the phosphoenolpyruvate carboxylase kinase (PEPCK) subtype. Next, these compounds are pumped into the Rubisco of bundle sheath cells where the decarboxylation reactions occur under a high concentration of CO_2.

Other than the activation mechanism by glucose-6-phosphate (G-6-P) and inhibition mechanism by malate, PEPC activity is controlled by a reversible phosphorylation process which is catalysed by a protein kinase or better known as PEPCK. On the other hand, the protein phosphatase type-2A can catalyse dephosphorylation (Nimmo, H. G., 2000; Izui K., et. al., 2004; O'Leary, B., et. al., 2011). Phosphorylated PEPC usually becomes more active and less sensitive to inhibition by malate. It also improves the sensitivity to activation by G-6-P (Chollet, R. et. al., 1996; Izui, K., et. al., 2004; Nimmo, H.G., 2003).

It would be interesting to investigate the effects of PEPC-derived phosphorylation in both C_3 and C_4 plants on the enzyme activity before comparing it with the equivalent nonphosphorylated enzymes. Therefore, the initial goal of this study is to obtain a purified PEPCK solution with soluble NusA-PEPCK fusion protein and phosphorylate PEPC in it with the purified PEPCK. The NusA tag was used since it acted as a solubility-enhancing tag that can be removed by the typical digestion method with the protease and thrombin. In addition to PEPCK, Protein Kinase A (PKA) was also capable of phosphorylating PEPC. After the purification, the PEPCK and PKA were used to phosphorylate PEPC via an *in vitro* phosphorylation protocol.

From the literature, the phosphorylation of PEPC by PEPCK was mainly assumed to be activated by the light source as many previous studies have found out that the enzyme activity of PEPC was higher during illumination, as compared to the dark phase (Bailey, K. J., et. al., 2007; Lara, M. V., et. al., 2006; Shen, Z., et. al., 2017). As the

phosphorylation of PEPC was performed by *in vitro*, the conventional SDS-PAGE was applied along with Pro-Q Diamond® and SYPRO® Ruby stain to ensure the reaction takes place on the target protein. In general, the phosphorylation of PEPC was detected at a serine residue which was located close to the *N*-terminal. The phosphorylation can be confirmed by the presence of the newly developed phosphate affinity electrophoresis, which is known as Phos-tag™. The Phos-tag™ is a binuclear metal complex that binds selectively to a phosphate monoester. Thus, it separates the phosphoprotein and nonphosphorylated PEPC (Kinoshita, E., et. al., 2004). The phosphoproteins obtained were further analysed by mass spectrometry to ascertain the presence of other phosphorylated residues in the phosphorylated PEPC.

As both malate and aspartate are significant biologically relevant inhibitors in the PEPC reaction, inhibition assays were performed to evaluate the enzyme activity after the phosphorylation process. The affinity of PEPC to HCO_3^- and PEP was also evaluated. Since the majority of the C_3 and C_4 plant model systems are only distantly related, a model system with both C_3 and C_4 species is necessary to allow a more comprehensive comparative research approach. In this work, *Panicum* genera were selected as the model system because it possessed both C_3 and C_4 species. *Panicum queenslandicum* and *Panicum pygmaeum* represent C_4 and C_3 species, respectively.

1.1 Expanding world population and food distribution around the globe.

From the analysis of the United Nations (UN), it was estimated that the current world population is about 7.7 billion. It is envisaged that the global population will reach 8.5 billion in 2030, 9.7 billion in 2050, and 10.9 billion in 2100. Up to 93 % of the world population growth is projected to occur in the developing countries, whose part of it was predicted to rise from 78 % in 1995 to 83 % in 2020 (Khush, G. S. 2005). On the contrary, the population of developed countries is expected to be declined by almost 59 million between 2025 and 2050 (Uncu, A. O., et. al., 2013).

In the context of regions, Sub-Saharan Africa, Northern Africa, Western Asia, Australia/New Zealand, and Oceania are projected to continue to grow by end of the century. Meanwhile, Central and Southern Asia, Eastern and South-Eastern Asia, Latin America, the Caribbean, Europe, and Northern America are projected to reach its peak population before start to decline before the end of the century (Table 1.1).

In 2019, China (1.43 billion) and India (1.37 billion) have long been the two most populous countries of the world, representing 19 % and 18 %, respectively, of the global population. Based on the present projections, India is expected to overtake China as the world's most populous country around 2027. Between 2019 and 2050, the population growth of the world's five largest countries is predicted to be remained largely unchanged by the end of the century, with India remains as the world's most populous country with a total of 1.45 billion inhabitants, followed by China with 1.06 billion, Nigeria with 733 million, the United States with 434 million, and Pakistan with 403 million populations (Table 1.2).

Based on the recent data from the UN (2019), the world's population is ageing. In 2018, people aged 65 years or above outnumbered children under five years of age. By 2050, it is predicted that the number of people aged above 65 will be twice that of children under five years of age. By 2050, the total global population aged 65 and over will surpass the population aged between 15 to 24. With the rapid population growth trend, the accessibility to adequate food supply remains limited up to 2015. The global level of the Prevalence of Undernourishment (PoU) has remained constant at a level slightly below 11%, while the total number of undernourished (NoU) has been slowly increasing. In another word, approximately 820 million people are still suffered from hunger today, corresponding to about one in every nine people in the world.

The increase in population will affect the food distribution system around the world as some parts of the world will not receive ample staple food supply for their daily dietary requirements. From Table 1.3, it was estimated that about 820 million people in the world were undernourished, with the vast majority occurred in the developing countries (FAO, 2019). If all these people are to be fed adequately, the overall food production will have to increase.

Table 1.1: Population of the world, SDG regions and selected groups of countries, with the total population from 2019, 2030, 2050 and 2100

Region	Projected population (millions)			
	2019	2030	2050	2100
World	**7 713**	**8 548**	**9 735**	**10 875**
Sub-Saharan Africa	1 066	1 400	2 118	3 775
Northern Africa and Western Asia	517	609	754	924
Central and Southern Asia	1 991	2 227	2 496	2 334
Eastern and South- Eastern Asia	2 335	2 427	2 411	1 967
Latin America and the Caribbean	648	706	762	680
Australia/New Zealand	30	33	38	49
Oceania*	12	15	19	26
Europe and Northern America	1 114	1 132	1 136	1 120

Data source: United Nations (2019). World population Prospects, 2019. Department of Economic and Social Affairs, Population Division.

*excluding Australia and New Zealand

Table 1.2: Ranking of the world's most populous countries, 1990 and 2019, and medium-variant projection, 2050 and 2100 (numbers in parentheses refer to the total population in millions)

Country	1990	2019	2050	2100
India	873	1 366	1 639	1 450
China	1 177	1 434	1 402	1 065
Nigeria	95	201	401	733
United States	252	329	379	434
Pakistan	108	217	338	403
Indonesia	181	271	331	321

Data source: United Nations (2019). World population Prospects, 2019. Department of Economic and Social Affairs, Population Division.

Table 1.3: Total undernourishment around the world in 2018

Country	Number of undernourished (NoU) (millions)	Prevalence (%) of undernourishment (PoU)
World	821.6	10.8
Developing countries	780.0	12.9
Developed countries	14.7	5.0
Africa	256.1	19.9
Asia	513.9	11.3
Latin America and Caribbean	42.5	6.5
Oceania	2.6	6.2

Source: FAO, 2019. The State of Food Security and Nutrition in the World 2019. Safe Guarding Against Economic Slowdowns and Downturns. Food and Agriculture Organization of the United Nations. Rome, FAO.

1.2 Challenges in crop productivity and food system

The exponential population growth has so far been sustained from the Green Revolution. In this third agricultural revolution, an extensive application of technology has been applied to accelerate and promote the agricultural crop production worldwide, specifically in the cereal-grain yields from many developing countries that began in the late 1960s (Kush, G. S. 2001). Unfortunately, the crop production output and yield in most of the developing countries were reported to be declined from 1980 (Evenson, R.E., and Gollin, D., 2003). A new 'Green revolution' is required to increase global agricultural production output and improve the resource use efficiency in crop production (Parry, M. A., and Hawkesford, M. J. 2010).

The agricultural demand is expected to grow by about 50 % by 2030 as the global population grows (Bruinsma, J. 2003). The global food systems need to change and intensify fundamentally to become more sustainable (Garnett, T., et. al., 2013). Besides, it was estimated that 2 billion people were suffered from micronutrient deficiencies in 2012 based on the health and nutrition indicators for development (Wheeler, T., and Von Braun, J. 2013). Other than the growing world population, some of the other challenges within the global food system in the upcoming decades include: (i) demographically changing population, (2) higher purchasing power with consequential change in eating habits, (3) resource scarcity, and (4) higher greenhouse gas (GHG) emissions (Godfray, H. C. J., and Garnett, T. 2014). Increasing global surface temperatures, water availability, and climate variability will adversely affect plant growth and carbon assimilation (Carmo-silva, E., et al., 2015).

Climate change is one of the significant challenges in food security, especially through its effect on the livelihoods of low-income workers and societies with less adaptability and reliance on highly climate-sensitive activities such as agriculture (Schmidhuber, J., and Tubiello, F, N. 2007).

Climate change can have both positive and negative effects on the crop like changes in phenology, heat stress, water pressure, and the existence of pests and diseases (Challinor, A. J. et. al., 2009; Chakraborty, S. and Newton, A. C. 2011; Bender, J. and Weigel, H. J. 2011). Some effects of the climate change can be helpful for food production. For example, secular temperature rises will allow the cultivation of marginal lands at higher latitudes which were previously deemed unsuitable for agricultural production. On the other hand, the rising atmospheric concentrations of CO_2 will improve the crop yields without any other factors limiting the plant growth. Nonetheless, lower crop yield was reported from a comprehensive analysis that investigated the net effect of climate changes on the plant production efficiency (Godfray, H. C. J., and Garnett, T. 2014).

Many previous studies have reported that anthropogenic global warming has triggered a series of extreme climate events that may negatively impact crop yields. With the incremental changes in temperature, rainfall, and extreme weather, climate change will affect the food supply chains, local food systems in small farm communities, food quality, food process, food security, reliability of delivery, and agricultural yields and remunerations in the future (Gornall, J., et. al., 2010; Vermeulen, S. J. 2012). It was predicted that the impacts of global climate change on food systems are expected to be widespread, complex, geographically, temporally variable, and profoundly influenced by socioeconomic conditions (Vermeulen, S. J., et. al., 2012). Under climate change, the sustainability of whole food systems may be at risk under global climate change due to the short-term variability in supply. The potential impacts on the country, however, are uncleared, although the weather instability and transition are most likely to exacerbate the food insecurity in areas with high risks of hunger and nutrition (Wheeler, T., and Von Braun, J. 2013). In short, a consistent global trend can be seen from the effects of climate change on crop production, which all demonstrated to have serious implications on food availability and accessibility. Climate change could potentially accelerate global progress toward a world without hunger.

1.3 A requirement to improve crop productivity and yield by photosynthesis.

As aspired by FAO (Food and Agriculture Organization of the United Nations), ending hunger and all forms of malnutrition by 2030 is an immense challenge. With real political commitment, bolder actions, and the right investments, a world without hunger is still achievable. A wide spectrum of approaches includes genetic improvement, molecular plant breeding, and improved crop nutrition are being introduced to increase global crop growth and yield. Other than that, another new approach is the application of crop-protection chemicals in the agricultural sector, which played a significant role in growing and maintaining arable crops in many industrialised countries (Jaggard, K. W., et. al., 2010). By increasing the availability of micronutrients in crops such as cassava, sorghum, and millet that grow under harsh environment, it will subsequently improve the dietary quality of such food staples. Thus, it will be very valuable to link breeding approaches for better crop yields, resilience, and nutrition value (Godfray, H. C. J., and Garnett, T. 2014).

Crop yields also can be improved by manipulating the rate of photosynthesis, depending on the type of photosynthesis carried out by the plants. Most of the higher plants exhibit one of three types of photosynthetic carbon fixation: three-carbon (C_3) compounds, four-carbon (C_4) compounds, and Crassulacean Acid Metabolism (CAM). Based on the primary product of carbon fixation, plants can be further classified into 3-phosphoglycerate

(3-PGA) in C_3 plants and oxaloacetate (OAA) in C_4 plants. The majority of the globally important crops include wheat (*Triticum aestivum* and *T. durum*), soybean (*Glycine max*), barley (*Hordeum sativum*), and rice (*Oryza sativa*) are C_3 species. Only maize (*Zea mays*) and sorghum (*Sorghum bicolor*) are C_4 species. Rice is a C_3 plant, hence its potential yield is limited by its photorespiration. Photorespiration generally reduces the rate of photosynthetic carbon fixation by around 25-35% and has a significant impact on a typical rice growth environment (Sage, T. L., and Sage, R. F. 2009).

Rice is one of the most important crops in the world. More people rely on it as their primary food source of calories and nutrition. Other crops like soybean are the fourth most important cereal crop in the world, followed by maize, rice, and wheat (Zhu, X. G., et. al., 2010). Globally, almost two-thirds of the calories are derived from all these four crops (Ray, D. K., et. al., 2013). A slow increment in the crop yields can be observed in China, India, and Indonesia. The rice yields per hectare were reported to be increased by an average of 36 % between 1970 and 1980, but the rate of yield between 2000 – 2010 was only increased by around 7% (Long, S. P. 2014). This raises the question of whether the present crop yield growth rate can meet the projected global demand or not.

The studies on the photosynthetic pathways of higher plants have been expanded over the last five decades since the start of the very first Green Revolution. Information on every photosynthetic reaction, the chemical structures of vital proteins, the internal mechanisms of the proteins, and the genes coding of each key component are widely reported in the literature (Long, S. P., et. al., 2015). With this vast amount of information available in the literature, the fundamental principles of the light capture reaction in photosynthesis by the pigment molecules for carbohydrate production can be easily understood.

To increase the growth rates of the world agricultural production, the productivity of the C_3 and C_4 plant species can be further improved by manipulating its inherent photosynthetic pathways. In general, C_4 species have a higher crop yield than C_3 species due to its higher nitrogen and water use efficiencies. This leads to the idea of improving the crop yield by integrating the desirable characteristics of the C_4 photosynthesis pathway into C_3 species (Hibberd, J. M., and Covshoff, S. 2010).

To incorporate the C_4 photosynthesis pathway into C_3 plants, one must identify and understand the function and structure of the specific genes (Furbank, R. T., et. al., 2009) in the leaf (Sage, T. L., and Sage, R. F. 2009). The conversion of C_3 plants into C_4 is challenging due to the complexity of C_4 photosynthesis. Thus, it is crucial to identify a suite of genes that can control the morphological and biochemistry of the photosynthesis reaction. Furthermore, many ongoing research works have indicated the high level of complexity in such work with an overwhelming amount of genes that require to produce a functional C_4 pathway. For example, *Flaveria* species requires a total of three thousand and five hundred and eighty-two genes in a C_4-related cluster (Gowik, U., et. al., 2011).

Instead of modifying the oxygenase activity, many previous researchers have attempted to improve the photosynthetic efficiency and carboxylation activity by changing the kinetic behavior of Rubisco (Carmo-silva, E., et. al., 2015). However, very little is known about which molecular features responsible for the control of specificity in Rubisco (Zhu, X. G., et. al., 2010).

In the literature, there are others several feasible approaches to improve the photosynthetic performance include a rational protein design that involves redesigning the electron transfer chain or carbon-fixing enzyme, multigene engineering of protein complexes in the electron transfer chain of carbon fixation pathways, and field phenotyping that involves the evaluation of design concepts under field conditions (Ort, D. R., et. al., 2015).

In this study, the phosphorylation of PEPC which is involved primarily in C_4 photosynthesis was addressed in detail. Furthermore, the changes in malate and aspartate were compared after the phosphorylation of PEPC. The photosynthetic isoforms of PEPC catalyse the primary fixation of CO_2, while PEPC is the major anapleurotic enzyme in non-photosynthetic tissue and C_3 leaves (O'Leary, M. H. 1982; Andreo, C. S., et. al., 1987; Chollet, R., et. al., 1996). PEPC in C_3 plants catalyses the replenishing cycle of tricarboxylic acid with other intermediates that were withdrawn for different biosynthetic pathways and nitrogen assimilation (O'Leary, B., et. al., 2011a).

1.4 C_3 photosynthesis mechanism.

In C_3 photosynthesis, CO_2 diffuses through the stomata, followed by the internal cellular air spaces before it arrives at the chloroplast of a mesophyll cell (Yamori, W., et. al., 2014). In the mesophyll cell, the CO_2 is anchored by ribulose-1,5-bisphosphate carboxylase (Rubisco) before produces 3-phosphoglycerate (3-PGA), a three-carbon compound (Paulus, J. K., et. al., 2013) (Figure 1.1).

Phosphorylated 3-PGA is then reduced to glyceraldehyde-3-phosphate (G-3-P) via a regenerative phase before the production of fructose-6-phosphate (F-6-P) and ribulose-5-phosphate. Next, F-6-P is converted into a starch component which is essential for plant growth and development. The regeneration of ribulose-1,5-biphosphate (RuBP) from ribulose-5-phosphate (Ru-5-P) ensures additional fixation of atmospheric CO_2 and carbohydrate (Raines, C. A., 2011). The primary obstacle hindering the high rates of photosynthesis in C_3 crops is the affinity of Rubisco towards O_2 rather than CO_2. This reaction is also known as oxygenation, where the closing of stomata is mainly stimulated under hot, dry, and high light intensity environments that induce stomata to close. The resulting high ratio of O_2 to CO_2 will suppress the affinity of Rubisco towards CO_2 (Ludwig, M. 2013).

Such a phenomenon should be avoided because C_3 photosynthesis produces sucrose and starch from triose and hexose phosphates, allow biosynthesis of amino acids and lignin from erythrose-4-P, G-3-P for the isoprenoid pathway, and promote the production of ribulose-5-phosphate (Ru-5-P) for cell wall biosynthesis (Raines, C. A. 2011). With all the metabolites produced from C_3 photosynthesis, it clearly showed that it has a central position in the carbon metabolism.

By manipulating this specific pathway, one can potentially improve the crop yield and carbon production for the synthesis of different products. A higher concentration of CO_2 in the atmosphere could raise the rate of carbon fixation in the mesophyll cell of C_3 plants, and promote the synthesis of metabolites. Since the concentration of atmospheric CO_2 has been increasing over the last 2 decades with the rate of ~2 ppm/year, there is a good chance for C_3 photosynthetic crop yields to increase in the future (Fischer, R. A. 2015).

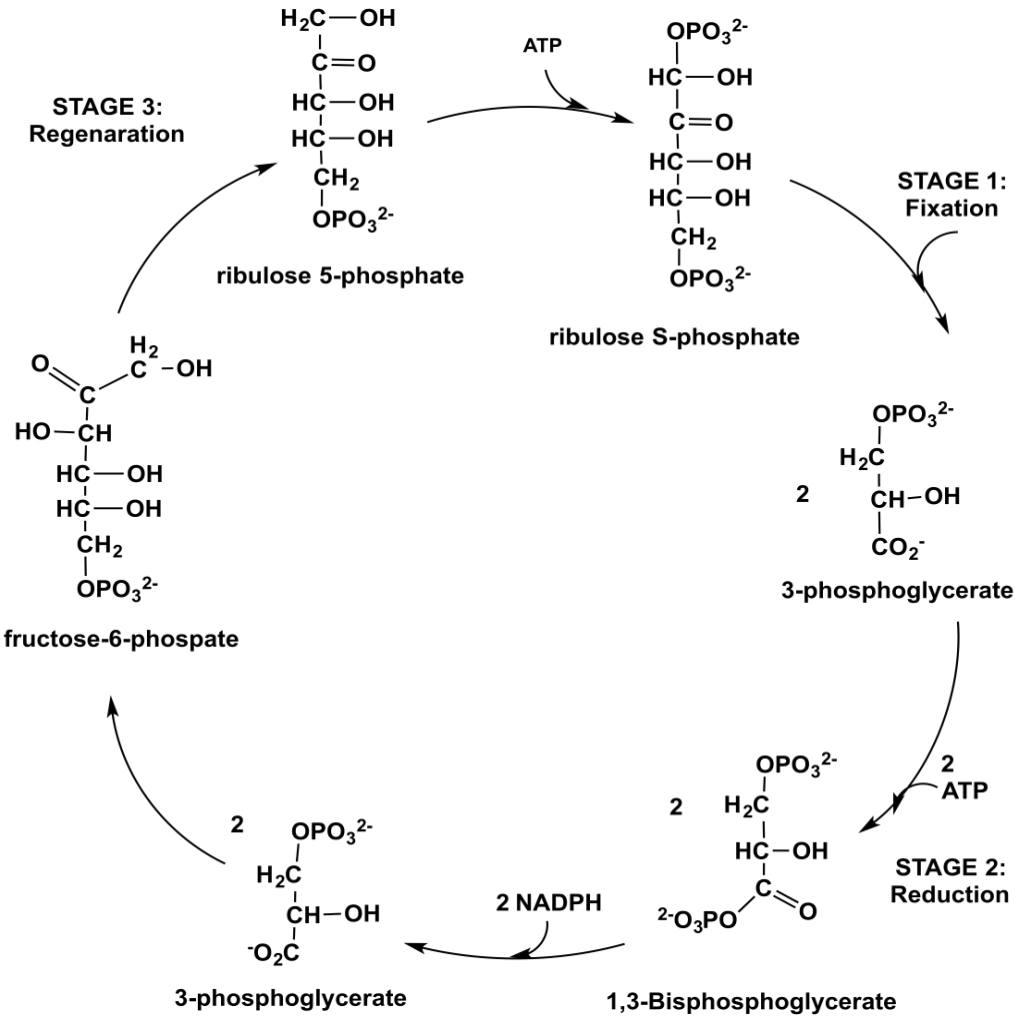

Figure 1.1: Scheme of the C_3 photosynthesis pathway. The atmospheric CO_2 is fixed by ribulose-1,5-bisphosphate carboxylase (Rubisco) producing 3-phosphoglycerate (3-PGA) in the chloroplasts of mesophyll cells. Phosphorylated 3-PGA is further reduced to fructose-6-phosphate (F-6-P) and ribulose-5-phosphate (Ru-5-P). The final step is regeneration of ribulose-1,5-biphosphate (RuBP) from Ru-5-P in the presence of ATP (Raines, C. A. 2011).

1.4.1 The photorespiratory cycle.

Photosynthesis can be easily retarded by photorespiration, which is the reaction of Rubisco with O_2 instead of CO2 (Jordan and Ogren, 1984). The reaction of Rubisco with CO_2 and ribulose-1,5-bisphosphate (RuBP) is known as carboxylation, while oxygenation is referred to as the reaction of Rubisco with O_2. In C_3 plants, carboxylation of RuBP produces a six-carbon compound, which is then divided into two molecules of 3-PGA, a three-carbon compound. Six of the 3-PGA molecules regenerate into six molecules of RuBP via the Calvin-Benson Cycle before forming a molecule of the six-carbon sugar, fructose-6-phosphate, via photosynthetic carbon reduction. This reaction route is desirable because both sucrose and starch are used to support plant growth (Yamori, W., et. al., 2014; Bloom, A. J. 2015). In contrast to C_4 plants, the downstream products of primary carbon fixation which include malate and aspartate are decarboxylated into pyruvate or PEP and CO_2. The resulting CO2 is then fixed by Rubisco in C_3 plants (Yamori, W., et. al., 2014).

The reaction of O2 with ribulose-1,5-bisphosphate (RuBP) produces two-carbon compound 2-phosphoglycolate (PG) and 3-phosphoglycerate acid (3-PGA) (Figure 1.2 and 1.3). 3-PGA is then recycled back to RuBP via the Calvin-Benson cycle. Next, the PG is transported into peroxisomes of mesophyll cells in the form of glycolate. In the peroxisome, glycolate is converted into glyoxylate before transformed into glycine. Following, two glycine molecules are diffused into mitochondria and before converted into serine. Next, the glycine decarboxylase releases CO_2, NH_3, and NADH. Then, serine transports to the peroxisome of bundle sheath cells and converted into hydroxypyruvate by an aminotransferase before reduced back to glycerate. Afterward, the glycerate diffuses back into the chloroplast of the mesophyll cells before it is converted into 3-PGA. Lastly, the 3-PGA molecules regenerate the RuBP (Tolbert, N. E. 1997; Sage, R. F., et. al., 2012).

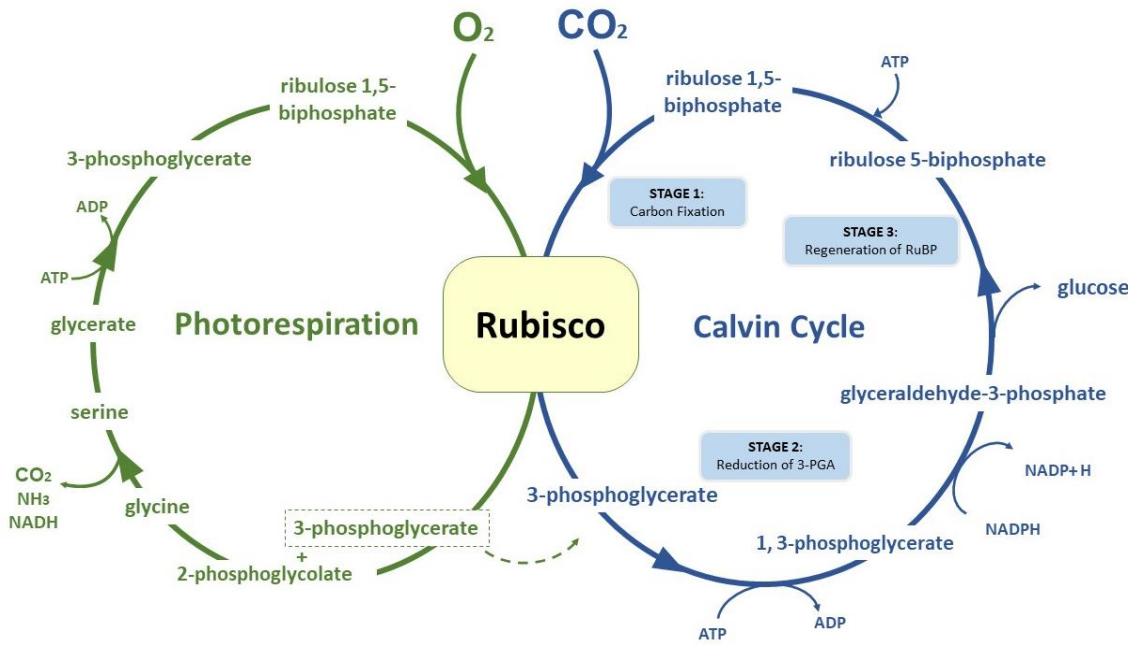

Figure 1.2: The reaction of Rubisco with O_2 or CO_2 (Tolbert, N. E. 1997).

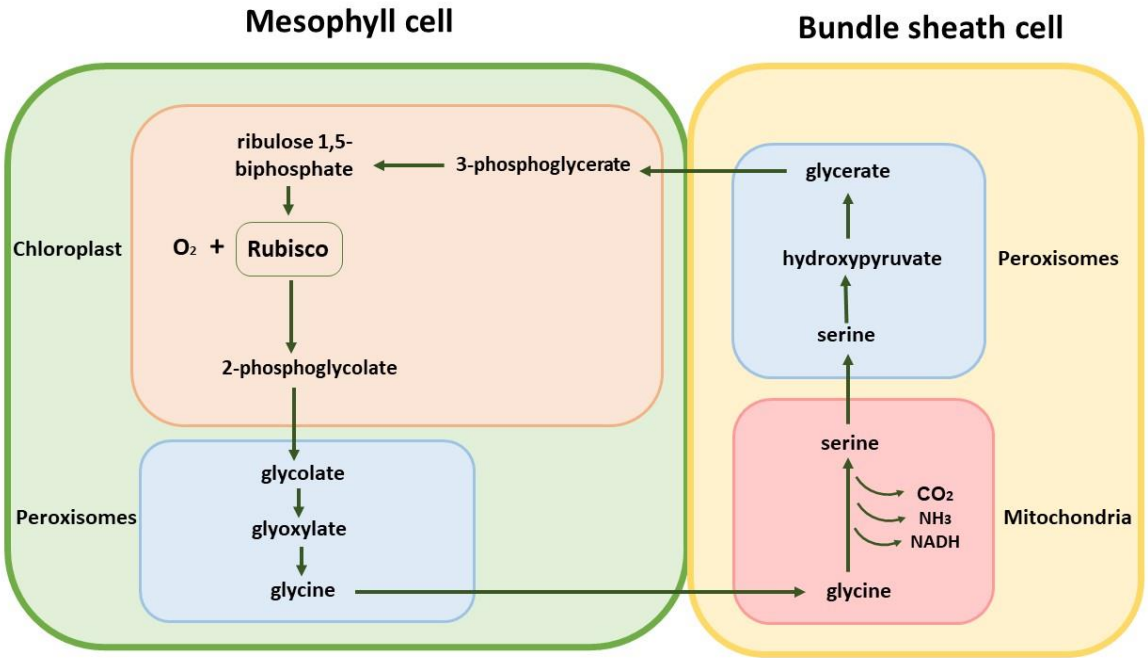

Figure 1.3: Schematic of photorespiration pathway (Tolbert, N. E. 1997; Sage, R. F., Sage, T. L. and Kocacinar, F. 2012).

1.5 What does it take to be C_4?

Edwards G. E., et. al., (2001) highlighted that there are several requirements for a CO_2 concentrating mechanism to fulfill, which include a cell-specific amplification of enzymes of C_4 photosynthesis. It should consist of PEPC (phosphoenolpyruvate carboxylase) in mesophyll cells and Rubisco in the bundle sheath cells, with complimentary adjustments of photosystem and electron transport activities. Besides, C_4 plants must express a novel set of cell-specific organelle metabolite translocators with a symplastic connection of the spatially separated sources and sinks of the 4C-dicarboxylic acid transport metabolites. Also, it should possess the CO_2 diffusion barriers between the CO_2 fixation sites by PEPC in mesophyll cells and the CO_2 release and refixation sites by the Rubisco in the bundle sheath cells.

These criteria have been fulfilled through the numerous independent evolutions of C_4 photosynthesis in different groups of terrestrial plants. Most of the terrestrial C_4 plants were presumed to have Kranz anatomy. Many early experiments that contributed to the discovery of C_4 plants were based on maize and sugarcane, which are derived from the members of family Poaceae (Hatch, M. D. 1999). Since then, C_4 plants have been identified in a total of nineteen families with the highest number of species reported from the families of Poaceae, Cyperaceae, and Chenopodiaceae.

Kranz means wreath in German, and the existence of Kranz anatomy was initially characterised by Haberlandt, G., (1884). The Kranz anatomy is a specific leaf structure that consists of a double concentric layer of chlorenchyma cells and forms Kranz tissues. The outer layer of the tissues captures the atmospheric CO_2 in the C_4 cycle, while the inner layer of the tissues donates CO_2 from the C_4 acids to the Rubisco in the C_3 cycle.

The outer layer is referred to as the mesophyll cells which consist of palisade parenchyma, and the inner layer is bundle sheath cells or Kranz cells. The mesophyll cells are closer to the atmosphere as compared to the bundle sheath cells because the bundle sheath cells have limited contact with the intercellular air space. Both mesophyll cell and bundle sheath cell layers are usually adjacent to one another, but they can be separated by an additional layer of cells in some situations. The ratios of mesophyll cells to bundle sheath cells are lower than those in C_3 plants and most of the mesophyll cells are in direct contact with bundle sheath cells.

C_4 plants also developed several specialised anatomical features and formed the inner compartment where Rubisco is localised and CO_2 is concentrated. Most of the C_4 plant leaf cells adapt a Kranz anatomy. In Kranz anatomy, an outer layer is derived from the mesophyll cells and the inner layer is derived from the cells located near or within the vascular bundle (Sage, R. F. 2004). This inner layer of cells or known as the bundle sheath surrounds each vascular bundle.

The intercellular transport system of the plant possesses two sets of transporters: one can be found in the organellar membranes within cells and another one located in between the cells of the two tissue types. Meanwhile, in C_4 photosynthesis, the transportation of small molecules between the mesophyll and bundle sheath cells occurs along a symplastic pathway via plasmodesmata (Bräutigam, A. and Weber, A. P. M. 2011).

After the mechanisms were discovered in the mid-1960s, much improvement has been made to understand the C_4 photosynthesis process that has been evolved independently over 50 times (Muhaidat, R., et. al., 2007). The C_4 pathway is a remarkable example of convergent evolution as most of the C_4 species come from the grass family, but with distinct C_4 lineages in all plant families. C_4 species is important because they account for about one-fourth of the earth's primary productivity. Most of them can be found in the grassland and arid shrubland plant communities within then warm temperate and tropical climates (Sage, R. F., et. al., 1999; Gillon, J., and Yakir, D. 2001).

Within C_4 grasses, nitrate and nitrite reductase are located in the mesophyll tissues. Thus, nitrogen reduction is localised in the mesophyll cells (Kopriva, S., 2011). In cold climates, C_4 species have poor performance because Rubisco has limited capacity under low temperatures. Under these circumstances, C_4 species tend to be poorly competitive against C_3 species, possibly due to the restrictions caused by the Rubisco, where it inhibits C_4 species from fully acclimating to the low-temperature environment (Sage, R. F., & McKown, A. D.; Sage, R. F., 2011).

1.5.1 The evolutionary origins of C4 photosynthesis.

It is widely accepted that the C_4 photosynthesis has evolved from the C_3 photosynthesis due to the decreasing concentration of atmospheric CO_2. With a lower level of atmospheric O_2 and a higher level of atmospheric CO_2 in the new environment, the evolution of primitive photosynthetic organisms began to occur within the plants (Ehleringer, J. R., et. al., 1991).

The evolution of primitive photosynthetic organisms began in an environment with a high level of atmospheric CO_2 and a low level of atmospheric O_2 (Ehleringer, J. R., et. al., 1991). In the C_4 photosynthetic pathway, a drop in the atmospheric CO_2 level around 30 million years ago is the primary driver for such evolution (Christin, P. A., et. al., 2008; Ehleringer, J. R., et. al., 1997; Sage, R. F., et. al., 2012). As compared to the C_4 types, a less effective response to the temperature changes is generally observed in the primitive C_3 photosynthetic types. This is because the C_4 plants usually prefer warm and humid climate as compared to C_3 plants which prefer colder climates (Collatz, G. J., et. al., 1998). The C_3 photosynthetic pathway generally reaches its optimum activity under a low-temperature environment with an atmospheric CO_2 concentration above 500 parts per million by volume (Cerling, T.E., et al., 1997).

C_3 species account for nearly 85 % of all higher plant species when compared to the other 5 % of C_4 species (Yamori, W., et. al., 2014). C_4 plants can sustain their growth due to its inherent ability to grow at a higher temperature and a lower atmospheric CO_2 concentration. Most importantly, they have a higher capability to concentrate CO_2 in bundle sheath cells for metabolism reactions.

The majority of C_4 species are derived from monocots. About 50 % of the total C_4 species are originated from the grasses, while sedges account for the remaining 25 % (Sage, R. F., et. al., 1999). Grasses and sedges are essential in providing food for the world population as they are the primary sources of grain, refined sugar, and

syrups. They can not only be served as the food staples for humans, but it can be used as fodder for the grazing animals which directly contribute to meat production (Brown, H.A. 1999).

Approximately four thousand and six hundred grass species and one thousand and six hundred sedge species exploit the C_4 photosynthesis pathway. From the total number, dicot plants derive from a total of one thousand and six hundred species and they also belong to sixteen families with 75 % of the clustering into the four different families of Amaranthaceae, Asteraceae, Chenopodiaceae, and Euphorbiaceae (Muhaidat, R., et. al., 2007). According to Leegood, R. C., and Walker, R. P. (1999), most of the C_4 species belong to the families of Poaceae, Cyperaceae, and Chenopodiaceae. Agronomically valuable crops such as *Zea mays* (maize), *Saccharum officinarum* (sugarcane), and *Sorghum bicolor* (sorghum) are from the family of Poaceae and they are also identified as the C_4 species (Ludwig, M. 2013).

Thus, the distribution of C_4 photosynthesis in the grass and sedge families should be understood by studying when and how these important species diversified in the recent geological time.

1.5.2 How C_4 species adapt to photorespiration.

As compared to the C_3 plant leaves, C_4 leaves have two types of cells; mesophyll cells and bundle sheath cells. Together, these two types of cells are capable of fixing the atmospheric CO_2 more efficiently. The coordinated function of these two cell types offers a high concentration of CO_2, which reduces the rate of the oxygenation reaction of Rubisco and the photorespiration rate (Kanai, R., and Edwards, G. E., 1999).

To counteract the inhibitory effects of low atmospheric CO_2 levels, the C_4 plants form a new CO_2 concentrating mechanism through a significant re-organisation of the leaf anatomy and metabolism (Sage, R. F. 2012). C_4 plants inhibit photorespiration by concentrating the atmospheric CO_2 in the chloroplast of bundle sheath cells near the Rubisco (Amthor, J.S. 2010). CO_2 in the form of HCO_3^- is assimilated into the mesophyll cells from the reaction of PEPC before converted into OAA. Next, the resulting four-carbon organic acid (malic or aspartic acid) diffuses into the bundle sheath cells and decarboxylated into CO_2 (Betti, M., et. al., 2016). Some of the CO_2 leakages from the bundle sheath cell is inevitable because the C_4 cycle generally operates faster than the C_3 cycle in C_4 plants (Amthor, J.S. 2010). This process also increases the CO_2 concentration to the saturation point for the Rubisco (Sage, R. F. 1999). The PEPC enzyme also plays a significant role in increasing CO_2 concentration.

The transportation of fixed carbon from the mesophyll cells to the bundle sheath cells must be coordinated with other metabolites from the photosynthetic cycle under different environmental conditions. For example, the rate of CO_2 fixation in the mesophyll cells and its sequential influx to the bundle sheath cells must be coordinated effectively with the assimilation rate of the Calvin-Benson cycle (Leegood, R. C., and Walker, R. P. 1999).

1.5.3 C_4 photosynthesis mechanism and the sub-types.

C_4 photosynthesis is mainly characterised by the separation of labour between the mesophyll and bundle sheath cells. The carboxylases PEPC can be found in the mesophyll cells, while the Rubisco is high metabolite fluxes

which are crucial for the proper function of C_4 photosynthesis. C_4 plants have been evolved independently over 50 times (Muhaidat, R., et. al., 2007) and have resulted in three biochemical subtypes of C_4 plant photosynthesis according to different types of decarboxylase enzymes. These are NADP-malic enzyme (NADP-ME), NAD-malic enzyme (NAD-ME), and PEPCK.

Each subtype transfers different types of metabolites between the mesophyll and bundle sheath cells. In all three subtypes, the primary carboxylation of PEP to OAA mainly occurs in the mesophyll cytoplasm under the aid of PEPC (Figure 1.4). The resulting OAA is then transformed into a more stable four carbon acid, which is malate in the NADP-ME subtype, aspartate in the NAD-ME subtype, or a combination of both malate and aspartate in the PEPCK subtype (Figure 1.5 and 1.6). In the bundle sheath cell, the malate in the NADP-ME type is decarboxylated by the NADP-malic enzyme. Aspartate in the NAD-ME type is deaminated into OAA before it is reduced to malate by malate dehydrogenase and then decarboxylated by NAD-ME. Aspartate in the PCK type is also deaminated into OAA before it is decarboxylated by PEPCK. These decarboxylation processes release CO_2 for the subsequent fixation process by the Rubisco in the Calvin-Benson Cycle (Aldous, S. H., et. al., 2014; Ludwig, M. 2013). Other products are pyruvate in the NADP-ME and NAD-ME types as well as pyruvate and PEP in the PCK type. PEP diffuses back into the mesophyll cells, whereas pyruvate is transaminated to the alanine before it is being transported back into the mesophyll cells.

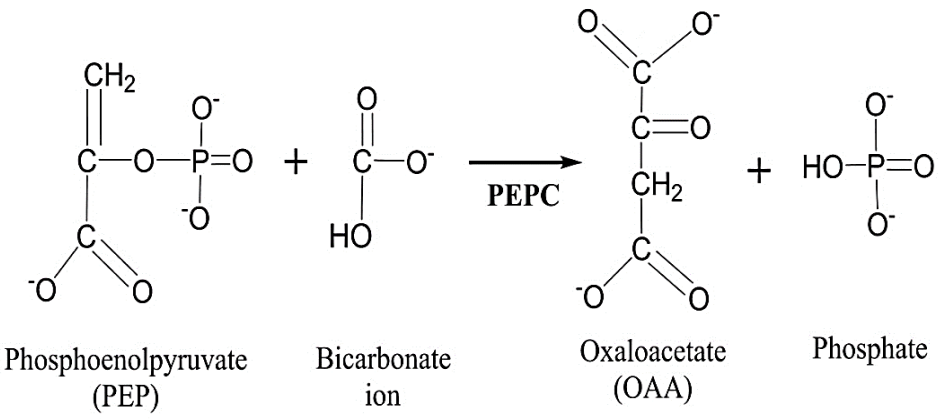

Figure 1.4: The carboxylation of PEP catalysed by phosphoenolpyruvate carboxylase (PEPC). PEPC will bind to the HCO_3^- and PEP to produce OAA (Svensson, P. et. al., 2003).

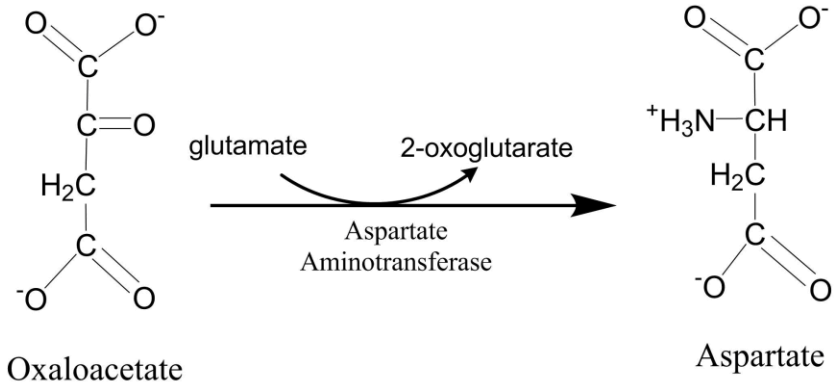

Figure 1.5: The four carbon acid, oxaloacetate was reduced by aspartate aminotransferase to produce aspartate and 2-oxoglutarate in NAD-ME type (Edwards, G., and Walker, D. 2003).

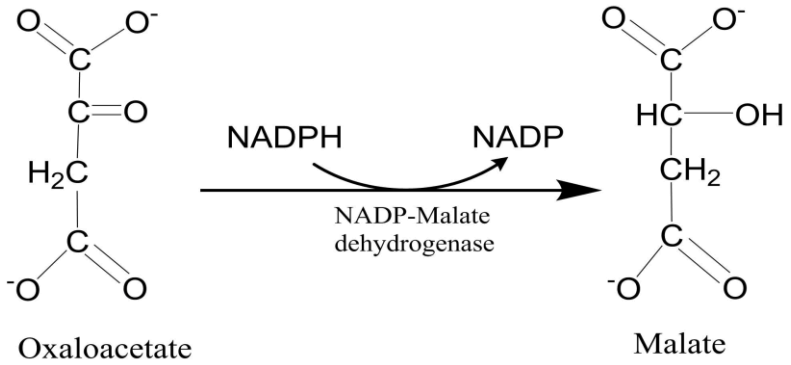

Figure 1.6: Oxaloacetate is reduced to malate by NADP-malate dehydrogenase in the NADP-ME type and malate is then diffused from mesophyll cell into the bundle sheath cell (Edwards, G., and Walker, D. 2003).

1.5.3.1 NADP-ME subtype.

The least complex C_4 subtype is the NADP-ME subgroup. The NADP-malic enzyme (NADP-ME; L-malate: NADP oxidoreductase [OAA decarboxylating], EC 1.1.1.40) involved in different metabolic pathways since it can be found in numerous types of animal and plant tissues, and also in prokaryotic and eukaryotic cells. NADP-ME catalyses the oxidative decarboxylation of L-malate to produce pyruvate, CO_2, and NADPH with either Mg^{2+} or Mn^{2+} as a cofactor. The decarboxylation reaction is the primary activity of this enzyme, but other researchers also found out that some isoforms can catalyse the reductive carboxylation of pyruvate, which is a reverse reaction of NADP-ME (Wheeler, M. C. G., et. al., 2008).

In C_4 crops like maize, sugarcane, and sorghum, NADP-ME exists as one of the most unique and significant decarboxylases in the chloroplasts of bundle sheath cells because malate is the predominant C_4 acid formed during photosynthesis (Fig. 1.7). Nonetheless, aspartate is also one of the significant transient fixed CO_2 in some NADP-ME species (Wingler, A., et. al., 1999). *Flaveria bidentis*, a dicot of an NADP-ME species, produces approximately an equal amount of malate and aspartate during photosynthesis, but, in this case, it was suggested that the aspartate is metabolised to malate before it is decarboxylated by chloroplastic NADP-ME (Meister, M., et. al., 1996). Early studies demonstrated that NADP-ME was derived from maize which was previously purified from mature green leaves (Drincovich, M.F., et. al., 1992; Drincovich, M.F. and Andreo, C.S. 1994). Other research activities in the literature have also characterised the five members of the NADP-malic enzyme family from *Zea mays* (Alvarez, C. E. 2013), and investigated the response of NADP-ME to the extreme climate environments likes drought (Hýsková, V. D. 2014).

1.5.3.2 NAD-ME subtype.

The NAD-Malic enzyme (NAD-ME; EC 1.1.1.38) catalyses the oxidative decarboxylation of malate to pyruvate and CO_2 in the presence of NAD, and cofactors like Mn^{2+} or Mg^{2+} to provide CO_2 for the Calvin-Benson cycle. NAD-ME exploits NADP in varying extents, but it still prefers NAD with the absolute requirements of a divalent cation and a potent activator, CoA (Drincovich, M. F., et. al., 2011). Plants with the NAD-ME subtype have high activities of aspartate and alanine amino transferases within both mesophyll and bundle sheath cells. As compared to malate that is decarboxylated in bundle sheath cell mitochondria (Fig. 1.7), aspartate is a major C_4 acid. To achieve high photosynthetic efficiency, the NADP-ME subtype has a high number of mitochondria in the bundle sheath cells as the photosynthetic isoform of NAD-ME can be found here.

In some C_4 plants, the activity of NAD-ME is fifty times higher than that of NAD-ME found in C_3 plants. The carbon flux within the bundle sheath cell mitochondria in the NAD-ME subtype is equivalent to the rate of photosynthesis. Thus, the bundle sheath mitochondria must have special features to allow a high rate of malate decarboxylation, especially during the daylight, where photosynthesis reactions are active (Agostino, A., et. al., 1996).

1.5.3.3 PEPCK subtype

In the PEPCK subtype (Figure 1.7), the decarboxylation enzyme is PEPCK. In the presence of HCO_3^-, Mg^{2+} or Mn^{2+}, the irreversible carboxylation of PEP to OAA and phosphate (Pi) is catalysed by PEPC in the mesophyll cell (Figure 1.4) (Chollet, R., et. al., 1996). OAA is transaminated into aspartate by aspartate aminotransferase before it is transported to the bundle sheath cells (Figure 1.5). Next, the aspartate is converted into OAA by 2-oxoglutarate before it is decarboxylated into PEP by PEPCK for the production and fixation of CO_2 for in the bundle sheath chloroplast (Brautigam, A., et. al., 2014). Following, the PEP is diffused back into the mesophyll cells for another round of carbon fixation. Plant PEPCK is a multimeric enzyme with identical subunits (Burnell, J. N., 1986; Walker, R. P., et. al., 1995). In PEPCK subtype plants, the enzyme is located at the cytosol of bundle sheath cells and works in tandem with the NAD-ME to supply the ATP required by the PEPCK (Hatch, M. D. 1987).

Based on Figure 1.7, each subtype of C_4 photosynthesis has its particular arrangement of cellular structure in terms of biochemistry and physiology, and each subtype has a different mechanism in regenerating PEP, which is the critical substrate of PEPC in the mesophyll cells. This specificity of cellular structure is vital to allow the effective operation of the C_4 cycle.

The particular arrangements of a cellular structure must occur to allow the efficient operation of the C_4 cycle. In C_4-NADP-ME-subtype species, the bundle sheath chloroplast has a rudimentary or deficient grana (the stacks of thylakoids embedded in the stroma of a chloroplast) with limited photosystem II expression. For C_4-NAD-ME-subtype species, the mitochondria in bundle sheath cells have a high decarboxylation rate of C_4 acid, thus possibly exhibit unusual respiratory characteristics. Finally, the cytosol in the C_4-PEPCK subtype species must generate adequate ATP to allow the decarboxylation of OAA (Drincovich, M. F., et. al., 2001)

As compared to C_3 species, C_4 plants have significant nitrogen and water use efficiencies. Depending on the C_4 subtype, NADP-ME has a higher nitrogen use efficiency than the NAD-ME subtype plants due to the higher Rubisco catalytic efficiency. On the contrary, NAD-ME species have a higher water use efficiency during drought as compared to the NADP-ME types. This situation may be explained by the higher frequency of NAD-ME grasses which can be found in dry regions (Ghannoum, O., et al., 2002).

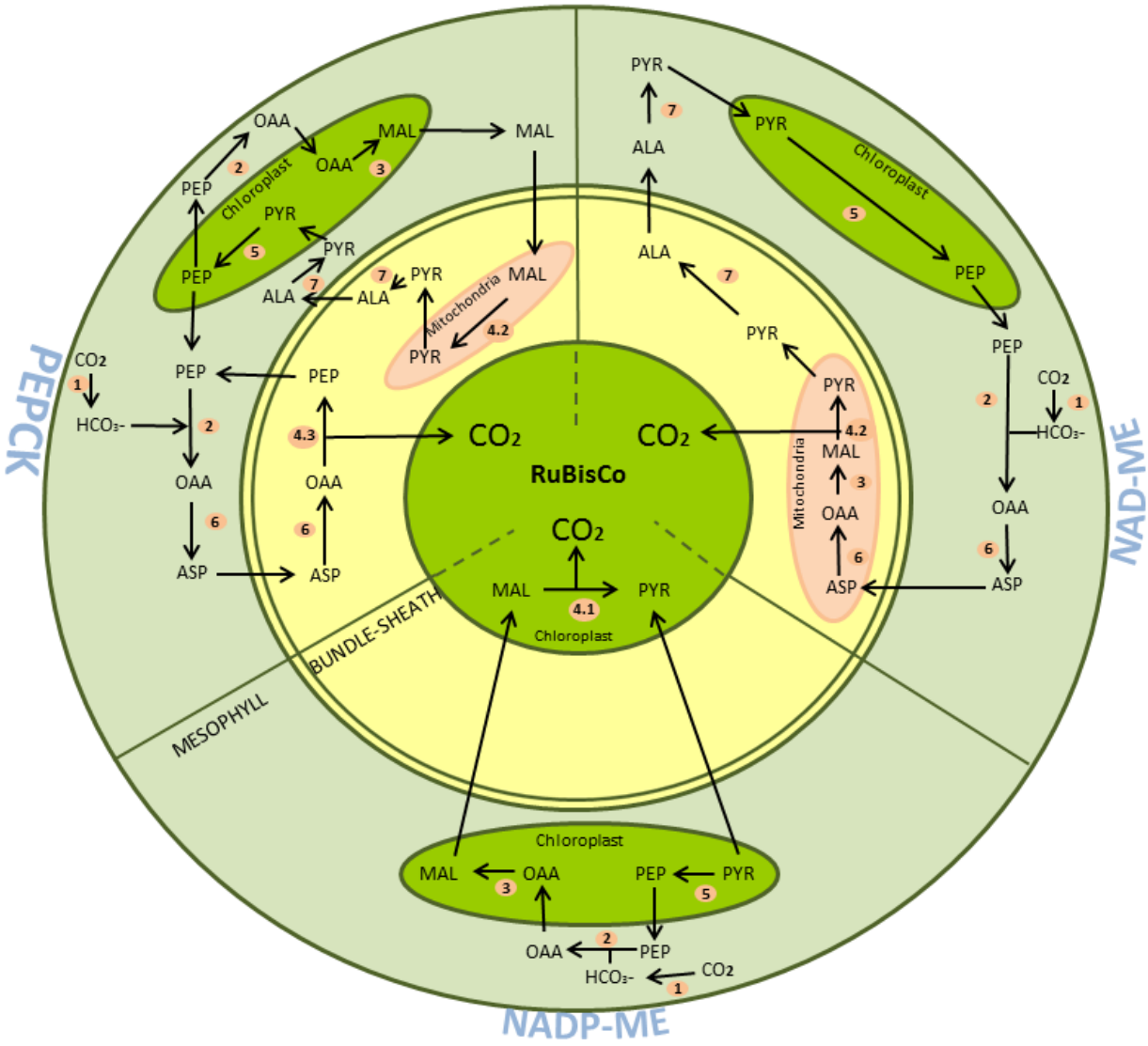

Figure 1.7: Schematic of C4 photosynthesis subtypes, NADP-ME, NAD-ME and PEPCK. Mesophyll surrounding bundle sheath cells. Chloroplast are in green and mitochondria in orange. MAL malate; OAA oxaloacetate; PEP phosphoenolpyruvate; ASP aspartate; ALA alanine; PYR; pyruvate. 1. Carbonic anhydrase. 2. Phosphoenolpyruvate carboxylase. 3. NAD/P-malate dehydrogenase, 4. Decarboxylases. 5. Aspartate amino acid transferase. 7. Alanine amino acids transferases. Atmospheric CO_2 is converted to HCO_3^- by carbonic anhydrase. All reactions released CO_2 that is fixed by Rubisco in Calvin-Benson Cycle. PEPC uses the HCO_3^- to carboxylate phosphoenolpyruvate (PEP), producing OAA. The OAA was either converted to malate or aspartate. In bundle sheath cell, malate is decarboxylated by NADP-ME producing pyruvate; aspartate is converted back to OAA by 2-oxoglutarate and decarboxylated by PEPCK producing PEP. Both reactions released CO_2 that is fixed by Rubisco in Calvin-Benson Cycle. The pyruvate and PEP diffuses back into the mesophyll cell and ready for another cycle. (Figure reference: Aubry, S., et. al., 2011).

1.6 Regulation of C_4 phosphoenolpyruvate carboxylase (PEPC).

PEPC was firstly isolated from spinach leaves in 1953 (Bandurski, R. S., and Greiner, C. M. 1953). Since then, PEPC has been found in many plants (Chollet, R., et. al., 1990), algae (Vanlerberghe, G. C., et. al., 1990), and bacteria (O'Leary, B. 2009) except animals and fungi. The largest PEPC catalytic subunit has been found in green algae known as *Chlamydomonas reinhardtii* which consists of about one thousand twenty and one amino acids with a molecular mass of one hundred and thirty-one kDa (Mamedov, T. G., et, al., 2005). In the active form, the PEPC enzyme is a homotetramer with four active sites with Mg^{2+} as a cofactor (Izui, K., et. al., 2004)

Phosphoenolpyruvate carboxylase (PEPC) is regulated allosterically by a wide range of metabolites. Photosynthetic PEPC catalyses the first carboxylation reaction of CO_2 uptake in C_4 photosynthesis (Figure 1.4) (Bailey, K. J., et. al., 2007). These photosynthetic isoforms are inhibited by the downstream products of CO_2 fixation such as malate (O'Leary, M. H. 1982). Non-photosynthetic PEPC usually replenishes the malate, oxaloacetate, and citric acid cycle intermediates that are required for the biosynthesis of amino acid and assimilation of nitrogen. Besides, intermediates inhibit these non-photosynthetic isoforms such as aspartate and glutamate in these pathways (O`Leary, B., et al., 2011; Murmu, J., and Plaxton, W. C. 2007). PEPC has many additional physiological roles in plants which include supplying carbon to the N_2-fixing legume root nodules and maintaining the cellular pH (Latzko, E., and Kelly, G. J. 1983).

C_4 PEPC has evolved from a non-C_4 isoform in each of the independent evolutionary lineages of C_4 photosynthesis (Sage, R, F. et. al., 2011). Since low-level expression of non-C_4 PEPCs was generally detected in the leaf tissues of C_3 plants, the expression of PEPC genes must have been altered during the C_4 evolution (Gowik, U., et. al., 2006). The PEPC activity in C_4 plants generally exhibits cold lability from the warm climates, whereas the PEPC of low-temperature C_4 plants remains stable under cold climates (Krall, J. P., and Edwards, G. E. 1993; Matsuba, K., et. al., 1997). PEPC levels were found to be declined by 30 % during the first week of exposure in the cold-tolerant species like *Spartina anglica* before it was stabilized afterward (Matsuba, K., et. al., 1997). Also, the PEPC activity of sugarcane was relatively stable at low temperatures (Du, Y. C., et. al., 1999a, 1999b). Besides, the PEPC activity of the cold-sensitive grass *Zoysia japonica* was reported to be decreased by more than two-thirds after being exposed to 10°C/7˚C day/night, which led to the assumption that it could be a critical limitation after prolonged exposure to the cold climate (Matsuba, K., et. al., 1997).

1.6.1 Small molecule inhibitors and activators.

The phosphoenolpyruvate carboxylase reaction is regulated by two different mechanisms: covalently through a reversible phosphorylation process of a conserved serine residue which is close to the *N*-terminus and non-covalently by binding various metabolite effectors include glucose-6-phosphate, malate, oxaloacetate, and aspartate (O'Leary, M. H. 1982; Fukuyama, H., et. al., 2006).

It is generally known that the metabolite products of C_4 photosynthesis, sugar phosphates like glucose-6-phosphate (G-6-P), hexose-phosphates, and triose-phosphates are allosteric activators of PEPC, which can

reduce the K_M for the substrate PEP (Svensson, P., et, al., 2003). In general, G-6-P increases the V_{max} of the enzyme and decreases the K_M for PEP (Andreo, C. S., et. al., 1987; Vidal, J., and Chollet, R. 1997). Other than sugar phosphates, other amino acid-based metabolites that act as activators include glycine (Gillinta, J., and Grover, S. D. 1995), alanine (Gao, Y., and Woo, K. C. 1996), and serine (Bandarian, V., et. al., 1992).

PEPC activation by G-6-P is accomplished by increasing the affinity of enzymes to PEP and by changing the affinity of PEPC to allosteric inhibitors. Although all PEPCs studied so far have a similar PEP affinity, the action of allosteric inhibitors may differ depending on the type of species. In the presence of G-6-P, the photosynthetic PEPC of maize, *F. pringlei* (C_3), and *F. pubescens* (C_3/C_4 intermediate) became less sensitive to malate (Engelmann, S., et. al., 2003; Takahashi-Terada, A., et. al., 2005). An opposite pattern was observed in the PEPC of *F. trinervia* (C4) and *F. brownii* (C_4-like) when it was activated by G-6-P as the enzyme became more sensitive towards malate (Engelmann, S., et. al., 2003).

In C_4 photosynthesis, PEPC uses bicarbonate to carboxylate PEP into OAA and phosphate (Pi). The role of Pi in C_4 photosynthesis has yet to be clarified in the literature. This is because there are contradictory findings on the effects of phosphate on the activity of C_4 PEPC as phosphate was reported to either inhibits (O'Leary, M. H. 1982; Doncaster, H. D. and Leegood, R. C. 1987), activates (Andreo, C. S., et. al., 1987), or does not affect the activity of C_4 PEPC (Wong, K. F., and Davies, D. D. 1973).

Particularly in the PEPCK subtype, malate accumulates as a result of the reduction of OAA. Malate is also a key player in the regulation of feedback in C_3 and CAM plants (Vidal, J., and Chollet, R. 1997). Aspartate is a downstream product of the carboxylation reaction in the NAD-ME and PEPCK types. It is also one of the major metabolites that transport between the mesophyll cell and bundle sheath cells (Andreo, C. S., et. al., 1987). Together, they act as feedback inhibitors of PEPC (Iglesias, A. A., et. al., 1986; Hatch, M. D., and Oliver, I. R. 1978). Aspartate was found to affect the non-photosynthetic PEPCs more severely than the C_4 isozymes (Svensson, P., et. al., 2003). Studies by Frank, J., et. al., (2001) and Gonzalez, D. H., et., al., (1984) showed that the maximum inhibition of PEPC by malate and aspartate were found at a pH of 7.0, but the inhibition effect was reported to be low or not detected at a pH of 8.0.

1.6.2 Phosphorylation of PEPC by Phosphoenolpyruvate Carboxylase Kinase (PEPCK).

Other than the activation and inhibition of specific metabolites, the activity of PEPC is also controlled by the reversible phosphorylation which is also catalysed by PEPCK (Chollet, R., et. al., 1996; Vidal, J., and Chollet, R. 1997; Nimmo, H. G. 2000). PEPCK phosphorylates PEPC specifically on Ser-15 in maize and Ser-8 in sorghum (Jiao, J. A. and Chollet, R. 1990). Phosphorylated PEPC shows less inhibition by malate (Jiao, J. A., et. al., 1991), which makes the enzyme more sensitive to the activation by glucose-6-phosphate (Chollet, R., et. al., 1996). As a result, the phosphorylated PEPC appears to be more active, although a reduction of the K_M towards PEP was observed instead of an increase in V_{max} (Duff, S. M. G. et. al., 1995; Tovar-Méndez, A., et. al., 2000; Takahashi-Terada, A., et. al., 2005). Ueno, Y., et. al., (2000) suggested that the PEPC in C_4 plants was phosphorylated in the light and de-phosphorylated in the dark. Vidal, J., and Chollet, R., (1997) showed that phosphorylation of PEPC

in sorghum was completed within two hours after being induced by light, with the final ratio of phosphorylated to non-phosphorylated PEPC was dependent on the light fluence rate.

The cloning and characterisation of the PEPCK gene were firstly reported in a CAM plant, *Kalanchoë fedtschenkoi* (Nimmo, H. G., 2003) and the C_3 species, *A. thaliana* (Hartwell, J., et. al., 1999). Echevarria, C., and Vidal, J., (2003) indicated that the PEPCK gene was encoded by a small multigene family, which was PEPCK-1 and PEPCK-2 in *A. thaliana* and *M. crystallinum,* respectively. Each gene has a single intron near to the 3' end of the coding region. The number of PPCK genes differs in several plant species. For example, two PPCK genes were detected in *A. thaliana* (Hartwell, J., et. al., 1999 and Fontaine, V., et. al., 2002), in tomato (*Lycopersicon esculentum* cv Alicante) (Marsh, J. T., et. al., 2003), and three in soybean (*Glycine max*) (Xu, W., et. al., 2007). Nimmo H. G. (2003) identified one PEPCK gene from sorghum, where the deduced amino acid sequence included a short and acidic insertion in contrast to other PEPCK. Furthermore, it was proposed that this sequence was located at the surface of the protein on the side opposite to that of the active sites. In tomato, the PECK gene (PPCK-2) contains two introns. One intron was located in the same position as that of the single intron in another PEPCK gene, and the other one lied in the middle of the coding sequence (Marsh, J. T., et. al., 2003).

The expression pattern of PEPCK genes also differs between plant organs. Nimmo, H. G., et. al., (2001) discovered that the PPCK-1 was highly expressed in rosette leaves of *Arabidopsis semialata*. Meanwhile, PPCK-2 was only expressed in flowers, roots, and carline leaves. The expression was promoted by the lighting and the addition of cycloheximide into the *Arabidopsis* cell culture. The expression of the PPCK gene also varied by an organ in soybean (Xu, W., et. al., 2007). The soybean PPCK-2 and PPCK-3 were highly expressed in root nodules, with the same transcripts in other organs.

Deficient PPCK polypeptide levels have also been described in other plant species, which included tomato, rice, soy-bean, and ice plant (Ermolova, N. V., et. al., 2003; Marsh, J. T., et. al., 2003; Xu, W., et. al., 2007; Fukayama, H., et. al., 2006). Murmu, J., and Plaxton, W. C. (2007) have purified PEPCK from castor oil seed with an approximate one thousand and five hundred-fold purifications. However, the analysis from Coomassie-blue stained SDS-PAGE gel showed that at least six protein bands, with none of which migrated with a M_r of about 31 kDa. This PEPCK derived from castor oil seeds had the same characteristics as that can be found in other PEPCKs. It has the molecular weight of approximately 30 kDa monomeric protein. Besides, it can phosphorylate PEPC specifically at highly conserved Serine residue near the *N*-terminus. Also, it can be reversibly inactivated under oxidative conditions and reactivated by dithiothreitol (DTT) (Murmu, J., and Plaxton, W. C. 2007).

Thus, this PEPCK can produce reactive thiol groups and led to a strong inhibition of enzymatic behavior when oxidised. However, a marked reactivation of the enzyme can be obtained if excess DTT is reduced. Other plant species with low PPCK polypeptide levels include tomato (Marsh, J. T., et. al., 2003), rice (Fukayama, H., et. al., 2006), soy-bean (Xu, W., et. al., 2003), and the ice plant (Ermolova, N. V., et. al., 2003).

PEPCK, a cytoplasmic enzyme, is a monomer of ca. 30 to 37 kDa (in C_4 plants) or ca. 32 to 39 kDa (in CAM plants) (Chollet, R., et. al., 1996). Nimmo, H. G. (2003) concluded that PEPCK was the smallest known protein kinase,

and it was a very low-abundance protein in maize leaves (Wang, Y. H., and Chollet, R. 1993; Saze, H., et. al., 2001). It was calcium-independent with limited calcium-binding domains. It also consisted of two hundred and sixty amino acid residues (Echevarria, C. and J. Vidal. 2003) and protein kinase catalytic domains with minimum insertions or extensions at the *N*- or *C*-termini (Nimmo, H. G., 2003). Taybi, T., et. al., (2000) purified PEPCK from a CAM plant, *Mesembryanthemum crystallinum* specifically phosphorylates PEPC at a single, *N*-terminal serine residue. Recognition elements of the *N*-terminal phosphorylation domain made the PEPC and PEPCK pairing highly specific (Li, B., et. al., 1997). The PEPCK is a Ca^{2+}-independent serine/threonine kinase with a high substrate specificity (Hartwell, J., et. al., 1999).

Phosphorylated PEPC is dephosphorylated by the protein phosphatase 2A (PP2A), and the regulation mechanism of this phosphatase is still unknown (Dong, L., et. al., 2001). Nimmo, H. G., et. al., (2001) mentioned that *in vitro*, PEPCK was inhibited by the 55-kDa inhibitor protein derived from *Zea mays* (C_4 plant) and *Kalanchoë fedtschenkoi* (CAM plant) leaf extracts. The inhibitor activity did not affect other serine/threonine protein kinases, which suggested that it may be specific for PEPCK. Another proposition is that a redox state might influence PEPCK activity in the assay. As reported by Saze, H., et. al., (2001), the PEPCK activity was low under mild oxidative conditions, but it became more active under a redox control mediated by thioredoxin and dithiothreitol (DTT).

The regulation of PEPCK activity was initially thought to be by continuous rapid degradation and *de novo* synthesis (Chollet, R., Vidal, J. and O'Leary, M. H., et. al., 1996). Further research works have discovered new PEPCK inhibitor protein, and possible redox regulation as another regulatory mechanism (Nimmo, H. G., et. al., 2001; Saze, H., et al., 2001). However, the *in vivo* mechanism of PEPCK regulation remains unclear.

The phosphorylation reaction also depends on the type of plants. It was observed that the PEPC purified from the leaves of CAM plants, and C_4 species like *P. maximum* was more susceptible to phosphorylation in the dark (Walker, R. P., and Leegood, R. C. 1995).

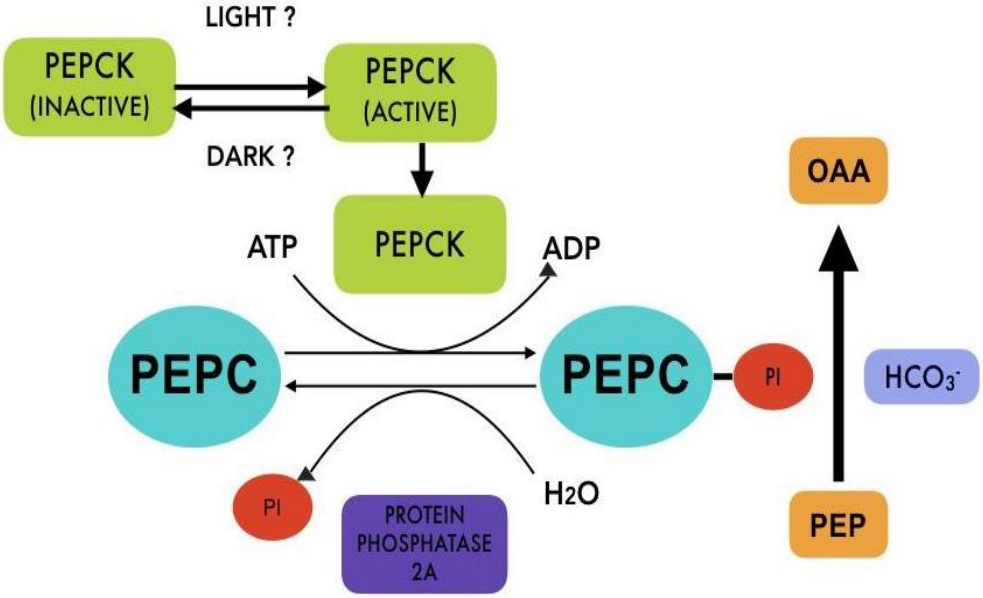

Figure 1.8: Regulation of cytosolic phosphoenolpyruvate carboxylase (PEPC) in C_4 plants. The regulation of PEPC kinases and phosphatase is still unknown, but it may involve additional post-translational modifications Friso, G., and van Wijk, K. J. 2015)

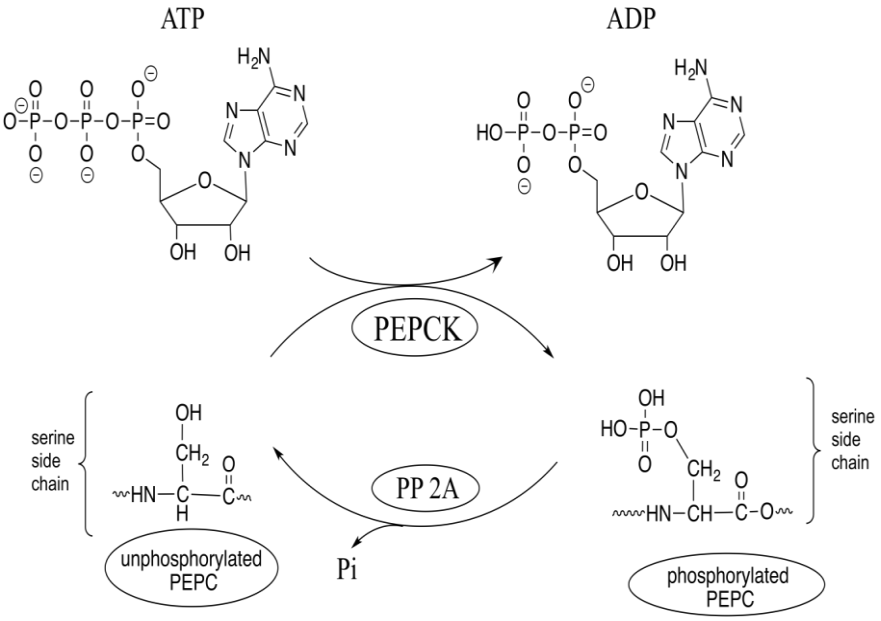

Figure 1.9: The attachment of the phosphate group from the ATP to the serine side chain. The phosphate is linked to the hydroxyl group of serine in the PEPC. Removal of phosphate is catalysed by protein phosphatase 2A (PP2A).

1.6.3 Phosphorylation of PEPC by PKA.

Some studies used PKA to phosphorylate PEPC. Meimoun, P., et. al., (2007) obtained a highly phosphorylated PEPC from dark-adapted sorghum leaves when the PEPC was incubated with PKA at 30°C for 40 minutes. The phosphorylated PEPC showed less inhibition by malate with 33 % after PKA treatment as compared to the 72 % inhibition before treatment. Pacquit, V., et. al., (1995) used PKA to phosphorylate sorghum PEPC and found out that the PEPC activity was about 5 to 6 folds higher when assayed in a pH of 7.1. Cotelle, V., et. al., (1999) phosphorylated PEPC from *Commelina communis L*. (Asiatic dayflower) with PKA. From the results, a 50 % increase in the V_{max} was observed under the presence of 1 mM malate (pH 7.3) and the sensitivity to L-malate inhibition was reduced from 84 % to 64 %.

Next, Terada, K., et. al., (1990) phosphorylated PEPC from maize leaf with PKA, and the phosphorylated acid amino residue was identified as Serine-15, which was located near the *N*-terminus by proteolytic digestion of 32P-labeled PEPC. In the context of kinetic properties, the half-saturation concentration of PEP ($S_{0.5}$) was decreased from 2 mM to 1.2 mM PEP after the phosphorylation. However, the V_{max} values were not affected significantly (Terada, K., et. al., 1990). Phosphorylation of PEPC from maize leaf (dark for 12 hours) with PKA produced a single serine residue (Ser-15) phosphorylated at the N-terminus of dark-form maize PEPC (Jiao, J. A., and Chollet, R. 1990).

To fully understand the function and regulation of C_4 and C_3 PEPCs, the recombinant enzymes from the C_3 plant, *Panicum pygmaeum*, and the C_4 plant, *Panicum queenslandicum* will be crucial. According to taxonomic principles, the Panicum genus is one of the major genera in Poaceace with up to five hundred species (Aliscioni, S. S., e.t al., 2003; Byng, J. W. 2014). The Panicum is also the most prominent group of Paniceae, which can be found primarily in tropical and subtropical areas around the world (Webster, R. D. 1988). The major types of photosynthetic in Poaceae are intermediate C_3, intermediate C4, C_3, and C4 and they are represented in the genus of Panicum (Zuloaga, F. O., et al. 2010). C_3 plant, *Panicum pygmaeum,* and the C4 plant, *Panicum queenslandicum* are two of the grasses species that belong to the same tribe, Paniceae.

In this thesis, the information on the PEPC from C_3 and C_4 plants were provided including the kinetic and regulatory properties of these enzymes, with or without the phosphorylation, and in the presence and absence of the key biologically relevant inhibitors.

CHAPTER 2

MATERIAL AND METHODS

2.1. Standard buffers, reagents and growth media.

Unless otherwise stated, all chemicals were analytical grade and purchased from Sigma-Aldrich. A Pre-packed HisTrap™ HP column was purchased from GE Healthcare (Uppsala, Sweden). All buffer and reagent solutions were made using distilled water purified by a Milli-Q system from Millipore. Luria-Bertani (LB) and Super Optimal broth with Catabolite repression (SOC) growth media were made up by using distilled water and sterilised by autoclaving. All buffer solutions were filtered through 0.2 µM cellulose nitrate membrane filters (Whatman). *E. coli* strains were from New England Biolabs® (NEB).

2.2 Cloning and expression of the PEPCK gene.

2.2.1. Construction of PEPCK gene into expression vector, pET-44a(+).

The PEPCK gene was constructed and expressed in a pET-44a(+) vector (Novagen). A schematic of the expression vector construction is shown in Figure 2.1. The Ppck gene was subcloned between BamH I and Xho I sites. The introduction of the Nde I, Spe I and Sac II site in the pET-44a(+) allowed for the introduction of the His-tag and NusA tag.

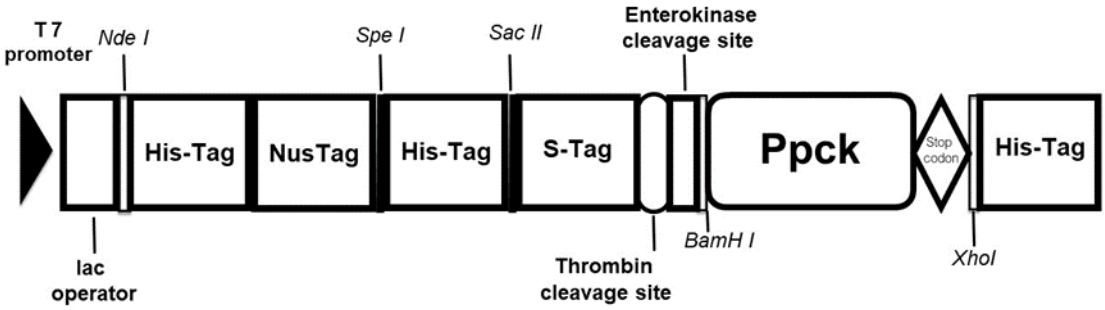

Figure 2.1: The pET-44a(+) vector design. The pET-44a(+) vector enables the expression of target protein attached to NusA tag and thrombin cleavage site will allow the separation during protein purification. His-tags present at the *N*-terminal allow for nickel affinity purification. The PEPCK gene was subcloned between BamH I and Xho I sites.

2.2.2 Complementary DNA (cDNA) synthesis.

The mRNA of *P. queenslandicum* (100 ng) was isolated, mixed with 1 µl of 500 µg/ml Oligo $(dT)_{12\text{-}18}$, 4 µl of 5x First-Strand (FS) buffer, 2 µl of 0.1 M dithiothreitol (DTT), 1 µl of deoxynucleotide (dNTP) mix, 1 µl of Superscript

II Reverse Transcriptase, 8 µl of Milli-Q water and then was reverse transcribed to generate a first strand of complementary DNA (cDNA).

2.2.3 DNA amplification by the thermo-cycling routine of Polymerase Chain Reaction (PCR).

Amplification of target DNA sequences was achieved using the polymerase chain reaction (PCR). The Forward and Reverse primers were designed and synthesized by Sigma. Primer DNA was diluted to the concentration of 10 µM. The first strand of cDNA then was used as a template for the polymerase chain reaction (PCR) by adding the following reagents; 3 µl of 100 % DMSO, 1 µl of 10 mM dNTPs, 10 µl of 5x Phusion GC Buffer, 2.5 µl of 10 mM Forward Primer, 2.5 µl of 10 mM Reverse Primer, 0.5 µl of Phusion Polymerase, 5 µl of cDNA and 25.5 µl of Mili-Q water to make the total volume of 50 µl.

Table 2.1: Forward and reverse sequence of PEPCK primer.

Primer	Forward	Reverse
PEPCK_PQu	5'-ATGAGTGCGGAGCTGAAGAGGGACTAC	5'-TCAGGTCGGCTGCTCCATTCCCCG
Pqu_PCK	5'-ATAGGATCCATGAGTGCGGAGCTGAAGAGG	5'-ATACTCGAGTCAGGTCGGCTGCTCCATTCC

PCR was performed with the initial denaturation of cDNA at 98˚C for 30 s, denaturation at 98˚C for 10 s, followed by annealing a short oligonucleotides primer to a single DNA strand at 72˚C for 30 s and synthesising a new strand at 72˚C for 1 min for 30 cycles. A final extension ended the PCR cycles at 72˚C for 10 mins, and the cycles were held for another 10 mins at 4˚C. A 1000 bp fragment was recovered from the 1 % agarose gel using the QIA quick Gel Extraction Kit and dephosphorylated by shrimp alkaline phosphatase (Exo Sap) to minimise the ligation background before submitted for DNA sequencing (Core Genomic Facility, Medical School, University of Sheffield) to confirm the nucleotide sequence.

2.2.4 Transformation of PEPCK plasmid DNA into Rosetta ™ competent cells by heat shock.

After confirmation by sequencing, 1 µl of purified plasmid DNA from the PCR (2.3.3) was added to 25 µl of Rosetta™ Competent Cells (Novagen) previously thawed on ice. The mixture was incubated on ice for 5 minutes before being heat-shocked at 42°C for 30 secs and then putting it on ice back for 5 mins. 75 µl of Super Optimal broth with Catabolite repression (SOC) medium was added, and the mixture was incubated at 37°C for 1 hour. The mixture (100 µl) was plated onto LB medium containing ampicillin (50 µg/µl) and incubated at 37°C overnight. After incubation overnight, a single colony then was inoculated into 10 ml LB medium and incubated at 37°C overnight.

2.2.5 Isolation of plasmid DNA.

The overnight culture that contains PEPCK DNA vector was purified with the QIAprep Plasmid Mini-Prep Kit (QIAGEN) by following the manufacturer's instructions. A two ml overnight culture was centrifuged at 13 000 rpm for 10 min, the pellet was resuspended in 100 µl of chilled P1 buffer and incubated on ice for 5 min. Next, the cells were lysed by addition of 250 µl of P2 buffer for 5 min. Then, lysis was stopped with 150 µl of chilled P3 buffer followed by a 5 min incubation on ice. Cell debris and precipitated protein were removed by centrifugation of the lysate at 10 rpm for 30 min, and the supernatant decanted into an 800 µl column. The matrix of these columns is based on silica, and this can bind dsDNA molecules of widely different sizes. Binding occurred by spinning the loaded columns at 10 000 rpm for a maximum of 1 min. Likewise, impurities were washed off the column with 750 µl of QC wash buffer. Finally, elution was performed with 30-50 µl of QE buffer.

The concentration of DNA vector was determined by NanoDrop 2000c Spectrophotometer (Thermo Scientific) as 101 ng/ µl. The preparation of Super Optimal broth with Catabolite repression (SOC) and Luria-Bertani (LB) medium is described in the Appendix section.

2.2.6 Vector restriction enzyme digests.

The expression vector was cut with BamHI-HF and Xho1 (New England, BioLabs) to insert the PEPCK gene into the correct reading frame. The reaction mixture contained 1 µg of vector DNA, 5 µl of 1X CutSmart® Buffer, 10 U of BamHI-HF, 10 U of Xho1 and was incubated at 37°C for 2 hours.

2.2.7 Purification of DNA from agarose gel.

Restriction digests products (DNA fragments) were separated and purified by electrophoresis in the 0.7 % agarose gels. 100 ml of Tris-acetate-EDTA (TAE) buffer was added into 70 g of agarose and then stirred softly. The agarose suspension was heated in a microwave at 300 watts for 10-15 min until the agarose was melted. Then, the suspension was poured into a plastic holder, a suitable comb (with 0.5-mm or 1-mm wells) was placed at the top end and allowed at least 30 min for solidification. Samples were then loaded alongside the DNA marker (5 µl) to estimate the sizes of DNA fragments. The samples were run at 90 Volts for 90 minutes in TAE buffer. The DNA fragment was visualised under 254 nm UV light, and the band containing the target DNA was excised with a clean scalpel.

To ensure high purity of plasmid DNA and/or PCR fragments, they were purified from excised agarose gel using the QIAQuick gel extraction kit (QIAGEN), following the manufacturer's instructions. Three volume were added per vol of agarose (100 µg corresponds approximately to 100 µl) in an Eppendorf tube, and then incubated at 50 C for 10 min with occasional vortexing. After the agarose dissolved completely, it was poured into a QIAQuick column and centrifuged for a 1 min at 13000 rpm in an Eppendorf tabletop centrifuged. Then, 750 µl of PE buffer was applied to the column and centrifuged as before. The DNA was eluted with 30-50 µl of buffer TB. The

concentration of DNA was then determined by NanoDrop 2000c Spectrophotometer (Thermo Scientific) as 10 ng/ µl.

2.2.8 Insert restriction enzyme digests and purification.

The restriction digestion procedure was the same as described above (2.3.6). The insert of DNA was then purified with the QIAquick PCR Purification Kit (QIAGEN) according to the protocol provided. The concentration of DNA was determined by NanoDrop 2000c Spectrophotometer (Thermo Scientific) which is 21 ng/ µl.

2.2.9 Ligation of DNA into expression vectors.

In a ligation reaction, a digested PCR fragment and a linearized vector are incubated with ATP and T4 DNA ligase to render a circularised vector containing the insert, by the formation of a phosphodiester bond between the 3' hydroxyl of one molecule and the 5' phosphate of another.

The insert containing the PEPCK gene was then ligated into the corresponding sites of the pET-44a(+) vector. This ligation process was carried out with 2 µl of 1X T4 ligase buffer (New England, BioLabs), 1 µl of 10U T4 DNA ligase (New England, BioLabs) with a molar ratio of purified insert DNA to vector of 3:1. The ligation reaction was performed at 16°C for 48 hours. The ligation product, pET-44a(+) plasmid that contains the PEPCK gene was purified by using QIAprep Plasmid Mini-Prep Kit (QIAGEN).

2.2.10 Transformation of purified plasmid into competent cells.

The 1 µl of purified plasmid from miniprep was incubated with 50 µl DH5 Alpha™ competent cells. The mixture was heat-shocked at 42°C for 20 secs and then put on ice for 5 mins. SOC medium was added to 950 µl total volume and incubated at 37°C for one hour with shaking at 250 rpm. Then 50 µl of the mixture was plated onto LB plate containing ampicillin (50 µg/µl) and incubated at 37°C for overnight. After overnight incubation, 93 colonies were observed growing on the LB plate.

2.2.11 Screening of expression clones.

To identify the presence of the PEPCK gene in a recombinant plasmid, 33 from 93 isolated colonies were selected to be analysed by PCR. The thermo-cycling routine of PCR was performed as in section 3.2.2.3. Then, the size of 33 colonies was identified with 1 % agarose gel by electrophoresis with untreated vector, pET-44a(+) was used as a negative control. From 33 colonies, three colonies (colony 4, 9 and 14) were purified from excised agarose gel using the QIAQuick gel extraction kit (QIAGEN), following the manufacturer's instructions followed by shrimp alkaline phosphatase (ExoSap) assay.

2.2.12 Dephosphorylation of DNA 5' termini

Dephosphorylation of the 5' terminal phosphate groups of digested plasmids avoiding recircularization and therefore decreases the background of false positives during colony screening. Dephosphorylation of 1-3 µg of DNA was performed with 1 U shrimp alkaline phosphatase (ExoSap) at 37°C for 30 min (Sambrook et al., 2001). SAP was heat-inactivated by incubation at 65°C for 15 min. The dephosphorylated plasmid was then purified with the QIAQuick PCR Purification kit (QIAGEN). The expression clones were then verified by DNA sequencing. All the sequencing was carried out by Medical School, University of Sheffield. Samples were prepared as recommended; in detail, 200-500 ng of pure DNA was re-purified with QIAQuick Plasmid Miniprep kit, ethanol-precipitated to remove salts before submitted.

2.3 Over-expression and purification of PEPCK-NusA protein.

2.3.1 Transformation of PEPCK-NusA fusion protein.

The recombinant Pqu_PCK: pET-44a(+) plasmid was transformed into Rosetta™ (Novagen) competent cells by the heat shock method. 1 µl of PEPCK DNA was added to an aliquot of competent cells previously thawed on ice. After 60 mins incubation in ice, a mixture of competent bacteria and DNA is placed at 42°C for 30 seconds (heat shock) and then put back in ice for another 60 mins. Then 100 µl of LB media was added into the mixture and incubated at 37°C for 60 min with agitation. A 50 µl of cell culture was then spread on agar-LB medium plates that contain ampicillin (50 µg/ml) and chloramphenicol (34 µg/ml) before incubation at 37°C for overnight.

2.3.2 PEPCK-NusA fusion protein induction.

Luria Bertani (LB) medium

The single colony from overnight incubation was then cultured into 20 ml of LB medium containing ampicillin and chloramphenicol and incubated at 37°C for overnight. After overnight incubation, 5 ml of the overnight culture was transferred into 500 ml of LB medium. The cells culture was further incubated at 18°C until the absorbance reading reached was around 0.5 - 0.6 at 600 nm (A_{600}). At this absorbance value, isopropyl-1-thio-β-D-galactopyranoside (IPTG) was added to a final concentration of 0.5 mM to induce PEPCK-NusA protein expression. The LB media that contain starter growth culture was further incubated at 18°C for another 18 hours. After 18 hours of incubation, the cell culture was centrifuged (Sorvall Lynx Superspeed 4000, Thermo Fisher) to separate cells containing target protein from the LB solution. After centrifuged at 4 000 rpm for 45 minutes at 4°C the supernatant was discarded and the pelleted cells now either used for further purification immediately or stored at – 80 °C for later purification.

2YT medium

The 2YT media was prepared from 16 g/l of tryptone, 10 g/l of yeast extract and 5 g/l of NaCl before being autoclaved at 121 °C for 15 minutes. The single colony that was transformed in Rosetta™ (Novagen) was then

cultured into 20 ml of 2YT medium containing 50 µg/ml ampicillin and 34 µg/ml chloramphenicol and incubated at 37°C overnight. The induction process was the same as LB medium except for the concentration of IPTG was increased to 1 mM. Induction took place at 18°C for 24 hours.

Auto-inducing growth medium.

The autoinduction media contained 1 % tryptone, 0.5 % yeast extract, 25 mM Na_2HPO_4, 25 mM KH_2PO_4, 50 mM NH_4Cl, 5 mM Na_2SO_4, 2 mM Mg_2SO_4, 100 µM FeCl3, 0.5 % glycerol, 0.0 5% glucose and 0.2 % lactose in 1 L water.

PEPCK-NusA constructs in pET44a(+) was transformed into the Rosetta™ (Novagen) host strains. Plate cultures were grown at 37°C in LB with ampicillin and chloramphenicol overnight. For a starter growth culture, a single colony was picked and added to the 25 ml of LB containing 50 µg/ml ampicillin and 34 µg/ml chloramphenicol. The culture was then incubated in a shaker (250 rpm) at 37°C for overnight. After overnight growth, 20 ml of culture was added to the 500 ml of auto-induction medium containing 50 µg/ml ampicillin and 34 µg/ml chloramphenicol. The medium was incubated at 18°C for another 48 hours.

2.3.3 Cell disruption.

Cell disruption by a sonicator

The pelleted cell from centrifugation was re-suspended in binding buffer, pH 7.4 (25 mM Tris-HCl, 0.5 M NaCl, 20 mM imidazole and 0.3 M glycerol). Protease inhibitor (Pefabloc®SC) was added to the pellet mixture to inhibit the activity of proteases that were released together with the protein during the cell disruption process. Cell disruption was performed with ultrasonication (Soniprep 150 Ultrasonic Disintegrator, MSE Sanyo), where ultrasonic vibrators will produce a high-frequency sound with a wave density. A transducer then converts the waves into mechanical oscillations through a titanium probe, which then immersed into the cell suspension. Sonication process was started at 15 micron amplitude for 30 s with 60 s intervals in an ice bath. This cycle was repeated six times for a total sonication time of 9 minutes. Then, the cell lysate was clarified by centrifugation at 32500 x *g*, for 60 minutes at 4°C. The pellet was discarded, and the supernatant was filtered with 0.45 µm Acrodisc syringe filter (Whatman) to clarify the solution and avoid clogging of the HisTrap™ HP column. Sonication can be very useful in small scale work, but when the volume of the resuspended pellet was substantially larger, a French press was used.

Cell disruption by the French press

Using a French press, the cell suspension was drawn through a valve into a pump cylinder. Then it was forced under pressure of up to 1500 bar through a narrow annular gap and discharge valve, where the pressure drops to atmospheric. Cell disruption is achieved due to the sudden drop in pressure upon the discharge, causing the cells to explode. In this experiment, the cells were disrupted twice with a French press at 20 psi. During the process, the lysate was kept cold by incubating on ice between rounds of lysis in the French press because warm lysate can cause target protein loss or degradation.

2.3.4 Affinity-purification of the intact, His-tagged (PEPCK-NusA) fusion protein with Ni-NTA affinity chromatography (HisTrap™ HP column).

Immobilised metal affinity chromatography (IMAC) makes use of the binding properties of metals towards protein for purification purpose; nickel-nitriloacetic (Ni-NTA) resin (QIAGEN) contains chelated nickel, which can specifically bind to stretches of polyhistidine in proteins. Many expression systems include His6 tags either at the *N*- or *C*-terminus or on both. 1 ml of resin need to be used for 20 mg of tagged protein since the resin has a maximum capacity of 50 mg protein/ml resin.

Prior to elution, the column was rinsed with MiliQ water to remove 20 % (v/v) ethanol and equilibrated with 20 ml (20 CV) of binding buffer pH 7.4, with 20 mM of imidazole (25 mM of Tris-HCl, 0.5 M of NaCl, and 0.3 M glycerol) to elute any remaining unwanted proteins. Once equilibrated, 20 ml (20 CV) of clarified supernatant was loaded into the column at the flow rate 1 ml per minute, and the colour of the resin was inspected. A beige colour was generally observed on protein binding, while no change of colour usually correlates with no binding. After loading, the column then was washed with 50 ml (50 CV buffer) of wash buffer, pH 7.4, with 100 mM of imidazole (25 mM of Tris-HCl, 0.5 M of NaCl, and 0.3 M glycerol) to remove loosely bound protein and other contaminants.

The fusion protein was eluted with 10 ml (10 CV) of elution buffer, pH 7.4 with 400 mM imidazole (25 mM of Tris-HCl, 0.1 M of NaCl, and 0.3 M glycerol). Eluted protein fractions were collected, and fractions containing protein (according to in-line absorbance reading on the instrument) were pooled and purity analysed by 10 % SDS-PAGE followed by Coomassie blue staining (2.4.11). The column was then washed with 50 ml (10 CV) of elution buffer to remove any remaining protein and stored in 20 % ethanol at 4°C.

2.3.5 Buffer exchange for removing the imidazole.

Desalting column containing Sephadex G-25 medium

Since the purified fusion protein was eluted in elution buffer that contains a high concentration of imidazole (400 mM) that can reduce thrombin cleavage, it needs to rebuffered in a thrombin cleavage buffer (TCB), pH 8.4 (20 mM Tris-HCl, 0.15 M NaCl, and 2.5 mM $CaCl_2$. Buffer was fully exchanged by dialysis or desalting chromatography on Sephadex G-25. The column was equilibrated with 20 ml (10 CV) of thrombin cleavage buffer (TCB) followed by applying the 5 ml of the purified fusion protein to the equilibrated column with the flow rate 1 ml per min. Five fractions with total volume 5 ml were collected from the column and pooled, analyzed for protein content by Bradford method (section 2.6).

Dialysis for buffer exchange

Dialysis can be used to replace buffer in the protein solution. The dialysis tubing cellulose membrane (D9777, Sigma-Aldrich) was submerged in a Mili-Q water for 30 minutes. One of the end of tube was sealed, then 5-10 ml of sample volume was loaded into the tube, air was expeled from the bag and sealed. The tube

was placed in 5 L beaker containing thrombin cleavage buffer (TCB), and agitate gently with magnetic bar at 4°C. The imidazole was removed by replacing with new TCB two or three times, to ensure full exchange of buffer.

2.3.6 On-column thrombin cleavage of the fusion protein (PEPCK - NusA).

Preparation of thrombin solution

The restriction grade of thrombin stock solution was prepared by dissolving 1000 Unit (U) of thrombin in 1 ml of thrombin storage buffer, pH 6.5 (50 mM sodium citrate, 200 mM NaCl, 0.1% PEG-800 and 50% glycerol) to make a stock concentration at 1U/µl.

Optimisation of thrombin cleavage reaction by time course in small scale

Small scale digestion reactions were conducted to optimize the thrombin to fusion protein concentration ratio so the NusA can completely separate from PEPCK. The purified fusion protein (section 3.4) was buffer exchanged into thrombin cleavage buffer, pH 8.4 (20 mM Tris-HCl, 20 mM NaCl, 2 mM $CaCl_2$) with dialysis tubing from Spectra/Por ® 1 Dry Standard. The concentration of purified fusion protein was determined by Bradford assay (2.6).

A serial dilution of thrombin (1 U/µl) in 8 tubes were made up so that there were five tubes with 1 U of thrombin and three tubes with 10 U of thrombin, respectively. 50 µg/ml of the fusion protein was added into each Eppendorf tube followed by thrombin cleavage buffer to make a total volume of reaction 50 µl. The cleavage reactions were incubated at room temperature with rotation. The reaction was stopped at various time by adding 50 µl 2X concentrated SDS-PAGE sample buffer into the aliquots and heated for 10 min at 75 °C. The level of cleavage of PEPCK was determined by SDS-PAGE.

On-column thrombin cleavage of the fusion protein (PEPCK - NusA)

Once the optimum concentration of thrombin and period of time was identified from the time course screening, large-scale cleavage reactions can be performed with the protein either bound on the column or in solution.

A HisTrap™ HP column was equilibrated with 10 ml (10 CV) of thrombin cleavage buffer, pH 8.4. The column was then loaded with 5 ml (1 CV) of the fusion protein in thrombin cleavage buffer containing thrombin. For each 1 mg of the fusion protein, 1 U of thrombin was added. The on-column thrombin cleavage process takes approximately 16 hours at 4°C.

Thrombin cleavage reaction in solution

The concentration of fusion protein was detected by BCA assay (1.11 mg/ml). Thus, 1.11 U of thrombin was added into the sample. The digestion was performed at room temperature for 2 hours or 16 hours at 4°C with agitation

2.3.7 Purification of PEPCK after thrombin cleavage reaction.

For on-column digestion, after 16 hours of reaction, the nickel column (HisTrap™ HP) was loaded with 10 ml of washing buffer, pH 7.4, (20 mM of imidazole) to elute the target protein, PEPCK that was tag free from NusA. PEPCK was collected in the wash buffer flow through. Finally, the bound, un-cleaved PEPCK-NusA was eluted with 20 ml of elution buffer, pH 7.4 (400 mM of imidazole). Fractions were pooled and analysed by 10 % SDS-PAGE followed by the Coomassie blue staining (2.5).

2.3.8 Digestion of the fusion protein with enterokinase.

Small Scale Optimization

Removal of NusA from PEPCK also can be achieved using enterokinase (GenScript). To determine the optimal enterokinase concentration and cleavage condition, small scale digestion reactions were performed. The purified fusion protein (section 3.4) was buffer exchanged into enterokinase cleavage buffer, pH 7.4 (20 mM Tris-HCl pH 7.4, 20 mM NaCl, 2 mM $CaCl_2$) with dialysis tubing from Spectra/Por ® 1 Dry Standard. The concentration of purified fusion protein was determined by Bradford assay (2.6).

A serial dilution of enterokinase (5 U/µl) was performed so that there was 1 U, 0.1 U, 0.01 U, 1X 10^{-3} U, 1X 10^{-4} U, 1X 10^{-5} U, 1X 10^{-6} U and 0 U enterokinase in 8 different tubes. 50 µg of the fusion protein was added into each tube followed by enterokinase cleavage buffer to make a total volume of reaction 50 µl. The digestion reaction was incubated at room temperature for 16 hours. The reaction was stopped by addition of 50 µl 2X concentrated SDS-PAGE sample buffer and heating for 10 min at 75°C. 5 µl from each tube was loaded on a SDS-PAGE gel to determine the extent of cleavage.

As no cleavage reaction was observed in this first attempt, digestion by enterokinase (5 U/µl) at higher concentrations was explored. The concentration of enterokinase was made up to 10U, 8U, 6U, 4U, 2U, 1U, 0.1 U, 0.01 U, 1X 10^{-3}U and 0 U enzymes respectively. The reaction and analysis were performed as described above.

2.3.9 Purification of PEPCK after enterokinase cleavage reaction.

After 16 hours digestion, the nickel column (HisTrap™ FF) was washed sequentially with 10 ml of washing buffer, pH 7.4, (20 mM imidazole) to elute the target protein, PEPCK that was tag free from NusA. PEPCK was collected in the wash buffer flow through. Finally, the bound, un-cleaved PEPCK-NusA was release with 20 ml of elution buffer, pH 7.4 (400 mM imidazole). Fractions from wash and elution buffer flow through that containing target protein were pooled and analysed by 10% SDS-PAGE followed by Coomassie blue staining (2.5).

2.4 Screening for PEPCK over-expression without NusA tag and purification

Rather than over-expression, induction and purification of PEPCK from the translation of the NusA-PEPCK fusion enzyme, it is acceptable to pursue other approaches to achieve an expression of of PEPCK with high active yield. An alternate technique for inducing high-level expression was to express PEPCK in the vector pET 100 / D-TOPO

as a single protein, without protein carrier, NusA. The primers were designed using PrimerX (http://www.bioinformatics.org/primerx/).

2.4.1. Transformation of PEPCK_Pqu in pET 100/D-TOPO PEPCK.

The recombinant PEPCK_Pqu: pET 100/D-TOPO plasmid was retransformed into Rosetta and BL21-DE3 strain (Novagen). After 30 mins of incubation in ice, a mixture of competent bacteria and DNA is placed at 42°C for 30 seconds (heat shock) and then put back in ice for another 30 mins. 100 µl of LB media was added, and the transformed cells are incubated at 37°C for 60 min with agitation. Then 50 µl of cells culture was spread on agar-LB medium containing ampicillin (50µg/ml) only or ampicillin with chloramphenicol (34 µg/ml) overnight at 37°C.

2.4.2. Over-Expression test and induction.

Small scale protein induction

The following protein induction strategy was applied after transformation as described in section 2.3. Initially, a starter culture from a single colony was grown in 20 ml of LB media with appropriate antibiotics at 28°C for overnight, with agitation, at 250 rpm. Small scale over-expression culture was then grown as follows: the overnight culture was added to 50 ml of LB medium at a dilution of 1:100. This then grew at 28°C (250 rpm) until the optical density (OD_{600}) was around 0.6. An aliquot was kept on ice as non-induced control, and the remaining cells were induced with different concentrations of IPTG. Depending on the host strain (Rosetta or BL21 DE3), some modifications were induced to the induction method such as the temperature, period time of incubation and types of antibiotics. Cells were harvested by centrifugation (Sorvall Lynx Superspeed 4000, Thermo Fisher) at 5000 rpm for 30 min and stored at – 80°C. Detailed conditions are given in Table 2.2 and 2.3.

Table 2.2: Small scale protein induction of PEPCK experimental design

Host strain	Rosetta				BL21-DE3			
Induction temperature	18°C				18°C			
Period of incubation	18 hrs				18 hrs			
IPTG (mM)	0.25	0.5	1.0	1.5	0.25	0.5	1.0	1.5

Table 2.3: Small scale protein induction of PEPCK experimental design

Host strain	Rosetta					BL21 DE3				
Induction temperature	20 °C		15 °C			20 °C		15 °C		
Period of incubation	18	24	18	24		18	24	18	24	
IPTG (mM)	0.5	0.5	0.5	0.5	1.0	0.5	0.5	0.5	0.5	1.0
	A1	A2	A3	A4	A5	B1	B2	B3	B4	B5

Large-scale induction

Over-expression in different expression vectors was performed using the same procedure described in section 2.4.2; Small scale protein induction. For preparative scale protein production, 8 L of LB medium with selected antibiotics were inoculated with 10 ml of an overnight preculture. The induction cultures were incubated at 18°C for 16 or 24 hours, as stated in Table 2.4.

Table 2.4: Large-scale PEPCK over-expression and induction experimental design

	BL21-DE3		Rosetta		
Period of incubation	18 hrs	24 hrs	18 hrs	24 hrs	
IPTG (mM)	0.5	1.0	0.5	0.5	1.0
	A	X	B	C	D

2.4.3. Purification of PEPCK protein by HisTrap™ HP column from pET 100/D-TOPO from different host strain, antibiotic, and temperature growth condition.

2.4.3.1 Cell lysis

The protein pellets were suspended with binding buffer containing 25 mM Tris-HCl (pH 7.4), 0.5 M NaCl, 20 mM imidazole and Pefabloc®SC was added later. The cell pellets were disrupted with a French press, as described in section 3.2.2.

2.4.3.2 Purification of PEPCK protein by HisTrap™ HP column

Prior to elution, the column was rinsed with MiliQ water to remove 20 % (v/v) ethanol and equilibrated with 20 ml (20 CV) of binding buffer pH 7.4 (25 mM Tris-HCl, 0.5 M of NaCl, 0.3 M glycerol, 20 mM imidazole) to elute any remaining unwanted proteins. Once equilibrated, 20 ml (20 CV) of clarified supernatant was loaded into the column at the flow rate 1 ml per minute. After loading, the column then was washed with 50 ml (50 CV buffer) of wash buffer, pH 7.4 (25 mM Tris-HCl, 0.5 M NaCl, 0.3 M glycerol, 100 mM imidazole) to remove loosely bound protein and other contaminants.

The fusion protein was eluted with 10 ml (10 CV) of elution buffer, pH 7.4 (25 mM Tris-HCl, 0.1 M NaCl, 0.3 M glycerol, 400 mM imidazole). Eluted protein fractions were collected, and fractions containing protein were pooled and analysed by 10 % SDS-PAGE followed by the Coomassie blue staining (2.5). The column was then washed with 50 ml (10 CV) of elution buffer to remove away any remaining protein and stored in 20% ethanol at 4°C.

2.5. Protein analysis by Sodium Dodecyl Sulphate–Polyacrylamide Gel Electrophoresis (SDS-PAGE).

Protein separation by SDS-PAGE gave an estimate of relative molecular mass and the relative abundance of a target protein in a sample. Two different layers of acrylamide gel were needed. The lower is the separating gel, which separates polypeptides by size. The upper layer or stacking gel is designed to load the protein sample. The final SDS concentration in the 0.75-mm-thick slab gels was 10 % (w/v) for the separating gel and 10 % for the stacking gel. Gels were run at a constant voltage of 200 volts for 50 minutes. The gel was stained with 0.12 % Coomassie blue R250 and then distained in 10 % acetic acid and 20 % ethanol. The gel image was analysed using the ChemiDoc MP Imaging System (BIO-RAD).

2.6. Protein quantification with Bradford assay.

The concentration of purified protein was estimated using the Bradford assay (Bradford, 1976) with modification using 96 well microplates. The assay was incubated at room temperature for 30 minutes before the absorbance reading was taken at 560 nm. Bovine serum albumin, molecular biology grade (New England BioLabs) was used as a standard. All the samples were analysed in triplicate.

2.7 Overexpression, Induction and Purification of PEPC from *P. queenslandicum* and *P. pygmaeum.*

The molecular cloning of PEPC was performed by Mr. Nick Moody started with the leaf samples of *P. queenslandicum* and *P. pygmaeum* were homogenised and the RNA was extracted from ground leaves using the RNeasy Kit (Qiagen). Libraries of cDNA were generated with SuperScript II Reverse Transcriptase (Thermo Fischer Scientific). The PEPC for *P. queenslandicum* was amplified using the primers PquFor1B and PquRev1B, and Q5 polymerase. The PEPC for *P. pygmaeum* was amplified using the primers PpyFor1B and PpyRev1B. Both genes were the cloned into the pET-1B His6 TEV LIC vector plasmid.

The expression, purification and quantification followed previously described methods by Moody, Nicholas., (2018).

2.7.1 Protein Overexpression of *P. queenslandicum* and *P. pygmaeum* PEPC.

The BL21 *λ* (DE3) *E. coli* strainwere transformed with each of the PEPC expression plasmids. A single colony from transformation was picked for overnight culture. An overnight culture was set up in 20 ml of LB with the addition of 30 mg/ml kanamycin. The starter cultures were grown in the LB media at 37°C until the OD_{600} reached 0.8. To induce recombinant protein, cultures were then cooled to 4°C about one hour before adding 0.5 mM IPTG, followed by incubation at 18°C for another 18 hours. Cells were harvested by centrifugation (Sorvall Lynx Superspeed 4000, Thermo Fisher) at 5000 rpm for 40 minutes, and the cells pellets were stored at -80°C for further analysis.

2.7.2 Protein purification with HisTrap™ HP column.

Cell pellets from 8.0 L of cultures was resuspended in 20 mL binding buffer, pH 7.4, 20 mM imidazole (25 mM Tris-HCl buffer, 0.5 M NaCl, 0.3 M glycerol) with DNase I and Pefabloc®SC (Sigma Aldrich). Cells were disrupted by using the French press (29 kPa at room temperature) and then centrifuged at 13000 rpm for 30 minutes twice. The supernatant was then filtered with a 0.45 µM pore filter (Elkay Labs.) The filtered supernatant was then loaded into a prepacked 1 ml nickel affinity column (HisTrap™ HP) previously equilibrated with five column volumes binding buffer, at a flow rate of 1.0 ml/min. Subsequently, the column was washed with 50 ml of wash buffer pH 7.4, containing 150 mM imidazole (25 mM Tris-HCl buffer, 0.5 M NaCl, 0.3 M glycerol) for PEPC *P. queenslandicum* and for *P. pygmaeum*, 100 mM imidazole was applied in wash buffer to remove any non-specific protein binders. PEPC was eluted with elution buffer, pH 7.4, 400 mM imidazole (25 mM Tris-HCl buffer, 0.5 M NaCl, 0.3 M glycerol) in a 10 ml total volume. The protein fractions from elution were pooled and buffer exchanged into phosphorylation buffer, (50 mM Tris-HCl, pH 8, 5 % glycerol and 1 mM DTT) using a Sephadex G-25M desalting column (Amersham Biosciences). About 5-10 ml of total protein fractions were collected and frozen at -80°C until use. All proteins were collected for analysis by SDS-PAGE to determine the purity of the samples.

2.7.3 Protein Quantification.

The PEPC enzyme concentration was quantified by absorption at 280 nm by using a Nanodrop 2000c Spectrophotometer. The enzyme extinction coefficient was calculated by Moody, Nicholas., (2018) using the ExPASy protein parameter tool. The extinction coefficient for *P. queenslandicum* PEPC was determined to be 105805 M^{-1} cm^{-1}, and the extinction coefficient for *P. pygmaeum* PEPC was determined to be 111514 M^{-1} cm^{-1}.

2.8.1 Small scale assay of *in vitro* phosphorylation assay of *P. queenslandicum* PEPC

Each assay contained phosphorylation buffer (50 mM Tris-HCl pH 8, 20 % glycerol), 5 mM $MgCl_2$, 200 µg/µl of PEPC *P. queenslandicum*, with or without 100 Units of the catalytic subunit of PKA from bovine heart (Sigma), and with or without 1 mM ATP in a total volume 500 µl. The catalytic subunit of Protein Kinase A (PKA) (P-2645; Sigma Chemical) was prepared following the manufacturer's recommendation. The lyophilized powder of PKA was prepared by adding 6 mg/ml (w/v) of DTT to make a stock at the concentration of 1 Unit/ µl and stored at -20°C until used. PEPC, PEPCK and PKA was added in different concentration in different experiments to find the optimum phosphorylation reaction.

In another assay ATP was excluded as a control. Addition of ATP is presumed essential for the activity of protein kinases to catalyse protein phosphorylation. Proteins samples without ATP served as controls. The reaction was started by addition of PEPC *P. queenslandicum*, followed by incubation at 30°C for 4 hours.

The phosphorylation reaction was initiated by adding 1 mM ATP and 20 µl aliquots were withdrawn at the specified times (1 min, 30 min, 1 hour, 2 hours, 3 hours, 4 hours and overnight) The phosphorylation reaction was terminated by adding with equal volume of SDS-sample buffer and heating for 10 min at 75°C. Each aliquot was analysed by 10% SDS-PAGE followed by the Coomassie blue staining (2.5). On another 10 % SDS-PAGE gel, the phosphorylated protein was probed using the Pro-Q® Diamond phosphoprotein stain. In this assay, only the SDS-PAGE gel from method C and D (Table 2.5) was stained with Sypro Ruby for total protein determination. Detail of the small-scale phosphorylation of PEPC is in Table 2.5.

Table 2.5: Small scale screening *in vitro* phosphorylation assay of PEPC from *P. queenslandicum* by PEPCK of *P. queenslandicum* or by Protein Kinase A.

Method	PEPC	PEPCK (1:0.5)	ATP (1 mM)	PKA (100 U)
A (1:0.5)	200 ug/ml	100 ug/ml	1 mM	X
B (1:0.5)	200 ug/ml	100 ug/ml	X	X
C (1:0.5)	50 ug/ml	X	1 mM	25 U
D (1:0.5)	200 ug/ml	X	X	100 U
E (1:0.2)	200 ug/ml	40 ug/ml	1 mM	X
F (1:0.1)	200 ug/ml	20 ug/ml	1 mM	X
G (1:0.01)	200 ug/ml	10 ug/ml	1 mM	X

2.8.2 Large scale *in vitro* phosphorylation of *P. queenslandicum* PEPC.

The reconstituted assay contained phosphorylation buffer (50 mM Tris-HCl pH 8, 20 % glycerol), 5 mM $MgCl_2$, 0.41 mg/ml of PEPC *P. queenslandicum* (total aliquots 6 ml), 200 Units of the catalytic subunit of PKA Catalytic Subunit from bovine heart (Sigma) and 1 mM ATP in a total volume of 7 ml. The phosphorylation reaction was performed at 30°C. The phosphorylation reaction was initiated by the addition of 1 mM ATP and 10 µl aliquots were withdrawn at the specified times (1, 15, 30, 45, 60, 90 and 120 mins) and the phosphorylation assay was terminated by adding with equal volume of SDS-sample buffer, 5 µl of water and heat up for 10 min at 75°C. Each aliquot was analysed in 10 % SDS-PAGE followed by the Coomassie blue staining (2.5). On the other 10 % SDS-PAGE gel, 0 the phosphorylated protein was determined by Pro-Q® Diamond phosphoprotein stain and then SYPRO Ruby staining for total protein determination.

2.8.3 Time course assay of *in vitro* phosphorylation assay of PEPC *P. pygmaeum.*

The reconstituted assay contained phosphorylation buffer (50 mM Tris-HCl pH 8, 20 % glycerol), 5 mM $MgCl_2$, 50 µg/µl of PEPC *P. pygmaeum*, 25 Units of the catalytic subunit of PKA Catalytic Subunit from the bovine heart (Sigma) and 1 mM ATP in a total volume 500 µl. The phosphorylation reaction was performed at 30°C. The phosphorylation reaction was initiated by the addition of 1 mM ATP and 10 µl aliquots were withdrawn at the specified times (1 min, 30 min, 1 hour, 2 hours, 3 hours and 4 hours). The phosphorylation reaction was terminated by addition of an equal volume of SDS-sample buffer with 10 µl of water and then heating for 10 min at 75 °C. Each aliquot was analysed by 10 % SDS-PAGE followed by the Coomassie blue staining (Section 2.5). On another 10% SDS-PAGE gel, phosphorylated protein was determined by Pro-Q® Diamond phosphoprotein stain and then SYPRO Ruby staining for total protein determination.

2.8.4 *In vitro* phosphorylation of PEPC *P. pygmaeum* by different ratios of PEPC to PKA.

Methods were similar to those described in Section 2.10.4, except that the ratio of PEPC *P. pygmaeum* to PKA were 6:1, 12:1 and 30:1. The concentration of PEPC *P. pygmaeum* is 0.297 µg/µl in 4 ml of assay total volume. The phosphoprotein was analyzed by Pro-Q® Diamond staining, SYPRO Ruby staining and Coomassie blue staining. The PEPC *P. pygmaeum* was incubated at 30°C for 2 hours in the presence of 1 mM ATP as indicated above.

2.9 Phosphoprotein analysis by Sodium Dodecyl Sulphate-Polyacrylamide Gel Electrophoresis (SDS-PAGE).

The SDS-PAGE gel was prepared according to the method in section 2.6. Preparation of the sample before loading in the well was also similar but replacing the protein marker with PeppermintStick™ (P33350; Molecular Probes (Eugene, OR, USA)) phosphoprotein molecular weight standards to ensure specific phosphoprotein labelling was achieved. The PeppermintStick™ phosphoprotein molecular weight standard marker contains two phosphorylated (ovalbumin and bovine β–casein) and four non-phosphorylated (β-galactosidase, bovine serum

albumin, avidin, and lysozyme) protein standards. Such protein markers are important to include in any Pro-Q® Diamond phosphoprotein stain-based experiments to exclude false-positive identification by normalising the detected phosphoprotein bands or spots against positive and negative phosphoprotein markers. Gels were run at a constant 10 Amps until the loading dye reached the bottom of the gel.

2.10 Determination of phosphoprotein by using Pro-Q® Diamond phosphoprotein stain.

After electrophoresis, gels were fixed in an aqueous solution containing 50 % (v/v) MeOH and 10 % (v/v) acetic acid for 30 minutes, and then fixed a second time overnight to ensure that all of the SDS is washed out of the gels and to ensure fixation of all proteins in the gel. During the fixation process, gels were incubated at room temperature (RT) with constant shaking on an orbital shaker at a speed of 35-55 rpm. The next day, fixed gels were washed in 100 ml of ultrapure water for 30 min with constant shaking, 3 times to remove all the fixative. The gels were then incubated with 20 ml of Pro-Q® Diamond phosphoprotein gel stain (P33300; Invitrogen™) for 3 hours, protected from light since the stain is light-sensitive. The gels were then de-stainined by immersing them in 100 ml wash solution containing 50 mM of sodium acetate (pH 4.0) buffer with 20 % (v/v) acetonitrile for 30 min, 3 times.

The de-staining process is crucial to reduce the gel background signal and the signal from nonspecific staining. The finel step was to wash the gels with 100 ml ultrapure water for 5 minutes per wash, and this step was repeated two more times. The gels were then visualised. The Pro-Q® Diamond–stained gel image was visualized using the ChemiDoc MP Imaging System (BIO-RAD) using an excitation wavelength of 532–560 nm. All the gels in the above process were incubated at room temperature (RT) with constant shaking on an orbital shaker at a speed of 35 -55 rpm.

2.11 Visualization of fluorescent signals from the Pro-Q® Diamond phosphoprotein stain

The Pro-Q® Diamond–stained gel image was scanned using the ChemiDoc MP Imaging System (BIO-RAD) with 555 nm excitation wavelength and 580 nm emission wavelength. The image was saved in 16-bit TIFF files (Image Gauge Analysis software, Fuji, Stamford, CT). After gel imaging, the gel was directly stained with a total-protein stain, which is SYPRO Ruby protein gel stain. This stain provides a landmark for excising the phosphoproteins for their identification by mass spectrometry and was useful in determining the relative phosphorylation state of a given protein.

2.12 Determination of total protein by SYPRO® Ruby protein gel stain

To confirm equal protein levels per sample, Pro-Q® Diamond stained gels were incubated with SYPRO® Ruby stain (10 ml volume of stain per gel) for overnight protected from light. After overnight staining, the gels were washed with the solution containing 10 % (v/v) MeOH and 7.0 % (v/v) acetic acid for 30 min, 3 times followed by washing twice with ultrapure water for 5 minutes per wash. All the gels in the above process were incubated at room temperature (RT) with constant shaking on an orbital shaker at a speed of 35-55 rpm. The gels were imaged at 450 nm (excitation) and 610 nm (emission) using the ChemiDoc MP Imaging System (BIO-RAD).

2.13 Phosphate affinity electrophoresis of phosphorylated PEPC *P. queenslandicum*

It appeared that the lack of sensitivity of Pro-Q® Diamond staining might have underestimated the amount of phosphorylated proteins in the enriched fractions. In order to assess these phosphoprotein-enriched samples further, *in vitro* phosphorylation of PEPC *P. queenslandicum* and *P. pygmaeum* was detected by using affinity-based Zn^{2+}-Phos-tag$^{(TM)}$ (Wako chemicals Ltd.) polyacrylamide electrophoresis according to the method described by Kinoshita, E. (2006) with modification. The Zn^{2+}-Phos-Tag$^{(TM)}$ acts as a selective phosphate-binding tag molecule and slow down the migration of the phosphorylated protein in an SDS-PAGE compared to the mobility of dephosphorylated protein thus producing two or more separated bands depended on the phosphorylation state of the target protein (Kinoshita, E. 2006).

Several trials were conducted to optimise the conditions of Phos-Tag$^{(TM)}$ gel electrophoresis and improve separation of the phosphorylated and non-phosphorylated protein. Trials including trying various Phos-Tag$^{(TM)}$ concentrations, (5-100 μM), duration of electrophoresis (1-14 hours), and electric current (3-10 Amps). Optimal concentrations of Phos-Tag$^{(TM)}$ to separate these phosphoproteins is 5μM for PEPC *P. queenslandicum* and 10 μM for PEPC *P. pygmaeum.*

2.13.1 Preparation of Phos-tag $^{(TM)}$ SDS-PAGE gel.

Phos-tag $^{(TM)}$ SDS-PAGE was prepared by using a 1-mm-thick, 8-cm-wide and 8-cm-long gel. A separating gel is consisting of 6 % (w/v) of acrylamide, 350 mM of Bis-Tris-base buffer, pH 6.8, 10 μl of TEMED, and 0.05 % APS. Phos-tag $^{(TM)}$ acrylamide (5 μM) and two equivalents of $ZnCl_2$ (50 μM) were added to the separating gel before polymerisation. An acrylamide stock solution was prepared containing an acrylamide and Bis- acrylamide mixture (37.5:1). The stacking gel contains 4.5 % (w/v) of acrylamide, 350 mM of Bis-Tris-base buffer, pH 6.8, 10 μl TEMED, and 0.05 % APS. The running buffer consisted 100 mM MOPS, 100 mM Tris HCl, 0.1 % SDS, pH 7.8 and 5 mM sodium bisulfite ($NaHSO_3$), that latter being added before use from a 1.0 M stock solution.

2.13.2 Sample preparation by protein precipitation.

Since the high concentration of salt in the sample will affect electrophoresis in the Phos-Tag $^{(TM)}$ gel, the protein precipitation is needed in order to give a better separation of a phosphoprotein. Protein precipitation was used in order to concentrate the target protein, decrease the salts concentration and other contaminants such as EDTA, inorganic salts and surfactant since it will affect the electrophoresis bands in the samples. Methanol precipitation was carried out as described in Wessel, et. al., (1984). 90 μl of methanol was added to 10 μl of the sample (PEPC *P. queenslandicum* or *P. pygmaeum*). The samples were mixed and incubated at -20°C overnight. Then the samples were centrifuged for 10 minutes at 13 000 rpm. After centrifugation, the supernatant was slowly removed by using a pipette, leaving a white translucent pellet at the bottom of the Eppendorf tube. The remaining supernatant was left open on the benchtop to dry completely. For acetone precipitation, the method was carried out the same as methanol, except the ratio of protein sample to acetone was 1:4. Finally, precipitated proteins were re-suspended in 20 μl Sample Buffer and heated for 5 minutes at 75 °C.

The gel was run at 5 mA/gel constant current until the Coomassie blue dye reached the bottom of the separating gel. Electrophoresis required 16 hours 30 min for completion.

2.14 Detection of Phosphorylated Protein detection and image analysis.

Staining and visualisation of the gel were performed as described in sections 2.5.

2.15 Determination of phosphorylation site by Mass spectrophotometry.

2.15.1 Mass Spectrophotometer analysis of protein from Phos-tag (TM) gel.

Destaining the Phos-Tag SDS-PAGE gel containing phosphorylated PEPC *P. queenslandicum* from Coomassie Blue staining was performed with 50 % acetonitrile and 50 mM ammonium bicarbonate. Once the stain was fully removed from the gel, the gels were washed and dehydrated with 50 % acetonitrile and 50 mM ammonium bicarbonate. Then 50 mM of Tris (2-carboxyethyl) phosphine (TCEP) was added into the dehydrated gel to reduce Cys residues followed by heating for 20 min at 70°C. 50 mM of iodoacetamide was added to alkylate reduced Cys and then incubated at room temperature in the dark for 30 minutes.

The supernatant was removed, and the protein sample was washed with 100 mM ammonium bicarbonate, followed by another wash with 50 mM ammonium bicarbonate and 50 % acetonitrile, 15 minutes each time. For the third cycle, gels were washed with 200 µl acetonitrile. The supernatant was removed, and the gel pieces were left for 5 minutes to ensure all acetonitrile had evaporated. Finally trypsin digestion was performed on the next day by adding 1 ng/µl of trypsin. The gel pieces were kept on ice until the trypsin solution is absorbed followed by incubating overnight in the oven at 37°C. The next day, the digestion reaction was stopped by adding 100 % acetonitrile and peptides were extracted by adding 50 % of formic acid and acetonitrile. The peptides now ready to be analysed by Mass-spectrometry.

2.15.2 Mass Spectrophotometry analysis of protein from protein precipitation.

Phosphorylated and non-phosphorylated PEPC was precipitated with methanol and acetone (Section 2.13.2) prior to addition of 6 M guanidine hydrochloride. For the reduction process, 1 µl of 50 mM Tris (2-carboxyethyl) phosphine (TCEP) was added followed by incubation on a thermal block for 10 min at 70°C. The samples were cooled down until room temperature and then wrapped with aluminium foil to create a dark environment. 2 µl of 50 mM iodoacetamide (IAA) was added to each sample and incubated at room temperature for 30 minutes while shaking. Trypsin digests were set up as follows. All samples were diluted 10 X by using freshly prepared ammonium bicarbonate buffer. 20 µl of samples were added to 180 µl of ammonium bicarbonate. Prior to adding trypsin, the pH value of samples was determined with pH-indicator strips (pH 8 is required for the digestion process). Then, 10 µl of 0.1 µg/ µl trypsin was added into 20 µg/ µl protein sample. The digests were incubated at 37°C for 4 hours. The digestion was then stopped by 10 % of formic acid until the aliquots reach pH 3. Samples were then stored at -20°C before the further steps. The next step is desalting of the peptide by using C18 micro-spin column. The column was equilibrated with 200 µl of 0.5 % formic acid. The

protein sample was then loaded into the column and wash with 200 µl of 0.5 % formic acid twice. The protein sample was eluted with 70 % of acetonitrile by centrifuge the column for 1 min at 1500 g twice. As the peptides eluted off the column, they now ready to be analysed by Mass-spectrometry.

2.16 Buffers and reagent solution preparation.

L-(–)-Malic acid disodium salt (L-malate) (M9138), malic dehydrogenase porcine heart (MDH) (M-2634), phospho(enol)pyruvic acid trisodium salt hydrate (PEP) and nicotinamide adenine dinucleotide (NADH) were purchased from Sigma (UK).

2.17 PEPC assay design with malate.

PEPC activity was examined by coupling the enzyme to a second enzyme, malate dehydrogenase (MDH). In the assay, PEPC will generate oxaloacetate (OAA) from phosphoenolpyruvate (PEP) and bicarbonate. Then the OAA was converted to malate by malate dehydrogenase (MDH) and NADH. The PEPC assay mixtures contain 5 nM PEPC, 50 mM Tricine-KOH (pH 8), 10 mM $MgCl_2$, 10 mM $KHCO_3$, 0.15 mM NADH and 1 U of malate dehydrogenase (porcine heart) and the indicated concentrations of PEP and L-malate, in a total volume of 150 µL. PEPC activity (NADH consumption rate) was coupled to a NADH-malate dehydrogenase reaction and measured spectroscopically at 340 nm (BMG FLUOstar OPTIMA Microplate Reader) at 25°C.

PEPC activity was expressed as the amount of enzyme extract which catalyzes the transformation of 1 µmol of substrate per minute and per µmolar of protein. Activity values presented are the average of at least three independent measurements. Apparent V_{max} and K_m values were determined from Michaelis-Menten plots over the range of 0.67 to 80 mM PEP for PEPC *P. queenslandicum* and 0.028 to 28 mM PEP for PEPC *P. pygmaeum.* To determine the inhibition constant (K_i) of PEPC, the ranges of malate concentration used as follows: PEPC *P. queenslandicum* (0, 20, 40, 80, 120, 240 mM), PEPC *P. pygmaeum* (0, 2, 6, 12, 30, 60 mM). Experimental data were fitted to the Michaelis-Menten (Equation 1) where $v_i/[E_T]$ is the steady state rate divided by the total enzyme concentration, k_{cat} is the first order rate constant, K_m is the Michaelis constant, and S is the substrate concentration.

For inhibition constant (Equation 2) where *v* is the apparent rate constant, *K* is the uninhibited constant, *I* is the inhibitor concentration, and K_i is the inhibition constant. Kinetic parameters were evaluated by non-linear regression analysis in Igor Pro (Version 7.0.8.1; Wavemetrics Inc., Lake Oswego Orgeon).

$$v_i/[E_T] = \frac{k_{cat} \times [S]}{K_m + [S]} \quad \text{(Equation 1)}$$

$$k^{app} = \frac{k}{1 + [i]/K_i} \quad \text{(Equation 2)}$$

2.18 PEPC assay design with aspartate.

The PEP assay mixture was the same as described above except malate was replaced with aspartate. The ranges of aspartate concentrations used to determine the inhibition constant, K_i were as follows: PEPC *P. queenslandicum* (0, 8, 16, 32, 60, 120 mM), PEPC *P. pygmaeum* (0, 2, 6, 12, 30, 60 mM).

2.19 PEPC Bicarbonate Assay System.

The reaction of PEPC was coupled to malic dehydrogenase (MDH) and the PEPC activity was determined from the NADH oxidation that was measured spectroscopically (Cary 300 Bio) at 340 nm. Precautions were taken to minimize the level of dissolved bicarbonate in the assay mixture, for K_m^{HCO3-} determination. CO_2 was removed from the MiliQ water and the assay buffers by continuously bubbling with N_2 gas for 2 hours before starting the assay. Maintenance of bicarbonate free medium is technically very difficult and almost impossible. After minimising bicarbonate, we measured the residual bicarbonate in the medium and used this average figure to arrive at the actual bicarbonate levels during the assay. The residual bicarbonate in the assay medium was determined, by monitoring NADH oxidation in the absence of any added bicarbonate and was found to be 14.55 µM for Tricine buffer, pH 7.4 and 22.45 µM for Tricine buffer, pH 8.

The assay mixture contained 50 mM Tricine.KOH pH 7.4 or pH 8, 5 mM PEP, 0.01 $U\mu l^{-1}$ MDH, 0.2 mM NADH, 5 mM $MgCl_2$ with total volume of 1.0 ml. The pH was adjusted with freshly prepared NaOH. Twelve $KHCO_3$ concentrations (0.012, 0.021, 0.041, 0.19, 0.28, 0.3, 0.37, 0.5, 1, 2, 5, 10 mM) were used to measure the PEPC-HCO_3^- kinetics. The reaction was initiated with the addition of PEPC enzyme at the concentration 5 nM, and the enzyme rate was measured by the reduction of absorbance of oxidation of NADH at 340 nm. Each PEPC enzyme activity was monitored the absorbance reading until 30 minutes at room temperature.

2.20 PEPC binding properties with 8-anilino-1-naphthalenesulfonic acid (ANS).

2.20.1 Preparation of samples.

8-anilino-1-naphthalenesulfonic acid (ANS) is a fluorescent probe for the characterization of protein binding sites. ANS was dissolved in 50 mM tricine-KOH (pH 8) buffer, and the concentration was determined by absorbance at 350 nm, using ε_{350} = 5000 M^{-1} cm^{-1}. The concentration of PEPC (*P. queenslandicum* and *P. pygmaeum)* in the assay was 0.2 µM. The buffer used for all measurements was 50 mM tricine-KOH (pH 8) with 10 mM $MgCl_2$.

2.20.2 Screening for optimum ANS concentration in malate inhibition.

To find the dissociation constant, (K_d) of PEPC, first, the binding of ANS to the PEPC *P. queenslandicum* was measured by the fluorescence signal upon binding using spectro-fluorometer, (FluoroMax®-3, Jobin Yvon Inc, NJ). Fluorescence of ANS was excited at 370 nm, and emission spectra were recorded between 400 and 650 nm while the temperature was maintained at 25°C. The concentration of ANS was from 100, 200, 300, 400 and 500 µM. Then the fluorescent measurement of PEPC *P. queenslandicum* in the presence of malate was also

carried out in the same manner as described above. The concentration of ANS measured was from 2, 2, 5, 10, 20, 30 µM with the addition of different range concentration of malate. Details of experimental design can be seen in Table 2.6.

Table 2.6: Different range concentration of ANS and malate to determine the binding ability of PEPC *P. queenslandicum*.

	ANS (µM)	Malate (mM)
A	2	0, 1, 2, 4, 6, 8, 10, 12, 14, 16, 18, 20,25, 30, 35, 40, 45, 50
B	5	0, 1, 2, 4, 6, 8, 10, 12, 14, 16, 18, 20,25, 30, 35, 40, 45, 50
C	10	0, 1, 2, 4, 6, 8, 10, 12, 14, 16, 18, 20,25, 30, 35, 40, 45, 50
D	20	0, 1, 2, 4, 6, 8, 10, 12, 14, 16, 18, 20,25, 30, 35, 40, 45, 50
E	30	0, 1, 2, 4, 6, 8, 10, 20, 30, 40, 50
F	100	0, 1, 2, 4, 6, 8, 10, 12, 14, 16, 18, 20, 30, 40, 50, 60, 70, 80, 90, 100

2.20.3 Fluorescent measurement phosphorylated and non-phosphorylated PEPC *P. queenslandicum* with ANS.

The results obtained by ANS concentration screening shows that ANS at the concentration of 10, 20 and 30 µM gave optimum fluorescence intensity (FI) on binding the PEPC. So, for the next experiment, these three concentrations were applied to determine the binding ability of non-phosphorylated and phosphorylated PEPC to ANS in the presence of malate with the same method as described above (2.20.2). Details of experimental design can be referred to in Table 2.7

Table 2.7: Different range concentration of ANS and malate to determine the binding ability of PEPC *P. queenslandicum*.

	PEPC	Malate (mM)	ANS (µM)
A	Non-phosphorylated *P. queenslandicum*	0, 0.05, 0.1,0.25, 0.5, 0.75 ,1, 2, 4, 6, 8, 10, 15, 20	10
B	Phosphorylated *P. queenslandicum*	0, 0.05, 0.1,0.25, 0.5, 0.75 ,1, 2, 4, 6, 8, 10, 15, 20	10
C	Non-phosphorylated *P. queenslandicum*	0, 0.05, 0.1,0.25, 0.5, 0.75 ,1, 2, 4, 6, 8, 10, 15, 20	20
D	Phosphorylated *P. queenslandicum*	0, 0.05, 0.1,0.25, 0.5, 0.75 ,1, 2, 4, 6, 8, 10, 15, 20	20
E	Non-phosphorylated *P. queenslandicum*	0, 0.05, 0.1,0.25, 0.5, 0.75 ,1, 2, 4, 6, 8, 10, 15, 20	30
F	Phosphorylated *P. queenslandicum*	0, 0.05, 0.1,0.25, 0.5, 0.75 ,1, 2, 4, 6, 8, 10, 15, 20	30

2.20.4 Fluorescent measurement of phosphorylated and non-phosphorylated PEPC *P. pygmaeum* with ANS.

The binding ability of non-phosphorylated and phosphorylated PEPC *P. pygmaeum* to 30 μM ANS in the presence of malate with the same method as described above (2.24.2). The range concentration of malate is from 0.05 to 40 mM.

CHAPTER 3

PEPCK PROTEIN EXPRESSION, PURIFICATION AND APPLICATION OF NusA TAG

3.1 Introduction

In plants, PEPCK exists at a much lower concentration than PEPC, which makes it challenging to purify from the native organism. To overcome such an obstacle, many studies include molecular cloning, over-expression, and purification of PEPCK in an active soluble protein have been performed. The PEPCK gene had previously been cloned from *Arabidopsis thaliana* (Fontaine, V., et. al., 2002) and *Kalanchoë fedtschenkoi* (Hartwell, J., et. al., 1999). However, it was overexpressed almost entirely in the inclusion bodies, which were insoluble protein aggregates that made the protein inactive. Thus, the protein must be refolded to its correct three-dimensional conformation in order to make it biologically active (Davis, G. D., et. al., 1999).

One previous study has described the over-expression of soluble PEPCK in the form of a PEPCK-NusA fusion protein (Ermolova, N. V., et. al., 2003). NusA is a bacterial transcription factor that promotes RNA polymerase to pause on some RNA motifs. Pauses in the RNA polymerase activity will decelerate the transcription (Kosobokova, E. N., et. al., 2016). Transcription and translation of the bacterial cells are coupled; therefore, inhibition or deceleration of transcription also results in decelerating translation. Thus, the synthesised amino acid chain was folded more slowly, which allowed more time for the protein to fold correctly and prevent the production of aggregations (Davis, G. D., et. al., 1999).

NusA does not have an intrinsic affinity property, thus it is necessary to add an affinity tag like a His-tag in the expression vector to produce the fusion protein with an affinity binding property. NusA will stabilise the passenger protein during translation, whereas the His-tag enables the affinity purification of the target protein. The NusA tag can be removed by the digestion method with thrombin or enterokinase since the expression vector pET-44a(+) contains a thrombin and enterokinase cleavage site between the NusA tag and the target protein gene.

To improve the expression and induction of target protein, different expression variables have been tested which included 1) expression host strain (BL21 DE3, Rosetta), 2) culture media (LB, 2YT, Auto-induction), 3) differing IPTG concentration, and 4) temperature and duration of induction. The application of the pET-44a(+) as a cloning vector in this present study will allow the over-expression of *Panicum queenslandicum*'s PEPCK gene as a NusA fusion protein and hopefully provide a soluble protein kinase.

3.2 Cloning the PEPCK gene.

The polymerase chain reaction (PCR) is a conventional method to amplify a template strand for gene cloning. At the end of the PCR reaction, the specific sequence will be accumulated in billions of copies. PCR is often used to

amplify the genes of interest from the plasmid templates and to introduce the appropriate restriction sites (Baneyx, F. 1999).

The pET-44a(+) vector was used in this study as it encoded an *N*-terminal NusA Tag /His Tag /S Tag fusion sequence followed by thrombin and enterokinase cleavage sites, (shown in detail in Figure 2.1; Chapter 2). After the restriction digestion procedure with BamHI-HF and Xho1 (New England, BioLabs), the insert of DNA was then purified with the QIAquick PCR Purification Kit (QIAGEN). The insert containing the PEPCK gene was then ligated into the corresponding sites of the pET-44a(+) vector before it was transformed into DH5 Alpha™ competent cells.

After overnight incubation, ninety-three colonies were observed on the LB plate and thirty-three colonies were screened, with up to 80% of them were found to be positive. After subjected to PCR, the size fragments of thirty-three colonies were identified by the visualisation of the agarose gel image. From figure 3.1, it can be seen that colonies 4, 9, and 14 have the correct size fragment. From the sequencing results, the colony 4, 9, and 14 showed the correct sequence.

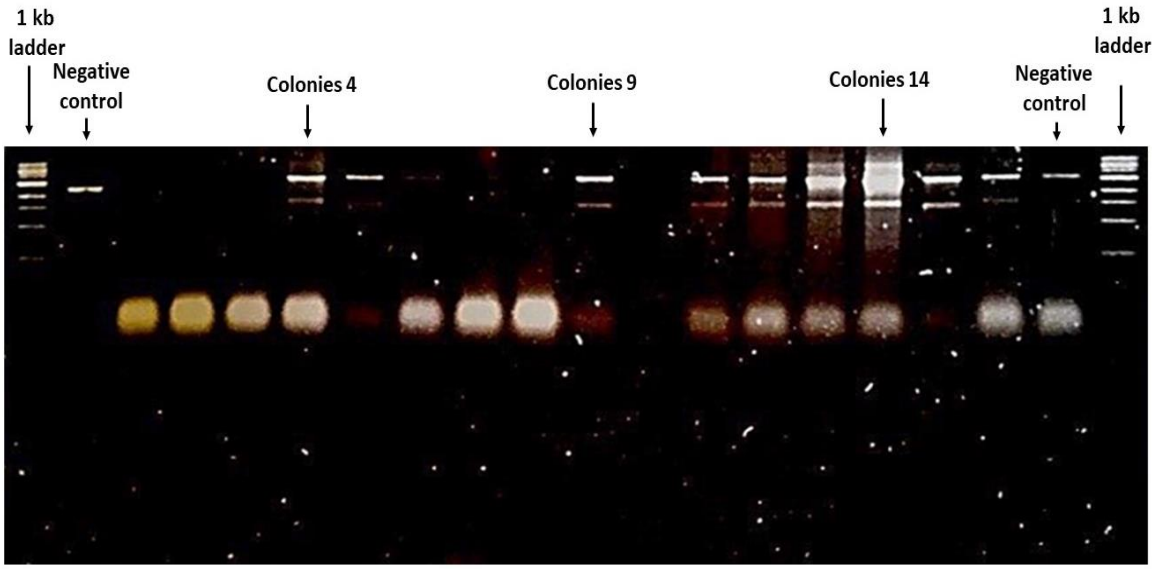

Figure 3.1: First and the last lane is 1 kb ladder (NEB). The second lane is a negative expression control (PCK with pET-44a/ containing pET-44a vector only). Colonies 4, 9 and 14 (arrows) were selected for mini prep and send to sequenced with PEPCK primers.

3.3 PEPCK-NusA over-expression and induction.

Transformed bacteria containing the PEPCK gene were cultured in LB medium and incubated at 37°C until the absorbance reading reached approximately 0.5-0.6 at 600 nm (A_{600}). The expression of the fusion protein was induced by 0.5 mM IPTG and followed by further growth at a temperature of 18°C for eighteen hours. The cell pellet was then stored at a temperature of -80°C.

The NusA-PEPCK culture medium was incubated at a temperature of 18°C, since a lower temperature was suggested to improve the protein folding and produce a soluble target protein (Kohl, T., et. al., 2008 and Korf, U., et. al., 2005). To determine whether the fusion protein was expressed or not, bacterial cell cultures that were either not induced (lane B) or induced (0.5 mM IPTG, Lane C) were compared with SDS-PAGE (Figure 3.2). The SDS-PAGE gel showed the expression of the fusion protein (arrow) near the band of 97 kDa marker protein, which was close to the size of the fusion protein. The ca. 37 kDa PEPCK protein was expressed as a fusion with ca. 57 kDa NusA, thus rendered the total size of this fusion protein ca. 92 kDa.

For purification, the protein pellet was re-suspended and lysed by ultrasonication before it was centrifuged and filtered. These methods disrupted the cells and released the soluble fusion protein into the resuspension buffer. Ultrasonication is a cell disintegration technique that can be applied for different cell suspension samples. It applies micro-scale high-pressure sound waves, shear forces, and cavitation to disrupt the cells and get rid of insoluble particles before extracting out the target protein (Scopes, R. K. 2013). Since bacterial cells contain a different type of protease, the addition of an inhibitor such as Pefabloc®SC can protect the target protein from degradation during the isolation and purification stages.

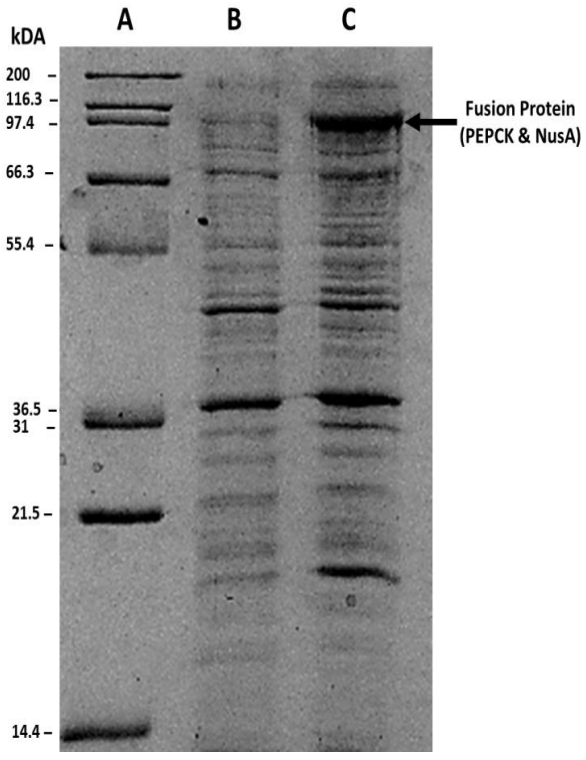

Figure 3.2: Over-expression of PEPCK as fusion protein to NusA; Lane A: Protein molecular weight marker; Lane B: Total crude extract before induction with 0.5 mM IPTG (200 µl of cell pellet was re-suspended in 100 µl of 2 X sample buffer, incubate at 75°C for 10 min, and 20 µl of the supernatant fluid was loaded; Lane C: Total crude extract after 18 hours induction at 18°C (sample was prepared and loaded as for non-induced cells).

3.4 Affinity purification of the His_6-NusA-PEPCK fusion protein.

The HisTrap™ High-Performance column was prepacked with Ni Sepharose 6 Fast Flow, which consists of highly cross-linked agarose beads with an immobilized chelating group. The medium was charged with Ni^{2+} ions. Ni Sepharose 6 HP can selectively bind with proteins if suitable complex-forming amino acid residues are exposed to the protein surface. Additional histidine such as histidine-tag increases the affinity of Ni^{2+}, which make the histidine-tagged protein the most potent binder as compared to other proteins like an *E. coli* extract. Using the HisTrap™ HP affinity column, the fusion protein was purified. From the analysis of the purified fusion protein on 10 % SDS-PAGE, it was revealed that a fusion protein band was located at around 100 kDa (Fig. 3.4; lane G) with a few contaminants. The next steps were buffer exchange from Elution buffer (400 mM imidazole) into Thrombin Cleavage Buffer (TCB) 20 mM of Tris-HCl, pH 8.4.

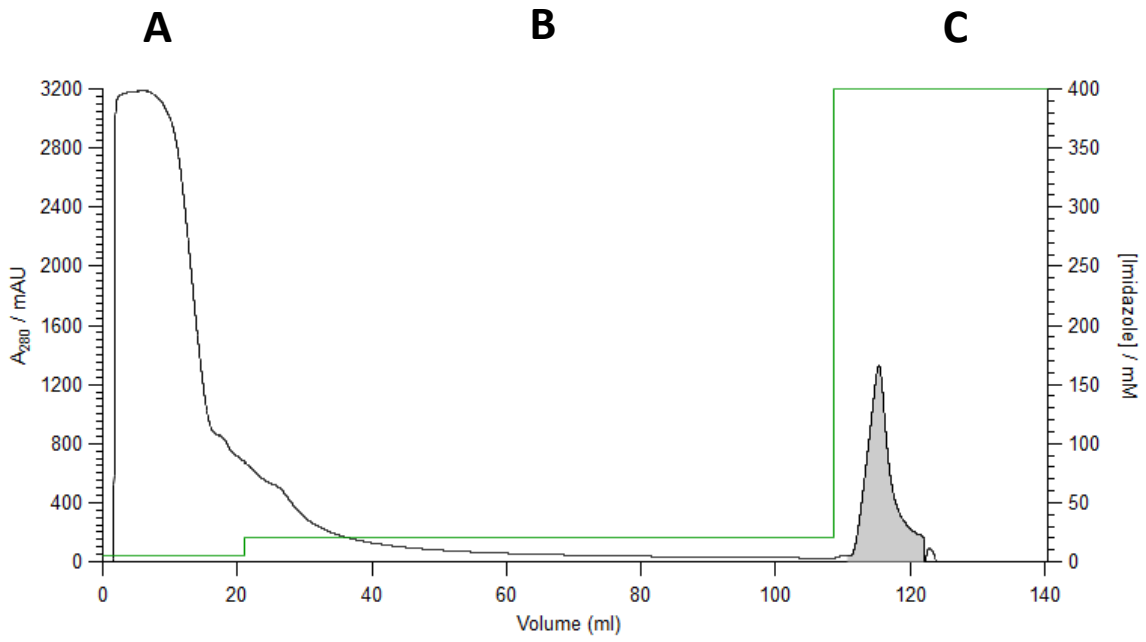

Figure 3.3: Purification of fusion protein (PEPCK-NusA) by using Ni-NTA column (HisTrap™ HP) on an AKTA. (A) The sample was loaded into column at the flow rate 1ml per min. (B) The column was washed with 20 mM imidazole. (C) The fusion protein was eluted with 400 mM imidazole. The fractions were pooled and subjected to SDS-PAGE to determine the level of purity, and then quantified by the Bradford method.

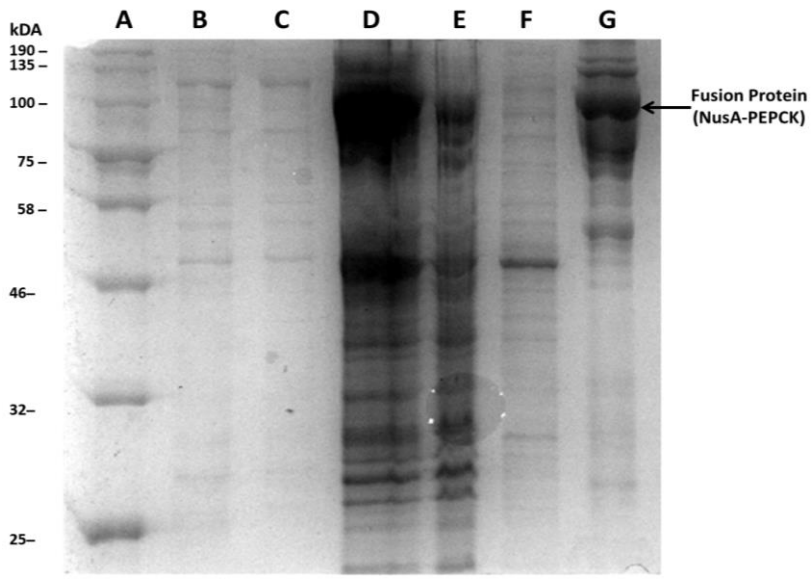

Figure 3.4: SDS-PAGE analysis of NusA-PECK fusion protein purification by HisTrap™ HP column. The fusion protein was over-expressed in Rosetta with 50 µg/ml of ampicillin and 34 µg/ml chloramphenicol, induced by 1 mM IPTG at 18°C for 18 hours. Lane A: Protein molecular weight marker; Lane B: Induced with 0.5 mM IPTG; Lane C: Cell lysate; Lane D: Supernatant from centrifugation; Lane E: Supernatant flow through from HisTrap™ HP column; Lane F: Flow through of wash buffer, 25 mM imidazole; Lane G: Fusion protein eluted from 400 mM imidazole.

3.5 Changing buffer of fusion protein aliquot by desalting column, containing Sephadex G-25 medium.

The desalting column was packed with Sephadex G-25 medium, a gel filtration product that separates molecules based on the molecular size. Desalting columns were used for buffer exchange and removal of small contaminant molecules from pure proteins. Small molecules like salt, free labels, and other impurities can be separated efficiently from the high molecular weight substances of interest. The chromatography technique used was gel filtration and the molecules can be separated based on the differences in molecular size. Molecules larger than the largest pores in the Sephadex matrix were excluded from the matrix and were eluted first, in or just after the void volume. The void volume is the column volume outside the Sephadex matrix. Molecules smaller than the largest pores in the Sephadex matrix will penetrate the pores to a varying extent. They have a higher accessible column volume than the large molecules. Thus, the small molecules will elute out of the column after the large molecules and just before one total column volume of the buffer passed through the column. From the automatic absorbance monitor of the ÄKTA, five fractions (a total volume of 5 ml) of the fusion protein were pooled from the column. This material was then loaded onto the HisTrap™ Fast Flow column equilibrated with thrombin cleavage buffer at a pH of 8.4 (20 mM Tris-HCl, 150 mM NaCl, and 2 % glycerol).

Removal of imidazole by desalting column containing Sephadex G-25 medium

Since the purified fusion protein was eluted in an elution buffer with a high concentration of imidazole (400 mM) that can inhibit the thrombin cleavage reaction, It is essential to transfer the fusion protein mixture into a buffer without imidazole. Thus, the fusion protein was buffer exchanged into a thrombin cleavage buffer at a pH of 8.4

(20 mM of Tris-HCl, 150 mM of NaCl, 2 % of glycerol) with a desalting column that contains Sephadex G-25 medium. The column was equilibrated with 200 ml (10 CV) of thrombin cleavage buffer before the addition of five ml of the purified fusion protein to the equilibrated column. Five fractions with a total volume of 5 ml were collected from the column and the protein contents obtained were pooled and analyzed by the Bradford method (Chapter 2; Section 2.7.3).

3.6 Small scale cleavage reactions of NusA-PEPCK with thrombin in solution

NusA not only can promote the solubility of aggregation-prone passenger proteins, but it also changes the target protein conformation (De Marco, V., et. al., 2004). Thus, the removal of the NusA tag from the protein is crucial to produce PEPCK in the form of a native, biologically active protein. From a preliminary digestion trial, it was demonstrated that the 1 U of thrombin was able to cleave NusA from the PEPCK in 1 mg of the fusion protein (NusA-PEPCK).

These results demonstrated that similar levels of PEPCK cleavage from the NusA tag can be obtained with the concentration of thrombin up to 10 U. The rate of cleavage reaction was unaffected by the duration of incubation from 2 hours to 19 hours under room temperature. This is because all the fusion protein was cleaved at all periods. In the next experiment, a large-scale cleavage reaction was performed. Instead of room temperature, 1 U of thrombin was applied to cleave 1 mg of fusion protein under an incubation temperature of 4°C to avoid protein degradation.

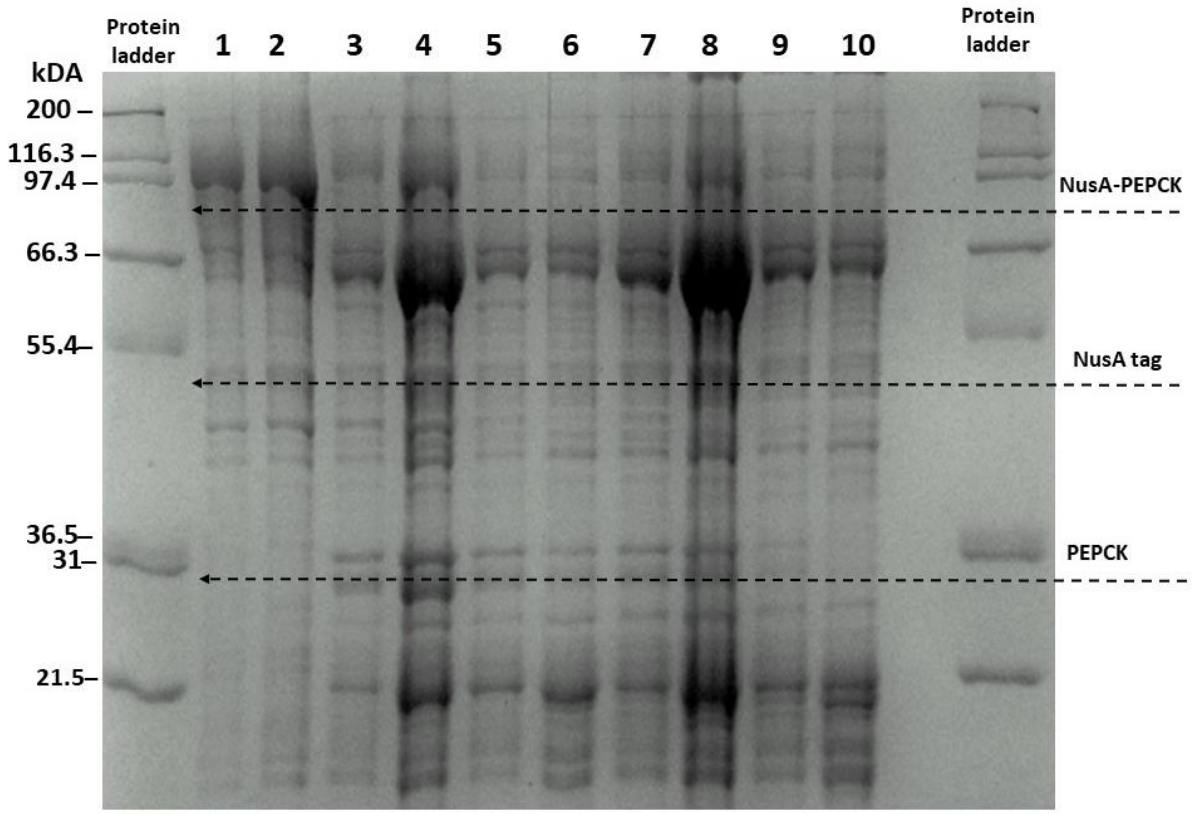

Figure 3.5: SDS-PAGE analysis of small-scale thrombin cleavage reactions with PEPCK-NusA fusion protein. Each aliquot contains 50 µg/ml of purified PEPCK-NusA fusion protein and varying amount of thrombin. The aliquots were incubated at room temperature for 16 hours with agitation. Lane 1: Fusion protein in elution buffer; Lane 2: Fusion protein in thrombin cleavage buffer. Lane 3: 1U of thrombin/mg of protein, 2hrs of incubation. Lane 4; 1U of thrombin/mg of protein, 4hrs of incubation. Lane 5; 1U of thrombin/mg of protein, 6hrs of incubation. Lane 6; 1U of thrombin/ mg of protein, 19 hrs of incubation. Lane 7; 10U of thrombin/ mg of protein, 2hrs of incubation. Lane 8; 10 U of thrombin/ mg of protein, 4hrs of incubation. Lane 9; 10U of thrombin/ mg of protein, 6hrs of incubation. Lane 10; 1U of thrombin/ mg of protein, 19hrs of incubation.

3.7. On-Column cleavage of fusion proteins with thrombin and purification of PEPCK from NusA tag.

On-column thrombin cleavage (Chapter 2; Section 2.3.6) was applied to remove the NusA tag from the target protein. As a result, it can be seen from Figure 3.6, lane K (arrow) the untagged protein was eluted from the wash buffer flow and it was free from the NusA tag. However, a secondary band was detected. This could be due to the presence of a contaminant that has an affinity for nickel ions almost the same as the target protein or could be due to the degradation of a cleavage product after prolonged incubation with thrombin.

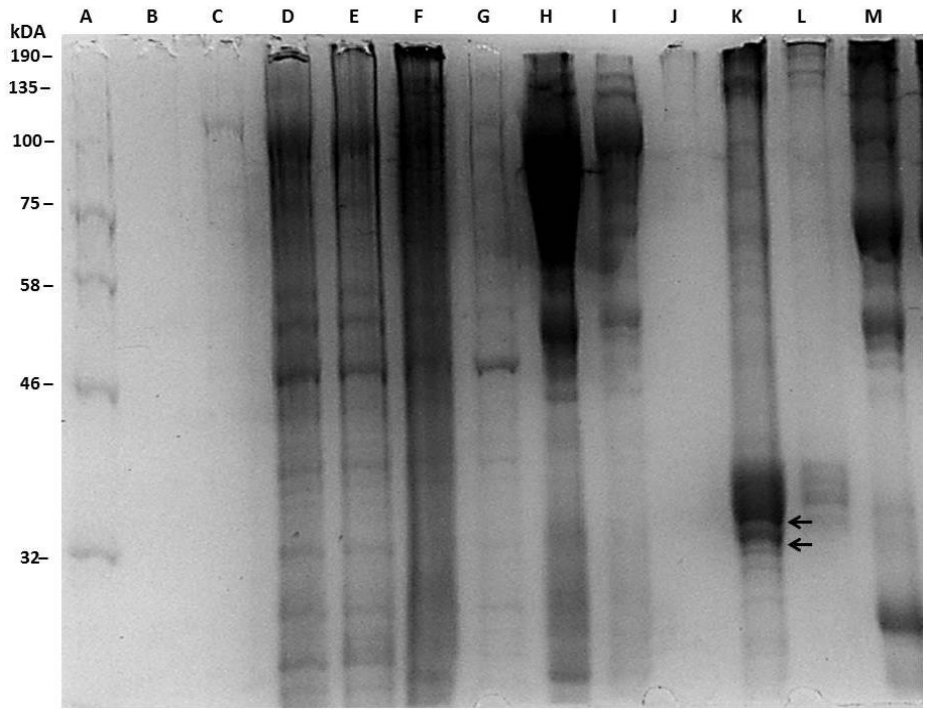

Figure 3.6: Expression and purification of PEPCK by HisTrap column; Lane A: Protein molecular weight marker; Lane B: Total crude extract before induction with 0.5 mM IPTG; Lane C: Total crude extract after 18 hours induction at 18°C; Lane D: Crude lysate ; Lane E: Lysate after sonication; Lane F: Flow-through of the supernatant; Lane G: Flow-through from wash buffer, 20 mM imidazole; Lane H and I: Fusion protein eluted from 400 mM imidazole; Lane J: Flow-through of the fusion protein after subjection to the column; Lane K and L: PEPCK (arrow) was detected in the flow through of wash buffer 20 mM imidazole, after overnight digestion with thrombin ; Lane M: Uncleaved fusion protein and NusA eluted from elution buffer, 400 mM imidazole.

From Figure 3.6, Lane K revealed two prominent bands that corresponded to the fusion protein/non-cleaved protein (94 kDa) and NusA tag (60 kDa). Such a result suggested that the un-optimised digestion condition of the fusion protein has caused the incomplete thrombin cleavage activity. It is widely reported that the efficiency of thrombin digestion may vary with different types of protein and tags (Hefti, M. H., et. al., 2001). Further optimisation of the reaction conditions is required to ensure complete cleavage of the NusA tag from the target protein. Jenny, R. J., et. al., (2003) suggested that the pH should be between 7.0 and 8.0 and the ionic strength equivalent should be between 0.1 and 0.15 M NaCl. The optimum ratio of enzyme to the substrate is also crucial for complete cleavage of NuSa tag from the fusion protein. The digestion rate can be improved by increasing the reaction temperature up to 37°C. However, the digestion temperature in this work was kept at 4°C since the target protein is easily degraded at high temperatures. With a lower digestion temperature, the reactions were performed overnight or for more than 16 hours for better digestion performance. On-column cleavage was used because many potential contaminants can be removed easily from the column and hence the target protein can be obtained with a higher level of purity.

3.8 Small scale of NusA-PEPCK cleavage with enterokinase.

Apart from thrombin, the NusA tag can be removed by digestion with enterokinase as the expression vector pET-44a(+) contains an enterokinase cleavage site located in between the NusA tag and the target protein gene. Enterokinase specifically recognises a five-amino-acid polypeptide (D-D-D-D-K-X1) and cleaves at the carboxyl site of lysine. The molecular weight of the light-chain of enterokinase is 26.3 kDa (Terpe, K. 2003). Enterokinase exhibits high activity over a broad range of pH and can work in the presence of denaturants and detergents (Racie, L.A.C., et. al., 1995).

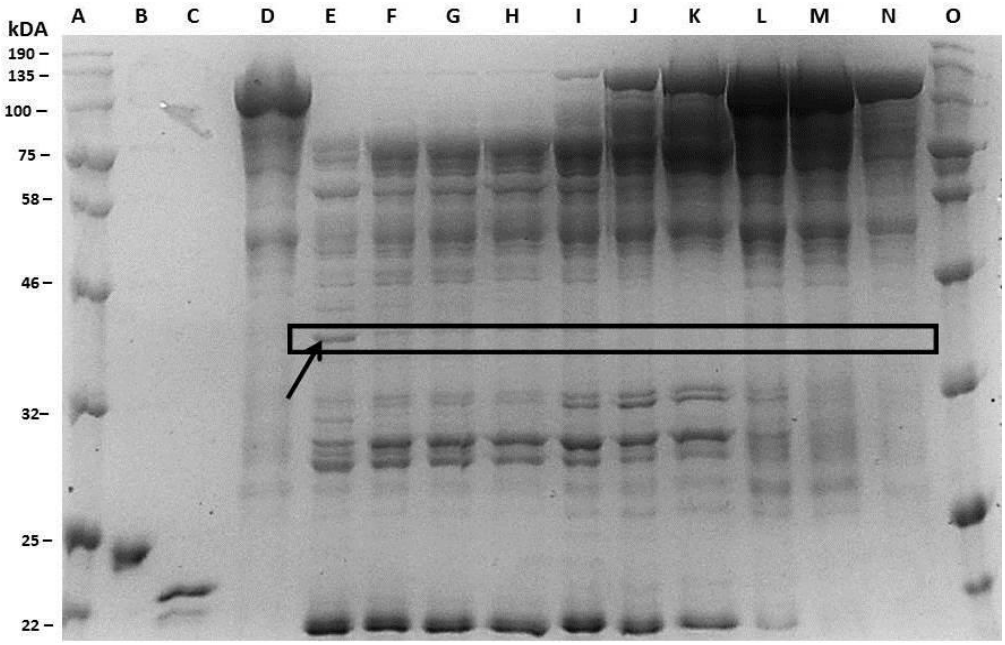

Figure 3.7: Enterokinase cleavage reactions with each aliquot contain 50 µg of purified PEPCK-NusA fusion protein and varying amount of enterokinase. The 50 µl of aliquots were incubated at 22°C for 16 hours and analysed on a Coomassie-stained SDS-PAGE (10%) without any purification with column. Lane A and O: Protein molecular weight marker; Lane B: Control protein (from company) without addition of enterokinase; Lane C: Control protein incubate with 10 U of enterokinase; Lane D: Fusion protein; without addition of enterokinase. Units of enzyme loaded per reaction is listed as follows: Lane E: 10 U; Lane F: 8U; Lane G: 6U; Lane H; 4U: Lane I; 2U: Lane J; 1U: Lane K: 0.1 U; Lane L: 0.01 U; Lane M: 1X 10^{-3}U; Lane N: 0 U. PEPCK. Box area enclosed the PEPCK (arrow).

As seen in Figure 3.7, almost all fusion proteins were cleaved between 4 U of enterokinase (Lane H) and 10 U (Lane E, F, G) but PEPCK was only detected at 10 U of enterokinase (Lane E, arrow). The intensity of the protein band was quite low, which indicated a small yield of PEPCK. No PEPCK was detected at 8, 6, or 4 U when enterokinase was applied. These results suggest that the enterokinase did not cleave the specific site of the Nusa and PEPCK. For the next stage, only thrombin was applied to cleave the Nusa from the PEPCK since thrombin demonstrated more efficient in cleaving the NusA tag from the fusion protein than enterokinase.

3.9 Difficulties in obtaining high amounts of PEPCK from thrombin cleavage reaction.

From the results, the yields of the fusion protein, NusA-PEPCK, target protein, and PEPCK from IMAC purification were found to be decreased under the over-expression and induction conditions as described. Thus, a screening of over-expression, induction, and purification conditions was performed to improve the yield of PEPCK. In this method, besides LB, two additional growth media include 2YT and autoinduction media were used. The inducer (IPTG) was used at two different concentrations (0.5 mM and 1.0 mM) to obtain an efficient concentration for protein induction. The duration of induction was 18 hours and 24 hours (Table 3.1). Once the fusion protein was induced, it was then purified by different methods (Table 3.2). After the NusA was removed by thrombin, the availability of PEPCK was recorded and tabulated in Table 3.3.

In general, except for method A (Table 3.1), no PEPCK was recovered after Ni-NTA purification of the products of the thrombin cleavage reaction. Therefore, it was impossible to yield any purified PEPCK protein despite a reasonable amount of soluble recombinant proteins was detected in the cell lysate and supernatant after the IPTG induction.

The amount of purified NusA-PEPCK obtained was very little from method B (Table 3.1) with thrombin cleavage reaction for 2 hours at 4°C. In method C (Table 3.1), no PEPCK was eluted from the column after the thrombin cleavage reaction was performed at 4°C for overnight. For method E and F (Table 3.1), the fusion protein in *Rosetta* was over-expressed. There was no purified fusion protein eluted from the Ni-NTA column, although the analysis results from SDS-PAGE showed that it was overexpressed in the lysate of medium culture. The condition details of methods B - G can be referred to the Appendix, section E.

Method A; A low amount of PEPCK was produced from over-expression in LB, BL21 DE3 host strain with 0.5 mM IPTG.

Followed by the addition of 2.27 U of thrombin, the concentration of purified fusion protein obtained was 2.27 mg/ml. The cleavage reaction was performed in the solution under room temperature for 2 hours. After two hours, the cleaved PEPCK was purified by Ni-NTA column and eluted with 20 mM imidazole and 25 mM Tris-HCl buffer. Next, the purified PEPCK was concentrated up to six-fold to obtain a visible band in the SDS-PAGE gel (arrow, Fig. 3.8). Several non-specific cleavage products can also be observed at Lane 1 (Fig. 3.8). The figure shows the uncleaved fusion protein, the NusA tag that was cleaved off, and the purified PEPCK. The size of PEPCK (37 kDA) fused to a NusA (55 kDA) was estimated to be 92 kDA approximately. At the step where NusA-PEPCK was cleaved, the yield of PEPCK was observed to be decreased.

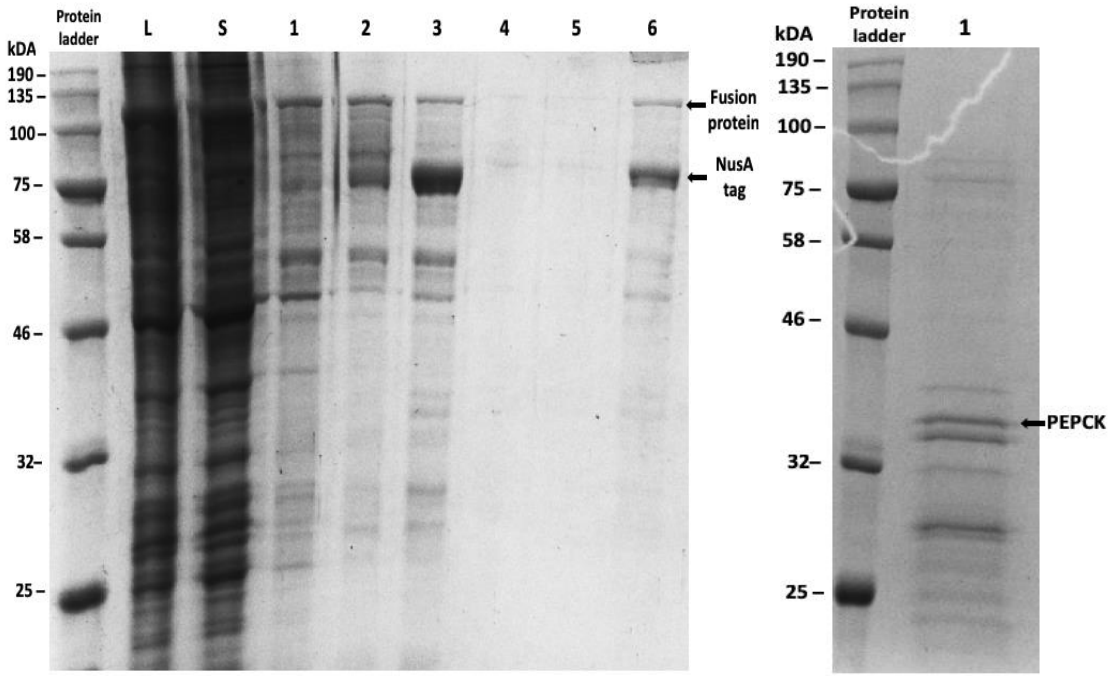

Fig. 3.8: SDS-PAGE analysis of PECK-NusA fusion protein purification by HisTrap™ HP column. The fusion protein was over-expressed in BL21-DE3 with 50 µg/ml of ampicillin and induced by 0.5 mM IPTG at 18°C for 18 hours. Lane L; Lysate after French press. Lane S; Supernatant from centrifugation of the lysate. Lane 1; Flow through of wash buffer, 50 mM imidazole. Lane 2; Fusion protein eluted from 400 mM Imidazole. Lane 3; Solution mixture of fusion protein with thrombin before loaded into the column. Lane 4; Supernatant flow through from column. Lane 5; Flow through from wash buffer, 20 mM imidazole. Lane 6; Uncleaved fusion protein from 400 mM imidazole. PEPC was detected as double band (arrow, Lane 1).

Table 3.1: Overexpression conditions of fusion protein (PEPCK-NusA) in LB, 2YT or autoinduction media with over-expression in BL21 DE3 or Rosetta host strain with IPTG.

Host strain	BL21-DE3			Rosetta		
Time of incubation	18 hrs	24 hrs	48 hrs	18 hrs	24 hrs	48 hrs
IPTG (mM)	0.5	1.0		0.5	1.0	
LB Media	A	G		E and F		
2YT Media					C	
Autoinduction Media			D			B

Table 3.2: The availability of NusA-PEPCK from the purification by using Ni-NTA column in different induction condition. All methods were using the same concentration imidazole in binding buffer (20 mM) and Elution buffer (400 mM).

Overexpression condition	Wash buffer Imidazole (mM)	The availability of NusA-PEPCK after purification
A	50 mM	NusA-PEPCK was successfully purified (2.27 mg/ml)
B	50, 150 mM	Very low yield of NusA-PEPCK was purified.
C	50, 150 mM	Only one ml of NusA-PEPCK was purified
D	50, 150 mM	Very low yield of PEPCK-NusA was purified.
E	50 mM	No NusA-PEPCK was detected
F	50mM	No NusA-PEPCK was detected
G	50 mM	No NusA-PEPCK was detected

Table 3.3: The availability of PEPCK from the purification by using Ni-NTA column after thrombin cleavage reaction.

Overexpression condition	Buffer exchange method	Cleavage reaction condition	The availability of PEPCK- after cleavage reaction with thrombin
A	Dialysis	In solution, RT for 2 hours	PEPCK was purified but in a low volume (500 µl).
B	Desalting column	In solution, RT for 2 hours	No PEPCK was detected
C	Desalting column	On-column, 4°C for, overnight	No PEPCK was detected
D	Desalting column	On-column, 4°C for, overnight	No PEPCK was detected
E	Dialysis	In solution, RT for 2 hours	No PEPCK was detected
F	Dialysis	On-column, 4°C for, overnight	No PEPCK was detected

3.10 Small-scale induction PEPCK without NusA in LB media.

Instead of conducting an over-expression, induction, and purification of PEPCK from NusA-PEPCK fusion protein, other methods were applied to obtain an expression of active high yield of PEPCK. An alternative strategy to induce high-level expression was to express the PEPCK as a single protein, without protein carrier, and NusA in the vector pET 100/D-TOPO.

The first preliminary overexpression tests were carried out on a small scale culture (Table 3.4). The bacteria were grown in an LB media at 18°C for 18 hours before it was induced with different concentrations of IPTG. From the analysis by 10 % SDS-PAGE gel, an inefficient overexpression (arrow, Fig. 3.9) was obtained from the transformation of Rosetta cells. In BL21 (DE3), this analysis showed that the possibility that PEPCK can be induced (arrow in Fig. 3.10). However, there was no difference in the protein expression for both strains when IPTG was increased from 0.25 mM to 1.5 mM.

Table 3.4: The first preliminary small scale induction of PEPCK from pET 100 plasmid.

Host strain	BL21-DE3				Rosetta			
Induction temperature	18°C				18°C			
Period of incubation	18 hrs				18 hrs			
IPTG (mM)	0.25	0.5	1.0	1.5	0.25	0.5	1.0	1.5

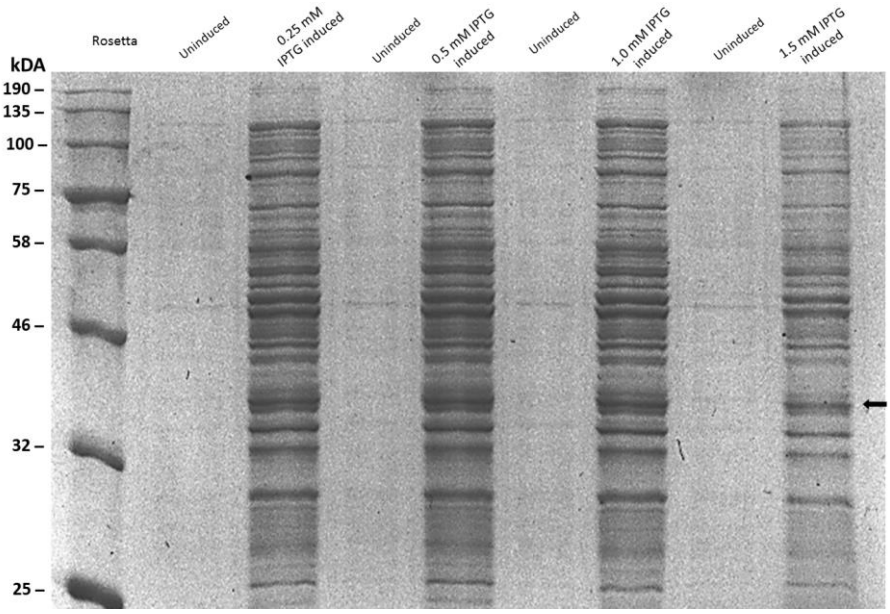

Fig. 3.9: SDS-PAGE analysis of small scale induction of PEPCK in pET 100/D-TOPO constructs, overexpress in Rosetta at different concentrations of IPTG, incubate for 18 hours at 18°C. IPTG was added at different range of final concentration (0.25 mM, 0.5 mM, 1.0 mM, 1.5 mM) as inducer.

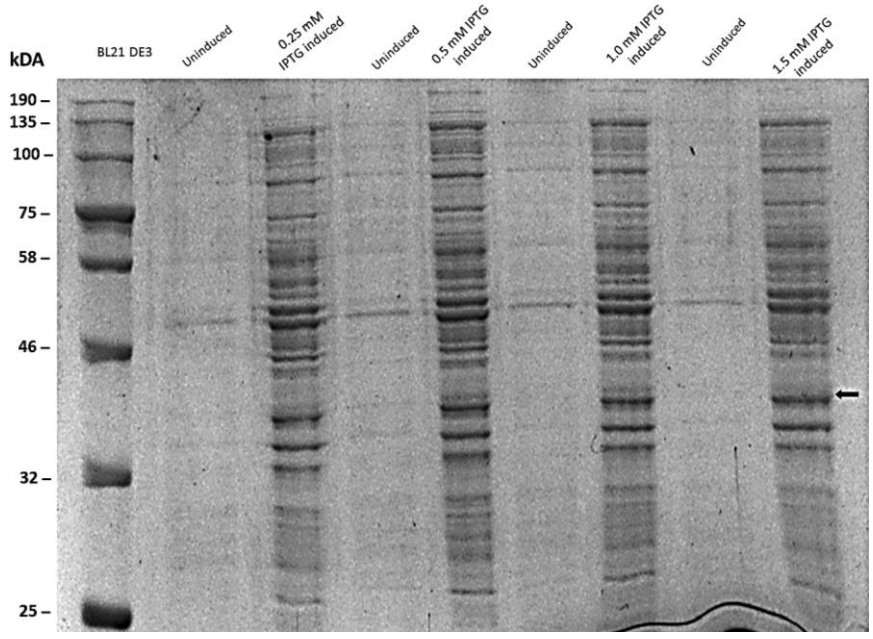

Fig. 3.10: SDS-PAGE analysis of small scales induction of PEPCK in pET 100/D-TOPO constructs, overexpress in BL21 DE3 at different concentrations of IPTG, incubate for 18 hours at 18°C**.** IPTG was added at different range of final concentration (0.25 mM, 0.5 mM, 1.0 mM, 1.5 mM) as inducer.

Small-scale (25 ml) cultures contain adequate material for rapid comparison of protein induction. The bacterial lysate from non-induced culture (without adding IPTG) and induced culture (adding IPTG) were analysed by SDS-PAGE to estimate the expression level of the target protein. From Figure 3.9 and 3.10 (arrow), PEPCK can be induced at all concentrations of IPTG in either Rosetta or BL 21 (DE3) cells under similar induction levels. Hence, only two concentrations of IPTG (0.5 mM and 1.0 mM IPTG) were applied with different host strains and induction temperatures for the next induction screening (Table 3.5).

In this second small-scale overexpression trial, PEPCK was induced under the same induction conditions as the first attempt (Table 3.4). However, it was conducted for a longer period. When the fusion protein NusA-PEPCK was induced with 0.5 mM IPTG, it was sufficient to induce the fusion protein. It is envisaged that a higher concentration of IPTG will increase the level of PEPCK induction. The methods for the second small scale screening are summarised in Table 3.5.

Table 3.5: The second preliminary small-scale induction of PEPCK from pET 100/D-TOPO

Host strain	Rosetta					BL21 DE3				
Induction temperature	20 °C		15 °C			20 °C		15 °C		
Period of incubation	18	24	18	24		18	24	18	24	
IPTG (mM)	0.5	0.5	0.5	0.5	1.0	0.5	0.5	0.5	0.5	1.0
Method	A1	A2	A3	A4	A5	B1	B2	B3	B4	B5

From the SDS-PAGE analysis (arrows of Fig. 3.11, 3.12 and 3.13) it can be concluded that PEPCK can be induced from Rosetta or BL21 DE3 host strain, with the concentration of IPTG were 0.5 or 1 mM at 15°C or 20°C. Incubation as long as 18 or 24 hrs seem to have the same level of protein induction.

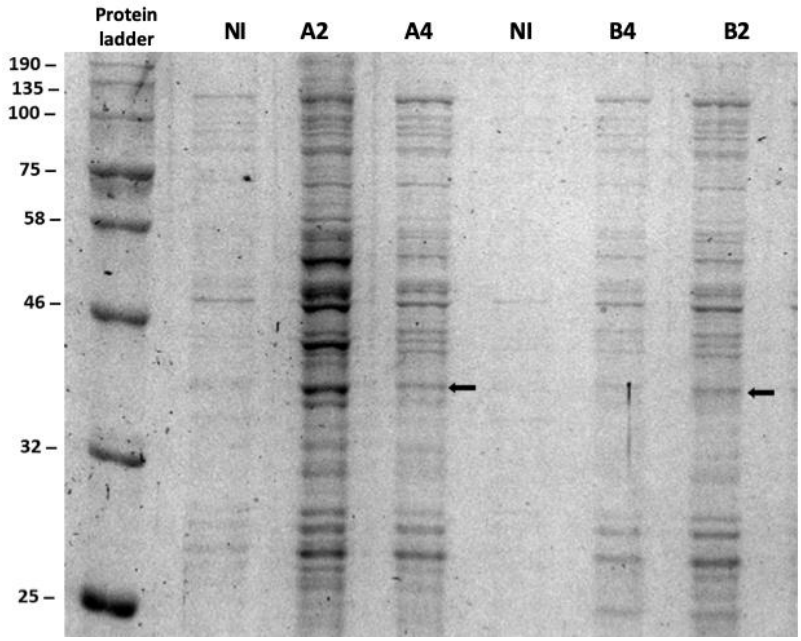

Figure 3.11: SDS-PAGE analysis of small scales induction of PEPCK in pET100 constructs. Lane NI; Non-induced. Lane A2: PEPCK was over-expressed in Rosetta, 0.5 mM IPTG, with 50 µg/ml of ampicillin and chloramphenicol at 34 µg/ml at 20°C for 24 hours. Lane A4: PEPCK was over-expressed in Rosetta, 0.5 mM IPTG, with 50 µg/ml of ampicillin and chloramphenicol at 34 µg/ml at 15°C for 24 hours. Lane B2: PEPCK was over-expressed in BL21 DE3, with 50 µg/ml of ampicillin, induced by 0.5 mM IPTG, with 50 µg/ml of ampicillin at 20°C for 24 hours. Lane B4: PEPCK was over-expressed in BL21 DE3, with 50 µg/ml of ampicillin, induced with 0.5 mM IPTG, incubated at 15°C for 24 hour.

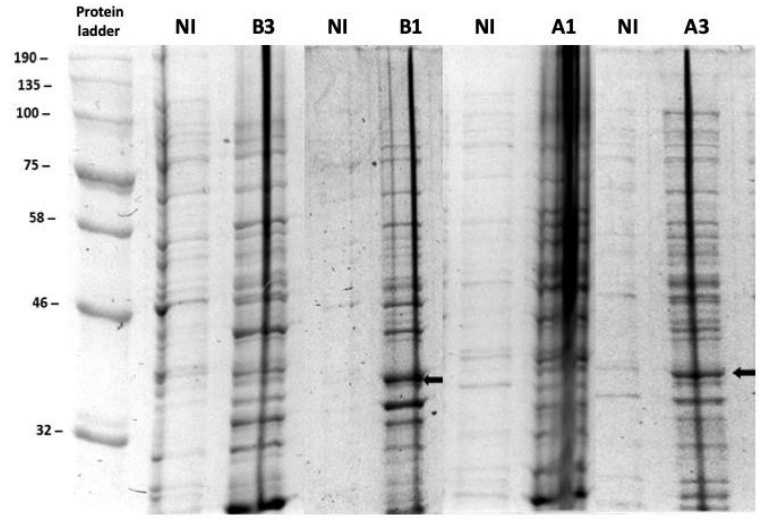

Figure 3.12: SDS-PAGE analysis of small scales induction of PEPCK in pET100 constructs. Lane NI; Uninduced. Lane A1: PEPCK was over-expressed in Rosetta, with 50 µg/ml of ampicillin and chloramphenicol at 34 µg/ml, induced by 0.5 mM IPTG at 20°C for 18 hrs. Lane A3: PEPCK was over-expressed in Rosetta, with 50 µg/ml of ampicillin and chloramphenicol at 34 µg/ml, induced by 0.5 mM IPTG at 15°C for 18 hrs (C2). Lane B1: PEPCK was over-expressed in BL21 DE3, with 50 µg/ml of ampicillin, induced by 0.5 mM IPTG, at 20°C for 18 hrs (A2). Lane B3: PEPCK was over-expressed in BL21 DE3, with 50 µg/ml of ampicillin, induced by 0.5 mM IPTG at 15°C for 18 hrs.

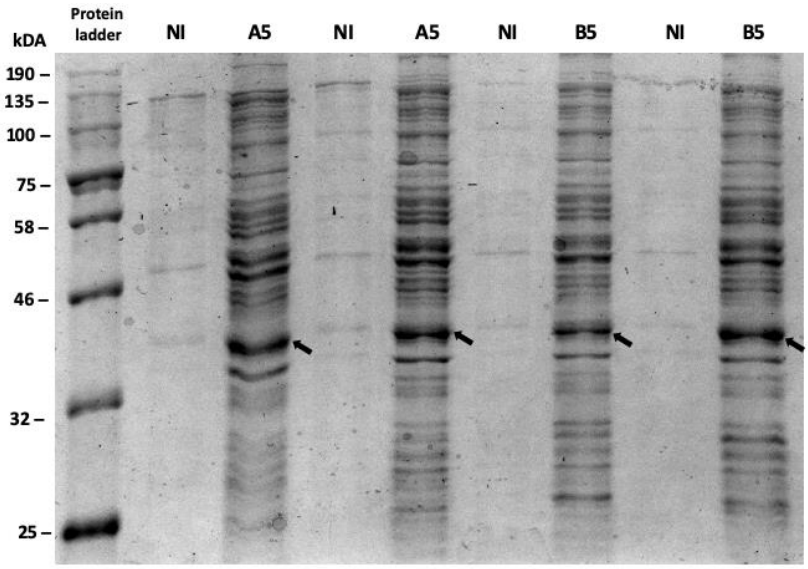

Figure 3.13: SDS-PAGE analysis of small scales induction of PEPCK. The PEPCK was over-expressed in Rosetta or BL21 DE3, induced by 1 mM IPTG at 18°C for 24 hours. Lane NI; Non-induced protein. Lane A5; PEPCK was over-expressed in Rosetta, with 50 µg/ml of ampicillin and 34 µg/ml chloramphenicol, 1 mM IPTG, at 15°C for 24 hrs. Lane B5; PEPCK was over-expressed in BL21 DE3, with 50 µg/ml of ampicillin, 1 mM IPTG, at 15°C for 24 hrs.

3.11 Purification of PEPCK with Ni-NTA column (HisTrap HP) from large scale induction in LB media.

Large-scale induction was performed as described in Table 3.6. PEPCK was extracted after the cells were disrupted with a French press and the resulting enzyme was purified by using a Ni-NTA column (HisTrap™ HP) on an AKTA. No pure protein was detected from Method A, B, C, and D (Table 3.6). From the inspection of the gel, the protein was found in the cell pellet, which was in the form of an insoluble fraction (Appendix F; Experiment PEPCK purification without NusA). Since PEPCK purified was in the form of an inclusion body, it is crucial to overexpress, induce, and purify the protein under different conditions. It is also essential to screen for a correct folding or effective refolding mechanism after a denaturing purification.

Table 3.6: Large scale induction of PEPCK from pET 100/D-TOPO in LB media.

Host Strain	BL21-DE3		Rosetta		
Time of incubation	18 hrs	24 hrs	18 hrs	24 hrs	
IPTG (mM)	0.5	1.0	0.5	0.5	1.0
Method	A		B	C	D

3.11.1 Purification of PEPCK overexpressed from LB and auto-induction medium with HisTrap™ HP column.

Besides LB media, auto-induction media also was applied as an induction media for PEPCK. Large-scale induction was performed as described in Table 3.7.

Table 3.7: Large scale induction of PEPCK from pET 100/D-TOPO from LB and autoinduction media

Host strain	BL21-DE3		Rosetta	
Time of incubation	18 hrs	48 hrs	18 hrs	48 hrs
IPTG (mM)	1.0	-	1.0	-
LB Media	D		A	
Autoinduction Media		B		C

For the LB medium (Method A, Table 3.7), the PEPCK was overexpressed in Rosetta before induced with 1 mM IPTG at 18°C. The protein was eluted with 20, 50, 100- and 200-mM imidazole in a tris-HCl buffer. From the gel image (Fig. 3.14), most of the protein PEPCK at 37 kDA (arrow) was detected in the cell pellet (Lane P), which suggests that it was insoluble.

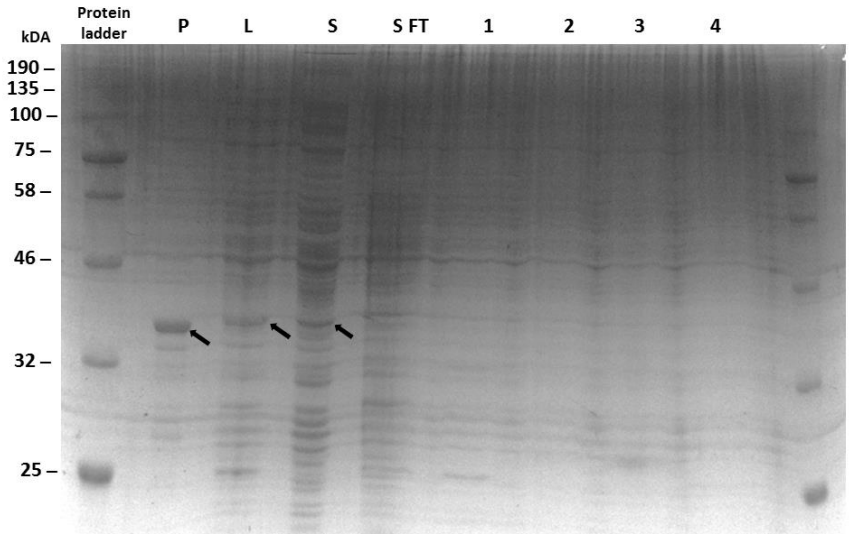

Fig. 3.14: SDS-PAGE analysis of PEPCK purification by HisTrap™ HP column. The PEPCK was over-expressed in Rosetta with 50 µg/ml ampicillin and 34 µg/ml chloramphenicol. Lane P; Cell Pellet contains insoluble PEPCK protein. Lane L; Lysate after French press. Lane S; Supernatant from centrifugation of the lysate. Lane S FT; Supernatant flow through. Lane 1; 20 mM imidazole. Lane 2; 50 mM imidazole. Lane 3 100 mM imidazole. Lane 4; 200 mM imidazole.

For the auto-induction medium (Method B and C, Table 3.7), the PEPCK was overexpressed in Rosetta or BL21 DE3 host strain with an incubation temperature of 18°C for 48 hours. The target protein was then eluted with 50, 100, 150- and 200-mM imidazole in a tris-HCl buffer.

From the gel image (Fig. 3.15 and 3.16) the PEPCK were induced from the autoinduction medium since the band of PEPCK at 37 kDA cell growth can be detected in the lysate (Fig. 3.15 and 3.16, Lane L; arrow), in the supernatant (Fig. 3.16 and 3.17, Lane P; arrow), and also in the pellet (Fig. 3.15 and 3.16, Lane S; arrow). The presence of protein PEPCK in the pellet suggested that it was in an inclusion body and no target protein was eluted from the elution buffer, 25 mM of Tris-HCl buffer, pH 7.4, with 0.5 M of NaCl, and 0.3 M glycerol with 100 or 200 mM of imidazole.

Although the protein was expressed in high amounts of *E. coli*, it was mostly expressed as insoluble inactive aggregates. Thus, the addition of urea could enhance the solubility of PEPCK protein.

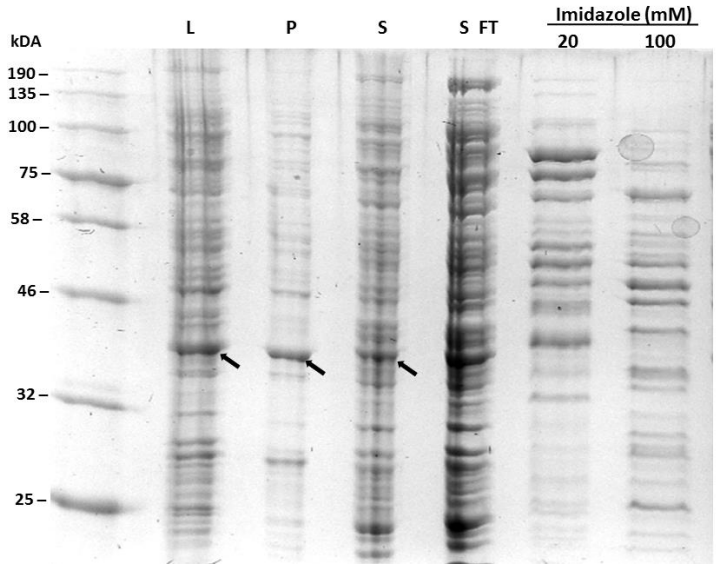

Fig. 3.15: SDS-PAGE analysis of PEPCK purification by HisTrap™ HP column. The protein was over-expressed in Rosetta with 50 µg/ml of ampicillin and 34 µg/ml of chloramphenicol in auto-induction medium with incubation at 18°C for 48 hours. Lane L; Cell lysate. Lane P; Cell pellet. Lane S; Supernatant. Lane S FT; Supernatant flow through from the column. Lane 20- and 100 mM imidazole; No presence of PEPCK protein from the elutions at this imidazole concentration.

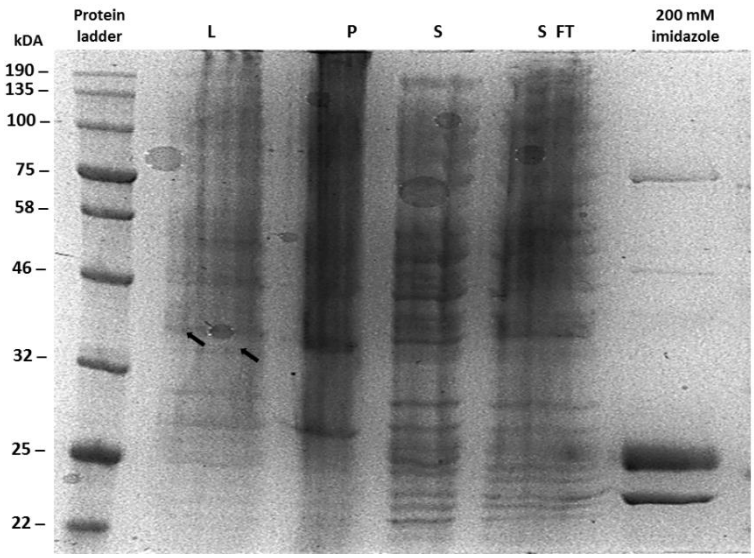

Fig. 3.16: SDS-PAGE analysis of PEPCK purification by HisTrap™ HP column. The protein was over-expressed in BL21 DE3 with 50 µg/ml of ampicillin in auto-induction medium with incubation at 18°C for 42 hours. Lane L; Cell lysate. Lane P; Cell pellet. Lane S; Supernatant. Lane S FT; Supernatant flow through from the column. Lane 200 mM Imidazole; No presence of PEPCK protein from the elution at this imidazole concentration.

3.11.2 Purification of PEPCK with His GraviTrap column with urea.

The PEPCK was overexpressed in BL21-DE3 and induced with 1 mM IPTG at 18°C (Method D, Table 3.7). The protein pellet was resuspended in the 50 mM Tris-HCL buffer with 100 mM KCl and 8 M of urea before centrifuging it to obtain a supernatant. The supernatant was loaded into the column which was equilibrated previously with binding buffer (50 mM Tris-HCl, pH 7.4, 100 mM KCl) and 8 M urea. The protein was washed with different concentrations of urea (7, 6, 5, 4, 3, 2, 1, 0 M), followed by the target protein elution with 50, 100, 200- and 300-mM imidazole in the elution buffer, (50 mM Tris-HCl, with 100 mM KCl, pH 7.4). From the gel image (Fig. 3.17), PEPCK at 37 kDA (Lane P; arrow) was detected in the binding buffer solution. However, it was undetected in the elution buffer.

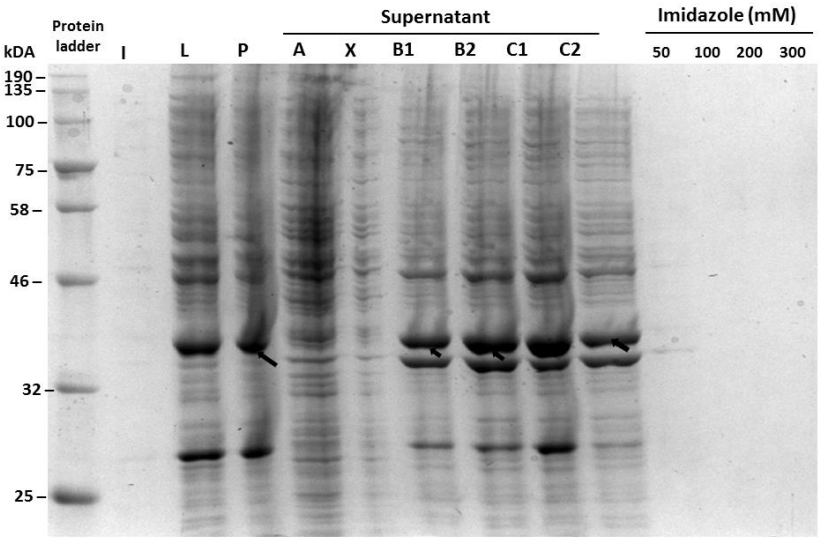

Fig. 3.17: SDS-PAGE analysis of PEPCK purification by HisTrap™ HP column. The PEPCK was over-expressed in BL21-DE3 with 50 µg/ml of ampicillin and induced by 1 mM IPTG at 18°C for 18 hours. Lane I; Cell lysate (non-induced). Lane L; Cell lysate (induced), Lane P; Pellet, Lane A; Supernatant; Lane B1 and B2 from the pellet that was resuspend in binding buffer (50 mM Tris, 100 mM KCl, 8 M Urea, solubilized for 60 mins at 4°C; Lane C1 and C2 from the centrifugation of supernatant B1 and B2 (13000 rpm, 4°C at 15 mins).

3-[(3-cholamidopropyl)dimethylammonio]-1-propanesulfonate or CHAPS is a sulfobetaine derivative of cholic acid, which can be served as a non-denaturing detergent in the protein purification. The target protein was unable to refold in a Tris-HCl wash buffer with 2 % (g/v) CHAPS and different concentrations of urea. From the gel image (Fig. 3.18), PEPCK was absent in the elution buffer (100-200 mM imidazole).

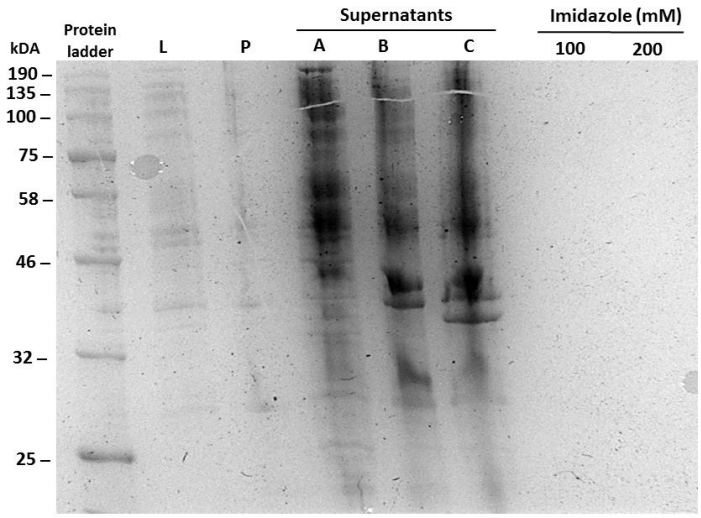

Fig. 3.18: SDS-PAGE analysis of PEPCK purification by HisTrap™ HP column. The protein was over-expressed in BL21-DE3 with 50 µg/ml of ampicillin and induced by 1 mM IPTG at 18°C for 18 hours. Lane L; Cell lysate. Lane P; Cell pellet. Lane A; Supernatant. Lane B; Supernatant from the pellet that was re-suspend in binding buffer (50 mM Tris, 100 mM KCl, 8 M urea, solubilized for 60 mins at 4°C. Lane C; supernatant from the centrifugation of Lane B (13 000 rpm, 4°C at 15 mins).

3.12 Discussion

In addition to *E. coli*, other hosts can be used as expression systems such as baculovirus/insect cell, yeast, and mammalian cell culture. Firstly, they have the same criteria as *E. coli.* Next, they have straightforward protocols. Lastly, they are commercially accessible and inexpensive for small-scale production (Zerbs, S. et. al., 2009). Among these systems, *E. coli* is preferable since it offers rapid growth in media and capable of providing high cell densities. Besides, *E. coli* can be manipulated genetically. Furthermore, they are cheap to grow in culture since it only requires cheap media. It also has a high protein expression level allowing large amounts of protein to be routinely produced in one day (Francis, D. M., and Page, R. 2010). Likewise, it is widely used in many structural studies, especially in isotope-labeling for NMR spectroscopy and X-ray crystallography (Yin, J., et. al., 2007).

In theory, the production of recombinant protein in *E. coli* is straightforward. It usually started with the identification of the target protein, followed by the cloning of the target gene into an appropriate vector and transformation of the construct into host strain, lastly the induction of amplified expression and protein purification. As a whole, the purified protein can be characterised by its sequencing, purity, structural integrity, and activity depending on the research aims.

In this study, an attempt was made to purify the recombinant PEPCK protein that was previously expressed and fused with NusA and a His_6 tag in a pET-44a(+) expression vector system. BL21 (DE3) and Rosetta were used as the expression cell lines, and the fusion protein was induced into three different types of growth media (LB, 2YT, and autoinducing media). Next, thrombin was applied to cleave the NusA tag from the target protein, PEPCK since the presence of NusA in the fusion protein could interfere with the activity of PEPCK.

From the analysis obtained by the SDS-PAGE, the presence of a double band in PEPCK from pET-44a(+) indicated that it was partially purified. At first, the amount of purified NusA-PEPCK was around 2.27 mg/ml and the purified PEPCK was around 0.1 mg/ml. Hence, this method can be deemed as unreliable and essentially irreproducible. The difficulty ascribed from the thrombin cleavage step. To achieve a high level of PEPCK protein without the thrombin cleavage reaction, the PEPCK was expressed as a single protein in the strain pET 100/D-TOPO. PEPCK was expressed in the absence of a protein carrier (NusA) to avoid any potential loss after the thrombin cleavage reaction. From the results, it was found out that the PEPCK was overexpressed in the inclusion bodies, which also suggested that it was not biologically active. In a comparative study of the effectiveness of a range of fusion proteins in solubilising target proteins, NusA enhanced the solubility of the fusion proteins (scFvs-NusA) partially. The expression amount of target protein (with NusA) was reported at around 15 % of the total *E. coli* protein and 60 % of that was soluble (Sun, W., et. al., 2012).

To obtain a high yield and quality of recombinant protein expression, many factors must be considered which include the promoter system, expression vector, expression host, and growth conditions (media, temperature) (Francis, D. M., and Page, R. 2010). It is crucial to choose a proper expression system because a poorly selected expression host will cause the target protein to be misfolded and poorly expressed with limited necessary

posttranslational modifications. In this study, pET-44a(+) from the pET system was chosen as the expression vector since it has NusA and His6 tag sites with T7 promoter and ampicillin resistance. For overexpression of PEPCK without NusA, the pET 100/D-TOPO vector (Invitrogen) was supplied by a commercial company. Both vectors share the same crucial feature which is the His-tag site, but both vectors differ in the length of the region between His-tag and the target protein.

It is well known in the literature that the pET vector is highly effective in cloning and expression of recombinant proteins in *E. coli*. In this system, the target genes were cloned in the pET plasmids under the control of bacteriophage T7 transcription and translational signals where the expression was induced by a source of T7 RNA polymerase in the host cell (Novagen, pET System Manual, 11th Edition). The gene expression was determined by the T7 RNA polymerase from the T7 bacteriophage. The T7 RNA polymerase was then transcribed into DNA, about five times faster than the bacterial RNA polymerase (Studier, F. W. 1990). T7 RNA polymerase was found to be absent in *E. coli*. Thus, it must be delivered to the cell by an inducible plasmid or an *E. coli* strain that contains a chromosomal copy of the T7 polymerase gene (Studier, F. W., and Moffatt, B. A. 1986). Without an inducer (lactose), the production of the polymerase from the lacUV5 promoter will be inhibited and the gene of interest will not be transcribed (Studier, F. W. 1990). Hence, the T7 RNA polymerase was transcribed and synthesised with the addition of IPTG as an analog of lactose.

Since T7 promoter systems generally provide a strong and robust expression (Francis, D. M., and Page, R. 2010), some translated proteins will aggregate and form inclusion bodies because they are unable to fold before react with another unfolded protein. To minimise this problem, NusA was expressed as a fusion protein with PEPCK. The pET-44a(+) vectors were designed for the cloning and high-level expression of peptide sequences fused with the 495 aa Nus•Tag™ protein and an additional *N*-terminal His•Tag (Novagen). NusA is a bacterial transcription factor that promotes RNA polymerase to pause on some of the RNA motifs. Pauses in the RNA polymerase activity will decelerate the transcription (Kosobokova, E. N., et. al., 2016), which causes the bacterial cells to be coupled. Therefore, inhibition or deceleration of transcription could result in decelerating translation. In another word, the amino acid chain synthesised will be folded more slowly, which renders it adequate time for the protein to fold correctly and the formation of aggregations with incorrectly folded protein chains can be avoided (Davis, G. D., et. al., 1999). The addition of NusA was reported to promote the solubility of the target protein as compared to other solubility tags such as glutathione-S-transferase (GST) and thioredoxin (Trx) (Shih, Y. P., et al., 2002); Previous studies have obtained correctly folded target protein from the expression and purification of cyclomaltodextrinase from *Anoxybacillus flavithermus* (Turner, P., et. al., 2005) and haemerythrin from *Methylococcus capsulatus* (Karlsen, O. A., et. al., 2005).

NusA has been expressed as a fusion partner with the target proteins which were very difficult to express in the active form such as d-gluconate) (GNAD), Yellow Fluorescent Proteins (EYFPs), and cyclomaltodextrinase from the α-amylase family (Dümmler, A., et. al., (2005); Kim, S., and Lee, S. B. (2008); Turner, P., et. al., (2005). De Marco, V., et. al., 2004 found out that NusA which was cloned and fused with target proteins (Tep3Ag, E8R, Xklp3a) gave a higher yield of the purified fusion protein and the target protein as compared to GST. Also, the

fusion proteins were highly soluble and can be purified to near homogeneity. This can be attributed to the natural solubility of NusA and its biological activity in *E. coli* which may decrease the rate of translation during the transcriptional pauses and provide sufficient time for the protein folding (Davis, G. D., et. al., 1999). Multiple studies have shown that the NusA can enhance the protein solubility for a diverse set of protein targets (De Marco, V., et. al., 2004; Douette, P., et. al., 2005; Niiranen et al., 2007). In fact, in some cases, it is even more effective than MBP (Kohl, T., et. al., 2008). Ermolova, N. V., et. al., (2003) have expressed and purified the soluble PEPCK from *Mesembryanthemum crystallinum* by applying NusA and pET-43a(+) (Novagen) as the expression vector systems. Meanwhile, the PEPCK expressed from the recent study has demonstrated highly active property in soluble form.

In the *E. coli* expression host system, the recombinant proteins are normally either directed to the cytoplasm or the periplasm and, to a lesser extent, secreted. When the proteins are directed to the cytoplasm, it can be expressed efficiently and offer yields of up to 30 % of the biomass (Jana, S., and Deb, J. K. 2005). However, the transcription and translation of *E. coli* are fast and tightly coupled since it is prokaryotic. The high rate of these reactions could lead to a partially folded, unfolded, or misfolded soluble protein (Oberg, K., et. al., 1994). A previous study from Vethanayagam, J. G., and Flower, A. M. (2005) found out that the repressed expression of the recombinant protein was mainly due to the occurrence of chromosomal mutations that diminished the level of functional T7 RNA polymerase, thus inhibited the expression from the plasmid.

Besides a low level of expression, the PEPCK was overexpressed as an inclusion body in the absence of a NusA tag. Various methods have been undertaken to avoid the formation of the inclusion body or to resolubilisation of the protein, however, these methods were unable to eliminate the insoluble aggregates. High solubility is one of the primary requirements to produce a biologically active recombinant protein. From this study, only a fraction of the polypeptide achieved proper/correct folding, and others were misfolded and accumulated as inclusion bodies. Thrombin is a protease that recognises LVPRG or LVPRGS and cleaves between arginine and glycine (Chang, J. Y. 1985). This linker sequence is derived from the sequence of bovine factor XIII, the native target of thrombin (Takagi, T. and Doolittle, R.F. 1974). Even though the thrombin cleavage at the designated sequence is relatively specific, many previous studies have demonstrated the occurrence of thrombin cleavage at alternative sites (Koehl, C., and Abecassis, J. 1976). Furthermore, the presence of impurities in the commercial thrombin was also observed. Most of the impurities were plasmin, which could contribute to the formation of non-specific cleavage products (Koehl, C., and Abecassis, J., 1976; Donaldson, V. H., and Kleniewski, J. 1979).

As thrombin stability decreases very rapidly with an increase of temperature, the cleavage reaction was performed at 4°C to maintain the stability of thrombin, avoid the aggregation of target protein, and the formation of inclusion bodies (Le Borgne, S., and Graber, M. 1994). From the SDS-PAGE analysis, it has appeared that thrombin cleaved the fusion protein more than it should be (Fig. 3.10). As a result, PEPCK may have endogenous target sequence or it could be a target for non-specific cleavage by the thrombin. The band appeared to be the products of non-specific digestion (Fig. 3.10). The poor cleavage of the fusion protein by thrombin may be due to the accessibility of the thrombin recognition site (Guan, K., and Dixon, J. E. 1991).

Additional bands can be seen before the and this could be due to the occurrence of proteolysis event by the host bacteria, *E. coli*.

Sometimes, a protease will fail to cleave the fusion protein. More often, this can be ascribed by the presence of steric hindrance, where the protease sites are inaccessible by the enzyme (Kapust, R. B., and Waugh, D. S., 2000; Lee, S., et. al., 2008). To alleviate such a problem, one could include a short linker of glycine, asparagine, or alanine residues between the protease site and the fusion protein (Esposito, D., and Chatterjee, D. K. 2006). Poor cleavage of fusion proteins can also be overcome by changing the cleavage conditions, such as increasing the protease concentrations, prolonging the cleavage time, and altering temperature. In this study, attempts to improve the thrombin specificity was unsuccessful under a low protease concentration and a shorter period of reaction.

Often, the expression and solubility of the protein can be improved with the induction process under low temperatures. In the literature, NusA fusion proteins have been reported to be more soluble when it was induced at a lower temperature of 20°C as compared to a higher temperature of 30°C (Korf, U., et. al., 2005). In this study, a lower expression temperature was applied after being inducted at 18-20°C. Bacteria cultivation under the low-temperature environment is widely reported in many previous studies to reduce protein aggregation. The low-temperature environment can slow down the protein synthesis and folding processes, hence minimising the occurrence of hydrophobic interactions and self-aggregation of the protein (Schumann, W., and Ferreira, L. C. S., 2004; Sørensen, H. P., and Mortensen, K. K. 2005b). Furthermore, it reduces the degradation of the protein which caused by the activity of proteases (Chesshyre, J. A., and Hipkiss, A. R. 1989; Spiess, C., et. al., 1999; Hunke, S., and Betton, J. M. 2003; Pinsach, J., et. al., 2008). Due to a lower protein synthesis rate, a longer induction period is necessary to obtain a higher protein yield (typical induction conditions are 4 hours at 37°C and 16 to 20 hours at 18°C). However, the reduction of temperatures can cause some drawbacks such as low replication, transcription, and translation rates, and poor bacterial growth and production yields (Mujacic, M., et. al., 1999).

PEPCK was also expressed without NusA as a protein carrier. The PEPCK was unable to purify because it was expressed in the form of an inclusion body. The inclusion bodies are commonly produced from an intracellular expression of recombinant proteins. It was accumulated as insoluble polypeptide aggregates of misfolded proteins which were required to be solubilised before refolded and recover back to its native state (Roe, S. 2001). The formation of inclusion bodies can be found on the overexpression of foreign eukaryotic proteins and soluble bacterial proteins. To recover back to its native state, the misfolded proteins need to be dissolved into denaturing agents such as urea and guanidine hydrochloride, which are water-soluble chaotropic agents and compatible with the protein folding (Zhu, S., et. al., 2013). In the refolding of the solubilised protein, the final concentration of denaturant should be high enough to solubilise the aggregates, but also low enough to promote proper folding (Clark, E. D. B., 1998). Urea has been used extensively as a denaturing agent in solubilising and refolding the protein back into its native state (Maeda, Y., et. al., 1996; Al-Samarrai, T. H., et. al., 2007). When

urea was applied to solubilise and refold PEPCK in this study, no PEPCK was detected after the IMAC purification (Section 3.11.2).

As aforementioned, T7 promoter systems provide a strong and robust expression that sometimes results in the formation of an inclusion body, where the overexpressed proteins are unable to fold before come across another unfolded protein (Francis, D. M., and Page, R. 2010). To solve this problem, the strength of the promoter can be altered. For expression systems with lac promoter, the level of expression is usually characterised as low and middle. With such a weak level of expression, it can be regulated easily and suitable for gene products at a very low intracellular level (Gronenborn, B. 1976). Other promoter systems such as the trc or tac promoters have a moderately high level of expression. Despite these promoter systems have a lower level of expression than the T7 system, it is still possible to regulate the level of expression in the protein. However, this tac promoter generally requires expensive induction procedures and a higher basal level of expression (Brosius, J., et. al., 1985). For the expression system with T7 RNA polymerase, the level of expression is very high. The basal level of expression usually depends on the type of strain used (pLys) (Studier, F. W., and Moffatt, B. A. 1986). By adjusting the concentration of inducer, IPTG as well as lowering the growth temperature, it is envisaged that the level of expression of the protein will increase with no formation of inclusion bodies. In this study, the fusion protein (NusA-PEPCK) and PEPCK were successfully induced at the final IPTG concentration of 0.5 mM.

3.13 Conclusion.

The presence of NusA tag in the fusion protein is essential for the expression and purification of PEPCK. The PEPCK can only be solubilised when it was expressed with the NusA tag. However, the yield of PEPCK was observed to be low after the thrombin cleavage due to the aggregation event of the target proteins during the cleavage processes. Many methods have been performed to purify the PEPCK. However, most of it did not achieve the desired outcomes, especially the removal of the NuSA tag after the thrombin cleavage and the formation of inclusion bodies from the over-expression of PEPCK without the NusA tag. Various methods were attempted to remove inclusion bodies, but many methods encountered the difficulty in eliminating the insoluble aggregates. Furthermore, expression from either the vector pET-43a(+) or pET 100/D-TOPO did not promote the production of active protein. Despite *E. coli* exhibited many advantages in recombinant protein expression, the production of active PEPCK from *E. coli* still appeared to be quite challengin

CHAPTER 4

Phosphorylation of PEPC with PEPCK or Protein Kinase A (PKA).

4.1 Introduction.

Post-translational modifications (PTMs) of proteins play a fundamental role in controlling the activity, localisation, interactions, and biological regulation of cells (Bi, Y. D., et. al., 2011). Among the PTMs, protein phosphorylation is widely studied due to its excellent regulation of protein function, subcellular localisation, and protein-protein interactions (Cohen, P. 2002). Phosphorylation is a common covalent post-translational modification that regulates the protein and enzyme activity in plants, animals, and microorganisms. It has been reported that the reversible phosphorylation of proteins and enzymes played a central role in regulating the enzyme in cellular metabolism (Krebs, E. G. and Beavo, J. A. 1979). Other functions related to reversible protein phosphorylation have also been reported, which include regulation of proteins in many fundamental cellular processes (Hunter, T. and Cooper, J.A. 1985; Edelman, A. M., et. al., 1987; Hanks, S. K., et. al., 1988; Ullrich, A. and Schlessinger, J. 1990).

In plants, phosphorylation of protein possesses many vital functions in the cellular processes such as regulation of the development, metabolism, and plant-pathogen interactions (Mori, I. C., et. al., 2006; De La Fuente van Bentem, S., 2006; Huber, S. C., and Hardin, S. C. 2004; Thurston, G., et. al., 2005). Besides, protein phosphorylation also regulates other activities like photosynthesis, photomorphogenesis, and gravitropism (Ma, H., 1993). Recently, different types of protein kinases have been reported and classified based on the substrate specificities and structural resemblances of the members in the same family (Dissmeyer, N., and Schnittger, A., 2011). Budde, R. J., and Chollet, R. (1988) proposed seven different types of specific enzymes in plants which responsible for the reversible phosphorylation: mitochondrial pyruvate dehydrogenase (EC 1.2.4.1), chloroplastic pyruvate, orthophosphate dikinase (EC 2.7.9.1), ribulose bisphosphate carboxylase/oxygenase (EC 4.1.1.39), cytoplasmic phosphoenolpyruvate carboxylase (PEPC) (EC 4,1.1.31) and 6 phosphofructo-2-kinase (EC 2.7.1.105), microsomal hydroxymethylglutaryl-CoA reductase (EC 1.1.1.34), and quinate: NAD^+ oxidoreductase (EC 1.1.1.24).

In higher plants, the reversible phosphorylation controls the activity of PEPC under the catalysis of PEPCK (Chollet, R., et. al., 1996; Vidal, J., and Chollet, R. 1997; Nimmo, H. G., 2003). Phosphorylated PEPC generally exhibits less inhibition effect when it is induced by malate (Jiao, J. A., et. al., 1991). However, it becomes more sensitive when it is activated by glucose-6-phosphate (G-6-P) (Chollet, R., et. al., 1996). Several researchers have reported that Protein Kinase A (PKA) can phosphorylate PEPC (Meimoun, P., et. al., 2007; Pacquit, V., et. al., 1995). In this chapter, PEPC was phosphorylated with PEPCK and PKA. Furthermore, ATP and phosphoprotein were detected by using sensitive fluorescent staining, Pro-Q® Diamond, and SYPRO Ruby. From the results, it was observed that the poor sensitivity of Pro-Q® Diamond staining might have underestimated the number of phosphorylated proteins in the enriched fractions. Thus, the Phos-Tag™ electrophoresis technique was applied

to isolate the phosphorylated proteins from the non-phosphorylated fraction before detecting the number of phosphorylation sites in the protein. The phosphorylation sites in PEPC were determined by using mass spectrophotometry (MS).

4.2 Purification of PEPC *P. queenslandicum* and *P. pygmaeum.*

Transformed BL21 *λ* (DE3) with the PEPC genes from both *P. queenslandicum* and *P. pygmaeum* was cultured in LB medium under an incubation temperature of 37°C until the absorbance reading reached approximately 0.7-0.8 at 600 nm (A_{600}). The recombinant protein was induced with 0.5 mM IPTG after cooled to 4°C for about one hour, followed by further growth at 18°C for another 18 hours. The cells were harvested by centrifugation and the resulting pellets were stored at -80°C. To determine whether the fusion protein was successfully expressed or not, the induced (Lane I) and un-induced (Lane Ni) bacterial cell cultures were compared with 10 % SDS-PAGE gel (Figure 4.2 and 4.4). From the 10 % SDS-PAGE gel, it was revealed that the expression of the PEPC protein was located around the band of 100 kDa marker protein, which was close to the size of the target protein.

For purification of target protein, the cell pellet was re-suspended in 25 mM Tris-HCl buffer with 20 mM imidazole. The cells were disrupted by using a French press before it was centrifuged and filtered to obtain a clear supernatant. Along the process, both DNase I and Pefabloc®SC were added because the bacterial cells contain a different type of protease, and the addition of protease inhibitors will protect the target protein from thermal degradation during isolation and purification of protein (Roche Diagnostics GmbH, 2004).

The filtered supernatant was loaded into a HisTrap™ HP column (GE Healthcare Life Sciences). The nickel-charged IMAC column was equilibrated with 25 mM Tris-HCl buffer which consists of 20 mM imidazole. The column resin was washed with 25 mM Tris-HCl buffer which consists of 150 mM imidazole (for *P. queenslandicum*) or 100 mM imidazole (for *P. pygmaeum*). The target protein was eluted from the column in 10 ml of elution buffer (25 mM Tris-HCl with 400 mM imidazole (Fig. 4.1). From the 10 % SDS-PAGE analysis of the purified protein, a protein band at around 100 kDa was observed (Fig. 4.2; Lane 3, arrow and Fig. 4.4; Lane 2, arrow). The purified proteins were obtained from the buffer exchange using a Sephadex G-25 column. The thrombin cleavage buffer (TCB) (20 mM of Tris-HCl, pH 8.4) was used to remove the imidazole before it was stored at 80°C.

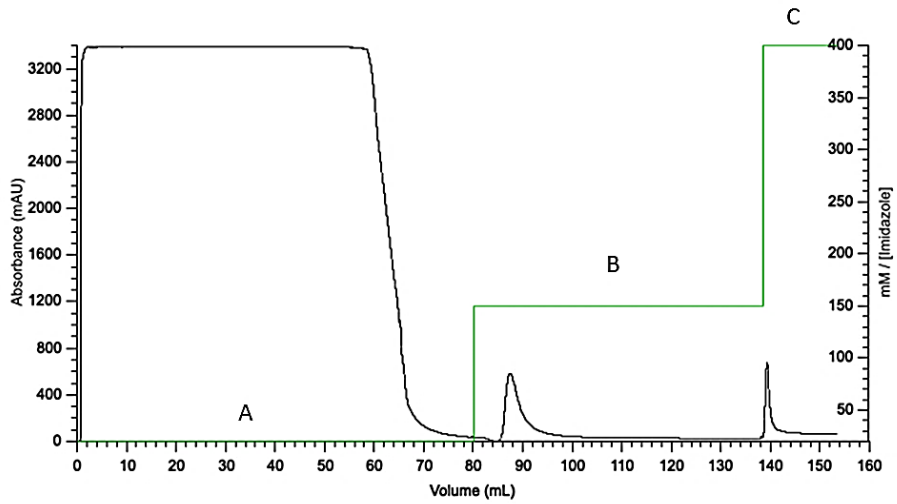

Fig. 4.1: Purification of PEPC *P. queenslandicum* by using Ni-NTA column (HisTrap™ HP) on a AKTA. (A) The sample was loaded into column at the flow rate 1 ml per min. (B) The column was washed with 150 mM of imidazole. (C) The fusion protein was eluted with 400 mM imidazole. The fractions were pooled and subjected to SDS-PAGE to determine the level of purity, and then quantify with Bradford method.

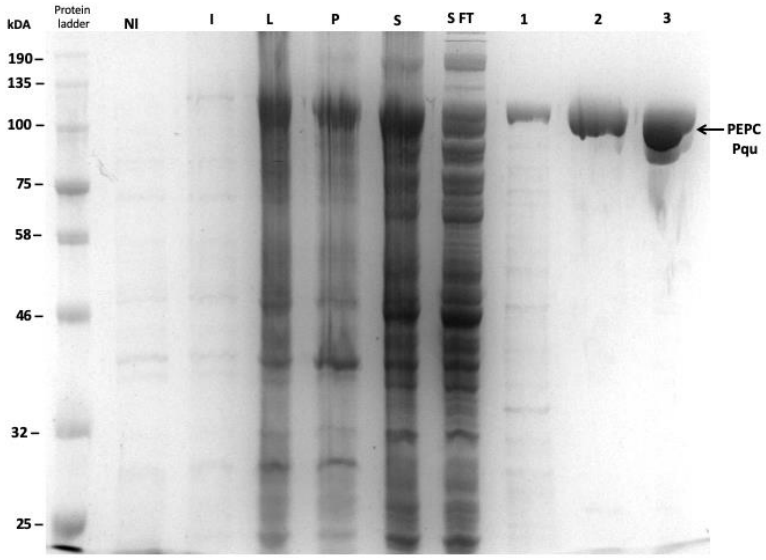

Fig. 4.2: 10 % SDS-PAGE analysis of PEPC *P. queenslandicum* protein purification. Lane NI: Protein molecular weight marker; Lane I: Induced with 0.5 mM IPTG; Lane L: Cell lysate; Lane P: Supernatant from centrifugation; Lane S FT: Supernatant flow through from HisTrap™ HP column; Lane 1: Flow through of wash buffer, 150 mM imidazole; Lane 2: PEPC protein eluted from 400 mM imidazole. Lane 3: PEPC protein rebuffered into phosphorylation buffer.

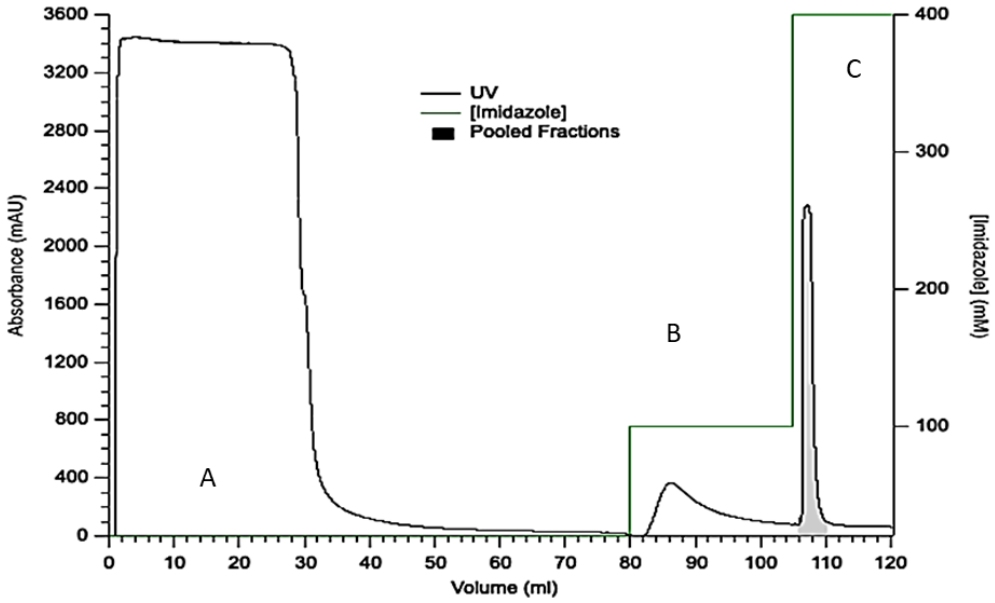

Fig. 4.3: Purification of PEPC *P. pygmaeum* by using Ni-NTA column (HisTrap™ HP) on a AKTA. (A) The sample was loaded into column at the flow rate 1ml per min. (B) The column was washed with 100 mM of imidazole. (C) The fusion protein was eluted with 400 mM imidazole. The fractions were pooled and subjected to SDS-PAGE to determine the level of purity, and then quantify with Bradford method.

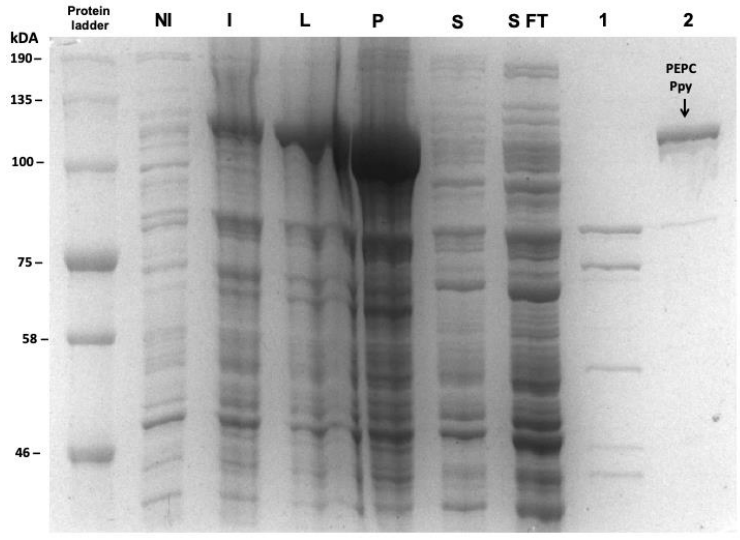

Fig. 4.4: 10% SDS-PAGE analysis of PEPC *P. pygmaeum* protein purification. Lane NI: Protein molecular weight marker; Lane I: Induced with 0.5 mM IPTG; Lane L: Cell lysate; Lane P: Supernatant from centrifugation; Lane S FT: Supernatant flow through from HisTrap™ HP column; Lane 1: Flow through of wash buffer, 100 mM imidazole; Lane 2: PEPC protein eluted from 400 mM imidazole. Lane 3: PEPC protein rebuffered into phosphorylation buffer.

4.3 Small scale *in vitro* phosphorylation assay of PEPC *P. queenslandicum* with PEPCK or Protein Kinase A (PKA).

The assay contained a phosphorylation buffer (pH 8) with 50 mM Tris-HCl and 5 mM $MgCl_2$. Various ratios of PEPC *P. queenslandicum* to PEPCK or PKA were added with or without 1 mM ATP to render a total volume of 500 µl (Table 4.1). Despite PEPCK was only partially purified, it was revealed from the gel of Pro-Q® Diamond staining, PEPCK can phosphorylate PEPC in this reconstituted *in vitro* phosphorylation assay (Fig. 4.5). Comparision of relative intensity to the control with ImageJ showed that it is slightly higher after incubated in two hours, four hours and overnight (Appendix H.ii, Table 1). These results suggesting that *in vitro* phosphorylation reaction were higher in these periods of times. PEPCK also can phosphorylate the fusion PEPC with a small ratio of PEPC to PEPCK (Table 4.1: Apendix H; Figure H. 9; Method G). Besides, incubation of PEPC with PEPCK or PKA in the absence of ATP produced less intense fluorescence bands and this can be explained by the little phosphorylation reaction occurred (Appendix G and H.i). Furthermore, PKA also able to phosphorylate PEPC *P. queenslandicum* (Appendix H; Figure H.3).

Table 4.1: Small scale screening *in vitro* phosphorylation assay of PEPC from *P. queenslandicum* by PEPCK of *P. queenslandicum* or by Protein Kinase A.

Method	PEPC	PEPCK (1:0.5)	ATP (1 mM)	PKA (100 U)
A (1:0.5)	200 ug/ml	100 ug/ml	1 mM	X
B (1:0.5)	200 ug/ml	100 ug/ml	X	X
C (1:0.5)	50 ug/ml	X	1 mM	25 U
D (1:0.5)	200 ug/ml	X	X	100 U
E (1:0.2)	200 ug/ml	40 ug/ml	1 mM	X
F (1:0.1)	200 ug/ml	20 ug/ml	1 mM	X
G (1:0.01)	200 ug/ml	10 ug/ml	1 mM	X

Complete results from Table 4.1 can be found in Appendix H. Based on the SDS-PAGE analysis from Pro-Q® Diamond stain (Appendix H; Figure H.1 till H.11), one can be observed that the PEPCK was capable to phosphorylate PEPC *P. queenslandicum* by *in vitro* phosphorylation assay.

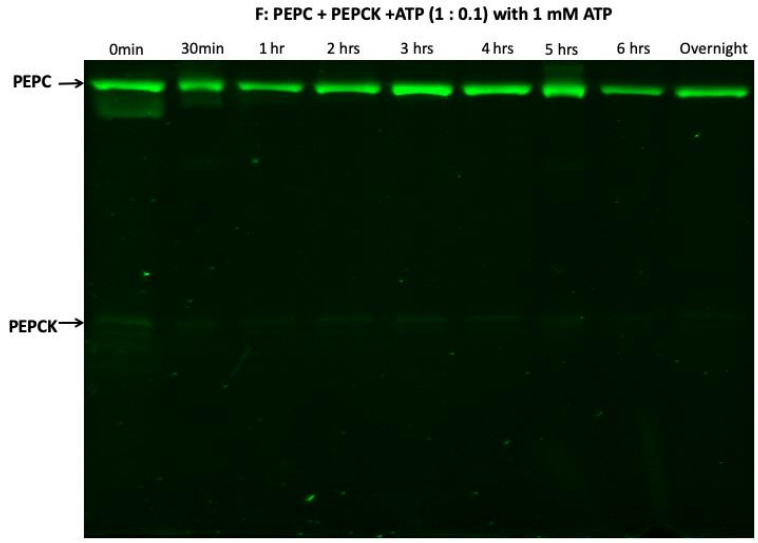

Fig. 4.5: 10% SDS-PAGE analysis of *in vitro* phosphorylation of PEPC *P. queenslandicum* by PEPCK (1: 0.1) from Pro-Q® Diamond stain by small scale assay. The assay was added with 1 mM ATP in different time course as indicated. The phosphorylation reaction was performed at 30°C and 5 µl aliquots were withdrawn at the specified times (0 min, 30 min, 1 hour, 2 hrs, 3 hrs, 4 hrs, 5 hrs, 6 hrs and overnight) and the phosphorylation assay was terminated by adding with equal volume of SDS-sample buffer. Each aliquot was analysed in 10 % SDS-PAGE followed by Pro-Q® Diamond stain.

4.4 Large scale *in vitro* phosphorylation assay of PEPC *P. queenslandicum* with Protein Kinase A (PKA).

In this work, the assay consists of a phosphorylation buffer (pH 8) with 50 mM Tris-HCl, 5 mM $MgCl_2$, PEPC *P. queenslandicum* to PKA ratio of 1 to 0.1, and with or without 1 mM ATP, which rendered a total volume of 6 ml. PEPCK was not used in this large scale assay since the PEPCK was unable to purify in earlier work (Chapter 3; Section 3.9). The phosphorylation reaction was initiated by the addition of 1 mM ATP and 10 µl aliquots were withdrawn at the specified times. In each well of 10 % SDS-PAGE gels, 0.42 µg of phosphorylated PEPC was loaded before run at 200 volts for 50 minutes. From the figure 4.6, it showed that after an incubation period of 1 min, the phosphoprotein staining displayed a low intensity of the fluorescence, which indicates incomplete phosphorylation of the PEPC (Fig. 4.6; A) (Appendix H.ii, Table 2). The band intensity was found to increase at 15 mins and reached the highest relative density at 60 mins. After 60 mins of incubation, the relative intensity start to decrease suggesting low reaction of *in vitro* phosphorylation (Appendix H.ii, Table 2). The results show that the phosphorylation reaction of PEPC by PKA was highest at 60 mins. From the literature, Pro-Q® Diamond dye has been shown to discriminate between phosphorylated and unphosphorylated proteins, and SYPRO Ruby dye signal had been applied in the same SDS-PAGE gel to characterise the total protein profile.

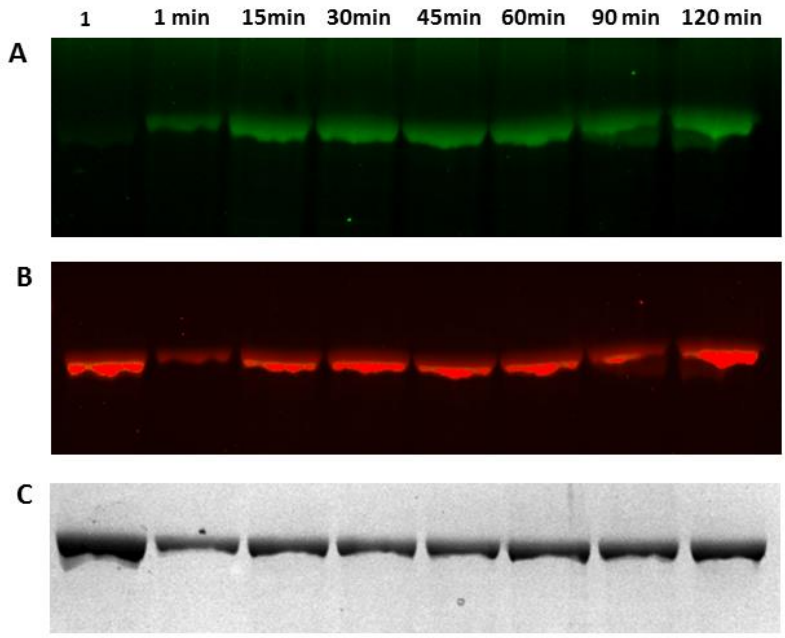

Fig. 4.6: 10 % SDS-PAGE analysis from time course of PEPC *P. queenslandicum in vitro* phosphorylation with PKA (1: 0.1) analyzed by A; Pro-Q® Diamond staining, B; SYPRO Ruby staining and C; Coomassie blue staining. The phosphorylation reaction was performed at 30°C and 10 µl aliquots were withdrawn at the specified times (1 min, 15 min, 30 min, 45 min, 60 min, 90 min and 120 min) and the phosphorylation assay was terminated by adding with equal volume of SDS-sample buffer. In each well of 10 % SDS-PAGE gel, 0.42 µg of phosphorylated PEPC was loaded. Lane 1 is unphosphorylated PEPC *P. queenslandicum*.

4.5 Time course of *in vitro* phosphorylation assay of PEPC *P. pygmaeum* with Protein Kinase A (PKA).

The assay contained phosphorylation buffer (pH 8) with 50 mM Tris-HCl, 5 mM $MgCl_2$, PEPC *P. pygmaeum* to PKA ratio of 1: 0.5, and with or without 1 mM ATP, which rendered a total volume of 500 µl. The phosphorylation reaction was performed at 30°C with 10 µl aliquots were withdrawn at the specified time intervals of 1 min, 30 min, 1 hour, 2 hours, 3 hours, and 4 hours. 10 µl of SDS-sample buffer with 10 µl of water was added to each aliquots and then heating for 10 min at 75 °C. In each well of 10 % SDS-PAGE gels, 50 µg of phosphorylated PEPC was loaded before run at 200 volts for 50 minutes. Figure 4.7 shows that the band intensities increased in a time-dependent manner (Appendix H.ii, Table 4) to an incubation period of 4 hours. The fluorescence intensities remained increased from 1 hour to 4 hours, which suggests that the phosphorylation reaction was completed in 4 hours (Appendix H.ii, Table 4). For *in vitro* phosphorylation assay without addition of ATP, the fluorescence intensities remained constant or slightly higher from 1 hour to 4 hours, which suggests that no or minimum phosphorylation reaction occur (Appendix H.ii, Table 5).

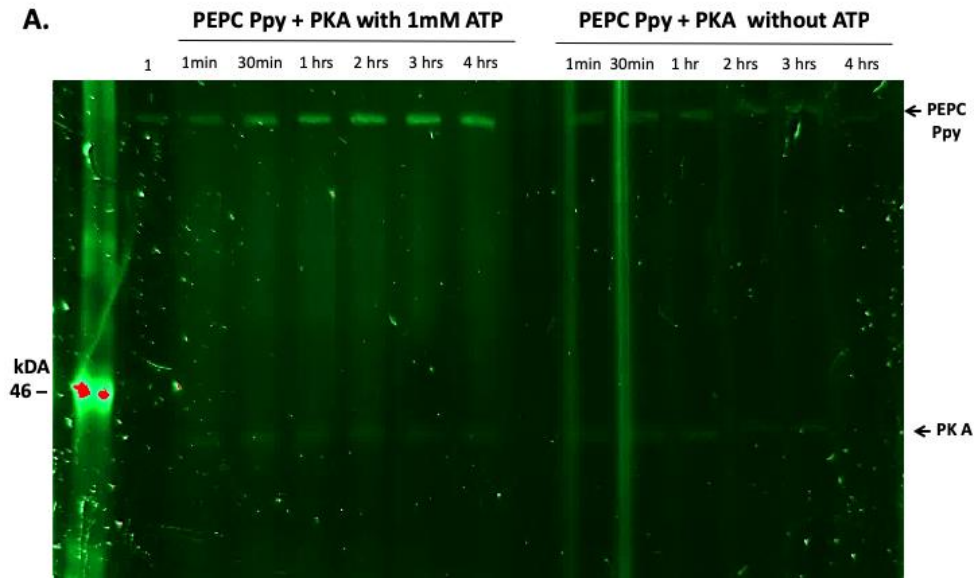

Fig. 4.7: 10 % SDS-PAGE analysis from time course of PEPC *P. pygmaeum in vitro* phosphorylation with PKA (12:1) from Pro-Q® Diamond stain. The gel shows two parts which is assay with ATP (left) and without ATP as a control (right) in different time course as indicated. The phosphorylation reaction was performed at 30°C and 3 µl aliquots were withdrawn at the specified times (0 min, 30 min, 1 hour, 2 hrs, 3 hrs and 4 hrs) and the phosphorylation assay was terminated by adding with equal volume of SDS-sample buffer. Lane 1 is unphosphorylated PEPC *P. pygmaeum*.

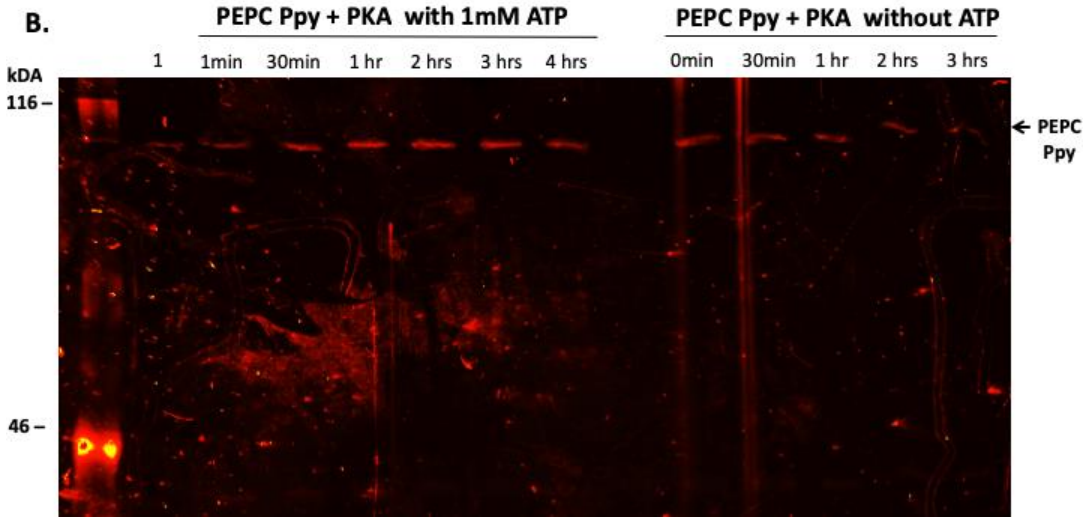

Fig. 4.8: 10 % SDS-PAGE analysis of *in vitro* phosphorylation of PEPC *P. pygmaeum* by PKA (12:1) from SYPRO Ruby stain. The gel shows two parts which is assay with ATP (left) and without ATP as a control (right) in different time course as indicated. The phosphorylation reaction was performed at 30°C and 10 µl aliquots were withdrawn at the specified times (0 min, 30 min, 1 hour, 2 hrs, 3 hrs and 4 hrs) and the phosphorylation assay was terminated by adding with equal volume of SDS-sample buffer. Lane 1 is unphosphorylated PEPC *P. pygmaeum*.

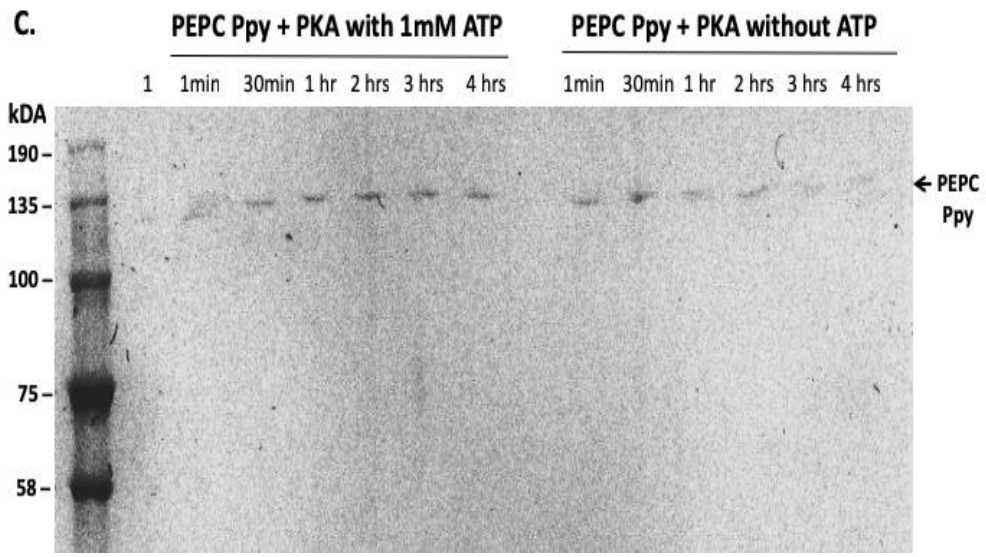

Fig. 4.9: 10 % SDS-PAGE analysis from time course of PEPC *P. pygmaeum in vitro* phosphorylation with PKA (12:1) from Coomassie blue staining. The gel shows two parts which is assay with ATP (left) and without ATP as a control (right) in different time course as indicated. The phosphorylation reaction was performed at 30°C and 10 µl aliquots were withdrawn at the specified times (1 min, 30 min, 1 hour, 2 hrs, 3 hrs and 4 hrs) and the phosphorylation assay was terminated by adding with equal volume of SDS-sample buffer. Lane 1 is unphosphorylated PEPC *P. pygmaeum*.

4.6 *In vitro* phosphorylation assay of PEPC *P. pygmaeum* with Protein Kinase A (PKA) with different ratio of PEPCK to PKA.

Instead of a time course, the phosphorylation assay was performed on a small scale at different ratios of PEPC *P. pygmaeum* to PKA. The phosphorylation reaction was performed at 30°C and incubated for 2 hours. In each well of 10 % SDS-PAGE gels, 0.59 µg of phosphorylated PEPC was loaded before run at 200 volts for 50 minutes. Based on the fluorescence intensity, the PEPC to PKA ratio of 6: 1 offered the highest level of intensity as compared to the two other ratios (30:1 and 12: 1) (Fig. 4.10). As the fluorescence signal intensity correlates with the number of phosphorylated residues on the protein (Steinberg, T. H., et. al., 2003), one can conclude that most of the proteins were phosphorylated at the PEPC *P. pygmaeum* to PKA ratio of 6: 1. (Appendix H.ii, Table 8).

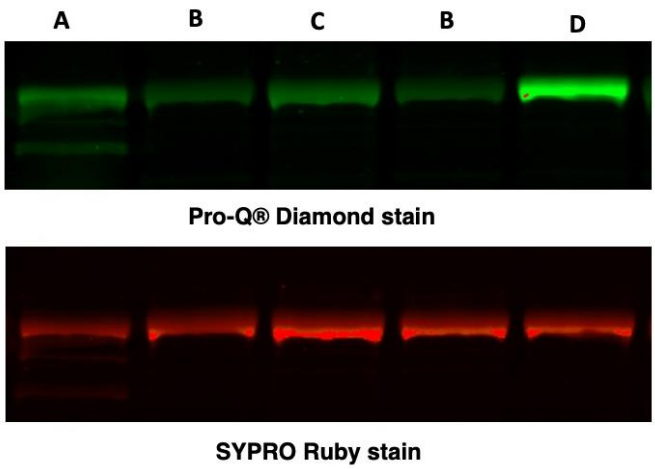

Fig. 4.10: 10 % SDS-PAGE analysis from *in vitro* phosphorylation of PEPC *P. pygmaeum* with PKA. The phosphorylation reaction was performed at 30°C for 120 min, then examined by Pro-Q® Diamond staining (upper) and SYPRO Ruby staining (lower). Lane A; Ratio of PEPC *P. pygmaeum* to PKA is 12:1, Lane B is unphosphorylated PEPC *P. pygmaeum*, Lane C; Ratio of PEPC *P. pygmaeum* to PKA is 30:1, Lane D; Ratio of PEPC *P. pygmaeum* to PKA is 6:1.

Once the optimum ratio of PEPC to PKA was determined, the phosphorylation assay was performed in different time courses. The assay contained phosphorylation buffer (pH 8) with 50 mM Tris-HCl, 5 mM $MgCl_2$, 0.396 mg/ml of PEPC *P. pygmaeum* to PKA ratio is (6: 1), and 1 mM ATP, which gave a total volume of 6 ml. The phosphorylation reaction was performed at 30°C and the phosphorylation rate was determined at the specified intervals of 1 min, 15 min, 30 mins, 45 mins, 60 mins, 90 mins, and 120 mins. The band intensities started to increase at 30 mins and the highest relative intensity was observed at 120 mins. The results show that the phosphorylation reaction of PEPC by PKA should be fully completed by 120 mins of incubation (Appendix H.ii, Table 10). Pro-Q® Diamond dye has been shown to discriminate between phosphorylated and unphosphorylated proteins, and the SYPRO Ruby dye signal had been applied in the same SDS-PAGE gel to define the full protein profile (Fig. 4.11; B) (Appendix H.ii, Table 11).

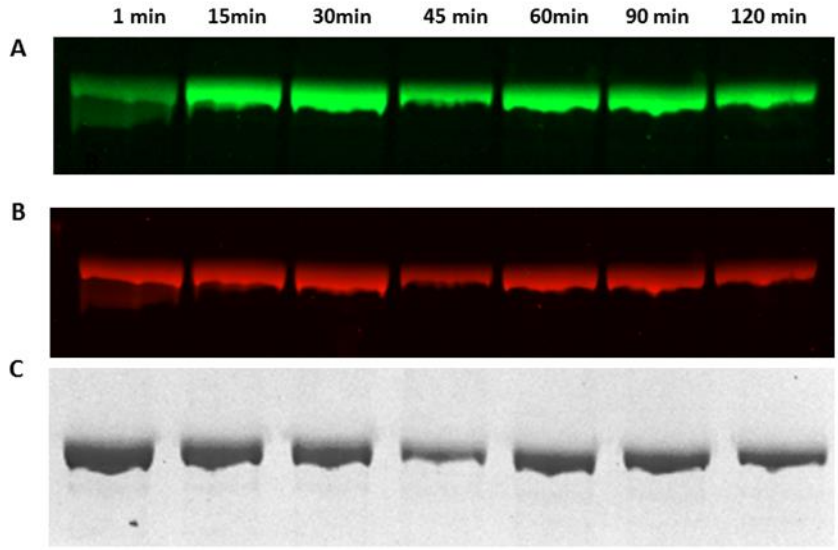

Fig. 4.11: 10% SDS-PAGE analysis from time course of PEPC *P. pygmaeum in vitro* phosphorylation with PKA (6: 1) analyzed by A; Pro-Q® Diamond staining, B; SYPRO Ruby staining and C; Comassie blue staining. The phosphorylation reaction was performed at 30°C and 5 µl aliquots were withdrawn at the specified times (1 min, 15 min, 30 min, 45 min, 60 min, 90 min and 120 min) and the phosphorylation assay was terminated by adding with equal volume of SDS-sample buffer. Lane 1 is unphosphorylated PEPC *P. pygmaeum*.

4.7 Banding profiles of phosphorylated PEPC *P. queenslandicum* in phos-tag™ SDS-PAGE.

Pro-Q® Diamond phosphoprotein gel stain is a fluorescence-based detection system that allows direct monitoring phosphorylation status of proteins in polyacrylamide gels. However, this technique is still unable to provide much information on the phosphorylated protein because the dye is specific for phosphoprotein. Therefore, the PEPC derived from PKA was analysed by using affinity-based Zn^{2+}-Phos-tag™, which was developed by Kinoshita, E., et. al., (2006). In this technique, a novel phosphate-binding tag molecule, Phos-Tag™ or {1,3-bis[bis(pyridin-2-ylmethyl)amino]propan-2-olatodizinc(II) complex} was added to separate SDS-PAGE gel prior the polymerisation. Phos-Tag™ consists of divalent metal ions that allow it to bind with phosphorylated protein and make it migrate slower in the gel as compared to the nonphosphorylated one. Thus, it separates the phosphorylated protein from the non-phosphorylated one. The number of migration bands usually depends on the amount of phosphorylation site in the protein.

First, the optimal concentrations of Phos-Tag™ and the percentage of SDS-PAGE were determined for efficient protein separation. Next, several trials were conducted to optimise the separation of the phosphorylated and non-phosphorylated protein such as varying the concentration of PEPC, changing the duration of electrophoresis from 1 hour to 14 hours, and altering the electric current from 3 Amp to 10 Amp. It was found out that PEPC *P. queenslandicum* and *P. pygmaeum* protein can be easily separated at the Phos-Tag™ concentrations of 5 µM and 10 µM, respectively. Besides, running the gel under as low as 6 mA overnight also improved the separation.

From both samples that were precipitated from acetone and methanol (Fig 4.12; A.i and B.i), the presence of phosphorylated PEPC *P. queenslandicum* was observed as one migration band. The unphosphorylated PEPC also exhibited the same trend, but the band intensity was lower than that of the phosphorylated one (Fig 4.12; A.ii and B.ii). This is because the migration rate of phosphorylated protein was slower than the non-phosphorylated one since the Phos-tag™ bind with the phosphorylated one. As the sample mixture contains both phosphorylated and non-phosphorylated, two migration bands were observed (Fig 4.12; A.iii and B.iii). In another word, the phosphorylated protein was effectively separated from the non-phosphorylated one.

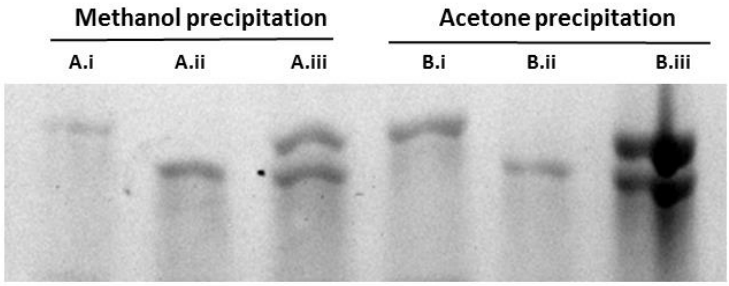

Fig 4.12: Separation of phosphorylated PEPC from the non-phosphorylated PEPC *P. queenslandicum* in the presence of the 5 µM Phos-Tag™. 2 µl of the sample was loaded in each well; A.i and B.i: Phosphorylated PEPC *P. queenslandicum*, A.ii and B.ii: Non-Phosphorylated PEPC *P. queenslandicum*, A.iii and B.iii: Mixture of the phosphorylated and non-phosphorylated PEPC *P. queenslandicum*. One major band was detected in A.i and B.i, which suggests that all PEPC *P. queenslandicum* were fully phosphorylated by the *in vitro* phosphorylation assay.

4.8 Banding profiles of phosphorylated PEPC *P. pygmaeum* in phos-tag™ SDS-PAGE.

Similar to PEPC *P. queenslandicum,* the PEPC *P. pygmaeum* was precipitated with methanol or acetone to remove salt and contaminants. The phosphorylated PEPC *P. pygmaeum* was taken from *in vitro* phosphorylation assay with the PEPC to PKA ratio of 30: 1 (Fig. 4.13). Once all the samples were eluted in the gel that contained 10 µM Phos-Tag™, migration of a single band was observed in the non-phosphorylated samples (Fig 4.13; A.ii and B.ii). For the control mixture with both phosphorylated and non-phosphorylated PEPC, two bands were observed (Fig 4.13; A.i and B.i). This also suggested that the phosphorylated protein was effectively separated from the non-phosphorylated. Two major bands were detected at the PEPC to PKA ratio of 30:1, which indicates incomplete phosphorylation of PEPC *P. pygmaeum* (Fig 4.13; A.iii and B.iii).

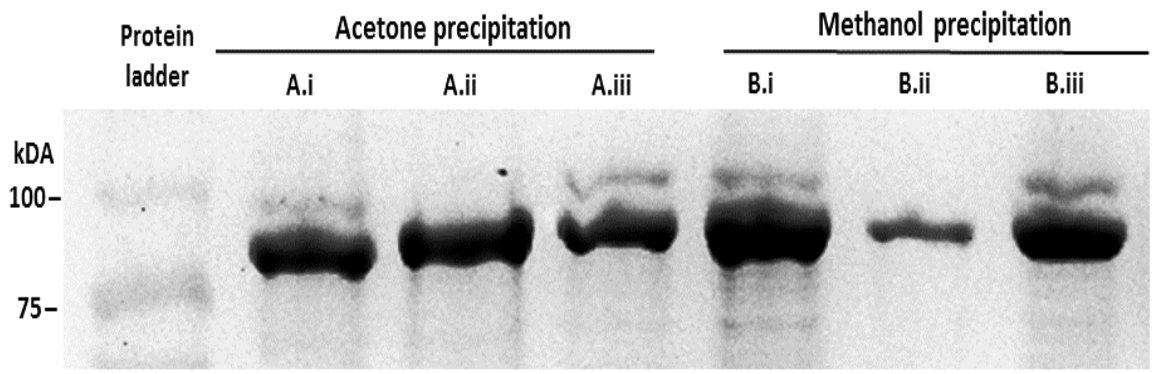

Fig. 4.13: Separation of phosphorylated PEPC *P. pygmaeum* in the presence of the 10 µM Phos-Tag™. The sample was loaded at 5 µl for each lane; A.i and B.i: The non-phosphorylated and phosphorylated PEPC mixtures, A.ii and B.ii: non-phosphorylated PEPC, A.iii and B.iii: phosphorylated PEPC with PKA (30: 1 U). Two major bands were detected, which suggested that not all PEPC was fully phosphorylated under the ratio of 30: 1.

Next, all the samples were run in the SDS-PAGE gel with 10 µM Phos-Tag™ and increased the ratio from 30: 1 to 6: 1, and 12: 1 (PEPC to PKA). The non-phosphorylated and phosphorylated PEPC mixtures presented two individual bands (Fig. 4.14 A.i and B.i), which indicates the phosphorylated protein was effectively separated from the non-phosphorylated. As expected, the non-phosphorylated PEPC *P. pygmaeum* (Fig 4.14; A.ii and B.ii) demonstrated a single migration band. For the phosphorylated PEPC *P. pygmaeum* with the PEPC to PKA ratio of 12: 1, two major bands were detected (Fig 4.14; A.iv and B.iv). Such results suggested that not all PEPC was fully phosphorylated by PKA under such ratio. With the PEPC to PKA ratio of 6: 1, one major band was observed (Fig 4.14; A.iii and B.iii). This suggests that all PEPC was fully phosphorylated by PKA. The high band intensity detected highlighted that several samples were overloaded and caused the bands to be distorted. Low sample loading usually leads to poor detection performance, which consequently contributes to the formation of faint bands in the photographic reproduction.

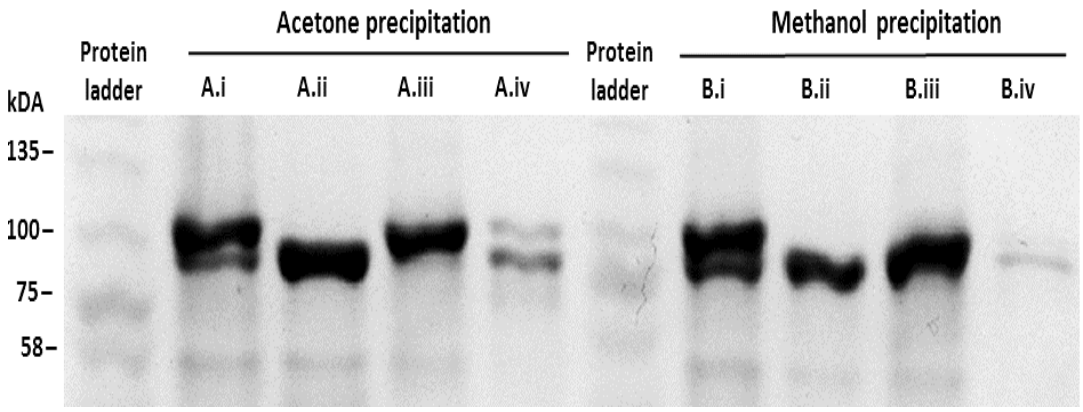

Fig. 4.14: Separation of phosphorylated PEPC *P. pygmaeum* in the presence of the 10 µM Phos-Tag™. The sample was loaded at 5 µl for each lane; A.i and B.i: The non-phosphorylated and phosphorylated PEPC mixtures, A.ii and B.ii: non-phosphorylated PEPC, A.iii and B.iii: phosphorylated PEPC with PKA (6: 1), A.iv and B.iv: Phosphorylated PEPC with PKA (12: 1): Two major bands were detected from A.iv (12: 1), which suggests that not all PEPC was fully phosphorylated. However, one major band was observed from A.iii and B.iii (6: 1), which suggests complete phosphorylation of PEPC.

4.9 Detecting the phosphorylation site of PEPC by Mass Spectrophotometry.

Once PEPC was phosphorylated by PKA, it is necessary to determine the phosphorylation site of the PEPC. PEPCK specifically phosphorylates an *N*-terminal serine, thus modulating the kinetic properties of PEPC (Echevarria, C. and Vidal, J. 2003). Mass spectrometry (MS) was performed to identify different types of phosphorylation sites in the PEPC. In general, MS measures the molecular weight of a protein-based on the mass-to-charge ratio. Based on this concept, MS also can analyse the phosphoproteins. For the analysis, the sample must be loaded in a gaseous state (Li, et al., 1997; Boersema, P. J., et. al., 2009; Mann, M., et. al., 2002). For a more detailed analysis of the phosphate attachment sites and stoichiometry, it is necessary to examine the peptide fragments of the phosphoprotein of interest. The peptides fragments are usually generated by digesting the phosphoprotein with site-specific proteases such as trypsin (McLachlin, D. T., and Chait, B. T. 2001). The peptides formed from the trypsin digestion of proteins are in the form of concentrated supernatant and desalted by purification over miniaturised reverse-phase C_{18} columns before it is analysed by electrospray MS (Mann, M., et al., 2002).

4.9.1 Identification phosphorylation site of PEPC *P. queenslandicum* from in gel digestion.

Before determining the phosphorylation sites analysis by MS, PEPC *P. queenslandicum* was phosphorylated by PKA via *in vitro* phosphorylation and separated by using Phos-Tag™ SDS-PAGE (Fig. 4.12). The phosphorylated band was isolated by using the Phos-Tag™ SDS-PAGE before it was digested with trypsin. The resulting peptides were used to identify the type of phosphorylation sites of PEPC.

From the spectrum of MS, it was revealed that one of the peptides was phosphorylated at the *N*-terminal of PEPC *P. queenslandicum* (Fig. 4.15). The peptide was phosphorylated at the serine residue.

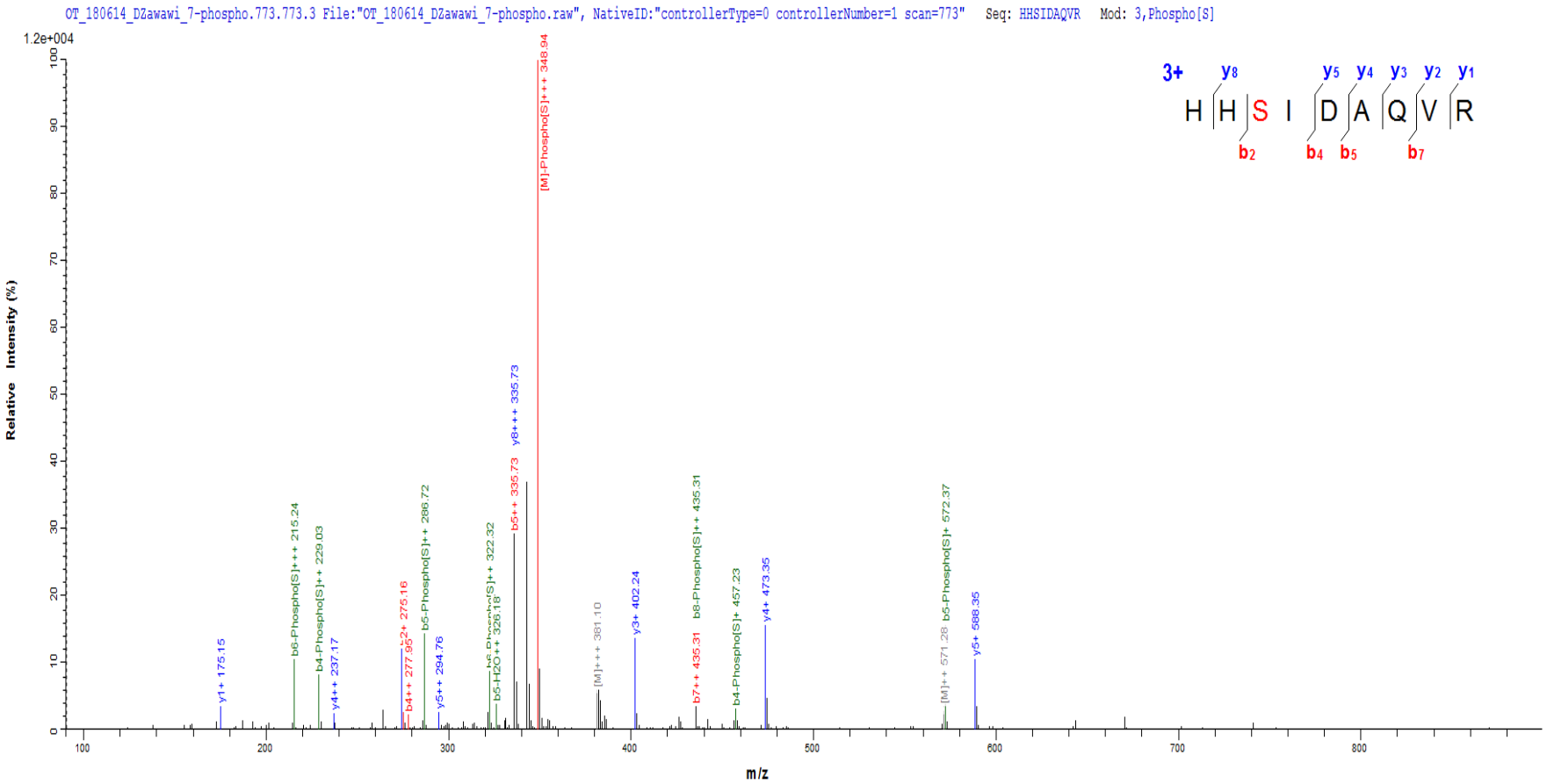

Fig. 4.15:MS/MS spectrum of a triply charged of sequence HHSIDAQVR from PEPC *P. queenslandicum*. The phosphorylation site was localized to the serine (S) in the peptide. The detected b (*N*-terminal) and y (C-terminal) fragment ions are labeled in the spectra.

4.9.2 Identification phosphorylation site of PEPC *P. queenslandicum* by protein digestion in solution.

To obtain more information on the phosphorylation of PEPC, the phosphorylated proteins were identified by using in-solution protein digestion. The disulfide bridges were reduced by using TCEP (Tris (2-carboxyethyl) phosphine), and the free SH-groups was alkylated by iodoacetamide as an alkylation regent. The alkylate procedure was performed in the dark. All preparations aimed to break the disulfide bonds of the protein and to protect the formation of thiols by the dissociation of the disulfide bonds.

Next, the trypsin digestion proceeded in a protein sample for overnight at 37°C. By using C18 resins that can retain the non-polar solutes such as peptides, proteins, and detergents, the digested peptides were desalted to remove salts and urea from the digestion buffer. These resins also removed the SDS from the peptide samples before the mass spectrometry analysis. From the MS spectrum, two peptides were phosphorylated at the *N*-terminus of PEPC P*. queenslandicum* (Fig. 4.16). Both peptides were phosphorylated at the serine residue (Table 4.2).

Table 4.2: The phosphopeptide detected and the phosphorylation site of PEPC P*. queenslandicum.*

Tryptic peptide	Phosphorylation site
HH**S**IDAQVR	serine
LK**S**GDFADEGSATTESNIDETIK	serine

MGSSHHHHHHENLYFQSNAMASSERHHSIDAQVRLLAPGKVSEDDKLVEYDVLLMDR
FLDILQDLHGPGIREFVQDCYELSAEYEGDRNSARLKDLGSRLASLAPADAILVAGSIQH
MLNLANLAEEVQIANRRRNKLKSGDFADEGSATTESNIDETIKRLVDLGKSKEEVFEALK
NQSVDLVLTAHPTQSVRRSLLQKHSRIRNCLTQLNAKDITDDEKQELDEALSREIQAAFR
TDEIRRAQPTPQDEMRYGMSYIHETIWKGVPKFLRRLDTALKNIGIDERLPYNVPLIQFC
SWMGGDRDGNPRVTPEVTRDVCLLARMMAANLYFSGLEELMFELSMWRCNDELRAR
AQEIHSAPKKAAKHYIEFWKQIPLSEPYRVVLGNVRDKLYNTRERARQLLTNEFSDIPEE
LVFSNVQEFLEPLELCYKSLCECGDKTIADGSLLDFLRQVSTFGLSLVKLDIRQESERHT
DVIDAITTHLGIGSYRSWPEDKRQEWLLSELRGKRPLLAPDMPQTEEIADVLGCFRVLAE
LPRDSFGPYIISMATAPSDVLAVELLQRECHVRDPLPVVPLFERLADLQNAPASMERLFS
VDWYLQRINGKQQVMIGYSDSGKDAGRLSAAWQLYRAQEELAQVAKRYGVKLTMFHG
RGGTVGRGGGPSHLAILSQPPDTINGSIRVTIQGEVIEHSFGEEHLCFRTLERFTAATLE
HGMHPPVSPKPEWRKLMDEMAVVATEEYRSIVFREPRFVEYFRSATPETEYGRMNIGS
RPAKRKPKGGIESLRAIPWIFSWTQTRFHLPVWLGVGAAFQYAIKKDSKNIQKLKDMYK
EWPFFRVTIDLLEMVFAKGDPSIAGLYDELLVAADLKPFGEQLRNKYLETQQFLLQIAGH
KEILEGDPYLKQGLRLRNPYITTLNVFQAYTLKLMRDPSFQVKKQPPMSKEFADEKKPA
GLVELNPASEYAPGLEDTLILTMKGIAAGMQNTG

Fig.4.16: Protein amino acid sequence of *P. queenslandicum* encoded by pET -1B.

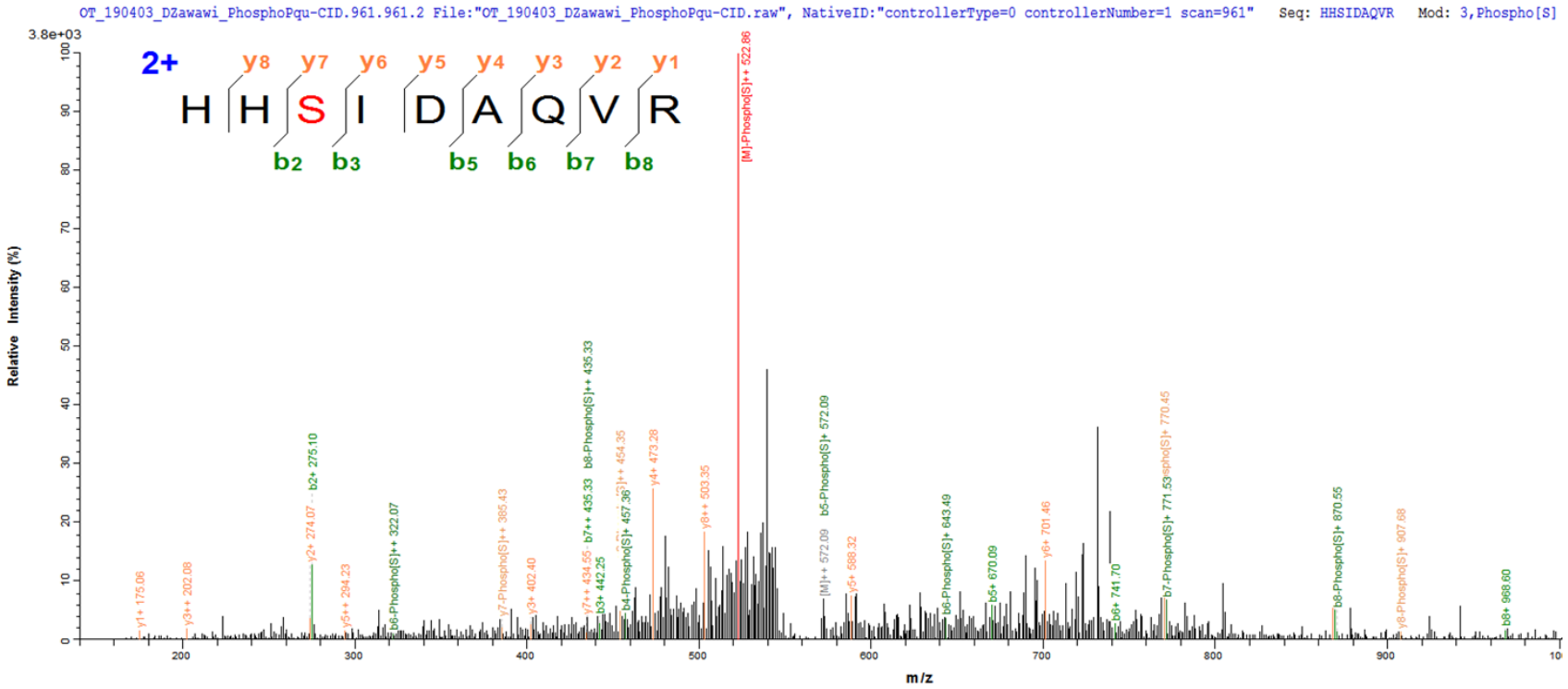

Fig. 4.17: MS/MS spectrum of a doubly charged of sequence HHSIDAQVR from PEPC *P. queenslandicum.* The phosphorylation site was localized to the serine (S) in the peptide. The detected b (*N*-terminal) and y (*C*-terminal) fragment ions are labeled in the spectra.

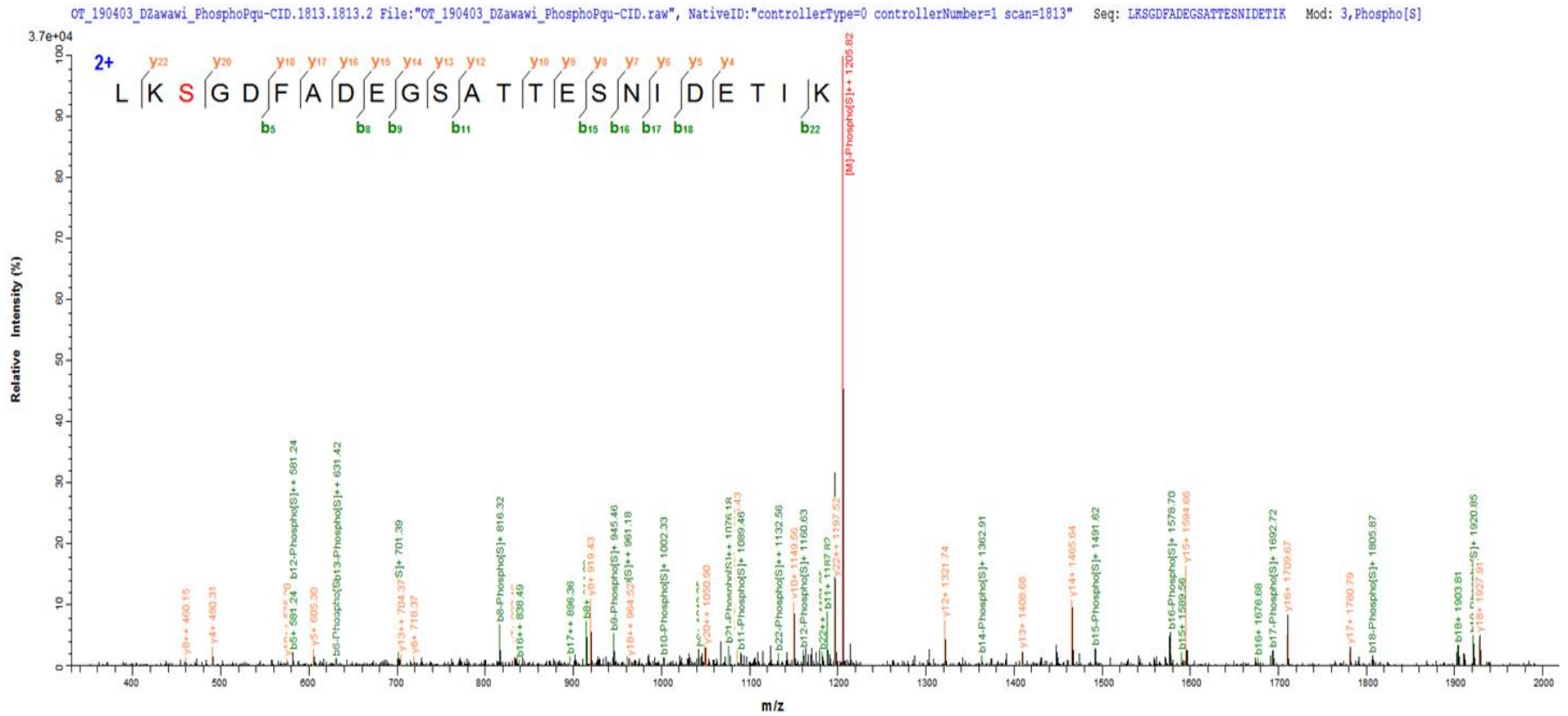

Fig. 4.18: MS/MS spectrum of a doubly charged of sequence LK**S**GDFADEGSATTESNIDETIK from PEPC *P. queenslandicum.* The phosphorylation site was localized to the serine (S) in the peptide. The detected b (*N*-terminal) and y (*C*-terminal) fragment ions are labeled in the spectra.

4.9.3 Identification phosphorylation site of PEPC *P. pygmaeum* by protein digestion in solution.

The phosphorylation sites of PEPC *P. pygmaeum* proteins were identified by using in-solution protein digestion. Reduction, alkylation, trypsin digestion, and peptides extraction were performed as that of PEPC *P. queenslandicum.* From the MS spectrums, six peptides were phosphorylated at the *N*-terminal of PEPC *P. pygmaeum* (Fig. 4.19). All peptides were phosphorylated at the serine residue (Table 4.3).

Table 4.3: The phosphopeptide detected and the phosphorylation site of PEPC *P. pygmaeum.*

No of peptides	Tryptic peptide of PEPC *P. pygmaeum*	Phosphorylation site
1	HQSIDAQLR	serine
2	LLAPGKVSEDDKLVEYDALLVDR	serine
3	GDFADEASATTESDIEETLKR	serine
4	LVSELGK	serine
5	NQTVDLVFTAHPTQSIRRSLLQK	serine
6	KPSGGIESLR	serine

MGSSHHHHHHENLYFQSNAMASSKAPGPVERHQSIDAQLRLLAPGKVSEDDKLVEYDALLVDR
FLDILQDLHGPSLREFVQECYELSAEYEGDRDAARLGELGDRLTGLAPADAIVVASSFSHMLNLA
NLAEEVQIAHRRRNKLKRGDFADEASATTESDIEETLKRLVSELGKSREEVFDALKNQTVDLVFT
AHPTQSIRRSLLQKHARIRNCLTQLYAKDITADDKQELDEALQREIQAAFRTDEIRRTQPTPQDEM
RAGMSYFHETIWKGVPKFLRRVDTALKNIGIDERLPYNAPLIQFSSWMGGDRDGNPRVTPEVTR
DVCLLARMMAANLYFSQIEELMFELSMWRCNDELRVRAEELHRASRKAAKHYIEFWKQIPPNEP
YRVILGYVRDKLYYTRERSRHLLTTGFSEIPEDSAFTNVEEFLEPLELCYRSLCACGDKTIADGSL
LDFLRQVSTFGLSLVKLDIRQESERHTDVLDAITTHLGIGSYREWPEEKRQEWLLSELRGKRPLL
GPDLPQTEEVADVLGTFRVLAELPPDSFGAYIISMATAPSDVLTVELLQRECHVRHPLRVVPLFE
KLADLEAAPAAVARLFSVDWYMDRINGKQEVMIGYSDSGKDAGRLSAAWQLYKAQEELVQVAK
RYGVKLTMFHGRGGTVGRGGGPTHLAILSQPPDTIHGSLRVTVQGEVIEHSFGEEHLCFRTLQR
FTAATLEHGMHPPVSPKPEWRALMDELAVVATEEYRSIVFKEPRFVEYFRSATPETEYGRMNIG
SRPSKRKPSGGIESLRAIPWIFAWTQTRFHLPVWLGFGAAFKHAMKKDIRNIQTLREMYNEWPF
FRVTLDLLEMVFAKGDPGIAGLYDELVVADDLKPFGEQLRNNYVETQQLLLQVAGHKDILEGDPY
LKQRLRLRDPYITTLNVCQAYTLKRIRDPSFQVTAQRPLSKEFADENQPAGLVKLNPASEYAPGL
EDTLILTMKGIAAGMQNTG

Fig. 4.19: Amino acid sequence of *P. pygmaeum* in PEPC as expressed. Phosphorylated peptides are highlighted.

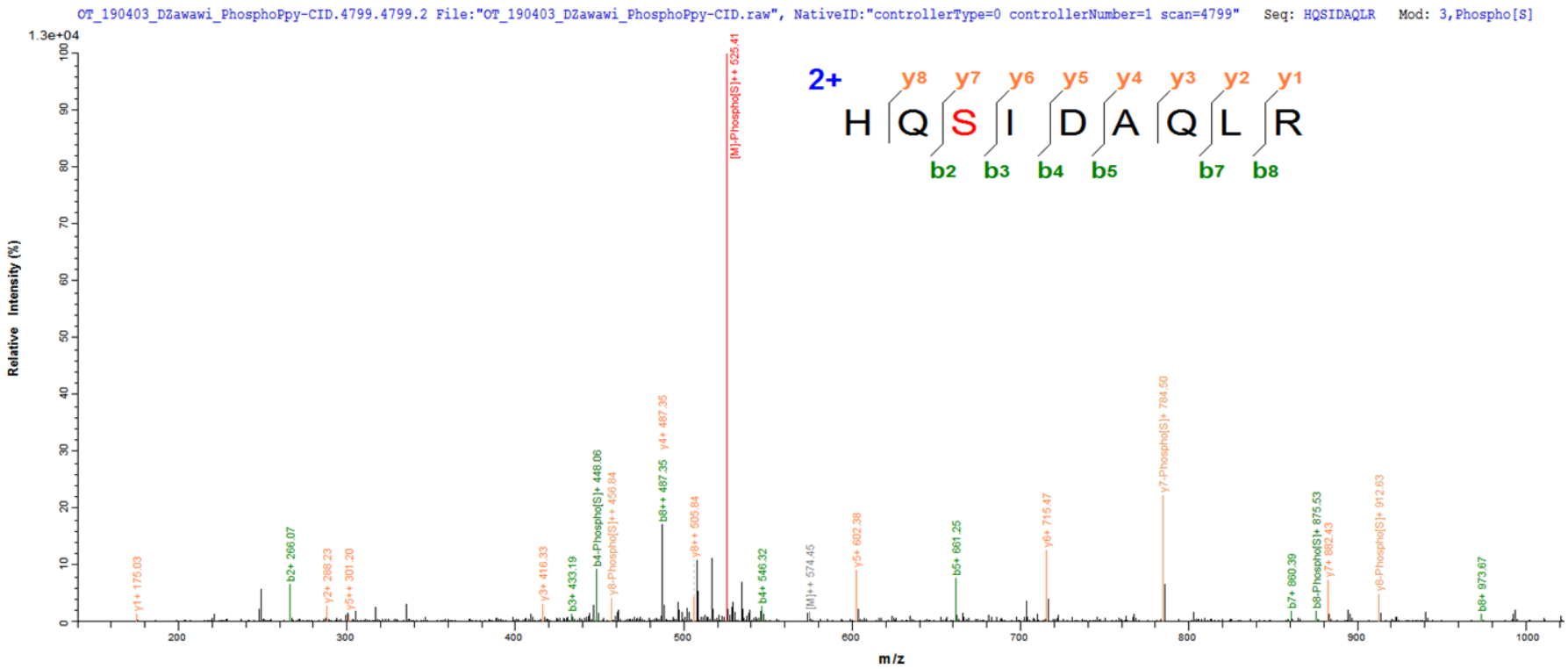

Fig.4.20: MS/MS spectrum of a doubly charged of sequence HQSIDAQLR from PEPC *P. pygmaeum.* The phosphorylation site was localized to the serine (S) in the peptide. The detected b (*N*-terminal) and y (*C*-terminal) fragment ions are labeled in the spectra.

4.10 Discussion.

Phosphorylation of protein is one of the most important post-translational modifications (PTMs), which helps to regulate the protein activity in primary metabolism, cellular processes, and biological functions (Parthibane, V., et. al., 2012; Krishna, R. G., and Wold, F. 1993). Serine, threonine, and tyrosine are some of the most common sites for the reversible phosphorylation that occurs in complex eukaryotic systems (Mann, M., and Jensen, O. N. 2003).

Previous studies have documented that the catalytic subunit of Protein Kinase A (PKA) from the bovine heart (Sigma) can transfer the terminal phosphate of ATP to phosphorylate C4 PEPC, specifically at the target Ser residue near the *N*-terminus (Jiao, J. A., and Chollet, R., 1990; Terada, K., et. al., 1990; Duff, S. M. G. et. al., 1995). Hence, for these peptide-phosphorylation studies, the purified PEPC *P. queenslandicum* and *P. pygmaeum* were phosphorylated with PKA as described in Chapter 2; Section 2.10.2 since purified PEPCK was unavailable (Chapter 3, Section 3.9). A comprehensive analysis of the PEPC protein phosphorylation usually involves the identification of the phosphoproteins and localisation of the phosphorylated residues.

Presently, many tools and techniques have been applied to determine the phosphorylation status of the proteins and peptides. This is because the phosphorylation profile of the proteins plays a prominent role in determining the variety of cellular processes including signal transduction, cell division, cell motility, apoptosis, differentiation, gene regulation, and carcinogenesis (Steinberg, T. H., et. al., 2003). For the most common conventional method, a radioactive isotope of phosphorus, phosphorus-32 (^{32}P), or phosphorous-33 (^{33}P) is usually incorporated into the cellular proteins with radio-labeled ATP before producing radioactive protein. The phosphorylation site (s) of radioactive protein can be detected and quantified by peptide sequencing. Such detection and quantification technique can be quite tedious and involves a considerable amount of radioactivity materials (Lukat, G. S., et. al., 1992; Hess, J. F., et. al., 1988; Buckler, D. R., and Stock, A.M. 2000).

Apart from radioactive isotopes, polyclonal and monoclonal antibodies can be used to detect the phosphorylated residues. From a wide spectrum of analytical techniques like enzyme-linked immunosorbent assay (ELISA), immunoblotting, or immunocytochemistry, the phosphopeptides will be measured in terms of fluorescence, luminescence, or polarisation signals. These methods generally require specific antibody-based reagents to express the functional monoclonal antibodies. Poor selection of antibodies can affect the outcome of the assay in some proteins (Kinoshita, E., et. al., 2012).

In the protein category, sodium dodecyl sulphate-polyacrylamide gel electrophoresis (SDS-PAGE) continues to be the most accepted and widespread method used for high-resolution separation of a protein mixture (Ong, S-E., and Pandey, A., 2001). The technique can estimate the molecular weights of the proteins and determines the purity level of the purified target protein (Weber, K., et. al., 1971; Chambach, A., and Rodbard, D. 1971).

To visualise the protein, SDS-PAGE gel can be stained with Coomassie blue to identify the type of protein of interest. Unfortunately, the Coomassie blue stain is unable to detect phosphoprotein. Thus, a fluorescence-

based detection technology, known as Pro-Q® Diamond phosphoprotein gel stain (Molecular Probes, Inc.), was applied for direct detection of phosphoprotein in polyacrylamide gels (Martin, K., et. al., 2003; Schulenberg, B., et. al., 2003). This phosphoprotein gel stain is a ready-to-use formulation, which was developed based on the principles of immobilised metal affinity chromatography for phosphopeptides. It utilises a fluorophore-conjugated metal chelating moiety in a solution which contains a metal ion, salts, and a water-miscible organic solvent that buffered to a pH of 4 (Agnew, B., et. al., 2006). By using Pro-Q® Diamond dye in the determination of phosphoprotein, one can avoid the usage of harmful radioactive materials, tedious electroblotting, or expensive antibodies (Schulenberg, B., et. al., 2004).

From figure 4.6 and figure 4.11, both PEPC *P. queenslandicum* and *P. pygmaeum* can be phosphorylated by PEPCK and PKA based on their gel image stained with Pro-Q® Diamond Phosphoprotein (Invitrogen). The unphosphorylated PEPC can be served as a control, while the phosphorylated PEPC without ATP demonstrated less or no fluorescence intensity, which suggests that no phosphorylation occurred. The Pro-Q® Diamond staining of PEPC *P. queenslandicum* from each assay showed significant enrichment of phosphoproteins, with PEPC *P. queenslandicum* had the higher overall intensity of phosphoprotein staining after incubated in two hours under a PEPC *P. queenslandicum* to PKA ratio of (1: 0.1) (Figure 4.5; Appendix H.ii, Table 1). For the Pro-Q® Diamond staining assay of PEPC *P. pygmaeum*, both *P. pygmaeum* to PKA ratio of 12:1 and 30:1 gave slightly lower phosphoprotein staining in the presented gel as compared to the *P. pygmaeum* to PKA ratio of 6:1 (Fig. 4.10). To determine the total protein content that had been loaded in the SDS-PAGE gel, SYPRO Ruby stain (Molecular Probes™ Invitrogen) was applied as it is one of the most commonly used total-protein detection technique.

Despite it has multiple advantages, the combination of Pro-Q® Diamond and SYPRO Ruby stains did not answer the question of whether all the protein had been phosphorylated or not. To address such a problem, the phosphate affinity electrophoresis technique was used as an alternative approach to isolate phosphorylated protein from the nonphosphorylated protein. In this method, the SDS-PAGE gels were copolymerised with a novel phosphate-binding tag molecule, {1,3-bis[bis(pyridin-2-ylmethyl)amino]propan-2-olato dizinc(II) complex} or also known as Phos-Tag™. The gel was stained with Coomassie Blue. Kinoshita, E., et. al., (2006) developed this method as a novel approach for the protein phosphorylation analysis.

The acrylamide pendant tag or Phos-Tag™ can slow down the migration of phosphorylated proteins by forming complex phosphate groups in the presence of Zn^{2+} (Kinoshita E., et. al., 2011, 2012). Hence, two or more separate bands were produced on the phosphorylation sites of the target protein (Kinoshita, E., et. al., 2006). Commercially known as Phos-Tag™, this dinuclear metal complex with two equivalents of Zn^{2+} (Kinoshita, E., and Kinoshita-Kikuta, E. 2011) or Mn^{2+} (Kinoshita-Kikuta, E., et. al., 2007), forms a specific noncovalent complex with the phosphomonoester dianion under a neutral pH.

The Phos-Tag™ method can be applied to detect the number of phosphorylation site(s) on the target protein and examine the differential phosphorylation which may occur in multiple residues of a single protein (Kinoshita-Kikuta E, et. al., 2012). If the target protein was fully phosphorylated by protein kinase and the protein has only

a single phosphorylation site, one migration bands on a Phos-Tag™ SDS-PAGE gel will be detected. If the kinase activity occurs at two or more residues of the protein, two or more migration bands may be observed with the assumption that all proteins were phosphorylated. In this work, phosphorylated PEPC *P. queenslandicum* and *P. pygmaeum* were observed as one single migration band from Phos-Tag™ SDS-PAGE after it was phosphorylated by PKA. Thus, the PEPCs have only one phosphorylation site. Besides PEPC, the Phos-Tag™ SDS-PAGE has been shown to selectively interact with other phosphorylated peptides or proteins containing phospho-Serine, phospho-Threonine, phospho-Tyrosine, and phospho-His residues from other types of protein (Kinoshita, E. et. al., 2006; Yamada, S. et. al., 2007).

To obtain well-separated bands, this method requires many parameters to be optimized, such as the percentage of acrylamide and the concentration of Phos-Tag™. It also requires a longer run time as compared to the conventional SDS-PAGE. However, this technique offers several advantages: (i) radioactive isotopes and chemical labels are unnecessary for phosphoprotein detection, (ii) the procedure is very similar to the conventional SDS-PAGE, (iii) the phosphate-binding potency is independent of the nature of the phosphorylated amino acid, (iv) can detect a vast number of phospho-histidine or phospho-aspartic acid intermediates from the phosphorylation reaction, (v) other analysis such as MS or immunoblotting can be applied once the gel is stained, (vi) several phosphoprotein species with the same number of phosphate groups can be separated, and (vii) the time course of the quantitative ratio of phosphorylated to non-phosphorylated proteins can be determined (Kinoshita, E., et. al., 2004; Kinoshita, E., et. al., 2012).

Since the Phos-Tag™ SDS-PAGE can only determine the number of phosphorylation sites and the Pro-Q® Diamond can bind directly to the phosphate moiety of phosphoproteins regardless of which amino acid residue is phosphorylated (Agrawal, G. K., and Thelen, J. J. 2009), mass spectrometry (MS) analysis was performed to determine at which residues the reaction occurs. This is because mass spectrometry (MS) seems to be the perfect method to analyse a large number of post-translational modifications (PTMs) because it is a rapid, sensitive, and nearly universal tools for the determination of PTMs (Neubauer, G., and Mann, M. 1999; Witze, E. S. 2007). This method can determine the modifications like the type and sites of the single purified protein, as well as capable to detect the type of protein structure (Aebersold, R., and Mann, M. 2003; Witze, E. S. 2007). One of the most common post-translational modifications of protein is the phosphorylation of serine, threonine, and tyrosine residues (Qiagen, 2011). MS analysis can be useful in many phosphorylation protein studies since this method allows the detection and mapping of phosphoprotein in a single or complex mixture. Besides, MS also provides a semi-quantitative measure of the phosphorylation state for an individual protein (Vener, A. V., et. al., 2001). To analyse the PTMs using MS, the essential key is to understand the reactivities of the solution and gas-phase as peptides with different compositions will cause a significant difference in the chemical behaviour of amino acids and other functional groups (Witze, E. S. 2007). Highly sensitive MS analysis can detect both phosphorylated and nonphosphorylated proteins simultaneously and measures the stoichiometry directly without an exogenous tracer (Vener, A. V., et. al., 2001) .

Various approaches have been proposed to determine the protein phosphorylation sites by using the MS method alone or a combination of MS and other methods such as Edman degradation and isolation of individual peptides by HPLC followed by MS sequencing of the fractions off-line (Palczewski, K., et. al., 1992; Taniguchi, H., et. al., 1994; Lombardo, C. R. et.al., 1995; Gold, M. R. et. al., 1994; Neubauer, G., and Mann, M. 1999).

From the MS spectrum, it was revealed that only one peptide was phosphorylated at the *N*-terminal of PEPC *P. queenslandicum* (Fig. 4.15) at the serine residue from the in-gel digestion of Phos-Tag™ SDS-PAGE gel. Besides, the MS spectrum also showed that two peptides were phosphorylated at the same *N*-terminal of PEPC P*. queenslandicum* (Fig. 4.17 dan 4.18) from the solution digestion. Both were phosphorylated at the expected serine residue (Table 4.2). Six peptides were phosphorylated at the *N*-terminal of PEPC *P. pygmaeum* (Fig. 4.19). As expected, all peptides were phosphorylated at the serine residue (Table 4.3). In plants, the occurrence of phosphorylation on serine, threonine, and tyrosine residues is about 75: 20: 5 (Huber, S. C. 2007).

In-gel digestion of samples with trypsin was performed in the sample preparation since it was challenging to analyse phosphorylated proteins derived from the crudes samples that may contain other proteins or contaminants. Therefore, Phos-Tag™ SDS-PAGE gel was performed in PEPC *P. queenslandicum* to separate non-phosphorylated and phosphorylated proteins. One migration band was detected, with the assumption that all PEPC was phosphorylated with a single phosphorylation site. From the MS analysis, it was revealed that the PEPC *P. queenslandicum* had only one phosphorylation site at the *N*-terminal, specifically at the serine residue (HH**S**IDAQVR). Two phosphorylation sites were detected when the PEPC *P. queenslandicum* from *in vitro* phosphorylation assay was phosphorylated with PKA and was precipitated with methanol and trypsin digestion. In this procedure, separation of the phosphorylated and non-phosphorylated PEPC *P. queenslandicum* by the phosphate affinity-Phos-Tag™ SDS-PAGE was unsuccessful. One peptide was similar to that of detected from in-gel digestion, HH**S**IDAQVR. The additional peptide detected was LK**S**GDFADEGSATTESNIDETIK. Both peptides were located at the *N*-terminal of PEPC and the phosphorylation sites were detected at the serine residue. The results demonstrate that the phosphorylation of PEPC *P. queenslandicum* was compatible with the PEPC from other C_4 species such as sorghum and maize (Table 4.4).

Table 4.3: Phosphorylation site from maize and sorghum by native kinase PEPCK and mammalian cyclic AMP-dependent protein kinase, Protein Kinase A (PKA).

Study	Plant	Enzyme	Phosphorylation site
Duff, S.M. et. al., (1995). *The FEBS Journal*, 228(1); 92-95.	C_4 species, Sorghum	PKA	Serine 8, *N*-terminal
Terada, K., et. al., (1990). *FEBS Letters*, 259(2); 241-244.	C_4 species, Maize	PKA	Serine 15, *N*-terminal
Jiao, J. A., and Chollet, R. (1990). *Arch Biochem Biophys*, 283(2); 300-305.	C_4 species, Maize	PEPCK	Serine 15, *N*-terminal
Jiao, J. A., et. al., (1991). *Plant Physiology*, 96(1); 297-301.	C_4 species, Sorghum	PEPCK	Serine 8, *N*-terminal

PEPC plays a crucial role in the photosynthesis process of C_3 and CAM plants (Hatch, M. D. 1992). Several isoforms of PEPC are involved in the physiological process of plants, with different catalytic and regulatory properties (Latzko, E., and Kelly, G. J. 1983). In CAM plants, the photosynthetic PEPC is responsible for the primary CO_2 fixation and is diurnally regulated by reversible phosphorylation (Rajagopalan, A. V., et. al., 1994; Terada, K., et. al., 1990; Ueno, Y., et. al., 2000. In C_3 plants, likes in C_4 and CAM species, it has been shown that illumination leads to PEPC phosphorylation *in vivo* and gene expression in response to light (Chollet, R., et. al., 1996). Many studies also have shown that the PEPCK activity was the primary mechanism that controlled the PEPC phosphorylation in C_3 plants like wheat, soybean, tobacco leaves, and barley seeds (Duff, S. and Chollet, R. 1995; Zhang, X.-Q., et. al., 1995; Li, B., et. al., 1996; Osuna, L. et. al., 1999), despite the mechanism controlling the kinase activity remains poorly understood. Small PEPCK gene families have been identified in many C_3 plant genomes such as PPCk1 and PPCk2 in Arabidopsis (Nimmo, H. G. 2003).

The regulatory serine was located in the conserved, plant-specific, *N*-terminal domain at each enzyme subunit of PEPC in C_3 species (Gousset-Dupont, A., et. al., 2005). *P. pygmaeum*, a C_3 species have shown that the phosphorylation was occurred at the serine residues, with six different types of phosphopeptides: HQ**S**IDAQLR, LLAPGKV**S**EDDKLVEYDALLVDR, GDFADEA**S**ATTESDIEETLKR, LV**S**ELGK, NQTVDLVFTAHPTQ**S**IRRSLLQK, and KP**S**GGIESLR. All phospho-peptides were detected at the N-terminal of PEPC and only KP**S**GGIESLR peptide were detected at *C*-terminal of PEPC protein (Table 4.2). It was also found out that the phosphorylation sites of PEPC *P. pygmaeum* were located at the *C*-terminal of the protein.

4.11 Conclusion

Since protein phosphorylation has a significant role in regulating a wide range of cellular processes, thus it is essential to understand the specificity of phosphorylation. In this chapter, a combination of Pro-Q® Diamond phosphoprotein stain with SYPRO Ruby protein gel stain was performed to allow fluorescence detection of phosphorylated PEPC protein in 1-D gels. Phosphate affinity Phos-Tag™ technique was used to characterise the

phosphorylation status of PEPC and it produced results similar to that obtained from established protocols. A single major migration band was detected from Phos-Tag™ SDS-PAGE gel in both PEPC *P. queenslandicum* and *P. pygmaeum,* which suggests complete phosphorylation of all PEPCs by PKA, with only one phosphorylation site. In summary, these results indicate that the staining method presented in this study is highly sensitive, simple, economical, and safe for a detailed analysis of the phosphorylation status of proteins. From the mass spectrophotometric analysis, it was revealed that the phosphorylation site(s) of PEPC *P. queenslandicum* and *P. pygmaeum* were at the same serine residue. These results show that the PKA can react properly/as it has to act. Two and six phosphopeptides were detected in PEPC *P. queenslandicum* and *P. pygmaeum*, respectively. Since both peptides are yet to be identified in the literature, hence analysis was performed to investigate how these peptides involve in this phosphorylation reaction. Lastly, a comprehensive model that clarifies the role of regulatory phosphorylation of PEPC *P. queenslandicum* and *P. pygmaeum* is highly sought-after.

CHAPTER 5

KINETIC BEHAVIOUR OF PHOSPHORYLATED AND NON-PHOSPHORYLATED PEPC

5.1 The enzyme and inhibition activity by malate or aspartate from phosphorylated and non-phosphorylated PEPC.

In C_4 photosynthesis, the first reaction to assimilate atmospheric CO_2 into the mesophyll cell is the irreversible carboxylation of PEP (phosphoenolpyruvate) to yield OAA and inorganic phosphate catalysed by PEPC (Hatch, M. D. 1992). The biological significance of this reaction is catalysed by photosynthetic PEPC in C_4 plants, which underlined by the complexity of its allosteric regulation (González-Segura, L., et. al., 2018). Many factors contribute to the regulation of the photosynthetic PEPC enzyme and one that is well characterised is its allosteric inhibition by downstream metabolites.

The allosteric inhibitors for PEPC such as L-malate (Jiao, J. A., and Chollet, R. 1992) and aspartate (Huber, S. C., and Edwards, G. E. 1975) are dicarboxylic acids which reduce its catalytic activity. Meanwhile the positive allosteric effectors like glucose-6-phosphate (Doncaster, H. D., and Leegood, R. C. 1987) and glycine (Nishikido, T., and Takanashi, H. 1973; Bandarian, V., et. al., 1992) activate the PEPC reaction. In addition, the substrate PEP can also act as a positive allosteric activator (Rodríguez-Sotres, R., and Muñoz-Clares, R. A. 1990; Tovar-Méndez, A., et. al., 1998). Reversible phosphorylation of a serine residue effectively activates the PEPC (Shane, M. W., et. al., 2013). Phosphorylation of an *N*-terminal serine residue not only makes PEPC less sensitive to inhibition by L-malate, but become more sensitive to activation by glucose-6-phosphate (Duff, S. M. G., et. al., 1995; Echevarria, C., et. al., 1994).

In order to analyse the importance of phosphorylation to PEPC feedback inhibitor sensitivity, a comparison was made between phosphorylated and non-phosphorylated PEPC in C_4 and C_3 plant species. The enzyme activity of PEPC *P. queenslandicum* and *P. pygmaeum* were determined by the phosphoenolpyruvate (PEP) kinetic assay previously described (Chapter 2; Section 2.16 and 2.17) and the effect of phosphorylation on sensitivity to bicarbonate was assayed as described above (Chapter 2; Section 2.19). The sensitivity of phosphorylated PEPC to inhibition by malate and aspartate can be determined either by a kinetic assay (Chapter 2; Section 2.16 and 2.17) or through determination of the inhibition constant (K_i) using the hydrophobic fluorescent probe, ANS (8-anilino-1-naphthalenesulfonic acid) (Chapter 2; Section 2.20). The range of malate and aspartate concentrations used in this study will be varied to encompass the inhibitor concentration which causes 50 % inhibition of initial PEPC activity (IC_{50}). The corresponding IC_{50} values will be estimated from a plot of PEPC activity vs malate concentration.

5.2.1 PEPC enzyme kinetic activity from PEP assay.

Phosphorylated and non-phosphorylated PEPC has been assayed by coupling the enzyme to a second enzyme, malate dehydrogenase (MDH) that will produced oxaloacetate (OAA) from phosphoenolpyruvate (PEP). OAA then was converted into malate by malate dehydrogenase (MDH) which also consumed NADH. PEPC activity (NADH consumption rate) was measured spectroscopically at 340 nm. PEPC activity was expressed as the amount of enzyme extract which catalyzes the transformation of 1 µmol of substrate per minute and per µmolar of protein. Assays performed with the presence of the inhibitors malate and aspartate were performed at limiting and saturating PEP and were initialled by the addition of PEPC. Aspartate and malate are fast acting inhibitors and PEPC did not need to be pre-incubated prior to assay initiation (Wedding, R. T., Black, M. K., and Meyer, C. R. 1989).

Phosphorylation increases the enzyme activity of PEPC from the C_4 plant species, *P. queenslandic*um based on the $k_{cat}s^{-1}$ value, which is 73 ± 4 for phosphorylated PEPC and 24 ± 1 for non-phosphorylated PEPC (Table 5.1). These values were obtained from an investigation of the effect of malate on the enzyme. A similar trend was observed when the inhibition by aspartate was being assayed although the values of k_{cat} were slightly lower, possibly reflecting loss of activity on storage. In this case, the enzyme activity (k_{cat} (s^{-1})) of the phosphorylated PEPC from *P. queenslandicum* is 32 ± 2, somewhat higher than that of non-phosphorylated PEPC from *P. queenslandicum* with a k_{cat} (s^{-1}) value is 21 ± 1. Although the phosphorylated enzyme shows a higher activity when compared to the non-phosphorylated one, the K_m value for PEP is not significant.

In the aspartate assays, the K_m value for non-phosphorylated PEPC *P. queenslandicum* was 3.5 ± 0.6 mM, and for phosphorylated PEPC, the K_m value is lower, which is 2.5 ± 0.7 mM PEP. In the context of the malate assays, a K_m value for non-phosphorylated PEPC from *P. queenslandicum* of 3.8 ± 0.3 mM and for phosphorylated PEPC of 5.0 ± 1.0 mM was observed (Fig. 5.1 A and B). Taken together these results suggest that there is no evidence that the K_m for PEP changes on phosphorylation.

It was observed that from results in Table 5.1, phosphorylation of PEPC does not increase the enzyme activity of PEPC from *P. pygmaeum* , the C_3 grass species based on the k_{cat} value observed in the aspartate or malate inhibition assays. From the malate assays, the k_{cat} (s^{-1}) for the non-phosphorylated PEPC *P. pygmaeum* is 12 ± 2 and for phosphorylated is 12 ± 1, showing no difference between non-phosphorylated and phosphorylated PEPC *P. pygmaeum*. From aspartate assay, the k_{cat} (s^{-1}) for non-phosphorylated PEPC *P. pygmaeum* is 32 ± 2 and for phosphorylated is 20 ± 1, suggesting that the non-phosphorylated PEPC *P. pygmaeum* gave higher activity compare to phosphorylated.

There is no difference at all between the K_m values of the non-phosphorylated and phosphorylated PEPC from *P. pygmaeum* for both inhibitors (Fig. 5.1 C and D). From the aspartate assay, the K_m value for non-phosphorylated PEPC *P. pygmaeum* is 0.18 ± 0.03 mM and for phosphorylated is 0.16 ± 0.03 mM. From the malate assay, the K_m value for the non-phosphorylated PEPC *P. pygmaeum* is 0.19 ± 0.07 mM, and phosphorylated is 0.20 ± 0.03 mM.

Comparing the enzymes from different species of plants, PEPC`s highest activity of was observed in C_4 species, phosphorylated PEPC *P. queenslandicum* (73.32 ± 4.44), but the apparent K_m^{PEP} (mM) did not change much compared to nonphosphorylated *P. queenslandicum*. In *P. pygmaeum*, the phosphorylated form of PEPC appears to have the same the apparent K_m^{PEP} (mM) as non-phosphorylated PEPC. In conclusion phosphorylation of a C_3 plant, *P. pygmaeum*, did not increase the activity.

Table 5.1: Summary of PEPC kinetic parameters from *P. queenslandicum* and *P. pygmaeum* in non-phosphorylated and phosphorylated form. Kinetic parameters were obtained from enzyme assay as described under Chapter 2: Section 2.17 and 2.18. The kinetic parameters (K_{cat} (s^{-1}), K_m^{PEP} (mM)) were determined using non-linear regression analysis. The K_{cat} (s^{-1}) value was estimated by the Equation 1. The K_m values are given in mM of PEP. The phosphorylated PEPCs were prepared as described under Chapter 2; Section 2.8.2 and 2.8.4.

PEPC Species	Type of assay	K_{cat} (s^{-1})	K_m^{PEP} (mM)	(K_{cat}/K_m^{PEP}) / ($s^{-1}M^{-1}$)
Non-phosphorylated *P. queenslandicum*	Aspartate	20.80 ± 1.11	3.50 ± 0.64	5.01 ± 0.77
	Malate	24.53 ± 0.59	3.77 ± 0.31	6.51 ± 0.11
Phosphorylated *P. queenslandicum*	Aspartate	32.20 ± 2.53	2.50 ± 0.74	15.12 ± 1.7
	Malate	73.32 ± 4.44	5.05 ± 0.95	14.34 ± 0.50
Non-phosphorylated *P. pygmaeum*	Aspartate	31.66 ± 2.32	0.18 ± 0.03	176.31 ± 19.1
	Malate	12.06 ± 1.59	0.19 ± 0.07	66.94 ± 1.66
Phosphorylated *P. pygmaeum*	Aspartate	19.75 ± 1.25	0.16 ± 0.03	125.46 ± 6.85
	Malate	11.66 ± 0.65	0.20 ± 0.03	57.93 ± 3.63

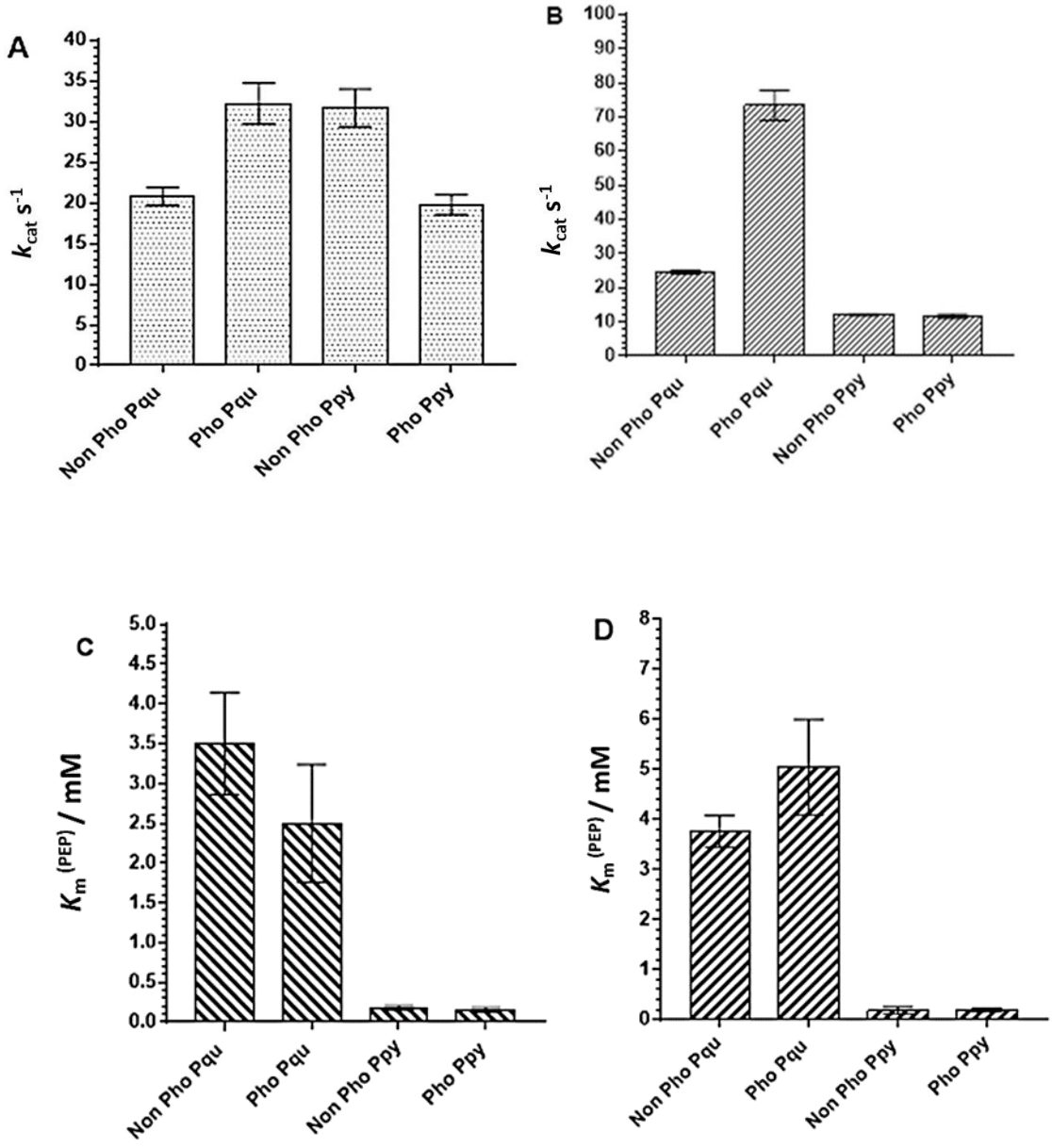

Fig. 5.1: Comparison of PEPC activity in aspartate (A) and malate (B) assay between non-phosphorylated and phosphorylated *P. queenslandicum* and *P. pygmaeum*. Phosphorylation effect on PEPC *P. queenslandicum* and *P. pygmaeum* kinetic parameter (K_m^{PEP} (mM)) from aspartate (C) and malate (D) assay.

5.2.2 Inhibition of PEPC by malate and aspartate.

The effect of phosphorylation on PEPC *P. queenslandicum* and *P. pygmaeum* from malate and aspartate inhibition assay was stated in Table 5.2 , 5.3 and Figure 5.4 for both limiting and saturating PEP. In this study, we are concerned with the concentration of the inhibitors malate and aspartate required to inhibit the enzyme activity of PEPC. The non-competitive inhibition constant (K_{IU}) was determined from the secondary plot of k_{cat} against inhibitor concentration. The competitive inhibition constant (K_{IC}) was determined from the secondary plot of k_{cat}/K_m against inhibitor concentration.

When PEP is limiting, non-phosphorylated PEPC *P. queenslandicum* is more sensitive to malate inhibition, as indicated by a lower K_{IC} value (K_{IC}^{Malate} (mM) = 12) when compared to phosphorylated PEPC which is less sensitive (K_{IC}^{Malate} (mM) = 33) (Appendix L; Fig. L. (A.ii), Table 5.2). In the saturating PEP, non-phosphorylated PEPC *P. queenslandicum* shows a lower sensitivity to malate inhibition as indicated by a high K_{IU} value (K_{IU}^{Malate} (mM) = 156) when compared to phosphorylated PEPC that shows a high sensitivity to malate (K_{IU}^{Malate} (mM) = 68) (Appendix L; Fig. L. (A.i), Table 5.2). In *P. pygmaeum*, phosphorylated PEPC is less sensitive to malate (K_{IC}^{Malate} (mM) = 3) in limiting PEP compared to the non-phosphorylated (K_{IC}^{Malate} (mM)=2) (Appendix L; Fig. L. (C.ii), Table 5.2). At saturating PEP the same pattern is observed, with phosphorylated PEPC from *P. pygmaeum* less sensitive to malate (K_{IU}^{Malate} (mM) = 184) than the non-phosphorylated form (K_{IU}^{Malate} (mM) = 124) (Appendix L; Fig. L. (C.i), Table 5.2). In comparing malate inhibition between C_4 and C_3 species, *P. queenslandicum* (C_4) phosphorylated PEPC showed least sensitivity to malate, followed by non-phosphorylated one, phosphorylated PEPC *P. pygmaeum* (C_3) and non-phosphorylated PEPC *P. pygmaeum* (C_3) showed high sensitivity to malate in limiting PEP (Table 5.2).

Phosphorylation of PEPC *P. queenslandicum* does not affect aspartate inhibition by saturation of PEP (K_{IU}) due to the unreasonably high K_{IU} value of both non-phosphorylated PEPC *P. queenslandicum* ($K_{IU}^{Aspartate}$ (mM) =1479) and phosphorylated PEPC ($K_{IU}^{Aspartate}$ (mM)=1473). These results clearly indicate that for saturation of PEP, uncompetitive inhibition is insignificant (Appendix L; Fig. L. (B.i); Table 5.2). However, with limiting PEP, phosphorylation of PEPC *P. queenslandicum* results in less aspartate sensitivity ($K_{IC}^{Aspartate}$ (mM) = 97) than the non-phosphorylated PEPC ($K_{IC}^{Aspartate}$ (mM) = 67) (Appendix L; Fig. L. (B.ii); (Table 5.2).

In saturating PEPC, non-phosphorylated PEPC *P. pygmaeum* shows the K_{IU} value that is estimated at 331 mM aspartate ($K_{IU}^{Aspartate}$ / mM = 331) and the result is insignificant (Appendix L; Fig. L. (C.i); Table 5.2). However, when PEP is limited PEP, the phosphorylated PEPC *P. pygmaeum* shows low aspartate inhibition ($K_{IC}^{Aspartate}$(mM) = 10) when compared to non-phosphorylated PEPC ($K_{IC}^{Aspartate}$ (mM) = 7) (Appendix L; Fig. L. (C.ii); Table 5.2).

There was no inhibition of aspartate in saturating PEP (K_{IU}) between C_3 (*P. pygmaeum*) and C_4 (*P. queenslandicum*) either in the phosphorylated or non-phosphorylated enzyme. However, in both cases the phosphorylation of PEPC demonstrate less aspartate sensitivity when limiting the PEP (K_{IC}) (Fig. 5.2; C, D.i and D.ii).

Table 5.2: Type of inhibition and inhibition constants for L-malate of PEPC *P. queenslandicum* and *P. pygmaeum.* Kinetic parameters were obtained from enzyme assay as describe under Chapter 2; Section 2.17 and 2.18 . PEPCs were assayed with at least six different concentrations of the inhibitor L-malate. The kinetic parameters (K_{cat} (s^{-1}), K_{cat}/K_m, K_{IU}^{Malate} (mM), K_{IC}^{Malate} (mM) were determined using non liner regression analysis. The K_{cat} (s^{-1}) value were estimated by the Equation 1. The K_{IU} and K_{IC} values are given in mM malate. The phosphorylated PEPCs were prepared as described under section Chapter 2; Section 2.8.2 and 2.8.4.

PEPC species	**K_{cat} (s^{-1})**	**K_{IU}^{Malate} (mM)**	**(K_{cat}/K_m^{PEP}) / ($s^{-1}M^{-1}$)**	**K_{IC}^{Malate} (mM)**
Non-phosphorylated *P. queenslandicum*	24.22 ± 1.82	156.47 ± 47.6	6.51 ± 0.11	11.90 ± 0.68
Phosphorylated *P. queenslandicum*	76.51 ± 6.5	68.44 ± 18.8	14.34 ± 0.50	32.52 ± 3.37
Non-phosphorylated *P. pygmaeum*	10.95 ± 0.43	123.85 ± 37.7	66.94 ± 1.66	1.95 ± 0.16
Phosphorylated *P. pygmaeum*	10.43 ± 0.66	183.98 ± 11	57.93 ± 3.63	3.08 ± 0.63

Table 5.3: Type of inhibition and inhibition constants for L-aspartate of PEPC from *P. queenslandicum* and *P. pygmaeum.* Kinetic parameters were obtained from enzyme assay as describe under "Materials and Method". PEPCs were assayed with at least six different concentrations of the inhibitor L-malate. The kinetic parameters (K_{cat} (s^{-1}), K_{cat}/K_m, $K_{IU}^{Aspartate}$ (mM), $K_{IC}^{Aspartate}$ (mM) were determined using non liner regression analysis. The K_{cat} (s^{-1}) value was estimated by the Equation 1. The K_{IU} and K_{IC} values are given in mM malate. The phosphorylated PEPCs were prepared as described under section Chapter 2; Section 2.8.2 and 2.8.4.

PEPC species	**K_{cat} (s^{-1})**	**$K_{IU}^{Aspartate}$ (mM)**	**(K_{cat}/K_m^{PEP}) / ($s^{-1}M^{-1}$)**	**$K_{IC}^{Aspartate}$ (mM)**
Non-phosphorylated *P. queenslandicum*	24.43 ± 3.31	1479.3 ± 5.82 X 10^3	5.01 ± 0.77	67.20 ± 42.7
Phosphorylated *P. queenslandicum*	32.75 ± 0.59	1472.5 ± 767	15.12 ± 1.7	96.99 ± 50.8
Non-phosphorylated *P. pygmaeum*	38.25 ± 3.98	331.27 ± 303	176.31 ± 19.1	6.99 ± 2.36
Phosphorylated *P. pygmaeum*	21.60 ± 1.37	N.A	125.46 ± 6.85	10.03 ± 1.65

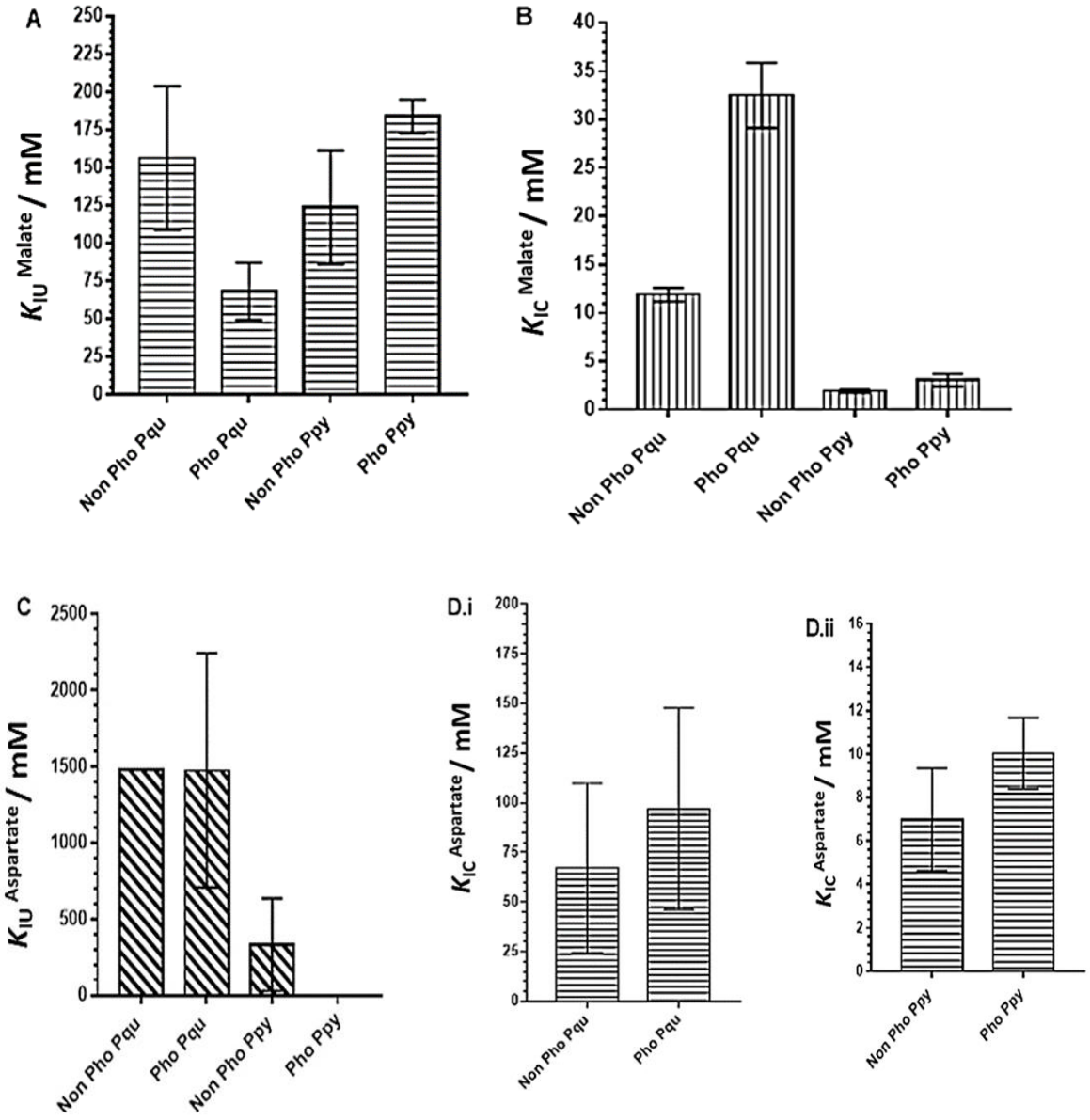

Fig. 5.2. Effect of malate and aspartate on non-phosphorylated and phosphorylated PEPC of *P. queenslandicum* and *P. pygmaeum.* Inhbition activity is expressed by the concentration of malate or aspartate in mM to inhibit activity of PEPC enzyme. (A) Uncompetitive inhibition of malate (B) Competitive inhibition of malate (C) Uncompetitive inhibition of malate (D.i) Competitive inhibition of aspartate in PEPC *P. queenslandicum*; (D.ii) Competitive inhibition of aspartate in PEPC *P. pygmaeum.*

5.3. Bicarbonate specificity of PEPC *P. quuenslandicum* and *P. pygmaeum*.

The specificity of PEPC to bicarbonate in phosphorylated and non-phosphorylate form was determined by the reactions of PEPC coupled to the malic dehydrogenase (MDH). The background bicarbonate in the water and tricine buffer were reduced by sparging with nitrogen gas. Assays were conducted using various concentrations of bicarbonate from freshly prepared potassium bicarbonate ($KHCO_3$).

The enzyme activity (k_{cat} (s^{-1})) for both phosphorylated (k_{cat} (s^{-1}) = 25) and non-phosphorylated PEPC from *P. queenslandicum* (k_{cat} (s^{-1}) = 24) showed almost similar rate at saturating bicarbonate in Tricine buffer, pH 7.4. At pH 8, the non-phosphorylated PEPC *P. queenslandicum* (k_{cat} (s^{-1}) =28) gave a slightly higher enzyme activity when compared to phosphorylated (k_{cat} (s^{-1}) = 24).

The apparent K_m for bicarbonate (HCO_3^-) of non-phosphorylated PEPC *P. queenslandicum* in Tricine buffer, pH 7.4 (K_m^{HCO3-} (mM)= 0.22) also show a similar K_m^{HCO3-} to the phosphorylated enzyme (K_m^{HCO3-} (mM) = 0.17). At pH 8, non-phosphorylated PEPC from *P. queenslandicum* has a significantly lower K_m^{HCO3-} value (K_m^{HCO3-} (mM) = 0.007) compared to phosphorylated PEPC (K_m^{HCO3-} (mM) = 0.5). Based on the results, non-phosphorylated PEPC *P. queenslandicum* showed a higher level of K_m^{HCO3-} and k_{cat} at pH 8 compared to pH 7.4, suggesting that pH 8 is the optimum pH for non-phosphorylated PEPC activity. Meanwhile for phosphorylated PEPC *P. queenslandicum,* K_m^{HCO3-} is higher in pH 7.4, but for enzyme activity (k_{cat}), the phosphorylated PEPC showed comparable activity rates for both pH values .

Phosphorylated PEPC *P. pygmaeum* showed a higher enzyme activity at pH 7.4 (k_{cat} (s^{-1}) = 49) compared to the non-phosphorylated PEPC (k_{cat}(s^{-1})= 38). The K_m^{HCO3-} also increased when PEPC was in the phosphorylated state (K_m^{HCO3-}(mM) = 0.09) compared to the non-phosphorylated enzyme (K_m^{HCO3-}(mM)= 0.21). The enzyme activity pattern was significantly different at pH 8. At this pH value, the non-phosphorylated PEPC *P. pygmaeum* has higher enzyme activity (k_{cat}(s^{-1}) = 32) compared to the phosphorylated one (k_{cat} (s^{-1}) = 26). the apparent K_m for bicarbonate for both types of PEPC *P. pygmaeum* are similar for non-phosphorylated PEPC *P. pygmaeum* (K_m^{HCO3-} (mM) = 0.26) and phosphorylated (K_m^{HCO3-}(mM) = 0.25).

Table 5.4: PEPC activity at pH 7.4 and pH 8 of both phosphorylated and non-phosphorylated PEPC from *P. queenslandicum* or *P. pygmaeum* in a varied bicarbonate concentration.

Tricine.KOH buffer	pH 7.4		pH 8	
PEPC speceis	K_{cat} (s^{-1})	K_m^{HCO3-} (mM)	K_{cat} (s^{-1})	K_m^{HCO3-} (mM)
Non-phosphorylated Pqu	23.83 ± 3.11	0.22 ± 0.10	28.37 ± 2.61	0.007 ± 0.009
Phosphorylated Pqu	24.62 ± 6.16	0.17 ± 0.17	24.43 ± 3.35	0.5 ± 0.22
Non-phosphorylated Ppy	37.85 ± 8.15	0.21 ± 0.17	31.93 ± 11.8	0.26 ± 0.34
Phosphorylated Ppy	48.77 ± 5.77	0.09 ± 0.05	25.94 ± 5.27	0.25 ± 0.70

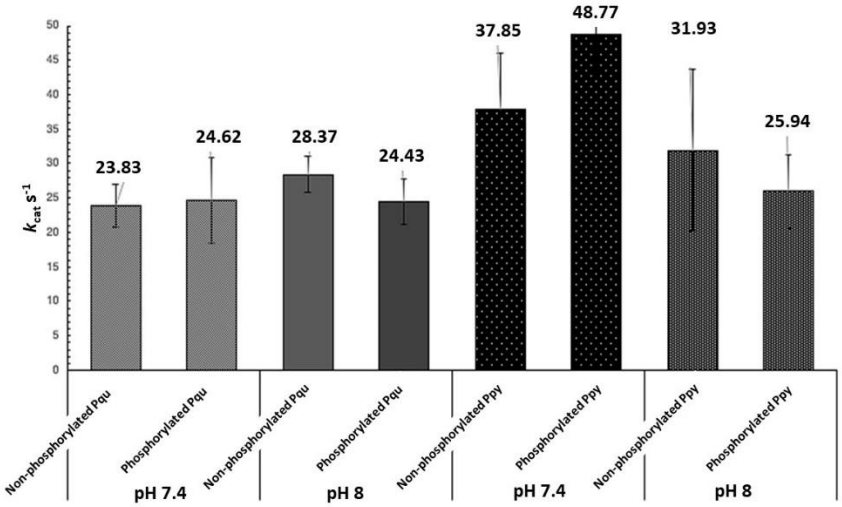

Fig. 5.3: PEPC activity in tricine.KOH buffer at pH 7.4 and 8 for both phosphorylated and non-phosphorylated PEPC *P. queenslandicum* and *P. pygmaeum* showing the effect of bicarbonate specificity on the rate of enzyme reaction.

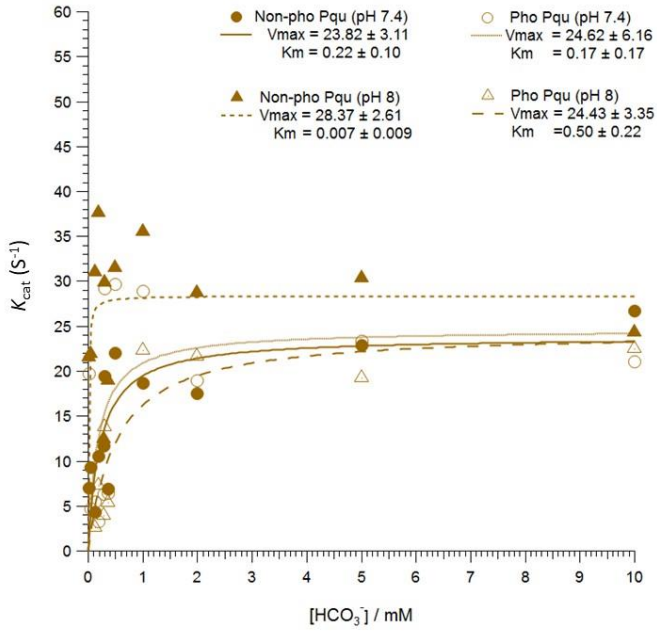

Fig. 5.4: Rate of oxaloacetic acid formation, catalysed by PEPC, both in phosphorylated and non-phosphorylated form with changing HCO^{3-} concentrations. The bicarbonate assays were conducted in 50 mM tricine.KOH buffer, pH 7.4 or pH 8, 5 mM $MgCl_2$, 0.2 mM NADH, 0.01 Uμl^{-1} MDH, 5 mM PEP, with total volume of 1.0 ml. Twelve $KHCO_3$ concentrations (0.012, 0.021, 0.041, 0.19, 0.28, 0.3, 0.37, 0.5, 1, 2, 5, 10 mM) were used to measure the PEPC-HCO_3^- kinetics. The enzyme rate was measured by the reduction of absorbance of oxidation of NADH at 340 nm. Each PEPC enzyme activity was monitored the absorbance reading until 30 minutes at room temperature. The symbols represent: ● Non-phosphorylated PEPC *P. queenslandicum*, pH 7.4; ▲ Non-phosphorylated PEPC *P. queenslandicum*, pH 8; ○ Phosphorylated PEPC *P. queenslandicum*, pH 7.4; ∆ Phosphorylated PEPC *P. queenslandicum*, pH 8.

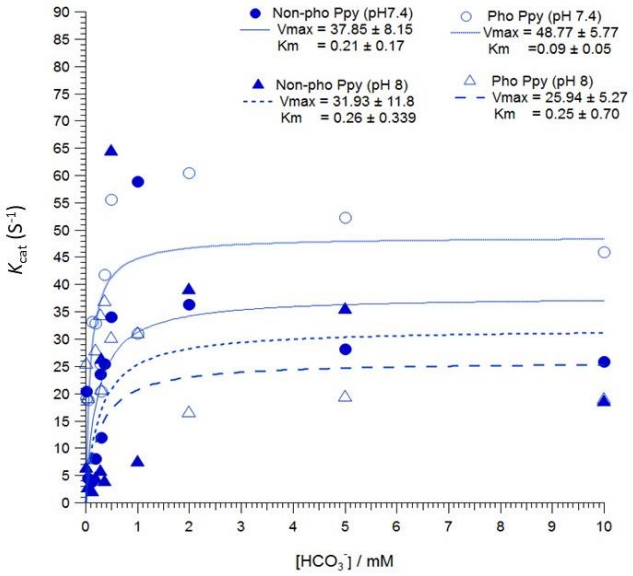

Fig. 5.5: Rate of oxaloacetic acid formation, catalysed by PEPC, both in phosphorylated and non-phosphorylated form. Assay conditions contained 50 mM Tricine.KOH buffer, pH 7.4 or pH 8, 5 mM $MgCl_2$, 0.2 mM NADH, 0.01 Uμl^{-1} MDH, 5 mM PEP, with total volume of 1.0 ml. Twelve $KHCO_3$ concentrations (0.012, 0.021, 0.041, 0.19, 0.28, 0.3, 0.37, 0.5, 1, 2, 5, 10 mM) were used to measure the PEPC-HCO_3^- kinetics. The enzyme rate was measured by the reduction of absorbance of oxidation of NADH at 340 nm. Each PEPC enzyme activity was monitored the absorbance reading until 30 minutes at room temperature. ●Non-phosphorylated PEPC *P. pygmaeum*, pH 7.4; ▲Non-phosphorylated PEPC *P. pygmaeum*, pH 8; ○ Phosphorylated PEPC *P. pygmaeum*, pH 7.4; ∆ Phosphorylated *P. pygmaeum*, pH 8.

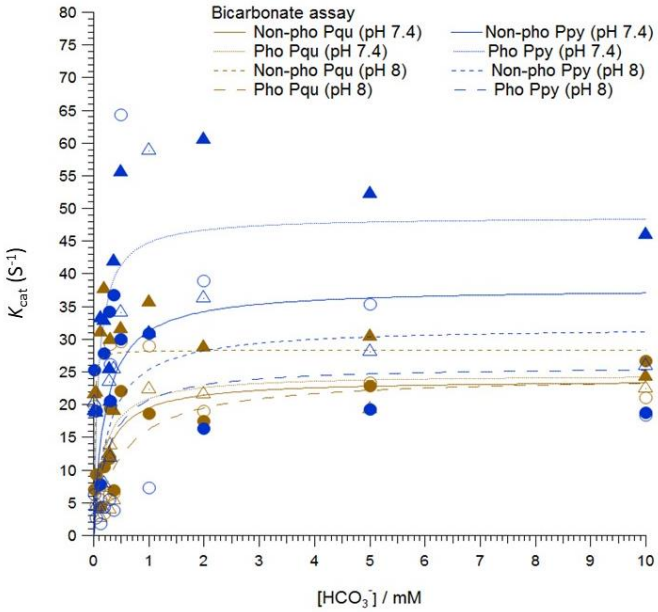

Fig. 5.6: Rate of oxaloacetic acid formation, catalysed by PEPC, both in phosphorylated and non-phosphorylated form. Assay conditions contained 50 mM Tricine.KOH buffer, pH 7.4 or pH 8, 5 mM $MgCl_2$, 0.2 mM NADH, 0.01 Uμl^{-1} MDH, 5 mM PEP, with total volume of 1.0 ml. Twelve $KHCO_3$ concentrations (0.012, 0.021, 0.041, 0.19, 0.28, 0.3, 0.37, 0.5, 1, 2, 5, 10 mM) were used to measure the PEPC-HCO_3^- kinetics. The enzyme rate was measured by the reduction of absorbance of oxidation of NADH at 340 nm. Each PEPC enzyme activity was monitored the absorbance reading until 30 minutes at room temperature.

5.4 Binding study of PEPC by using 8-anilino-1-naphthalenesulfonic acid (ANS).

Malate is one of the main downstream products of the PEP carboxylase reaction and can inhibit the PEPC reaction as PEPC has a feedback regulation. The ANS (8-anilino-1-naphthalenesulfonic acid) coupled binding assay was performed to investigate whether phosphorylation would inhibit the binding of malate to PEPC, with unphosphorylated PEPC as a control. The inhibition binding of PEPC was measured by the extrinsic fluorescence of the ANS that binds to the PEPChydrophobic regions, where the displacement of the ANS from malate leads to a fluorescence signal change. ANS hydrophobic fluorescent molecule that is a negatively charged and widely used in the characterisation of protein as it can also bind to native and partially unfolded proteins, as well as its role in the characterisation of protein binding sites (Cattoni, D. I. 2009).

ANS contains aromatic rings aniline and naphthalene that are fluorescence. The excitation wavelength of ANS is 350 to 380 nm and the emission maximum of ANS in water is 500 nm. So, when the ANS binds to hydrophobic regions of the protein, the emission maximum is shifted to a lower wavelength range. The level of blue shift is depends on the structure of the protein but produces an increased emission intensity. The emergence of intense fluorescence and blue shift of emission maximum upon dye binding to protein is easily distinguishable to the emission signals from the free dyes in solution, so the measurement of fluorescence can be a good signal for the degree of ligand binding, protein folding or protein denaturation (Lee, C. H. 2010).

5.4.1 Screening for ANS saturation concentration in non-phosphorylated PEPC *P. queenslandicum.*

To find the dissociation constant (K_d) of PEPC-ANS complex, first, the binding of ANS to the PEPC *P. queenslandicum* was measured by the fluorescence signal upon binding using spectrofluorometer, (FluoroMax®-3, Jobin Yvon Inc, NJ). The buffer used for all measurements was 50 mM tricine-KOH (pH 8) with 10 mM $MgCl_2$. The concentration of PEPC *P. queenslandicum* in the assay was 0.2 µM. Fluorescence of ANS was excited at 370 nm, and emission spectra were recorded between 400 and 650 nm. The addition of the enzyme to the ANS (100 µM) resulted in a large increase in fluorescence. The fluorescence signal upon the interaction of PEPC *P. queenslandicum* with ANS is established rapidly (i.e., in less than 5 sec), and increasing the molar concentration of ANS up to 500 µM results in a saturation curve (Fig. 5.7).

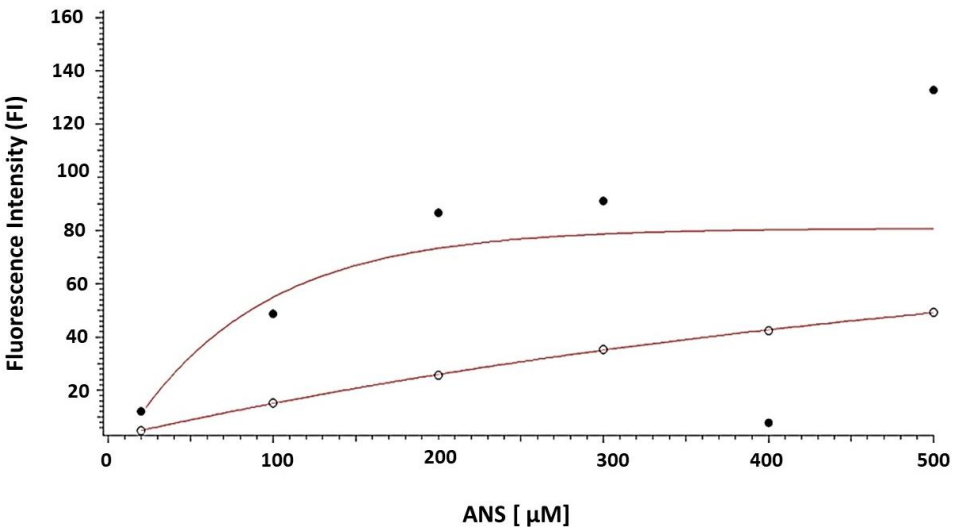

Fig. 5.7: The fluorescence intensity was measured and plotted versus the ANS concentration in µM. When the enzyme was titrated with ANS (100-500 µM), the fluorescence intensity (FI) increased in a hyperbolic manner, showing a tendency to reach a maximum at 200 µM of ANS (●). The symbols represent; ● Assay containing 50 mM of tricine buffer, pH 8, 0.2 µM of PEPC, and ANS; ○ Assay containing 50 mM of tricine buffer, pH 8, and ANS only.

5.4.2 Screening for optimum ANS concentration in malate inhibition for non-phosphorylated and phosphorylated PEPC *P. queenslandicum.*

The ANS-PEPC binding assay for phosphorylated PEPC *P. queenslandicum* was performed to determine whether phosphorylation will reduce the dissociation constant (K_d) in *P. queenslandicum*. The assay was performed at different ANS concentration (10, 20, 30 µM) in the presence of 20 mM malate (Fig. 5.10). At 10 µM ANS, the K_d of non-phosphorylated PEPC was determined to be 3 ± 2.0 mM and 42 ± 49 mM for phosphorylated PEPC (Table 5.6 and Appendix M; Fig. M.3). The K_d of non-phosphorylated PEPC from 20 µM ANS was 4 ± 3.8 mM and 22 ± 29 mM for phosphorylated PEPC (Table 5.6 and Appendix M; Fig. M.4). These results suggest that at 20 µM ANS, the inhibitory effects of malate are low on phosphorylated PEPC *P. queenslandicum*. Howeveer in 30 µM ANS, the binding was relatively high to phosphorylated PEPC with a K_d at 0.6 ± 0.5 compare to non-phosphorylated PEPC with K_d at 6.26 ± 6.49 (Table 5.6 and Appendix M; Fig. M.5) . Based on three different concentrations of ANS, it was observed that high quality emission spectrum from the concentration of 30 µM. So, for the next experiment, the dissociation constant (K_d) of non-phosphorylated and phosphorylated PEPC *P. pygmaeum* will be detected at 30 µM of ANS.

Table 5.6: Fluorescence intensity (FI) and dissociation constant (K_d) of non-phosphorylated and phosphorylated PEPC *P. queenslandicum* in different concentration of ANS by malate in different concentration of ANS (10, 20, 30 µM).

PEPC *P. queenslandicum*	ANS (µM)	K_d	FI
Non-phosphorylated	10	3.51 ± 2.06	3.50×10^{6}
Phosphorylated	10	41.85 ± 49.8	9.57×10^{7}
Non-phosphorylated	20	3.98 ± 3.76	3.94×10^{7}
Phosphorylated	20	22.34 ± 28.9	1.28×10^{8}
Non-phosphorylated	30	6.26 ± 6.49	5.39×10^{7}
Phosphorylated	30	0.63 ± 0.50	4.83×10^{7}

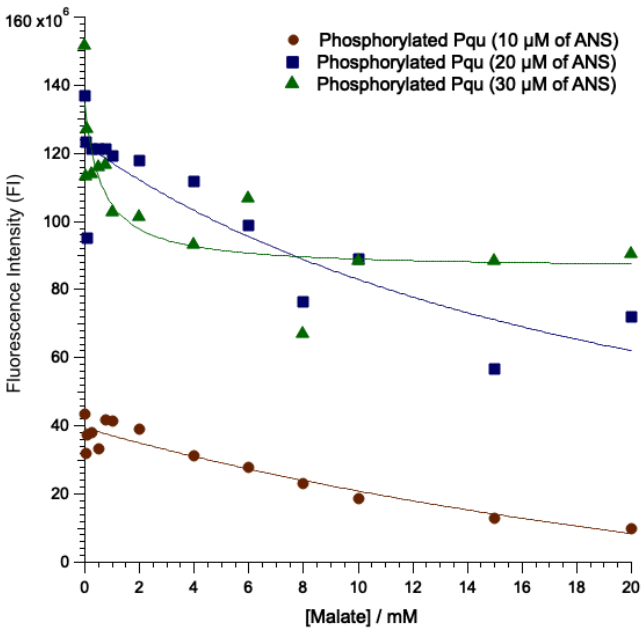

Fig. 5.8: Determination of dissociation constant (K_d) for phosphorylated of *P. queenslandicum* by using hydrophobic fluorescence probe, ANS. The inhibition activity was measured in the ANS fluorescence assay mixture contained 50 mM tricine-KOH buffer, pH 8, 10 mM $MgCl_2$, 0.2 µM PEPC, varying concentrations of malate (0-20 mM malate) and ANS (10, 20, 30 µM) at 25°C. The symbols represent: ● 10 µM of ANS, ■ 20 µM of ANS, ▲ 30 µM of ANS.

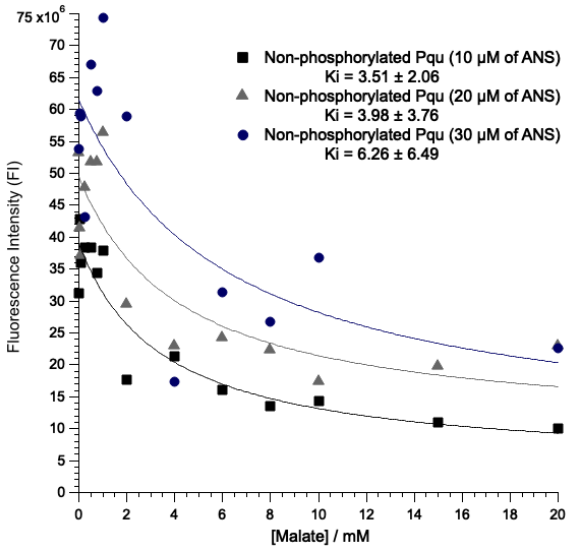

Fig. 5.9: Determination of dissociation constant (K_d) for non-phosphorylated of *P. queenslandicum* by using hydrophobic fluorescence probe, ANS. The inhibition activity was measured in the ANS fluorescence assay mixture contained 50 mM tricine-KOH buffer, pH 8, 10 mM $MgCl_2$, 0.2 µM PEPC, varying concentrations of malate (0-50 mM malate) and ANS (10, 20 and 30 µM) at 25°C. The symbols represent: The symbols represent: ● 10 µM of ANS, ■ 20 µM of ANS, ▲ 30 µM of ANS.

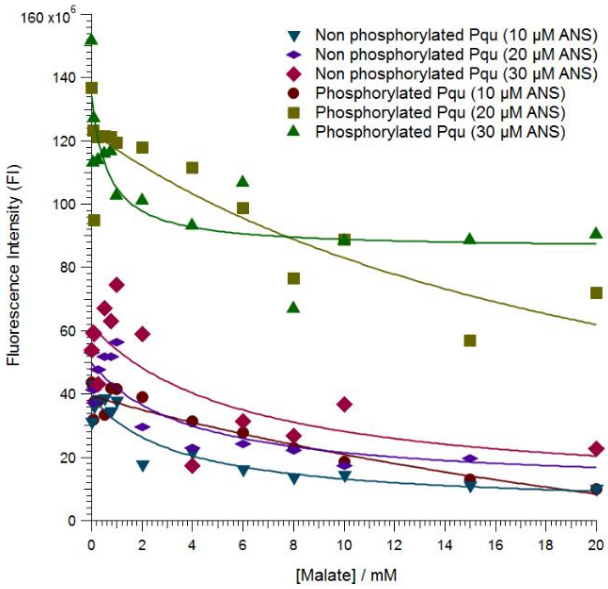

Fig. 5.10: Determination of dissociation constant (K_d) for non-phosphorylated and phosphorylated of *P. queenslandicum* by using hydrophobic fluorescence probe, ANS. The inhibition activity was measured in the ANS fluorescence assay mixture contained 50 mM tricine-KOH buffer, pH 8, 10 mM $MgCl_2$, 0.2 µM PEPC, varying concentrations of malate (0-20 mM malate) and ANS (10, 20, 30 µM) at 25°C. The symbols represent: ▼ Non-phosphorylated PEPC, 10 µM of ANS, ◄►Non-phosphorylated PEPC, 20 µM of ANS, ◆ Non-phosphorylated PEPC, 30 µM of ANS, ● Phosphorylated PEPC, 10 µM of ANS, ■ Phosphorylated PEPC, 20 µM of ANS, ▲ Phosphorylated PEPC, 30 µM of ANS.

5.4.3 ANS binding to non-phosphorylated and phosphorylated PEPC from *P. pygmaeum.*

The sensitivity of PEPC *P. pygmaeum* to malate was detected in the same method as PEPC *P. queenslandicum*. The ANS fluorescence assay was performed at 30 µM of ANS with the concentration of malate ranging from 0 – 40 mM. As shown in Table 5.7, the binding affinity of non-phosphorylated PEPC *P. pygmaeum* was 5.09 ± 2.01 mM and for phosphorylated PEPC, the K_d detected was at 1.06 ± 0.61 mM.

Table 5.7: Fluorescence intensity (FI) and dissociation constant (K_d) of non-phosphorylated and phosphorylated PEPC *P. pygmaeum* at 30 µM ANS in concentration of malate ranging from 0 – 40 mM.

PEPC *P. pygmaeum*	Baseline	FI	K_d
Non-phosphorylated	1.36 X10^7	4.01X10^7	5.09 ± 2.01
Phosphorylated	2.91X10^6	1.26 X10^6	1.06 ± 0.61

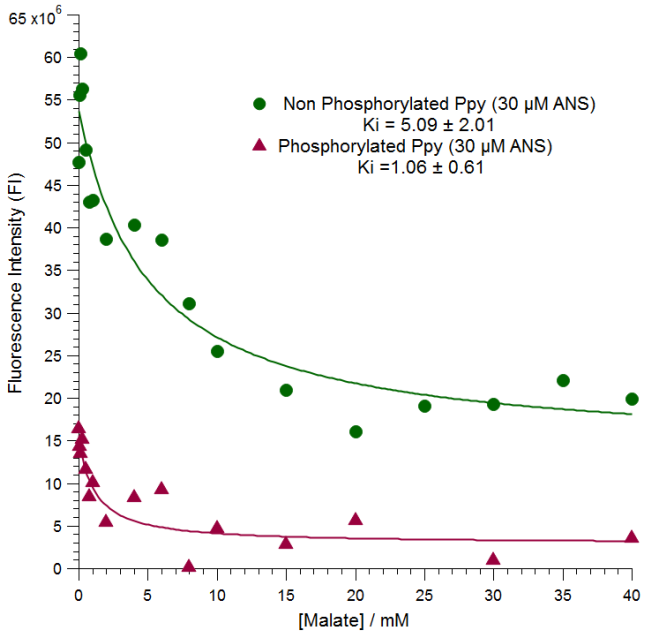

Fig. 5.11: Determination of dissociation constant (K_d) for non-phosphorylated and phosphorylated of *P. pygmaeum* by using hydrophobic fluorescence probe, ANS. The inhibition activity was measured in the ANS fluorescence assay mixture contained 50 mM tricine-KOH buffer, pH 8, 10 mM $MgCl_2$, 0.2 µM PEPC, varying concentrations of malate (0-40 mM malate) and 30 µM ANS at 25°C. The symbols represent: ● Non-phosphorylated PEPC *P. pygmaeum*: ▲ Phosphorylated *P. pygmaeum*.

5.5 Discussion

Results from the PEP, bicarbonate and ANS assays demonstrate that phosphorylation of PEPC from C_3 and C_4 plants species has significantly changes the activity of PEPC enzyme as well as its sensitivity to malate or aspartate. From the PEP assay, *P. queenslandicum* PEPC enzyme activity was increased in phosphorylated formed, but the K_m value is lower than the non-phosphorylated. Meanwhile, in the non-C_4 PEPC from *P. pygmaeum*, the K_m value showed slightly different between the phosphorylated and non-phosphorylated form of the enzyme, so there is no significant increase in the enzyme activity. Comparing species, PEPC`s highest enzyme activity was observed from the phosphorylated PEPC *P. queenslandicum*, a C_4 species.

The phosphorylated PEPC *P. queenslandicum* showed less malate sensitivity than non-phosphorylated when PEP is limiting (K_{IC}). At saturated PEP (K_{IU}), unphosphorylated PEPC *P. queenslandicum* was found to be less sensitivity to malate ($K_{IU}{}^{Malate}$(mM) = 156) compared to phosphorylated ($K_{IU}{}^{Malate}$(mM) = 68). In comparision, for PEPC *P. pygmaeum,* the level of sensitivity to malate was not quite different whether phosphorylated or not in limited PEP. At saturated PEP (K_{IU}), phosphorylated PEPC *P. pygmaeum* ($K_{IU}{}^{Malate}$(mM) = 184) showed less sensitivity to malate inhibition compare to non-phosphorylated PEPC ($K_{IU}{}^{Malate}$(mM) = 124). These results showed that phosphorylation of PEPC *P. pygmaeum* reduce its sensitivity to malate at saturating PEP.

The susceptibility to aspartate inhibition was detected at limiting PEP (K_{IC}), since no aspartate inhibition was observed by saturating PEP (K_{IU}) for both plant species. Phosphorylated PEPC *P. pygmaeum* showed lower sensitivity to aspartate than non-phosphorylated when limiting the PEP (K_{IC}), but the inhibition rate was not significant when PEP was saturated (K_{IU}). In *P. queenslandicum*, inhibition by aspartate also was not detected when PEP was saturated (K_{IU}) but at limited PEP, phosphorylated PEPC ($K_{IC}{}^{Aspartate}$ (mM)= 97) showed less sensitivity to aspartate inhibition compare to non-phosphorylated ($K_{IC}{}^{Aspartate}$ (mM)= 67).

The results obtained demonstrate that malate and aspartate exhibits mixed inhibition of both phosphorylated and non-phosphorylated PEPC from C_3 and C_4 plant species with the inhibition rates differs quantitively between type of enzymes (Table 5.3). Phosphorylation had decreased malate and aspartate sensitivity of PEPC *P. queenslandicum* in limited PEP (K_{IC}). When saturated the PEP (K_{IU}), aspartate inhibition rates were not significant for both formed of PEPC and it was observed that non-phosphorylated PEPC *P. queenslandicum* is less sensitive to malate.

It is well established that malate acts as an inhibitor to PEPC and comparative work from other species of *Flaveria* has shown that the C_4-specific form of the enzyme is less sensitive to malate than the C_3 form (Westhoff, P., et. al., 1997; Paulus, J. K., et. al., 2013). This pattern was also observed in *Panicum* species, which the PEPC from *P. queenslandicum* showed less sensitivity to malate compared to non-C_4 enzyme from *P. Pygmaeum* when limiting PEP. Many studies reported aspartate inhibition of PEPC and proposed possibilities for how this compound inhibits enzyme activity (Meister, M., et. al., 1996; Gillinta, J., and Grover, S. D., 1995; Endo, T., et. al., 2008). In C_4 photosynthesis, particularly in the NAD-ME and PCK types, aspartate is the primary carboxylation product

that transports between the mesophyll cell and bundle sheath cell (Andreo, C. S., et. al., 1987). However, aspartate was found to have negative effect to non-photosynthetic PEPCs than C_4 isozymes (Svensson, P., et. al., 2003). This could be the reason why there was no inhibition of aspartate was detected in C_4 species, *P. queenslandicum,* at saturating PEP (K_{IU}).

Previous studies have shown that sorghum and maize phosphorylated PEPC increased the affinity to PEP, become less sensitive to inhibitor malate and increased ezyme activation by glucose-6-phosphate, thereby attaining a higher maximum activity (Echevarria, C., et. al., 1994; Takahashi-Terada, A., et. al., 2005). Moreover, an *in vitro* study with sorghum PEPC, a C_4 species shows that phosphorylation has only a minor effect on enzyme activity in terms of V_{max} and K_m but phosphorylated PRPC was less sensitive to malate (seven-fold increase in K_i) and more susceptible to glucose-6-phosphate activation (fivefold increase in K_a) (Duff, S. M., et. al., 1995).

Results from the bicarbonate assay indicate that phosphorylation affects PEPC kinetic activities from *P. queenslandicum* and *P. pygmaeum* where bicarbonate act as a substrate. Phosphorylation had increase the PEPC *P. pygmaeum* activity by lowering the K_m value for bicarbonate and increasing the V_{max} in bicarbonate pH 7.4 assay. However at pH 8, the activity of the phosphorylated and non-phosphorylated PEPC almost remained constant. Phosphorylation of PEPC *P. queenslandicum* does not increase the PEPC activity at either K_m or V_{max} value in pH 7.4 or pH 8 compared with non- phosphorylated PEPC activity. It was expected that PEPC kinetic activity will showed significant difference between phosphorylated and non-phosphorylated at pH 7.4 since this pH value is near-physiological pH. These data suggest that despite the fact that PEPC was phosphorylated, the expected results can be varied depending on the pH value and the plant species. There was no significant change in the enzyme activity of PEPC from both C_4 and C_3 species, either in phosphorylated or non-phosphorylated form. Other steady-state kinetic assays were performed on the non-phosphorylated, phosphorylated and phosphorylation-site mutant of PEPC from sorghum, and its showed significant differences in certain kinetic parameters between these three types of enzyme forms when activity was assayed at pH 7.3, but not at pH 8.0 (Duff, S. M., et. al., 1995). Higher enzyme kinetics rate was observed from Parvathi, K. et. al., (2000) study that showed the apparent K_m for HCO_3^- for illuminated leaves *Amaranthus hypochondriacus L.*, a C_4 plant had decreased by half and the V_{max} had increased by five-fold compared to the non-illuminated leaves.

Maintaining the assay mixture free from bicarbonate can be challenging in this assay. In current method, CO_2 was removed from water and the assay buffers by continuously bubbling with N_2 gas for minimum 2 hours before starting the assay. After that, the residue bicarbonate in the assay medium was determined by monitoring NADH oxidation in the absence of any added bicarbonate. Thus, to completely remove the CO_2 completely, it was suggested that water and tricine buffer must be sparged with nitrogen for more than 2 hours or maximum overnight prior to use in assay.

An ANS binding assay was performed at 30 µM ANS for PEPC *P. queenslandicum* and *P. pygmaeum* to investigate whether phosphorylation will inhibit the binding capacity of malate. It was expected that when PEPC was phosphorylated, the ability of malate as an inhibitor to bind to the active site PEPC will decrease, thereby

preventing a reduction in enzyme activity. Table 5.8 indicates that phosphorylation does not suppress the binding of malate to PEPC based on the constant dissociation value for both plant species.

Although recent study has not shown the advantage of phosphorylation on PEPC in terms of binding capacity, ANS had the sensitivity and selectivity to hydrophobic regions of proteins is very high, so this compound can be good tools for studying the structure, function and mechanism of inter-molecular interaction of proteins (Lee, C. H. 2010). Besides that ANS can bind to folded or partially folded hydrophobic region of proteins. It is minimally fluorescent in polar environments, such as aqueous solutions but its fluorescence emission dramatically increases in non-polar environments (Wang, S., et. al., 2008; Fukunaga, Y., et. al., 2008).

Binding of malate to PEPC is a fast reaction which occurs in the millisecond time range (Appendix M, N, and O). Thefore, the kinetic analysis needed the application of fast reaction methodology such as stopped flow (SF) fluorimetry. Besides ANS, other fluoresenct compound such as 2-p-toluidinonaphthalene-6-sulfonate (TNS) can be applied to determined the binding reaction of malate to PEPC as a sensitive reporter fluorophore. The fluorescent probe TNS can efficiently be used to study ligand binding to PEPC and does not disturb the ligand binding (Frank, J., et al., 2001). Similar to ANS, TNS is a weakly fluorescent in polar solvents, dissolved in unpolar solvents, can bound to hydrophobic are of proteins, the dye`s fluorescence will increases sharply and the maximum of the fluorescence spectrum is changes to shorter wavelengths.This compound also reacts as an environmentally sensitive probe which detects polarity and viscosity changes in its surroundings.

Table 5.8: Fluorescence intensity (FI) and dissociation constant (K_d) of non-phosphorylated and phosphorylated PEPC *P. queenslandicum* and *P. pygmaeum* in 30 µM ANS.

PEPC *P. queenslandicum*	K_d
Non-phosphorylated	6.26 ± 6.49
Phosphorylated	0.63 ± 0.50
PEPC *P. pygmaeum*	K_d
Non-phosphorylated	5.09 ± 2.01
Phosphorylated	1.06 ± 0.61

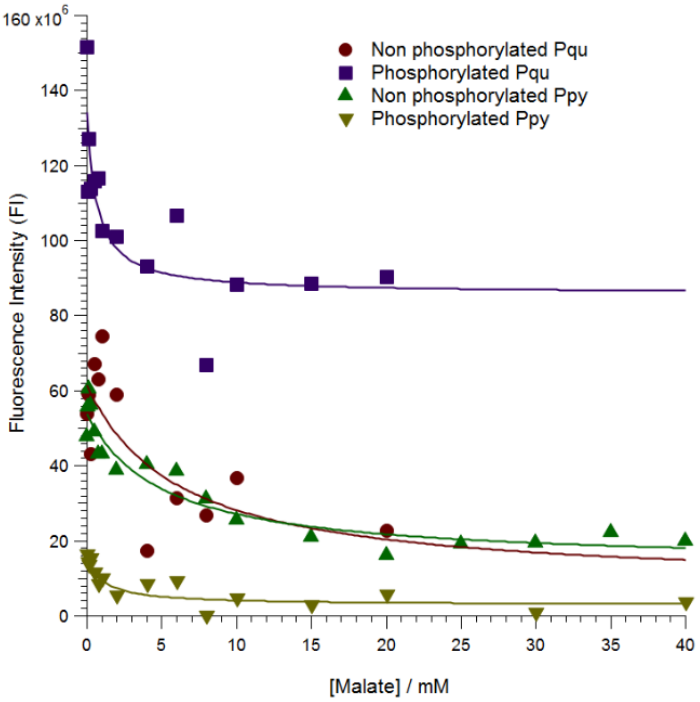

Fig. 5.12: Determination of malate dissociation constant (K_d) for phosphorylated and non-phosphorylated of PEPC *P. quenslandicum* and *P. pygmaeum*. Inhibition activity was measured in the fluorescence assay mixture contained 50 mM tricine-KOH (pH 8), 10 mM $MgCl_2$, 0.2 µM PEPC, 30 µM of ANS varying concentrations of malate (0-40 mM malate) and 30 µM ANS at 25°C. The symbols represent: ● non-phosphorylated of PEPC *P. quenslandicum*, ■ phosphorylated of PEPC *P. quenslandicum*, ▲ non-phosphorylated of PEPC *P. pygmaeum*, ▼ phosphorylated of PEPC *P. pygmaeum*

5.6 Conclusion

Phosphorylation changes the enzyme activity in both C_4 and non-C_4 forms of the enzyme. Phosphorylation increases the activity of the enzyme from *P. queenslandicum*, a C_4 plant, but not the enzyme from *P. pygmaeum*, a C_3 plant. Comparing between species, the highest activity of PEPC was observed from phosphorylated PEPC from P. *queenslandicum*, a C_4 species. Phosphorylation increases the specificity of PEPC towards bicarbonate in the enzyme from *P. queenslandicum* and *P. pygmaeum* at pH 8. Overall, the lowest K_m for HCO_3^- was observed from the non-phosphorylated *P. queenslandicum* enzyme at pH 8 followed by phosphorylated PEPC of *P. pygmaeum* at pH 7.4. Phosphorylation does not inhibit the binding of malate to PEPC *P. queenslandicum* and *P. pygmaeum* based on the dissociation experiments with ANS.

CHAPTER 6

GENERAL DISCUSSION AND CONCLUSION

C_4 plants have evolved from C_3 ancestors by producing a CO_2 concentrating mechanism that enables the concentration of CO_2 at the active site of Rubisco from a combination of anatomical and biochemical features (Hatch, M. D. 1987). In the C_4 plants, there are three types of carboxylase enzyme which is Rubisco, carbonic anhydrase and PEPC that control the levels of CO_2 assimilation and CO_2 concentrating mechanism (von Caemmerer, S., and Furbank, R. T., 2003; von Caemmerer, S., et. al., 2004; Studer, R. A., et. al., 2014). PEPC and carbonic anhydrase are localised in the cytosol of mesophyll cells, and Rubisco is localised in the chloroplast of bundle sheath cells (Burnell, J. N., and Hatch, M. D., 1988).

Rubisco catalyses the reaction of ribulose-1,5-bisphosphate (RuBP) either with CO_2 or oxygen in the Calvin cycle (Boyd, R. A., et. al., 2015). However, Rubisco tends to react with O_2 in a concentration-dependent manner (Chang, K. S., et. al., 2014) especially in the hot, dry and light environment that led to closure of stomata which increased the ratios of O_2 to CO_2 and decrease the specificity of Rubisco for CO_2 (Jordan, D. B., and Ogren, W. L. 1984). Carbonic anhydrase catalysing the CO_2 hydration reaction that produces bicarbonate and reverses dehydration reaction from bicarbonate to CO_2. This maintains the chemical equilibrium between CO_2 and bicarbonate even in the presence of significant consumption of bicarbonate by PEPC (Edwards, G., and Walker, D. 1983; Matsuda, Y., et. al., 2011).

The carboxylase enzyme that was analysed in current study is PEPC. This enzyme catalyses the conversion of PEP (phosphoenolpyruvate) to OAA (oxaloacetate) by using bicarbonate as a substrate (Svensson, P., et. al., 2003). In contrast with Rubisco, the PEPC does not react with O_2 and it has a higher affinity to bicarbonate than Rubisco to CO_2 (Badger, M. R., et. al., 1998). The lower K_m value of PEPC as compared to Rubisco can result in a higher CO_2 fixation rate (Moroney, J. V., and Somanchi, A. 1999).

Photosynthetic isoforms of PEPC catalyse primary fixation of CO_2, and in non-photosynthetic tissue and C_3 leaves, PEPC is the major anapleurotic enzyme (O'Leary, M. H. 1982; Andreo, C. S., et. al., 1987; Chollet, R., et. al., 1996). C_3 PEPC allows replenishing of the tricarboxylic acid cycle with intermediates that were withdrawn for a variety of biosynthetic pathways and nitrogen assimilation (O'Leary, B. et. al., 2011). In addition, non-photosynthetic PEPC is also involved in physiological and developmental process such as providing malate in stomatal guard cells, legume root nodules, and developing seed and ripening fruit (Andreo, C. S., et. al., 1987; Chollet, R., et. al., 1996; Vidal, J., and Chollet, R. 1997). To achieve these wide ranges of roles, PEPC is encoded by a small multigene family and expressed in various types of plant tissue (Lepiniec, L., et. al., 1994).

The purpose of the work desrcibed in this study is to generate phosphorylated versions of PEPC from C_4 and C_3 plant species and to compare kinetic changes of phosphorylated PEPC, particularly as reflected in the malate or aspartate sensitivity. In my study, the PEPC genes were expressed in *E. coli* and purified by using Ni-NTA affinity chromatography, which facilitated the analysis of homogenous protein. This is because PEPC enzymes that were

isolated directly from plant leaves indeed had a potential to represent a mixture of those encoded by different alleles, as well as paralogs. Additionally, the PTM state of PEPC enzymes purified from leaves depends on the time of the day the plant leaves are harvested, plus variation results among plant species (Doncaster, H. D. and Leegood, R. C. 1987; Nimmo, G. A., et. al., 1987; McNaughton, G. A. L., et. al., 1989).

Besides ability to concentrate CO_2, the C_4 PEPC catalytic properties also undergo changes on light/dark transitions. Nimmo, G. A., et. al., (1987) showed that illumination and darkness caused an increase and decrease, respectively of PEPC activity in maize leaf, a C_4 plant. Since than many *in vivo* studies have evaluated the enzyme activity of PEPC that was purified from illuminated leaves or dark leaves (Jiao, J. A., and Chollet, R. 1988; Nimmo, G. A., et.al, 1987; Jiao, J. A., et. al., 1991; Vidal, J. et. al., 1990). Besides C_4 plants, the phosphorylation of PEPC had been observed from C_3 plants (*Nicotiana tabacum* L.; Wang, Y. H., and Chollet, R., 1993), CAM plants (*Kalanchoë pinnata*, *K. daigremontiana* and *Ananas comosus*; Theng, V., et. al., 2008), and green algae (*Selenastrum minutum*; Rivoal, J., et. al., 2002). Several studies have performed on the effects of phosphorylation of PEPC by *in vitro*, commenced by Jiao, J.A., and Chollet, R. (1989), with a homologous reconstituted phosphorylation assay, using a purified dark-form maize PEPC, a partially purified protein kinase(s) from illuminated maize leaf and MgATP.

An attempt had been made to express and purify the recombinant protein PEPCK (Chapter 2, Section 2.3); however, it was partially purified when expressed with NusA and localised to inclusion bodies when overexpressed without tag (Chapter 2; Section 2.4). Other researchers have observed that the PEPCK can only be partially purified (Jiao, J. A., and Chollet, R. 1989, 1990; Wang, Y. H., and Chollet, R. 1993) although in some of these cases this may be as it is a very low-abundance protein in maize leaves (Wang, Y. H., and Chollet, R., 1993; Saze, H., et. al., 2001). Protein kinase A (PKA) had been applied to phosphorylate PEPC in this recent study. Previous studies have shown that PKA will phosphorylate PEPC from dark-adapted sorghum leaves, *Commelina communis* L. (Asiatic dayflower) and maize leaves (Meimoun, P., et. al., 2007; Cotelle, V., et. al., 1999; Pacquit, V., et. al., 1995; Jiao, J. A., and Chollet, R., 1990). PEPC phosphorylated by PKA shows similar enzymatic properties to that phosphorylated by PEPCK. The phosphorylated PEPC showed 33 % inhibition by malate after PKA treatment and 72 % inhibition before the treatment (Meimoun, P., et. al., 2007). Cotelle, V., et. al., (1999) phosphorylated PEPC with PKA resulting in a 3-fold increase in the V_{max} in the presence of 1 mM malate (pH 7.3), and reduction in L-malate inhibition when compared to the dephosphorylation PEPC.

The *P. queenslandicum*, a C_4 species encoded by the orthologous gene from the C_3 *P. pygmaeum* and belongs to the same tribe. The purified PEPC enzymes from both species were assayed at controlled concentrations of phosphoenolpyruvate (PEP) and bicarbonate (HCO_3). In the controlled concentrations of a PEP assay, phosphorylation increased the specific activity (k_{cat} (s^{-1})) of the enzyme from *P. queenslandicum* but not in the PEPC from *P. pygmaeum*. However, the phosphorylated PEPC of *P. queenslandicum* shows the lowest activity for PEP of the four enzymes compared, with K_m^{PEP} = 5.05 ± 0.95 mM, followed by the non-phosphorylated PEPC of *P. queenslandicum*. Phosphorylation does not increase the specificity for PEP in the enzyme from the C_3 *P. pygmaeum;* the K_m^{PEP} value was similar between the phosphorylated or non-phosphorylated enzyme (Table 5.1).

Since the major role of C_4 PEPC is fixing atmospheric CO_2 in the form of bicarbonate, the PEPCs enzymes were also assayed at controlled concentrations of bicarbonate as a substrate. An apparent decrease in K_m^{HCO3-} from 0.22 mM (pH 7.4) to 0.007 mM (pH 8) was observed in the enzyme from the C_4 *P. queenslandicum* but not for the enzyme from the C_3 *P. pygmaeum* where the K_m^{HCO3-} increased slightly from 0.21 mM (pH 7.4) to 0.26 mM (pH 8). Phosphorylation did increase the apparent K_m of PEPC for bicarbonate (K_m^{HCO3-}(mM)) in C_4 *P. queenslandicum* when assayed at pH 7.4 but not at pH 8. Meanwhile, phosphorylation of PEPC *P. pygmaeum* increases the K_m^{HCO3-} (mM) at pH 7.4 only. Comparing the two the pH values, the enzyme activity of PEPC was optimum at pH 7.4 compared to pH 8 since it shows that increasing of PEPC activity when both *Panicum* enzymes were phosphorylated. At pH 8, the activity results were not consistent as at pH 7.4 when both PEPCs were phosphorylated.

In this study, PEPC *P. pygmaeum* showed highest specific activity once phosphorylated (49 ± 5.8) k_{cat} (s^{-1}), followed by non-phosphorylated PEPC (38 ± 8.2), phosphorylated C_4 *P. queenslandicum* (25 ± 6.2) and non-phosphorylated PEPC (24 ± 3.1) at the same concentration of bicarbonate (Table 5.4). PEPC from *P. pygmaeum* showed a higher PEPC activity when compared to the PEPC from *P. queenslandicum*. This results can be observed in other research, when the level of atmospheric CO_2 concentration was doubled, the growth of C_3 plants is stimulated about 40-45 % more than the 10-20 % stimulation seen in C_4 plants (Ghannoum, O., et. al., 2000). This is because if atmospheric CO_2 levels was increased, it will slow down photorespiration, thus increasing the photosynthesis rate because of improved fixation of CO_2 by Rubisco, and the photosynthetic rate will be higher in C_3 than C_4 or CAM plants (Monson, R. K., and Sage, R. F. 1999). Generally, all plants contain the CO_2 fixation enzymes, Rubisco and PEPC, but the proportions vary with different photosynthetic pathways. In C_4 plants, the ratio of Rubisco to PEPC is near 1:1 (Latzko, E., and Kelly, G. J., 1983) but C_3 plants contain a vast, typically 15:1, excess of Rubisco over PEPC (Melzer, E., and O'Leary, M. H. 1987) that stimulates C_3 photosynthesis rather than C_4 photosynthesis

The purified PEPCs were also assayed in the presence of the inhibitors malate and aspartate at limiting and saturating of phosphoenolpyruvate (PEP). It is well known that malate acts as an inhibitor of PEPC and comparative work from other species, Flaveria has shown that the C_4-specific form of the enzyme is less sensitive to malate than C_3 form (Paulus, J. K., et. al., 2013). Particularly in the PCK subtype, malate accumulates as a result of the reduction of OAA. Malate is also a key player in feedback regulation in C_3 and CAM plants (Vidal, J., and Chollet, R., 1997). This pattern was also observed in *Panicum* species, in which the PEPC from *P. queenslandicum* showed less sensitivity to malate compared to the enzyme from the C_3 species, *P. pygmaeum* when PEP is limiting. The results presented in Chapter 5 (Section 5.2.1 and 5.2.2) show that malate and aspartate exhibit mixed inhibition of both types of PEPC from C_3 and C_4 plant species and inhibition differs quantitively between the two enzymes.

Phosphorylation made the PEPC from *P. queenslandicum* less sensitive to malate and aspartate when PEP was limiting (K_{IC}), but at saturating PEP (K_{IU}), the unphosphorylated PEPC becomes less sensitive to malate and has the same level of inhibition by aspartate when compared to phosphorylated PEPC. In the enzyme from the C_3

species *P. pygmaeum*, phosphorylation of PEPC had slightly increased the sensitivity to malate at limited PEP (K_{IC}) and at saturating PEP (K_{IU}). However, in the case of aspartate inhibition, only at limiting PEP (K_{IC}) the sensitivity of PEPC to aspartate was determined, since no aspartate inhibition was detected at saturating PEP(K_{IU}) .

Comparing the enzymes from the C_3 and C_4 plants, the C_4 *P. queenslandicum* PEPC (both phosphorylated and non-phosphorylated) showed less sensitivity to malate than the C_3 *P. pygmaeum* PEPC, at limiting PEP (K_{IC}). At saturating PEP, it is interesting to observe that the phosphorylated C_3 *P. pygmaeum* PEPC (K_{IU}^{Malate} (mM) = 184) shows less sensitivity to inhibition by malate when compared to the non-phosphorylated enzyme (K_{IU}^{Malate} (mM) = 124), and C_4 *P. queenslandicum* PEPC when both non-phosphorylated (K_{IU}^{Malate} (mM) = 156) and phosphorylated (K_{IU}^{Malate} (mM) = 68). The results presented here show that malate exhibits mixed inhibition of both phosphorylated and non-phosphorylated PEPC from C_3 and C_4 plant species. The inhibition differs quantitively between the two enzymes (Table 5).

Protein phosphorylation is among one of the most studied PTM along with protein ubiquitination, protein carbonylation or *N*-Linked and *O*-linked glycosylation. Protein phosphorylation can cause changes in protein conformation, the interaction between proteins, subcellular location and protein activity (Mithoe, S. C., and Menke, F. L., 2011; Schönberg, A., and Baginsky, S. 2012; van Wijk, K. J., et. al., 2014; Silva-Sanchez, C., et. al., 2015). Due to the vital role of phosphorylation in regulation, the development of techniques for characterising protein phosphorylation has been an active area of research. In addition, plant genomes encode approximately twice as many kinases as mammalian genomes (Zulawski, M., et. al., 2013); for example, the Arabidopsis genome encodes 1052 protein kinases and 162 phosphatases (Wang, Y., et. al., 2013), indicating the significant function of protein phosphorylation in plants.

In general, phosphorylation is catalysed by kinases that typically transfer a phosphoryl group from ATP to the hydroxyl group of specific Ser, Thr, or Tyr residues within their target protein. Phosphorylation is detected on average 75-80 % on Ser, 15-20 % on Thr, and 1-5 % on Tyr, respectively (Champion, A., et. al., 2004). In C_4 photosynthesis, PEPC in the cytosol of mesophyll cells is phosphorylated by the kinase, PEPCK. It was purposed that light will activate the PEPCK, but the specific mechanism is still unknown, and may itself involve one or more PTMs. In turn, on a conserved Ser residue, the kinase phosphorylates PEPC, thus activating PEPC to generate oxaloacetate. Dephosphorylation of PEPC is catalysed by an unidentified phosphatase from the Protein Phosphatase 2A family in the dark to reduce PEPC activity (Dong, L., et. al., 2001; Izui, K., et. al., 2004). The regulation of this phosphatase is still unknown. Studies of maize (Jiao, J. A., et. al., 1991; Nimmo, G.A. et. al., 1987) and sorghum (Jiao, J. A., et. al., 1991; Vidal, J., et. al., 1990) leaf tissue demonstrated that when C_4 PEPC was purified from the light and therefor phosphorylated, the activity is less susceptible to malate when compared to PEPC purified from the dark, PEPC become more sensitive to malate.

In this study, PEPC enzymes from both C_3 and C_4 plants were over-expressed in *E. coli*, purified and then phosphorylated by PKA. Then, phosphorylated PEPC was detected by Pro-Q® Diamond stain since this

fluorescent dye technology is appropriate to detect phosphoprotein directly in SDS-PAGE gels (Steinberg, T. H., et. al., 2003). PEPCs that were phosphorylated by PKA and PEPCK showed high fluorescent intensity compared to non-phosphorylated PEPC (Chapter 4; Section 4.4 and 4.6). Although the fluorescence signal intensity from the Pro-Q® Diamond stain is correlated with the number of phosphorylated residues, this dye also capable of staining non-phosphorylated protein. Therefore, in the same gel SYPRO Ruby gel stain was applied to verify detection and to normalise to total protein concentration (Arias-Baldrich, C., et. al., 2017; Stasyk, T., et. al., 2005).

An additional method was been applied in my study to further analyse whether all the PEPC was phosphorylated by PKA from *in vitro* phosphorylation assay: phosphate affinity- Phos-Tag™ electrophoresis. Phos-Tag™ is a dinuclear metal complex that acts as a phosphate-binding agent and can be conjugated to analytical materials such as acrylamide. This method had widely applied to analyse protein phosphorylation in plants (Bekesova, S., et. al, 2015); *E. coli* (Barbieri, C. M., and Stock, A. M. 2008); and human cells (Aguilar, H. N., et. al., 2011; Messer, A. E. 2009). It was observed that the PEPC of *P. queenslandicum* and *P. pygmaeum* gave one band in Phos-Tag™-SDS-PAGE gel suggesting that all of the protein was phosphorylated when *in vitro* phosphorylation assay was performed. In addition, one band detected, suggesting that there was one phosphorylation site in the polypeptide for both PEPCs.

The primary step to understand signal transduction based on changes in phosphorylation is by identifying the phosphorylated residues on the target protein. In this study, although Phos-Tag™ technique is unable to determine the phosphorylated residues, the band from the gel can be used as a sample to determine the phosphorylation site by applying MS (Mass Spectrophotometer). This is as the Phos-Tag™ affinity method can be effectively used in combination with other methods such as by capillary isoelectric focusing with laser-induced fluorescence detection (Takeya, K., et. al., 2008), MALDI-TOF-MS (Tatematsu, K., et. al., 2008), and gel electrophoresis (Kinoshita, E., et. al., 2009) in order to characterise phosphorylated proteins. MS is the most flexible and exact procedure since it can recognise numerous, diverse, PTMs and significantly, determine which residue or residues carry the PTM (Friso, G., and van Wijk, K. J. 2015).

MS (mass spectrometry) has been applied to analyse protein phosphorylation since this method is highly sensitive, thus making it capable of scanning the complex mixture of phosphoproteins and of evaluating the phosphorylation state of target protein (Vener, A. V., et. al., 2001). In this study, the phosphorylation site detected in phosphorylated PEPC from C_4 *P. queenslandicum* was at the *N*-terminal of the polypeptide. For C_3 *P. P. pygmaeum*, phosphorylation was detected at multiple residues, even at the C-terminal. The results obtained from both C_3 and C_4 PEPC in this study showed some similarities with previous studies. Terada, K., et al., (1990) phosphorylated the PEPC from maize leaf with PKA and the phosphorylated acid amino residue was identified as a Serine (Ser-15) located near the *N*-terminal end. Jiao, J. A., and Chollet, R. (1990) also identified a single serine residue (Ser-15) close to the *N*-terminal that was phosphorylated with PKA in PEPC, purified from leaves in the dark.

The primary sequences of PEPC isoforms are available from a wide range of species including *E. coli* (Fujita, N., et. al., 1984; Ishijima, S., et. al., 1985); C_3 plants (Rickers, J., et. al, 1989; Cushman, J.C., et. al., 1989); and C_4 plants (Jiao, J. A. et. al., 1990). Comparisons between these sequences show that the *C*-terminal region is relatively conserved, including the active-site domain, while the *N*-terminal region is more variable (Jiao, J. A., & Chollet, R. (1991).

CONCLUSION

Plant proteins will undergo post-translational modifications in order to respond to their surrounding changing conditions, mostly by protein phosphorylation. Many protein phosphorylations occured in C_4 photosynthesis pathway, but this study was focusing on the phosphorylation of PEPC, a decarboxylase enzyme. In this study, an attempt to purify the PEPCK cloned from the C_4 plant *P. queenslandicum*, was unsuccessful as the PEPCK purified insoluble (Chapter 3). Over-expression of PEPCK with the solubility tag, NusA produced a protein that soluble but in meagre amounts, especially after the thrombin cleavage reaction, yielding insufficient amounts of active kinase to be applied in further experiments. PEPCK is challenging to produce in an active form in *E. coli* despite *E. coli* having many advantages for recombinant protein expression. PKA seems to be a suitable kinase to phosphorylated PEPC, although greater confidence in the relevance of the behaviour of the phosphorylated PEPC would be possible if PEPCK had been used. Since the purified PEPCK purified exist as the insoluble protein, other methods will have to be developed to produce soluble, active kinase.

Since PKA phosphorylated the PEPC enzymes, it is crucial to detect if PKA performed the phosphorylation correctly (Chapter 4). The use of two fluorescent dyes, Pro-Q® Diamond phosphoprotein stain and SYPRO Ruby protein gel stain, allowed fluorescence detection of phosphorylated PEPC by PKA in SDS-PAGE gels. Then, the in-gel phosphate affinity Phos-Tag™ system was used to ensure that all PEPCs present were fully phosphorylated by the *in vitro* phosphorylation was performed. The bands from the phosphate affinity Phos-Tag™ SDS-PAGE gels were applied to mass spectrometry to determine the phosphorylation site of these PEPCs. Two phosphopeptides had been detected in PEPC *P. queenslandicum* and six in *P. pygmaeum* respectively with the phosphorylation site(s) of both PEPCs were detected at the serine residue. These findings indicate that PKA can act to phosphorylate PEPC. Phosphopeptides detected from PEPC *P. queenslandicum,* and *P. pygmaeum* have not been identified previously and how these peptides involve in phosphorylation reaction will be interesting for further study.

Phosphorylation of PEPC by PKA changes the catalytic activity, as well as both malate and aspartate sensitivity between phosphorylated and non-phosphorylated enzyme (Chapter 5). The phosphorylation increases the PEPC enzyme activity (V_{max}) in the enzyme from *P. queenslandicum*, but not from *P. pygmaeum.* In terms of K_m for PEP, the phosphorylated PEPC from *P. queenslandicum,* has a lower K_m value than the non-phosphorylated one. In contrast, for the C_3 *P. pygmaeum* enzyme*,* phosphorylation does not change the K_m (PEP) value or the specific

activity. Phosphorylation does increase the specificity of PEPC to bicarbonate in C4 *P. queenslandicum* and C_3 *P. pygmaeum* at pH 8.

The PEPC from *P. queenslandicum* becomes less sensitive to malate and aspartate inhibition once phosphorylated at limiting the PEP substrate. However, at saturating PEP, non-phosphorylated PEPC is less sensitive to malate than the phosphorylated form of the enzyme and for inhibition by aspartate, phosphorylated PEPC becomes less sensitive in limited PEP. In the *P. pygmaeum* enzyme, phosphorylation also makes PEPC less sensitive to malate compare to the non-phosphorylated PEPC. For inhibition by aspartate, phosphorylation makes the PEPC from *P. pygmaeum* less sensitive but only at low concentrations of PEP.

This study shows that the phosphorylation of PEPC changes its catalytic activity differently in the enzyme from C_3 and C_4 plants. The study of the enzymatic properties of phosphorylated PEPC found *in vivo* in C_3 and C_4 plants will be needed to test the predictions from my *in vitro* studies. This study on phosphorylation of PEPC can be further developed by involving ambient parameters essential for crops and wild C_4 plants such as temperature, the level of CO_2, nutrients and water to observe their respond on phosphorylation along with global climate change, in order to build a comprehensive study.

REFERENCES

1. Aebersold, R., and Mann, M. (2003). Mass spectrometry-based proteomics. Nature, 422(6928), 198.
2. Agnew, B., Beechem, J., Gee, K., Haugland, R., Liu, J., Martin, V., Patton, W., and Steinberg, T. (2006). Compositions and methods for detection and isolation of phosphorylated molecules. United States Patent 7102005.
3. Agostino, A., Heldt, H.W., Hatch, M.D. (1996). Mitochondrial respiration in relation to photosynthetic C4 acid decarboxylation in C4 species. Australian Journal of Plant Physiology, 23, 1–7.
4. Agrawal, G. K., & Thelen, J. J. (2009). A high-resolution two dimensional Gel-and Pro-Q DPS-based proteomics workflow for phosphoprotein identification and quantitative profiling. In Phospho-proteomics, (pp. 3-19). Humana Press.
5. Aguilar, H. N., Tracey, C. N., Tsang, S. C. F., McGinnis, J. M., & Mitchell, B. F. (2011). Phos-tag-based analysis of myosin regulatory light chain phosphorylation in human uterine myocytes. PloS One, 6(6), e20903.
6. Aldous, S. H., Weise, S. E., Sharkey, T. D., Waldera-Lupa, D. M., Stühler, K., Mallmann, J., & Arsova, B. (2014). Evolution of the phosphoenolpyruvate carboxylase protein kinase family in C_3 and C_4 Flaveria spp. Plant Physiology, 165(3), 1076-1091.
7. Aliscioni, S.S., Giussani, L.M., Zuloaga, F.O. and Kellogg, E.A. (2003). A molecular phylogeny of Panicum (Poaceae: Paniceae): tests of monophyly and phylogenetic placement within the Panicoideae. American Journal of Botany, 90, 796- 821.
8. Al-Samarrai, T. H., Kirk, C. A., Jones, W. T., Harvey, D., & Sun, X. (2007). Expression in Escherichia coli and *in vitro* refolding of the plant transcription factor Arabidopsis thaliana RGL3. Protein expression and purification, 53(2), 289-292.
9. Alvarez, C. E., Saigo, M., Margarit, E., Andreo, C. S., & Drincovich, M. F. (2013). Kinetics and functional diversity among the five members of the NADP-malic enzyme family from Zea mays, a C_4 species. Photosynthesis Research, 115(1), 65-80.
10. Amthor, J.S. (2010). From sunlight to phyto-mass: On the potential efficiency of converting solar radiation to phyto-energy. New Phytologist, (188), 939–959.
11. Andreo, C.S., González, D.H. & Iglesias, A.A. (1987). Higher plant phosphoenolpyruvate carboxylase: structure and regulation. FEBS Letter, (213), 1–8.
12. Arias-Baldrich, C., de la Osa, C., Bosch, N., Ruiz-Ballesta, I., Monreal, J. A., & García-Mauriño, S. (2017). Enzymatic activity, gene expression and posttranslational modifications of photosynthetic and non-photosynthetic phosphoenolpyruvate carboxylase in ammonium-stressed sorghum plants. Journal of Plant Physiology, 214, 39-47.
13. Aubry, S., Brown, N. J., & Hibberd, J. M. (2011). The role of proteins in C_3 plants prior to their recruitment into the C_4 pathway. Journal of Experimental Botany, 62(9), 3049-3059.
14. Badger, M. R., and Price, G. D. (1994). The role of carbonic anhydrase in photosynthesis. Annual Review of Plant Biology, 45(1), 369-392.
15. Bailey, K. J., Gray, J. E., Walker, R. P., & Leegood, R. C. (2007). Coordinate regulation of phosphoenolpyruvate carboxylase and phosphoenolpyruvate carboxykinase by light and CO2 during C4 photosynthesis. Plant Physiology, 144(1), 479-486.
16. Bandarian, V., Poehner, W. J., & Grover, S. D. (1992). Metabolite activation of Crassulacean acid metabolism and C_4 phosphoenolpyruvate carboxylase. Plant Physiology, 100(3), 1411-1416.
17. Bandurski, R. S., and Greiner, C. M. (1953). The enzymatic synthesis of oxalacetate from phosphoryl-enolpyruvate and carbon dioxide. Journal of Biological Chemistry, 204(2), 781-786.
18. Baneyx, F. (1999). Recombinant protein expression in Escherichia coli. Current Opinion in Biotechnology, 10(5), 411-421.

19. Barbieri, C. M., and Stock, A. M. (2008). Universally applicable methods for monitoring response regulator aspartate phosphorylation both *in vitro* and *in vivo* using Phos-tag-based reagents. Analytical Biochemistry, 376(1), 73-82.

20. Bekesova, S., Komis, G., Krenek, P., Vyplelova, P., Ovecka, M., Luptovciak, I., & Samaj, J. (2015). Monitoring protein phosphorylation by acrylamide pendant Phos-Tag™ in various plants. Frontiers in Plant Science, 6, 336.

21. Bender, J., and Weigel, H. J. (2011). Changes in atmospheric chemistry and crop health: A review. Agronomy for Sustainable Development, 31, 81–89.

22. Berggren, K., Chernokalskaya, E., Steinberg, T. H., Kemper, C., Lopez, M. F., Diwu, Z., & Patton, W. F. (2000). Background-free, high sensitivity staining of proteins in one-and two-dimensional sodium dodecyl sulfate-polyacrylamide gels using a luminescent ruthenium complex. Electrophoresis: An International Journal, 21(12), 2509-2521.

23. Betti, M., Bauwe, H., Busch, F. A., Fernie, A. R., Keech, O., Levey, M. & Walker, B. (2016). Manipulating photorespiration to increase plant productivity: Recent advances and perspectives for crop improvement. Journal of Experimental Botany, 10, 2977-2988.

24. Bi, Y. D., Wang, H. X., Lu, T. C., Li, X. H., Shen, Z., Chen, Y. B., & Wang, B. C. (2011). Large-scale analysis of phosphorylated proteins in maize leaf. Planta, 233(2), 383-392.

25. Bigeard, J., Rayapuram, N., Pflieger, D., & Hirt, H. (2014). Phosphorylation-dependent regulation of plant chromatin and chromatin-associated proteins. Proteomics, 14(19), 2127-2140.

26. Bloom, A. J. (2015). Photorespiration and nitrate assimilation: a major intersection between plant carbon and nitrogen. Photosynthesis Research, 123(2), 117-128.

27. Boersema, P. J., Mohammed, S., & Heck, A. J. (2009). Phosphopeptide fragmentation and analysis by mass spectrometry. Journal of Mass Spectrometry, 44(6), 861-878.

28. Boyd, R. A., Gandin, A., & Cousins, A. B. (2015). Temperature responses of C4 photosynthesis: biochemical analysis of Rubisco, phosphoenolpyruvate carboxylase, and carbonic anhydrase in Setaria viridis. Plant Physiology, 169(3), 1850-1861.

29. Bradford, M. M. (1976). A rapid and sensitive method for the quantitation of microgram quantities of protein utilizing the principle of protein-dye binding. Analytical Biochemistry, 72(1-2), 248-254.

30. Bräutigam, A and Weber, A. P. M. (2011). Transport processes: Connecting the Reactions of C4 Photosynthesis. In C4 Photosynthesis and Related CO_2 Concentrating Mechanism. Edited by Raghavendra, A.S. and Sage, R.F. Springer Science, Dordrecht, The Netherlands.

31. Brosius, J., Erfle, M., & Storella, J. (1985). Spacing of the-10 and-35 regions in the tac promoter. Effect on its in vivo activity. Journal of Biological Chemistry, 260(6), 3539-3541.

32. Brown, H.A. (1999). Agronomic implications of C4 photosynthesis. In C4 Plant Biology (Sage, R.F. and Monson, R.K., eds), pp. 473–508, Academic Press.

33. Bruinsma, J. (2003). World agriculture: towards 2015/2030: an FAO perspective. Earthscan. Food and Agriculture Organization, London/Rome.

34. Buckler, D. R., & Stock, A. M. (2000). Synthesis of [32P] phosphoramidate for use as a low molecular weight phosphodonor reagent. Analytical Biochemistry, 283(2), 222-227.

35. Budde, R. J., & Chollet, R. (1988). Regulation of enzyme activity in plants by reversible phosphorylation. Physiologia Plantarum, 72(2), 435-439.

36. Burnell, J. N. (1986). Purification and properties of phosphoenolpyruvate carboxykinase from C_4 plants. Functional Plant Biology, 13(5), 577-587.

37. Burnell, J. N., & Hatch, M. D. (1988). Low bundle sheath carbonic anhydrase is apparently essential for effective C_4 pathway operation. Plant Physiology, 86(4), 1252-1256.

38. Byng, J.W. (2014). The flowering plants handbook: a practical guide to families and genera of the world (Plant Gateway, Hertford, United Kingdom).

39. Carmo-silva, E, Scales, J. C., Madgwick, P. J., & Parry, M. A. (2015). Optimizing Rubisco and its regulation for greater resource use efficiency. Plant, Cell & Environment, 38(9), 1817-1832.

40. Cattoni, D. I., Kaufman, S. B., & Flecha, F. L. G. (2009). Kinetics and thermodynamics of the interaction of 1-anilino-naphthalene-8-sulfonate with proteins. Biochimica et Biophysica Acta (BBA)-Proteins and Proteomics, 1794(11), 1700-1708.

41. Cerling, T.E., Harris, J.M., MacFadden, B.J., Leakey, M.G., Quade, J.,Eisenmann, V. & Ehleringer, J.R. (1997) Global vegetation change throughthe Miocene/Pliocene boundary. Nature, 389, 153–158.

42. Chakraborty S, Newton AC. 2011. Climate change, plant diseases and food security: an overview. Plant Pathology, 60,2–14.

43. Challinor AJ, Ewert F, Arnold S, Simelton E, Fraser E. 2009. Crops and climate change: progress, trends, and challenges in simulating impacts and informing adaptation. Journal of Experimental Botany, 60:2775–89.

44. Champion, A., Kreis, M., Mockaitis, K., Picaud, A., & Henry, Y. (2004). Arabidopsis kinome: after the casting. Functional and Integrative Genomics, 4(3), 163-187.

45. Chang, J. Y., Thrombin specificity. Requirement for apolar amino acids adjacent to the thrombin cleavage site of polypeptide substrate. European Journal of Biochemistry, 1985, 151, 217–224.

46. Chang, K. S., Jeon, H., Seo, S., Lee, Y., & Jin, E. (2014). Improvement of the phosphoenolpyruvate carboxylase activity of Phaeodactylum tricornutum PEPCase 1 through protein engineering. Enzyme and Microbial Technology, 60, 64-71.

47. Chesshyre, J. A., and Hipkiss, A. R. (1989). Low temperatures stabilize interferon a-2 against proteolysis inMethylophilus methylotrophus and Escherichia coli. Applied Microbiology and Biotechnology, 31, 158–162.

48. Chollet, R., Vidal, J. & O'Leary, M.H. (1996). Phosphoenolpyruvate carboxylase: A ubiquitous, highly regulated enzyme in plants, Annu. Rev. Plant Physiol. Plant Molecular Biology, (47), 273-298.

49. Chrambach, A., & Rodbard, D. (1971). Polyacrylamide gel electrophoresis. Science, 172(3982), 440-451.

50. Christin, P. A., & Osborne, C. P. (2013). The recurrent assembly of C 4 photosynthesis, an evolutionary tale. Photosynthesis Research, 117(1-3), 163-175.

51. Christin, P. A., Salamin, N., Muasya, A. M., Roalson, E. H., Russier, F., & Besnard, G. (2008). Evolutionary switch and genetic convergence on rbcL following the evolution of C4 photosynthesis. Molecular Biology and Evolution, 25(11), 2361-2368.

52. Clark, E. D. B. (1998). Refolding of recombinant proteins. Current Opinion in Biotechnology, 9(2), 157-163.

53. Cohen, P. (2002). The origins of protein phosphorylation. Nature Cell Biology, 4(5), E127.

54. Collatz, G. J., Berry, J. A., & Clark, J. S. (1998). Effects of climate and atmospheric CO_2 partial pressure on the global distribution of C_4 grasses: present, past, and future. Oecologia, 114(4), 441-454.

55. Cong, W. T., Hwang, S. Y., Jin, L. T., & Choi, J. K. (2008). Sensitive fluorescent staining for proteomic analysis of proteins in 1-D and 2-D SDS-PAGE and its comparison with SYPRO Ruby by PMF. Electrophoresis, 29(21), 4304-4315.

56. Cotelle, V., Pierre, J. N., & Vavasseur, A. (1999). Potential strong regulation of guard cell phospho enol pyruvate carboxylase through phosphorylation. Journal of Experimental Botany, 50(335), 777-783.

57. Cousins, A. B., Baroli, I., Badger, M. R., Ivakov, A., Lea, P. J., Leegood, R. C., & von Caemmerer, S. (2007). The role of phosphoenolpyruvate carboxylase during C_4 photosynthetic isotope exchange and stomatal conductance. Plant Physiology, 145(3), 1006-1017.

58. Cushman, J. C., Meyer, G., Michalowski, C. B., Schmitt, J. M., & Bohnert, H. J. (1989). Salt stress leads to differential expression of two isogenes of phosphoenolpyruvate carboxylase during Crassulacean acid metabolism induction in the common ice plant. The Plant Cell, 1(7), 715-725.

59. Davis, G. D., Elisee, C., Newham, D. M., & Harrison, R. G. (1999). New fusion protein systems designed to give soluble expression in Escherichia coli. Biotechnology and Bioengineering, 65(4), 382-388.

60. De La Fuente van Bentem, S., Roitinger, E., Anrather, D., Csaszar, E., & Hirt, H. (2006). Phosphoproteomics as a tool to unravel plant regulatory mechanisms. Physiologia Plantarum, 126(1), 110-119.

61. De Marco, V., Stier, G., Blandin, S., & De Marco, A. (2004). The solubility and stability of recombinant proteins are increased by their fusion to NusA. Biochemical and Biophysical Research Communications, 322(3), 766-771.

62. Dissmeyer, N., & Schnittger, A. (2011). The age of protein kinases. In Plant Kinases (pp. 7-52). Humana Press.

63. Donaldson, V. H., & Kleniewski, J. (1979). The role of plasmin in kinin-release by preparations of human thrombin. Thrombosis Research, 16(3-4), 401-406.

64. Doncaster, H. D. & Leegood, R. C. (1987). Regulation of Phosphoenolpyruvate Carboxylase Activity in Maize Leaves. Plant Physiology, 84, 82-87.

65. Dong, L., Ermolova, N. V., & Chollet, R. (2001). Partial purification and biochemical characterization of a heteromeric protein phosphatase 2A holoenzyme from maize (*Zea mays* L.) leaves that dephosphorylates C4 phosphoenolpyruvate carboxylase. Planta, 213(3), 379-389.

66. Dong, L., Ermolova, N. V., & Chollet, R. (2001). Partial purification and biochemical characterization of a heteromeric protein phosphatase 2A holoenzyme from maize (Zea mays L.) leaves that dephosphorylates C4 phosphoenolpyruvate carboxylase. Planta, 213(3), 379-389.

67. Douette, P., Navet, R., Gerkens, P., Galleni, M., Lévy, D., & Sluse, F. E. (2005). Escherichia coli fusion carrier proteins act as solubilizing agents for recombinant uncoupling protein 1 through interactions with GroEL. Biochemical and Biophysical Research Communications, 333(3), 686-693.

68. Drincovich, M. F., Casati, P., & Andreo, C. S. (2001). NADP-malic enzyme from plants: a ubiquitous enzyme involved in different metabolic pathways. FEBS Letters, 490(1-2), 1-6.

69. Drincovich, M.F. and Andreo, C.S. (1994) Redox regulation of maize NADP-malic enzyme by thiol–disulfide interchange: effect of reduced thioredoxin on activity. Biochemical and Biophysical, Acta 1206, 10–16.

70. Drincovich, M.F., Lara, M.V., Andreo, C.S. and Maurino, V.G. (2011) C4 decarboxylases: different solutions for the same biochemical prob- lem, the provision of CO2 to RubisCO in the bundle sheath cells. In C4 Photosynthesis and Related CO2 Concentrating Mechanism. Edited by Raghavendra, A.S. and Sage, R.F. pp. 277–300. Springer Science, Dordrecht, The Netherlands.

71. Drincovich, M.F., Spampinato, C.P. and Andreo, C.S. (1992) Evidence for the existence of two essential and proximal cysteinyl residues in NADP-malic enzyme from maize leaves. Plant Physiology, 100: 2035–2040.

72. Du, Y. C., Nose, A., & Wasano, K. (1999). Thermal characteristics of C4 photosynthetic enzymes from leaves of three sugarcane species differing in cold sensitivity. Plant and Cell Physiology, 40(3), 298-304.

73. Du, Y. C., Nose, A., & Wasano, K. (1999a). Effects of chilling temperature on photosynthetic rates, photosynthetic enzyme activities and metabolite levels in leaves of three sugarcane species. Plant, Cell and Environment, 22(3), 317-324.

74. Duff, S. M., Andreo, C. S., Pacquit, V., Lepiniec, L., Sarath, G., Condon, S. A., Chollet, R. (1995). Kinetic analysis of the non-phosphorylated, *in vitro* phosphorylated, and phosphorylation-site-mutant (Asp8) forms of intact recombinant C_4 phosphoenolpyruvate carboxylase from sorghum. European Journal of Biochemistry, 228(1), 92-95.

75. Duff, S. M.G., and Chollet, R. (1995). In vivo regulation of wheat-leaf phosphoenolpyruvate carboxylase by reversible phosphorylation. Plant Physiology, 107(3), 775-782.

76. Duff, S.M.G. (1995). Kinetic analysis of the non-phosphorylated, *in vitro* phosphorylated, and phosphorylatian-site-mutant (Asp8) forms of intact recombinant C_4 phosphoenolpyruvate carboxylase from sorghum, European Journal Biochemistry, 228, 92-95.

77. Dümmler, A., Lawrence, A. M., & De Marco, A. (2005). Simplified screening for the detection of soluble fusion constructs expressed in E. coli using a modular set of vectors. Microbial Cell Factories, 4(1), 34.

78. Echevarria, C. & J. Vidal (2003). The unique phosphoenolpyruvate carboxylase kinase. Plant Physiology and Biochemistry, (41), 541-547.

79. Echevarria, C., Pacquit, V., Bakrim, N., Osuna, L., Delgado, B., Arriodupont, M., & Vidal, J. (1994). The effect of pH on the covalent and metabolic control of C4 phosphoenolpyruvate carboxylase from Sorghum leaf. Archives of Biochemistry and Biophysics, 315(2), 425-430.

80. Edelman, A. M., Blumenthal, D. K., & Krebs, E. G. (1987). Protein serine/threonine kinases. Annual review of biochemistry, 56(1), 567-613.

81. Edwards, G. E., Furbank, R. T., Hatch, M. D., & Osmond, C. B. (2001). What does it take to be C_4? Lessons from the evolution of C4 photosynthesis. Plant Physiology, 125(1), 46-49.

82. Edwards, G., & Walker, D. (1983). C_3, C_4: mechanisms, and cellular and environmental regulation of photosynthesis. University of California Press.

83. Ehleringer, J. R., Cerling, T. E., & Helliker, B. R. (1997). C4 photosynthesis, atmospheric CO_2, and climate. Oecologia, 112(3), 285-299.

84. Ehleringer, J. R., Sage, R. F., Flanagan, L. B., & Pearcy, R. W. (1991). Climate change and the evolution of C4 photosynthesis. Trends in Ecology & Evolution, 6(3), 95-99.

85. Elvin, C. M., Thompson, P. R., Argall, M. E., Hendr, N. P., Stamford, P. J., Lilley, P. E., & Dixon, N. E. (1990). Modified bacteriophage lambda promoter vectors for overproduction of proteins in *Escherichia coli*. Gene, 87(1), 123-126.

86. Endo, T., Mihara, Y., Furumoto, T., Matsumura, H., Kai, Y., & Izui, K. (2008). Maize C4-form phosphoenolpyruvate carboxylase engineered to be functional in C_3 plants: mutations for diminished sensitivity to feedback inhibitors and for increased substrate affinity. Journal of Experimental Botany, 59(7), 1811-1818.

87. Engelmann, S., Bläsing, O. E., Gowik, U., Svensson, P., & Westhoff, P. (2003). Molecular evolution of C_4 phosphoenolpyruvate carboxylase in the genus Flaveria—a gradual increase from C_3 to C_4 characteristics. Planta, 217(5), 717-725.

88. Ermolova, N. V., Cushman, M. A., Taybi, T., Condon, S. A., Cushman, J. C., & Chollet, R. (2003). Expression, purification, and initial characterization of a recombinant form of plant PEP-carboxylase kinase from CAM-induced Mesembryanthemum crystallinum with enhanced solubility in *Escherichia coli*. Protein Expression and Purification, 29(1), 123-131.

89. Ernst, S. M., Budde, R. J., & Chollet, R., (1986). Partial purification and characterization of pyruvate, orthophosphate dikinase from *Rhodospirillum rubrum*. Journal of Bacteriology, 165(2), 483-488.

90. Esposito, D., & Chatterjee, D. K. (2006). Enhancement of soluble protein expression through the use of fusion tags. Current Opinion in Biotechnology, 17(4), 353-358.

91. Evenson, R.E., & Gollin, D. (2003). Assessing the impact of the green revolution, 1960 to 2000. Science, (300), 758–762.

92. FAO, (2015). The state of food insecurity in the world 2015. Meeting the 2015 International Hunger Targets: Taking Stock on Uneven Progress. Food and Agriculture Organisation, Rome. Retrieved from http://www.fao.org/3/ca5162en/ca5162en.pdf.

93. FAO, (2019). The State of Food Security and Nutrition in the World 2019. Safe Guarding Against Economic Slowdowns And Downturns. Food and Agriculture Organization of the United Nations. Rome, FAO. Reterived from https://www.unicef.org/media/55921/file/SOFI-2019-full-report.pdf.

94. Fischer, R. A. (2015). Definitions and determination of crop yield, yield gaps, and of rates of change. Field Crops Research, (182), 9-18.

95. Fontaine, V., Hartwell, J., Jenkins, G. I., & Nimmo, H. G. (2002). Arabidopsis thaliana contains two phosphoenolpyruvate carboxylase kinase genes with different expression patterns. Plant, Cell & Environment, 25(1), 115-122.

96. Francis, D. M., & Page, R. (2010). Strategies to optimize protein expression in *E. coli*. Current Protocols in Protein Science, 61(1), 5-24.

97. Frank, J., Clarke, R.J., Vater, J., & Holzwarth, J.F. (2001). Influence of allosteric effectors on the kinetics and equilibrium binding of phosphoenolpyruvate (PEP) to phosphoenolpyruvate carboxylase (PEPC) from *Zea mays*. Biophysical Chemistry, 92, 53–64.

98. Friso, G., & van Wijk, K. J. (2015). Posttranslational protein modifications in plant metabolism. Plant Physiology, 169(3), 1469-1487.

99. Fujita, N., Miwa, T., Ishijima, S., Izui, K., & Katsuki, H. (1984). The primary structure of phosphoenolpyruvate carboxylase of Escherichia coli. Nucleotide sequence of the ppc gene and deduced amino acid sequence. The Journal of Biochemistry, 95(4), 909-916.

100. Fukayama, H., Tamai, T., Taniguchi, Y., Sullivan, S., Miyao, M., & Nimmo, H. G. (2006). Characterization and functional analysis of phosphoenolpyruvate carboxylase kinase genes in rice. The Plant Journal, 47(2), 258-268.

101. Fukunaga, Y., Nishimoto, E., Otosu, T., Murakami, Y., & Yamashita, S. (2008). The unfolding of α-momorcharin proceeds through the compact folded intermediate. Journal of Biochemistry, 144(4), 457-466.

102. Furbank, R. T., von Caemmerer, S., Sheehy, J., & Edwards, G. (2009). C_4 rice: a challenge for plant phenomics. Functional Plant Biology, 36(11), 845-856.

103. Gao, Y., & Woo, K. C. (1996). Site-directed mutagenesis of *Flaveria trinervia* phosphoenolpyruvate carboxylase: Arg450 and Arg767 are essential for catalytic activity and Lys829 affects substrate binding. FEBS letters, 392(3), 285-288.

104. Garnett, T., Appleby, M. C., Balmford, A., Bateman, I. J., Benton, T. G., Bloomer, P., & Herrero, M. (2013). Sustainable intensification in agriculture: premises and policies. Science, 341(6141), 33-34.

105. Gerland, P., Raftery, A. E., Ševčíková, H., Li, N., Gu, D., Spoorenberg, T. & Bay, G. (2014). World population stabilization unlikely this century. Science, 346(6206), 234-237.

106. Ghannoum, O., Caemmerer, S. V., Ziska, L. H., & Conroy, J. P. (2000). The growth response of C4 plants to rising atmospheric CO2 partial pressure: a reassessment. Plant, Cell & Environment, 23(9), 931-942.

107. Ghannoum, O., Evans, J. R., & von Caemmerer, S. (2010). Nitrogen and water use efficiency of C 4 plants. In C4 photosynthesis and related CO2 concentrating mechanisms (pp. 129-146). Springer, Dordrecht.

108. Ghannoum, O., Evans, J. R., & von Caemmerer, S. (2010). Nitrogen and water use efficiency of C 4 plants. In C4 photosynthesis and related CO2 concentrating mechanisms (pp. 129-146). Springer, Dordrecht.

109. Gillinta, J., & Grover, S. D. (1995). Kinetic interactions of glycine with substrates and effectors of phosphenolpyruvate carboxylase from maize leaves. Photosynthesis Research, 45(2), 121-126.

110. Gillon J. & Yakir D. (2001) Influence of carbonic anhydrase activity in terrestrial vegetation on the O-18 content of atmospheric CO_2. Science, 291, 2584–2587

111. Godfray, H. C. J., & Garnett, T. (2014). Food security and sustainable intensification. Philosophical transactions of the Royal Society B: Biological Sciences, 369(1639), 20120273.

112. Gonzalez, D. H., Iglesias, A. A., & Andreo, C. S. (1984). On the regulation of phosphoenolpyruvate carboxylase activity from maize leaves by L-malate. Effect of pH. Journal of Plant Physiology, 116(5), 425-434.

113. González-Segura, L., Mújica-Jiménez, C., Juárez-Díaz, J. A., Güémez-Toro, R., Martinez-Castilla, L. P., & Muñoz-Clares, R. A. (2018). Identification of the allosteric site for neutral amino acids in the maize C4 isozyme of phosphoenolpyruvate carboxylase: The critical role of Ser-100. Journal of Biological Chemistry, 293(26), 9945-9957.

114. Gornall J, Betts R, Burke E, Clark R, Camp J, Willett K, Wiltshire A. (2010). Implications of climate change for agricultural productivity in the early twenty-first century. Philosophical Transactions of the Royal Society B, 365, 2973–2989.

115. Gousset-Dupont, A., Lebouteiller, B., Monreal, J., Echevarria, C., Pierre, J. N., Hodges, M., & Vidal, J. (2005). Metabolite and post-translational control of phosphoenolpyruvate carboxylase from leaves and mesophyll cell protoplasts of Arabidopsis thaliana. Plant Science, 169(6), 1096-1101.

116. Gowik, U., & Westhoff, P. (2010). C 4-phosphoenolpyruvate carboxylase. In C_4 photosynthesis and related CO_2 concentrating mechanisms (pp. 257-275). Springer, Dordrecht.

117. Gowik, U., Brautigam, A., Weber, K.L., Weber, A.P. & Westhoff, P. (2011). Evolution of C_4 photosynthesis in the genus Flaveria: how many and which genes does it take to make C_4? Plant Cell, (23), 2087-2105.

118. Gowik, U., Engelmann, S., Bläsing, O. E., Raghavendra, A. S., & Westhoff, P. (2006). Evolution of C_4 phosphoenolpyruvate carboxylase in the genus Alternanthera: gene families and the enzymatic characteristics of the C_4 isozyme and its orthologues in C_3 and C_3/C_4 Alternantheras. Planta, 223(2), 359-368.

119. Grodberg, J., & Dunn, J. J. (1988). ompT encodes the *Escherichia coli* outer membrane protease that cleaves T7 RNA polymerase during purification. Journal of Bacteriology, 170(3), 1245-1253.

120. Gronenborn, B. (1976). Overproduction of phage lambda repressor under control of the lac promotor of *Escherichia coli*. Molecular and General Genetics MGG, 148(3), 243-250.

121. Guan, K., and Dixon, J. E. (1991). Eukaryotic proteins expressed in Escherichia coli: an improved thrombin cleavage and purification procedure of fusion proteins with glutathione S-transferase. Analytical Biochemistry, 192(2), 262-267

122. Haberlandt, G. (1884). Physiologische Pflanzenanatomie. Engelmann, Leipzig.

123. Haldimann, A., Daniels, L. L., & Wanner, B. L. (1998). Use of new methods for construction of tightly regulated arabinose and rhamnose promoter fusions in studies of the *Escherichia coli* phosphate regulon. Journal of Bacteriology, 180(5), 1277-1286.

124. Hanks, S. K., Quinn, A. M., & Hunter, T. (1988). The protein kinase family: conserved features and deduced phylogeny of the catalytic domains. Science, 241(4861), 42-52.

125. Harrison, R. G. NusA Protein as a Solubility-Promoting Tag: A Review. Novagen . inNovation

126. Hartwell, J., Gill, A., Nimmo, G. A., Wilkins, M. B., Jenkins, G. I., & Nimmo, H. G. (1999). Phosphoenol pyruvate carboxylase kinase is a novel protein kinase regulated at the level of expression. The Plant Journal, 20(3), 333-342.

127. Hatch, M. D. (1987). C_4 photosynthesis: a unique elend of modified biochemistry, anatomy and ultrastructure. Biochimica et Biophysica Acta (BBA)-Reviews on Bioenergetics, 895(2), 81-106.

128. Hatch, M. D. (1992). C_4 photosynthesis: an unlikely process full of surprises. Plant and Cell Physiology, 33(4), 333-342.

129. Hatch, M. D. (1999). C_4 photosynthesis: a historical overview. In Sage, R. F., and Monson, R. K. (eds) C_4 Plant Biology. Physiological Ecologiy Series, pp 17-46. Academic Press, San Diego.

130. Hatch, M. D., & Oliver, I. R. (1978). Activation and inactivation of phosphoenolpyruvate carboxylase in leaf extracts from C4 species. Functional Plant Biology, 5(5), 571-580.

131. Hefti, M. H., Dixon, R., & Vervoort, J. (2001). A novel purification method for histidine-tagged proteins containing a thrombin cleavage site. Analytical Biochemistry, 295(2), 180-185.

132. Hess, J.F. Oosawa, K. Kaplan, N. Simon, M.I. (1988) Phosphorylation of three proteins in the signaling pathway of bacterial chemotaxis, Cell, 53; 79–87.

133. Heyl, A., Brault, M., Frugier, F., Kuderova, A., Lindner, A. C., Motyka, V.,& Schaller, G. E. (2013). Nomenclature for members of the two-component signaling pathway of plants. Plant physiology, 161(3), 1063-1065.

134. Hibberd, J. M., & Covshoff, S. (2010). The regulation of gene expression required for C4 photosynthesis. Annual Review of Plant Biology, (61), 181-207.

135. Huber, S. C. (2007). Exploring the role of protein phosphorylation in plants: from signalling to metabolism. Biochemical Society Transactions, 35(1), 28-32.

136. Huber, S. C., & Edwards, G. E. (1975). Regulation of oxaloacetate, aspartate, and malate formation in mesophyll protoplast extracts of three types of C4 plants. Plant Physiology, 56(2), 324-331.

137. Huber, S. C., & Hardin, S. C. (2004). Numerous posttranslational modifications provide opportunities for the intricate regulation of metabolic enzymes at multiple levels. Current Opinion in Plant Biology, 7(3), 318-322.

138. Hunke, S., & Betton, J. M. (2003). Temperature effect on inclusion body formation and stress response in the periplasm of *Escherichia coli*. Molecular Microbiology, 50(5), 1579-1589.

139. Hunter, T., & Cooper, J. A. (1985). Protein-tyrosine kinases. Annual Review of Biochemistry, 54(1), 897-930.

140. Hýsková, V. D., Miedzińska, L., Dobrá, J., Vankova, R., & Ryšlavá, H. (2014). Phosphoenolpyruvate carboxylase, NADP-malic enzyme, and pyruvate, phosphate dikinase are involved in the acclimation of *Nicotiana tabacum* L. to drought stress. Journal of Plant Physiology, 171(5), 19-25.

141. Iglesias, A. A., González, D. H., & Andreo, C. S. (1986). The C_4 pathway of photosynthesis and its regulation. Biochemical Education, 14(3), 98-102.

142. Ishijima, S., Katagiri, F., Kodaki, T., Izui, K., Katsuki, H., Nishikawa, K., & Ooi, T. (1985). Comparison of amino acid sequences between phosphoenolpyruvate carboxylases from Escherichiacoli (allosteric) and anacystisnidulans (non-allosteric): Identification of conserved and variable regions. Biochemical and Biophysical Research Communications, 133(2), 436-441.

143. Izui, K., Matsumura, H., Furumoto, T., & Kai, Y. (2004). Phospho enol pyruvate carboxylase: a new era of structural biology. Annual Review of Plant Biology, 55, 69-84.

144. Jaggard, K. W., Qi, A., & Ober, E. S. (2010). Possible changes to arable crop yields by 2050. Philosophical Transactions of the Royal Society B: Biological Sciences, 365(1554), 2835-2851.

145. Jana, S., & Deb, J. K. (2005). RETRACTED ARTICLE: Strategies for efficient production of heterologous proteins in Escherichia coli. Applied Microbiology and Biotechnology, 67(3), 289-298.

146. Jenny, R. J., Mann, K. G., & Lundblad, R. L. (2003). A critical review of the methods for cleavage of fusion proteins with thrombin and factor Xa. Protein Expression and Purification, 31(1), 1-11.

147. Jensen, O. N. (2004). Modification-specific proteomics: characterization of post-translational modifications by mass spectrometry. Current Opinion in Chemical Biology, 8(1), 33-41.

148. Jiao, J. A., & Chollet, R. (1988). Light/dark regulation of maize leaf phosphoenolpyruvate carboxylase by in vivo phosphorylation. Archives of Biochemistry and Biophysics, 261(2), 409-417.

149. Jiao, J. A., & Chollet, R. (1989). Regulatory seryl-phosphorylation of C4 phosphoenolpyruvate carboxylase by a soluble protein kinase from maize leaves. Archives of Biochemistry and Biophysics, 269(2), 526-535.

150. Jiao, J. A., & Chollet, R. (1990). Regulatory phosphorylation of serine-15 in maize phosphoenolpyruvate carboxylase by a C4-leaf protein-serine kinase. Archives of Biochemistry and Biophysics, 283(2), 300-305.

151. Jiao, J. A., & Chollet, R. (1992). Light activation of maize phosphoenolpyruvate carboxylase protein-serine kinase activity is inhibited by mesophyll and bundle sheath-directed photosynthesis inhibitors. Plant Physiology, 98(1), 152-156.

152. Jiao, J. A., Vidal, J., Echevarría, C., & Chollet, R. (1991). In vivo regulatory phosphorylation site in C_4-leaf phosphoenolpyruvate carboxylase from maize and sorghum. Plant Physiology, 96(1), 297-301.

153. Jordan, D. B., & Ogren, W. L. (1984). The CO_2/O_2 specificity of ribulose 1, 5-bisphosphate carboxylase/oxygenase. Planta, 161(4), 308-313.

154. Kanai, R., and Edwards, G. E. (1999). The biochemistry of C_4 photosynthesis.C_4 plant biology. 49: 87.

155. Kapust, R. B., & Waugh, D. S. (1999). Escherichia coli maltose-binding protein is uncommonly effective at promoting the solubility of polypeptides to which it is fused. Protein Science, 8(8), 1668-1674.

156. Karlsen, O. A., Ramsevik, L., Bruseth, L. J., Larsen, Ø., Brenner, A., Berven, F. S., & Lillehaug, J. R. (2005). Characterization of a prokaryotic haemerythrin from the methanotrophic bacterium Methylococcus capsulatus (Bath). The FEBS Journal, 272(10), 2428-2440.

157. Kemp, B. E., & Pearson, R. B. (1991). Intrasteric regulation of protein kinases and phosphatases. Biochimica et Biophysica Acta (BBA)-Molecular Cell Research, 1094(1), 67-76.

158. Khush, G. S. (2001). Green revolution: The way forward. Nature Reviews Genetics, 2(10), 815-822.

159. Khush, G. S. (2005). What it will take to feed 5 billion rice consumers in 2030. Plant Molecular Biology, 59(1), 1-6.

160. Kim, S., & Lee, S. B. (2008). Soluble expression of archaeal proteins in Escherichia coli by using fusion-partners. Protein Expression and Purification, 62(1), 116-119.

161. Kinoshita, E., & Kinoshita-Kikuta, E. (2011). Improved Phos-tag SDS-PAGE under neutral pH conditions for advanced protein phosphorylation profiling. Proteomics, 11(2), 319-323.

162. Kinoshita, E., Kinoshita-Kikuta, E., & Koike, T. (2009). Separation and detection of large phosphoproteins using Phos-tag SDS-PAGE. Nature Protocols, 4(10), 1513.

163. Kinoshita, E., Kinoshita-Kikuta, E., & Koike, T. (2012). Phos-tag SDS-PAGE systems for phosphorylation profiling of proteins with a wide range of molecular masses under neutral pH conditions. Proteomics, 12(2), 192-202.

164. Kinoshita, E., Kinoshita-Kikuta, E., Matsubara, M., Aoki, Y., Ohie, S., Mouri, Y., and Koike, T. (2009). Two-dimensional phosphate-affinity gel electrophoresis for the analysis of phosphoprotein isotypes. Electrophoresis, 30, 550–559

165. Kinoshita, E., Kinoshita-Kikuta, E., Takiyama, K., & Koike, T. (2006). Phosphate-binding tag, a new tool to visualize phosphorylated proteins. Molecular & Cellular Proteomics, 5(4), 749-757.

166. Kinoshita, E., Takahashi, M., Takeda, H., Shiro, M., & Koike, T. (2004). Recognition of phosphate monoester dianion by an alkoxide-bridged dinuclear zinc (II) complex. Dalton Transactions, (8), 1189-1193.

167. Koehl, C., & Abecassis, J. (1976). Determination of oxalic acid in urine by atomic absorption spectrophotometry. Clinica Chimica Acta, 70(1), 71-77.

168. Kohl, T., Schmidt, C., Wiemann, S., Poustka, A. & Korf, U. (2008). Automated production of recombinant human proteins as resource for proteome research. Proteome Science, 6(1), 1-10.

169. Kopriva, S. (2011). Nitrogen and Sulfur Metabolism in C4 Plants. In C4 Photosynthesis and Related CO2 Concentrating Mechanism. Edited by Raghavendra, A.S. and Sage, R.F. Springer Science, Dordrecht, The Netherlands.

170. Korf, U., Kohl, T., van der Zandt, H., Zahn, R., Schleeger, S., Ueberle, B. & Wiemann, S. (2005). Large-scale protein expression for proteome research. Proteomics, 5(14), 3571-3580.

171. Kosobokova, E. N., Skrypnik, K. A., & Kosorukov, V. S. (2016). Overview of fusion tags for recombinant proteins. Biochemistry (Moscow), 81(3), 187-200.

172. Krall, J. P., & Edwards, G. E. (1993). PEP carboxylases from two C4 species of Panicum with markedly different susceptibilities to cold inactivation. Plant and Cell Physiology, 34(1), 1-11.

173. Krebs, E. G., & Beavo, J. A. (1979). Phosphorylation-dephosphorylation of enzymes. Annual Review of Biochemistry, 48(1), 923-959.

174. Krishna, R. G., & Wold, F. (1993). Post-translational modifications of proteins. In Methods in protein sequence analysis (pp. 167-172). Springer, Boston, MA.

175. Kubien, D. S., & Sage, R. F. (2003). C 4 grasses in boreal fens: their occurrence in relation to microsite characteristics. Oecologia, 137(3), 330-337.

176. Latzko, E., & Kelly, G. J. (1983). The many-faceted function of phosphoenolpyruvate carboxylase in C_3 plants. Physiologie végétale (Paris), 21(5), 805-815.

177. Le Borgne, S., & Graber, M. (1994). Amidase activity and thermal stability of human thrombin. Applied Biochemistry and Biotechnology, 48(2), 125-135.15:36

178. Leakey, A. D. (2009). Rising atmospheric carbon dioxide concentration and the future of C4 crops for food and fuel. Proceedings of the Royal Society B: Biological Sciences, 276(1666), 2333-2343.

179. Lee, C. H. (2010). 1-Anilinonaphthalene-8-sulfonate (ANS); A versatile fluorescent probe from protein folding study to drug design. BioWave Cooperation, 12(6), 1.

180. Leegood, R. C., & Walker, R. P. (1999). Regulation of the C4 Pathway. In C_4 Plant Biology. Academic Press. Sage, R. F., & Monson, R. K. Academic Press. San Diego.

181. Lepiniec, L., Vidal, J., Chollet, R., Gadal, P., & Crétin, C. (1994). Phosphoenolpyruvate carboxylase: structure, regulation and evolution. Plant Science, 99(2), 111-124.

182. Li, B., Pacquit, V., Jiao, J. A., Duff, S. M., Maralihalli, G. B., Sarath, G., & Chollet, R. (1997). Structural requirements for phosphorylation of C4-leaf phosphoenolpyruvate carboxylase by its highly regulated protein-serine kinase. A comparative study with synthetic-peptide substrates and mutant target proteins. Functional Plant Biology, 24(4), 443-449.

183. Lombardo, C. R., Consler, T. G., & Kassel, D. B. (1995). *In vitro* phosphorylation of the epidermal growth factor receptor autophosphorylation domain by c-src: identification of phosphorylation sites and c-src SH2 domain binding sites. Biochemistry, 34(50), 16456-16466.

184. Long, S. P. (2014). We need winners in the race to increase photosynthesis in rice, whether from conventional breeding, biotechnology or both. Plant, Cell & Environment, 37(1), 19-21.

185. Long, S. P., Marshall-Colon, A., & Zhu, X. G. (2015). Meeting the global food demand of the future by engineering crop photosynthesis and yield potential. Cell, 161(1), 56-66.

186. Lopez, M. F., Berggren, K., Chernokalskaya, E., Lazarev, A., Robinson, M., & Patton, W. F. (2000). A comparison of silver stain and SYPRO Ruby Protein Gel Stain with respect to protein detection in two-dimensional gels and identification by peptide mass profiling. Electrophoresis, 21(17), 3673-3683.

187. Ludwig, M. (2013). Evolution of the C_4 photosynthetic pathway: Events at the cellular and molecular levels. Photosynthesis Research, 117(1-3), 147-161.

188. Lukat, G.S. McCleary, W.R. Stock, A.M. Stock, J.B. (1992) Phosphorylation of bacterial response regulator proteins by low molecular weight phospho-donors, Proceedings of the National Academy of Sciences, 89; 718–722.

189. Ma, H. (1993). Protein phosphorylation in plants: enzymes, substrates and regulators. Trends in Genetics, 9(7), 228-230.

190. Maeda, Y., Ueda, T., & Imoto, T. (1996). Effective renaturation of denatured and reduced immunoglobulin G *in vitro* without assistance of chaperone. Protein Engineering, Design and Selection, 9(1), 95-100.

191. Mamedov, T. G., Moellering, E. R., & Chollet, R. (2005). Identification and expression analysis of two inorganic C-and N-responsive genes encoding novel and distinct molecular forms of eukaryotic phosphoenolpyruvate carboxylase in the green microalga Chlamydomonas reinhardtii. The Plant Journal, 42(6), 832-843.

192. Mann, M., & Jensen, O. N. (2003). Proteomic analysis of post-translational modifications. Nature Biotechnology, 21(3), 255.

193. Mann, M., Ong, S. E., Grønborg, M., Steen, H., Jensen, O. N., & Pandey, A. (2002). Analysis of protein phosphorylation using mass spectrometry: deciphering the phosphoproteome. Trends in Biotechnology, 20(6), 261-268.

194. Marsh, J. T., Sullivan, S., Hartwell, J., & Nimmo, H. G. (2003). Structure and expression of phosphoenolpyruvate carboxylase kinase genes in Solanaceae. A novel gene exhibits alternative splicing. Plant Physiology, 133(4), 2021-2028.

195. Martin, K., Steinberg, T. H., Cooley, L. A., Gee, K. R., Beechem, J. M., & Patton, W. F. (2003). Quantitative analysis of protein phosphorylation status and protein kinase activity on microarrays using a novel fluorescent phosphorylation sensor dye. Proteomics: International Edition, 3(7), 1244-1255.

196. Matsuba, K., Imaizumi, N., Kaneko, S., Samejima, M., & Ohsugi, R. (1997). Photosynthetic responses to temperature of phosphoenolpyruvate carboxykinase type C_4 species differing in cold sensitivity. Plant, Cell & Environment, 20(2), 268-274.

197. Matsuda, Y., Nakajima, K., & Tachibana, M. (2011). Recent progresses on the genetic basis of the regulation of CO_2 acquisition systems in response to CO_2 concentration. Photosynthesis Research, 109(1-3), 191-203.

198. Maxwell, K., Badger, M. R., & Osmond, C. B. (1998). A comparison of CO_2 and O_2 exchange patterns and the relationship with chlorophyll fluorescence during photosynthesis in C_3 and CAM plants. Functional Plant Biology, 25(1), 45-52.

199. McLachlin, D. T., & Chait, B. T. (2001). Analysis of phosphorylated proteins and peptides by mass spectrometry. Current Opinion In Chemical Biology, 5(5), 591-602.

200. McNaughton, G. A. L., Fewson, C. A., Wilkins, M. B., & Nimmo, H. G. (1989). Purification, oligomerization state and malate sensitivity of maize leaf phosphoenolpyruvate carboxylase. Biochemical Journal, 261(2), 349-355.

201. Meimoun, P., Ambard-Bretteville, F., Colas-des Francs-Small, C., Valot, B., & Vidal, J. (2007). Analysis of plant phosphoproteins. Analytical Biochemistry, 371(2), 238-246.

202. Meister, M., Agostino, A., & Hatch, M. D. (1996). The roles of malate and aspartate in C_4 photosynthetic metabolism of Flaveria bidentis (L.). Planta, 199(2), 262-269.

203. Melzer, E., & O'Leary, M. H. (1987). Anapleurotic CO2 fixation by phosphoenolpyruvate carboxylase in C_3 plants. Plant Physiology, 84(1), 58-60.

204. Messer, A. E., Gallon, C. E., McKenna, W. J., Dos Remedios, C. G., & Marston, S. B. (2009). The use of phosphate-affinity SDS-PAGE to measure the cardiac troponin I phosphorylation site distribution in human heart muscle. Proteomics–Clinical Applications, 3(12), 1371-1382.

205. Mithoe, S. C., & Menke, F. L. (2011). Phosphoproteomics perspective on plant signal transduction and tyrosine phosphorylation. Phytochemistry, 72(10), 997-1006.

206. Mithoe, S. C., Boersema, P. J., Berke, L., Snel, B., Heck, A. J., & Menke, F. L. (2011). Targeted quantitative phosphoproteomics approach for the detection of phospho-tyrosine signaling in plants. Journal of Proteome Research, 11(1), 438-448.

207. Moffatt, B. A., & Studier, F. W. (1987). T7 lysozyme inhibits transcription by T7 RNA polymerase. Cell, 49(2), 221-227.

208. Monson, R. K., & Sage, R. F. (Eds.). (1999). C_4 plant biology. Academic Press.

209. Moody, Nicholas., (2018). Comparative enzymology of the convergent co-option of phosphoenolpyruvate carboxylase for C_4 photosynthesis (Doctoral dissertation thesis) University of Sheffield;Chemsitry Sheffield, United Kingdom.

210. Mori, I. C., Murata, Y., Yang, Y., Munemasa, S., Wang, Y. F., Andreoli, S., ... & Kwak, J. M. (2006). CDPKs CPK6 and CPK3 function in ABA regulation of guard cell S-type anion-and Ca2+-permeable channels and stomatal closure. PLoS Biology, 4(10), e327.

211. Moroney, J. V., & Somanchi, A. (1999). How do algae concentrate CO_2 to increase the efficiency of photosynthetic carbon fixation?. Plant Physiology, 119(1), 9-16.

212. Muhaidat, R., Sage, R. F., & Dengler, N. G. (2007). Diversity of Kranz anatomy and biochemistry in C_4 eudicots. American Journal of Botany, 94(3), 362-381.

213. Mujacic, M., Cooper, K. W., & Baneyx, F. (1999). Cold-inducible cloning vectors for low-temperature protein expression in Escherichia coli: application to the production of a toxic and proteolytically sensitive fusion protein. Gene, 238(2), 325-332.

214. Murmu, J., & Plaxton, W. C. (2007). Phosphoenolpyruvate carboxylase protein kinase from developing castor oil seeds: partial purification, characterization, and reversible control by photosynthate supply. Planta, 226(5), 1299-1310.

215. Nakagami, H., Sugiyama, N., Ishihama, Y., & Shirasu, K. (2011). Shotguns in the front line: phosphoproteomics in plants. Plant and Cell Physiology, 53(1), 118-124.

216. Neubauer, G., & Mann, M. (1999). Mapping of phosphorylation sites of gel-isolated proteins by nanoelectrospray tandem mass spectrometry: potentials and limitations. Analytical Chemistry, 71(1), 235-242.

217. Nimmo, G. A., McNaughton, G. A., Fewson, C. A., Wilkins, M. B., & Nimmo, H. G. (1987). Changes in the kinetic properties and phosphorylation state of phosphoenolpyruvate carboxylase in Zea mays leaves in reponse to light and dark. FEBS Letters, 213(1), 18-22.

218. Nimmo, H. G. (2000). The regulation of phosphoenolpyruvate carboxylase in CAM plants. Trends in Plant Science, 5(2), 75-80.

219. Nimmo, H. G. (2003). Control of the phosphorylation of phosphoenolpyruvate carboxylase in higher plants. Archives of Biochemistry and Biophysics, 414(2), 189-196.

220. Nishikido, T., & Takanashi, H. (1973). Glycine activation of PEP carboxylase from monocotyledoneous C4 plants. Biochemical and Biophysical Research Communications, 53(1), 126-133.

221. O'Leary B., Rao, S.K., Kim, J., Plaxton, W.C. (2009) Bacterial-type phosphoenolpyruvate carboxylase (PEPC) functions as a catalytic and regulatory subunit of the novel class-2 PEPC complex of vascular plants. Journal of Biological Chemistry, 284, 24797–24805.

222. Oberg, K., Chrunyk, B. A., Wetzel, R., & Fink, A. L. (1994). Native-like secondary structure in interleukin-1. beta. Inclusion bodies by attenuated total reflectance FTIR. Biochemistry, 33(9), 2628-2634.

223. O'Leary, B., Park, J., & Plaxton, W. C. (2011). The remarkable diversity of plant PEPC (phosphoenolpyruvate carboxylase): Recent insights into the physiological functions and post-translational controls of non-photosynthetic PEPCs. Biochemical Journal, 436(1), 15-34.

224. O'Leary, M. H. (1982). Phosphoenolpyruvate carboxylase: an enzymologist's view. Annual Review of Plant Physiology, 33(1), 297-315.

225. Ong, S. E., & Pandey, A. (2001). An evaluation of the use of two-dimensional gel electrophoresis in proteomics. Biomolecular Engineering, 18(5), 195-205.

226. Ort, D. R., Merchant, S. S., Alric, J., Barkan, A., Blankenship, R. E., Bock, R., Croce, R., Hanson, M.R., Hibberd, J.M., Long, S.P & Moore, T. A. (2015). Redesigning photosynthesis to sustainably meet global food and bioenergy demand. Proceedings of the National Academy of Sciences, 112(28), 8529-8536.

227. Osakabe, Y., Yamaguchi-Shinozaki, K., Shinozaki, K., & Tran, L. S. P. (2013). Sensing the environment: key roles of membrane-localized kinases in plant perception and response to abiotic stress. Journal of Experimental Botany, 64(2), 445-458.

228. Osuna, L., Pierre, J. N., González, M. C., Alvarez, R., Cejudo, F. J., Echevarría, C., & Vidal, J. (1999). Evidence for a slow-turnover form of the Ca2+-independent phosphoenolpyruvate carboxylase kinase in the aleurone-endosperm tissue of germinating barley seeds. Plant Physiology, 119(2), 511-520.

229. Pacquit, V., Giglioli, N., Crétin, C., Pierre, J. N., Vidal, J., & Echevarria, C. (1995). Regulatory phosphorylation of C 4 phosphoenolpyruvate carboxylase from Sorghum: an immunological study using specific anti-phosphorylation site-antibodies. Photosynthesis Research, 43(3), 283-288.

230. Palczewski, K., Buczyłko, J., Van Hooser, P., Carr, S. A., Huddleston, M. J., & Crabb, J. W. (1992). Identification of the autophosphorylation sites in rhodopsin kinase. Journal of Biological Chemistry, 267(26), 18991-18998.

231. Parry, M. A., & Hawkesford, M. J. (2010). Food security: increasing yield and improving resource use efficiency. Proceedings of the Nutrition Society, 69(04), 592-600.

232. Parthibane, V., Iyappan, R., Vijayakumar, A., Venkateshwari, V., & Rajasekharan, R. (2012). Serine/threonine/tyrosine protein kinase phosphorylates oleosin, a regulator of lipid metabolic functions. Plant Physiology, 159(1), 95-104.

233. Parvathi, K., Bhagwat, A. S., Ueno, Y., Izui, K., & Raghavendra, A. S. (2000). Illumination increases the affinity of phosphoenolpyruvate carboxylase to bicarbonate in leaves of a C4 plant, Amaranthus hypochondriacus. Plant and Cell Physiology, 41(8), 905-910.

234. Paulus, J. K., Schlieper, D., & Groth, G. (2013). Greater efficiency of photosynthetic carbon fixation due to single amino-acid substitution. Nature Communications, 4, 1518.

235. Phos-tag SDS-PAGE Guidebook, Wako chemicals Ltd.

236. Pinsach, J., de Mas, C., López-Santín, J., Striedner, G., & Bayer, K. (2008). Influence of process temperature on recombinant enzyme activity in Escherichia coli fed-batch cultures. Enzyme and Microbial Technology, 43(7), 507-512.

237. Qiagen, (2011). PhosphoProtein Handbook, Second edition.

238. Racie, L.A.C., McColgan, J.M. , Grant, K.L. , Smith, E.A.D. , McCoy, J.M., Lavallie, E.R. (1995). Production of recombinant bovine enterokinase catalytic subunit in Escherichia coli, using the novel secretory fusion partner DsbA, Biotechnology, 13, 982–987.

239. Raines, C. A. (2011). Increasing photosynthetic carbon assimilation in C3 plants to improve crop yield: current and future strategies. Plant Physiology, 155(1), 36-42.

240. Rajagopalan, A. V., Devi, M. T., & Raghavendra, A. S. (1994). Molecular biology of C 4 phosphoenolpyruvate carboxylase: structure, regulation and genetic engineering. Photosynthesis Research, 39(2), 115-135.

241. Ray, D. K., Mueller, N. D., West, P. C., & Foley, J. A. (2013). Yield trends are insufficient to double global crop production by 2050. PloS One, 8(6), e66428.

242. Rickers, J., Cushman, J. C., Michalowski, C. B., Schmitt, J. M., & Bohnert, H. J. (1989). Expression of the CAM-form of phosphoenol pyruvate carboxylase and nucleotide sequence of a full length cDNA from Mesembryanthemum crystallinum. Molecular and General Genetics MGG, 215(3), 447-454.

243. Rivoal, J., Turpin, D. H., & Plaxton, W. C. (2002). *In vitro* phosphorylation of phosphoenol pyruvate carboxylase from the green alga *Selenastrum minutum*. Plant and Cell Physiology, 43(7), 785-792.

244. Roche Diagnostics GmbH. (2004). The Complete Guide for Protease Inhibition. Mannheim, Germany.

245. Rodríguez-Sotres, R., & Muñoz-Clares, R. A. (1990). Kinetic evidence of the existence of a regulatory phosphoenolpyruvate binding site in maize leaf phosphoenolpyruvate carboxylase. Archives of Biochemistry and Biophysics, 276(1), 180-190

246. Roe, S. (Ed.). (2001). Protein purification techniques: a practical approach (Vol. 244). OUP Oxford.

247. Ross, E. M. (1989). Signal sorting and amplification through G protein-coupled receptors. Neuron, 3(2), 141-152.

248. Sage, R. F. (2004). The evolution of C_4 photosynthesis. New Phytologist, 161(2), 341-370.

249. Sage, R. F. (2011). C4 Photosynthesis and Temperature. In C4 Photosynthesis and Related CO_2 Concentrating Mechanism. Edited by Raghavendra, A.S. and Sage, R.F. Springer Science, Dordrecht, The Netherlands.

250. Sage, R. F., & Kubien, D. S. (2003). An ecophysiological perspective on global change and the future of C 4 plants. Photosynthesis Research, 77(2-3), 209-225.

251. Sage, R. F., & McKown, A. D. (2005). Is C_4 photosynthesis less phenotypically plastic than C_3 photosynthesis?. Journal of Experimental Botany, 57(2), 303-317.

252. Sage, R. F., Christin, P. A., & Edwards, E. J. (2011). The C_4 plant lineages of planet Earth. Journal of Experimental botany, 62(9), 3155-3169.

253. Sage, R. F., Sage, T. L. & Kocacinar, F. (2012). Photorespiration and the evolution of C_4 photosynthesis. Annual Review of Plant Biology, 63, 19-47.

254. Sage, R. F., Wedin, D. A., & Li, M. (1999). The biogeography of C4 photosynthesis: patterns and controlling factors. C_4 plant biology, 313-373.

255. Sage, T. L., & Sage, R. F. (2009). The functional anatomy of rice leaves: implications for refixation of photorespiratory CO_2 and efforts to engineer C_4 photosynthesis into rice. Plant and Cell Physiology, 50(4), 756-772.

256. Saze, H., Ueno, Y., Hisabori, T., Hayashi, H., & Izui, K. (2001). Thioredoxin-mediated reductive activation of a protein kinase for the regulatory phosphorylation of C_4-form phosphoenolpyruvate carboxylase from maize. Plant and Cell Physiology, 42(12), 1295-1302.

257. Schmidhuber, J., and Tubiello, F.N. (2007). Global food security under climate change. Proceedings of the National Academy of Sciences of the USA, 104, 19703–8.

258. Schönberg, A., & Baginsky, S. (2012). Signal integration by chloroplast phosphorylation networks: an update. Frontiers In Plant Science, 3, 256.

259. Schindelin, J., Arganda-Carreras, I., and Frise, E. (2012). Fiji: an open-source platform for biological-image analysis. Nature Methods, 9(7), 676-682.

260. Schulenberg, B., Aggeler, R., Beechem, J. M., Capaldi, R. A., & Patton, W. F. (2003). Analysis of steady-state protein phosphorylation in mitochondria using a novel fluorescent phosphosensor dye. Journal of Biological Chemistry, 278(29), 27251-27255.

261. Schulenberg, B., Goodman, T. N., Aggeler, R., Capaldi, R. A., & Patton, W. F. (2004). Characterization of dynamic and steady-state protein phosphorylation using a fluorescent phosphoprotein gel stain and mass spectrometry. Electrophoresis, 25(15), 2526-2532.

262. Schumann, W., and Ferreira, L. C. S. (2004). Production of recombinant proteins in Escherichia coli. Genet. Mol. Biol. 27, 442–453.

263. Scopes, R. K. (2013). Protein purification: Principles and practice. Springer Science & Business Media.

264. Shane, M. W., Fedosejevs, E. T., & Plaxton, W. C. (2013). Reciprocal control of anaplerotic phosphoenolpyruvate carboxylase by in vivo monoubiquitination and phosphorylation in developing proteoid roots of phosphate-deficient harsh hakea. Plant Physiology, 161(4), 1634-1644.

265. Shih, Y. P., Kung, W. M., Chen, J. C., Yeh, C. H., Wang, A. H. J., & Wang, T. F. (2002). High-throughput screening of soluble recombinant proteins. Protein Science, 11(7), 1714-1719.

266. Silva-Sanchez, C., Li, H., & Chen, S. (2015). Recent advances and challenges in plant phosphoproteomics. Proteomics, 15(5-6), 1127-1141.

267. Skerra, A. (1994). Use of the tetracycline promoter for the tightly regulated production of a murine antibody fragment in *Escherichia coli*. Gene, 151(1-2), 131-135.

268. Sørensen, H. P., & Mortensen, K. K. (2005a). Soluble expression of recombinant proteins in the cytoplasm of Escherichia coli. Microbial Cell Factories, 4(1), 1.

269. Sørensen, H. P., & Mortensen, K. K. (2005b). Advanced genetic strategies for recombinant protein expression in Escherichia coli. Journal of Biotechnology, 115(2), 113-128.

270. Spiess, C., Beil, A., & Ehrmann, M. (1999). A temperature-dependent switch from chaperone to protease in a widely conserved heat shock protein. Cell, 97(3), 339-347.

271. Spreitzer, R. J., & Salvucci, M. E. (2002). Rubisco: structure, regulatory interactions, and possibilities for a better enzyme. Annual Review of Plant Biology, 53.

272. Stasyk, T., Morandell, S., Bakry, R., Feuerstein, I., Huck, C. W., Stecher, G., ... & Huber, L. A. (2005). Quantitative detection of phosphoproteins by combination of two-dimensional difference gel electrophoresis and phosphospecific fluorescent staining. Electrophoresis, 26(14), 2850-2854.

273. Steinberg, T. H., Agnew, B. J., Gee, K. R., Leung, W. Y., Goodman, T., Schulenberg, B., ... & Patton, W. F. (2003). Global quantitative phosphoprotein analysis using multiplexed proteomics technology. Proteomics: International Edition, 3(7), 1128-1144.

274. Studer, R. A., Christin, P. A., Williams, M. A., & Orengo, C. A. (2014). Stability-activity tradeoffs constrain the adaptive evolution of RubisCO. Proceedings of the National Academy of Sciences, 111(6), 2223-2228.

275. Studier, F. W. (1990). Use of T7 RNA polymerase to direct expression of cloned genes. Methods Enzymology, 185, 60-89.

276. Studier, F. W., & Moffatt, B. A. (1986). Use of bacteriophage T7 RNA polymerase to direct selective high-level expression of cloned genes. Journal of Molecular Biology, 189(1), 113-130.

277. Sun, W., Xie, J., Lin, H., Mi, S., Li, Z., Hua, F., & Hu, Z. (2012). A combined strategy improves the solubility of aggregation-prone single-chain variable fragment antibodies. Protein Expression and Purification, 83(1), 21-29.

278. Svensson, P., Blasing, O. E., Westhoff, P. (2003). Evolution of C4 phosphoenolpyruvate carboxylase. Archives of Biochemistry and Biophysics, 414, 180–88.

279. Takagi, T., & Doolittle, R. F. (1974). Amino acid sequence studies on factor XIII and the peptide released during its activation by thrombin. Biochemistry, 13(4), 750-756.

280. Takahashi-Terada, A., Kotera, M., Ohshima, K., Furumoto, T., Matsumura, H., Kai, Y., & Izui, K. (2005). Maize Phosphoenolpyruvate Carboxylase mutations at the putative binding site for glucose 6-phosphate caused desensitization and abolished responsiveness to regulatory phosphorylation. Journal of Biological Chemistry, 280(12), 11798-11806.

281. Takeya, K., Loutzenhiser, K., Shiraishi, M., Loutzenhiser, R., and Walsh, M. P. (2008) A highly sensitive technique to measure myosin regulatory light chain phosphorylation: the first quantification in renal arterioles. American Journal of Physiology-Renal Physiology. 294, F1487–F1492

282. Taniguchi, H., Suzuki, M., Manenti, S., & Titani, K. (1994). A mass spectrometric study on the in vivo posttranslational modification of GAP-43. Journal of Biological Chemistry, 269(36), 22481-22484.

283. Tatematsu, K., Yoshimoto, N., Okajima, T., Tanizawa, K., & Kuroda, S. I. (2008). Identification of ubiquitin ligase activity of RBCK1 and its inhibition by splice variant RBCK2 and protein kinase Cβ. Journal of Biological Chemistry, 283(17), 11575-11585.

284. Taybi, T., Patil, S., Chollet, R., & Cushman, J. C. (2000). A minimal serine/threonine protein kinase circadianly regulates phosphoenolpyruvate carboxylase activity in crassulacean acid metabolism-induced leaves of the common ice plant. Plant Physiology, 123(4), 1471-1482.

285. Terada, K., Kai, T., Okuno, S., Fujisawa, H., & Izui, K. (1990). Maize leaf phosphoenolpyruvate carboxylase: phosphorylation of Ser15 with a mammalian cyclic AMP-dependent protein kinase diminishes sensitivity to inhibition by malate. FEBS Letters, 259(2), 241-244.

286. Terpe, K. (2003). Overview of tag protein fusions: from molecular and biochemical fundamentals to commercial systems. Applied Microbiology and Biotechnology, 60(5), 523-533.

287. Theng, V., Agarie, S., & Nose, A. (2008). Regulatory phosphorylation of phosphoenolpyruvate carboxylase in the leaves of *Kalanchoe pinnata, K. daigremontiana* and *Ananas comosus*. Biologia Plantarum, 52(2), 281-290.

288. Thomason, P., & Kay, R. (2000). Eukaryotic signal transduction via histidine-aspartate phosphorelay. Journal of Cell Science, 113(18), 3141-3150.

289. Thurston, G., Regan, S., Rampitsch, C., & Xing, T. (2005). Proteomic and phosphoproteomic approaches to understand plant–pathogen interactions. Physiological and Molecular Plant Pathology, 66(1-2), 3-11.

290. Tolbert, N. E. (1997). The C_2 oxidative photosynthetic carbon cycle. Annual Review of Plant Biology, 48(1), 1-25.

291. Tovar-Méndez, A., Mújica-Jiménez, C., & Muñoz-Clares, R. A. (2000). Physiological implications of the kinetics of maize leaf phosphoenolpyruvate carboxylase. Plant Physiology, 123(1), 149-160.

292. Tovar-Méndez, A., Rodríguez-Sotres, R., López-Valentín, D. M., & Muñoz-Clares, R. A. (1998). Re-examination of the roles of PEP and Mg^{2+} in the reaction catalysed by the phosphorylated and non-phosphorylated forms of phosphoenolpyruvate carboxylase from leaves of *Zea mays*. Biochemical Journal, 332(3), 633-642.

293. Turner, P., Holst, O., & Karlsson, E. N. (2005). Optimized expression of soluble cyclomaltodextrinase of thermophilic origin in Escherichia coli by using a soluble fusion-tag and by tuning of inducer concentration. Protein Expression and Purification, 39(1), 54-60.

294. Ueno, Y., Imanari, E., Emura, J., Yoshizawa-Kumagaye, K., Nakajima, K., Inami, K., & Izui, K. (2000). Immunological analysis of the phosphorylation state of maize C_4-form phosphoenolpyruvate carboxylase

with specific antibodies raised against a synthetic phosphorylated peptide. The Plant Journal, 21(1), 17-26.

295. Ullrich, A., & Schlessinger, J. (1990). Signal transduction by receptors with tyrosine kinase activity. Cell, 61(2), 203-212.

296. Uncu, A. O., Doganlar, S., & Frary, A. (2013). Biotechnology for enhanced nutritional quality in plants. Critical Reviews in Plant Sciences, 32(5), 321-343.

297. United Nations. (2019). World Population Prospects 2019. Department of Economic and Social Affairs, Population Division.

298. van Bentem, S. D. L. F., Anrather, D., Roitinger, E., Djamei, A., Hufnagl, T., Barta, A., & Hirt, H. (2006a). Phosphoproteomics reveals extensive in vivo phosphorylation of Arabidopsis proteins involved in RNA metabolism. Nucleic Acids Research, 34(11), 3267-3278.

299. van Wijk, K. J., Friso, G., Walther, D., & Schulze, W. X. (2014). Meta-analysis of Arabidopsis thaliana phospho-proteomics data reveals compartmentalization of phosphorylation motifs. The Plant Cell, 26(6), 2367-2389.

300. Vanlerberghe, G. C., Schuller, K. A., Smith, R. G., Feil, R., Plaxton, W. C., & Turpin, D. H. (1990). Relationship between $NH^{+}{}^{4}$ assimilation rate and *in vivo* phosphoenolpyruvate carboxylase activity: regulation of anaplerotic carbon flow in the green alga selenastrum minutum. Plant Physiology, 94(1), 284-290.

301. Vermeulen, S. J., Campbell, B. M., & Ingram, J. S. (2012). Climate change and food systems. Annual Review of Environment And Resources, 37.

302. Vener, A. V., Harms, A., Sussman, M. R., & Vierstra, R. D. (2001). Mass spectrometric resolution of reversible protein phosphorylation in photosynthetic membranes of *Arabidopsis thaliana*. Journal of Biological Chemistry, 276(10), 6959-6966.

303. Venter, J. C., Adams, M. D., Myers, E. W., Li, P. W., Mural, R. J., Sutton, G. G., & Gocayne, J. D. (2001). The sequence of the human genome. Science, 291(5507), 1304-1351.

304. Vethanayagam, J. G., & Flower, A. M. (2005). Decreased gene expression from T7 promoters may be due to impaired production of active T7 RNA polymerase. Microbial Cell Factories, 4(1), 3.

305. Vidal, J., & Chollet, R. (1997). Regulatory phosphorylation of C_4 PEP carboxylase. Trends in Plant Science, 2(6), 230-237.

306. von Caemmerer, S., & Furbank, R. T. (2003). The C_4 pathway: an efficient CO_2 pump. Photosynthesis Research, 77(2-3), 191.

307. von Caemmerer, S., Lawson, T., Oxborough, K., Baker, N. R., Andrews, T. J., & Raines, C. A. (2004). Stomatal conductance does not correlate with photosynthetic capacity in transgenic tobacco with reduced amounts of Rubisco. Journal of Experimental Botany, 55(400), 1157-1166.

308. Walker, R. P., & Leegood, R. C. (1995). Purification, and phosphorylation in vivo and *in vitro*, of phosphoenolpyruvate carboxykinase from cucumber cotyledons. FEBS letters, 362(1), 70-74.

309. Walker, R. P., Acheson, R. M., Técsi, L. I., & Leegood, R. C. (1997). Phosphoenolpyruvate carboxykinase in C4 plants: its role and regulation. Functional Plant Biology, 24(4), 459-468.

310. Walker, R. P., and Leegood, R. C., (1996) Phosphorylation of phosphoenolpyruvate carboxykinase in plants: studies in plants with C4 photosynthesis and Crassulacean acid metabolism and in germinating seeds. Biochemical Journal, 317, 653–658

311. Walker, R. P., Trevanion, S. J., & Leegood, R. C. (1995). Phosphoenolpyruvate carboxykinase from higher plants: purification from cucumber and evidence of rapid proteolytic cleavage in extracts from a range of plant tissues. Planta, 196(1), 58-63.

312. Wang, S., Liu, W. F., He, Y. Z., Zhang, A., Huang, L., Dong, Z. Y., & Yan, Y. B. (2008). Multistate folding of a hyperthermostable Fe-superoxide dismutase (TcSOD) in guanidinium hydrochloride: The importance of the quaternary structure. Biochimica et Biophysica Acta (BBA)-Proteins and Proteomics, 1784(3), 445-454.

313. Wang, Y. H., & Chollet, R. (1993). *In vitro* phosphorylation of purified tobacco-leaf phosphoenolpyruvate carboxylase. FEBS Letters, 328(1-2), 215-218.

314. Wang, Y. H., & Chollet, R. (1993). Partial purification and characterization of phosphoenolpyruvate carboxylase protein-serine kinase from illuminated maize leaves. Archives of Biochemistry and Biophysics, 304(2), 496-502.

315. Wang, Y., Liu, Z., Cheng, H., Gao, T., Pan, Z., Yang, Q., & Xue, Y. (2013). EKPD: a hierarchical database of eukaryotic protein kinases and protein phosphatases. Nucleic Acids Research, 42(D1), D496-D502.

316. Weber, K., & Kuter, D. J. (1971). Reversible denaturation of enzymes by sodium dodecyl sulfate. Journal of Biological Chemistry, 246(14), 4504-4509.

317. Webster, R.D. 1988. Genera of the North American Paniceae (Poaceae: Panicoideae). Systematic Botany, 13, 576-609.

318. Wedding, R. T., Black, M. K., & Meyer, C. R. (1989). Activation of higher plant phosphoenolpyruvate carboxylases by glucose-6-phosphate. Plant Physiology, 90(2), 648-652.

319. Westhoff, P., Svensson, P., Ernst, K., Bläsing, O., Burscheidt, J., & Stockhaus, J. (1997). Molecular evolution of C4 phosphoenolpyruvate carboxylase in the genus Flaveria. Functional Plant Biology, 24(4), 429-436.

320. Westhoff, P., Svensson, P., Ernst, K., Bläsing, O., Burscheidt, J., & Stockhaus, J. (1997). Molecular evolution of C4 phosphoenolpyruvate carboxylase in the genus Flaveria. Functional Plant Biology, 24(4), 429-436.

321. Wheeler, M. C. G., Arias, C. L., Tronconi, M. A., Maurino, V. G., Andreo, C. S., & Drincovich, M. F. (2008). Arabidopsis thaliana NADP-malic enzyme isoforms: high degree of identity but clearly distinct properties. Plant Molecular Biology, 67(3), 231-242.

322. Wheeler, T., & Von Braun, J. (2013). Climate change impacts on global food security. Science, 341(6145), 508-513.

323. Wingler, A., Walker, R. P., Chen, Z. H., & Leegood, R. C. (1999). Phosphoenolpyruvate carboxykinase is involved in the decarboxylation of aspartate in the bundle sheath of maize. Plant Physiology, 120(2), 539-546.

324. Witze, E. S., Old, W. M., Resing, K. A., & Ahn, N. G. (2007). Mapping protein post-translational modifications with mass spectrometry. Nature Methods, 4(10), 798.

325. Wong, K. F., & Davies, D. D. (1973). Regulation of phosphoenolpyruvate carboxylase of Zea mays by metabolites. Biochemical Journal, 131(3), 451-458.

326. Xu, W., Zhou, Y., & Chollet, R. (2003). Identification and expression of a soybean nodule-enhanced PEP-carboxylase kinase gene (NE-PpcK) that shows striking up-/down-regulation in vivo. The Plant Journal, 34(4), 441-452.

327. Yamada, S., Nakamura, H., Kinoshita, E., Kinoshita-Kikuta, E., Koike, T., & Shiro, Y. (2007). Separation of a phosphorylated histidine protein using phosphate aYnity polyacrylamide gel electrophoresis. Analytical Biochemistry, 360, 160-162.

328. Yamori, W., Hikosaka, K., & Way, D. A. (2014). Temperature response of photosynthesis in C3, C4, and CAM plants: temperature acclimation and temperature adaptation. Photosynthesis Research, 119(1-2), 101-117.

329. Yan, J. X., Packer, N. H., Gooley, A. A., & Williams, K. L. (1998). Protein phosphorylation: technologies for the identification of phosphoamino acids. Journal of Chromatography A, 808(1-2), 23-41.

330. Yin, J., Lin, J. H., Li, W. T., & Wang, D. I. (2003). Evaluation of different promoters and host strains for the high-level expression of collagen-like polymer in *Escherichia coli*. Journal of Biotechnology, 100(3), 181-191.

331. Zhang, X. Q., Li, B., & Chollet, R. (1995). *In vivo* regulatory phosphorylation of soybean nodule phosphoenolpyruvate carboxylase. Plant Physiology, 108(4), 1561-1568.

332. Zhu, S., Gong, C., Ren, L., Li, X., Song, D., & Zheng, G. (2013). A simple and effective strategy for solving the problem of inclusion bodies in recombinant protein technology: His-tag deletions enhance soluble expression. Applied Microbiology and Biotechnology, 97(2), 837-845.

333. Zhu, X. G., Long, S. P., & Ort, D. R. (2010). Improving photosynthetic efficiency for greater yield. Annual Review of Plant Biology, 61, 235-261.

334. Zulawski, M., Braginets, R., & Schulze, W. X. (2012). PhosPhAt goes kinases—searchable protein kinase target information in the plant phosphorylation site database PhosPhAt. Nucleic Acids Research, 41(D1), D1176-D1184.

335. Zuloaga, F.O., Scataglini, M.A. and Morrone, O. (2010). A phylogenetic evaluation of Panicum sects. Agrostoidea, Megista, Prionitia and Tenera (Panicoideae, Poaceae): Two new genera, Stephostachys and Sorengia. Taxonomy, 59, 1535-46.

APPENDIX

A. Super Optimal broth with Catabolite repression (SOC) medium preparation

Reagent	Concentration	Mass for 1.0 L stock (g)	Mass for 50 ml stock (g)
Tryptone	–	–	1.0
Yeast extract	–	–	0.25
NaCl	5.0 M	292.2	14.61
KCl	1.0 M	74.55	3.73
$MgCl_2$	1.0 M	95.21	4.76
$MgSO_4$	1.0 M	120.36	6.02
Glucose	1.0 M	180.15	9.0

All the reagents were mixed together and bring the volume to 50 ml with MiliQ water. The solution was filtered with 0.2 µm Acrodisc syringe filter (Whatman) and stored at -80 °C.

B. Luria-Bertani (LB) medium preparation

1. 10.0 g of tryptone, 10.0 g of NaCl and 5.0 g of yeast extract was added in 800 ml distilled water and bring the volume to 1000 ml.
2. The medium were autoclaved and allowed the solution to cool up to room temperature before adding the antibiotics.
3. 7.5 g of agar was added in 1 litter of LB medium for LB plate.

C. Antibiotic preparation

1. Kanamycin:

   0.5 g of kanamycin was dissolved in 10 ml MiliQ water to make 50 mg/ml water stock concentration. 500 µl from the stock was added to 500 ml of LB to make the final concentration of kanamycin at 50 µg/ml. The solution was stored at -20 °C.

2. Ampicillin:

   0.5 g of ampicillin was dissolved in 10 ml MiliQ water to make 50 mg/ml water stock concentration. 500 µl from the stock was added to 500 ml of LB to make the final concentration of ampicillin at 50 µg/ml. The solution was stored at -20 °C.

3. Chloramphenicol:

   0.34 g of ampicillin was dissolved in 10 ml ethanol to make 34 mg/ml stock concentration. 500 µl from the stock was added to 500 ml of LB to make the final concentration of ampicillin at 34 µg/ml. The solution was stored at -20 °C.

D. Sodium dodecyl sulphate–polyacrylamide gel electrophoresis (SDS-PAGE) buffer recipes.

4 X Separating gel buffer:	1.5 M Tris HCl, pH 8.8, 0.4 % SDS
4 X Stacking gel buffer:	0.5 M Tris HCl, pH 6.8, 0.4 % SDS
Running Buffer :	1 X TGS (25 mM Tris, 192 mM glycine, 0.1 % SDS, pH 7.3) (1 in 10 dilution of 10 X pre-made stock)
2 X Sample Buffer :	250 mM Tris.HCl pH 6.8, 2 % SDS, 20 % glycerol, 0.01 % bromophenol blue. Add 14 l of B-mercaptoethanol to 200 l of sample buffer.
Stain:	50 % tricholoroacetic acid, 0.12 % Coomassie blue R250, 0.02 % SDS, 0.03 % glycine, 0.05 % tris.
Destain:	50 % tricholoroacetic acid, 0.02 % SDS, 0.03 % glycine, 0.05 % tris.

E. Difficulties in obtaining high amounts of PEPCK from thrombin cleavage reaction.

Method B; Have low amount of PEPCK from auto-induction growth medium from Rosetta host strain at 18°C for 48 hours.

NusA-PEPCK purified was very low from this method. The NusA-PEPCK was eluted from 25 mM Tris-HCl buffer, consisting of 400 mM imidazole (Fig. 3.9; C and D). The thrombin cleavage reaction of NusA-PEPCK was performed in solution at room temperature for 2 hours. No PEPCK protein was eluted from 50 mM imidazole wash (Fig. 3.10) purified by using Ni-NTA column. The uncleaved protein was eluted with 25 mM Tris-HCl buffer, pH 7.4, 400 mM Imidazole.

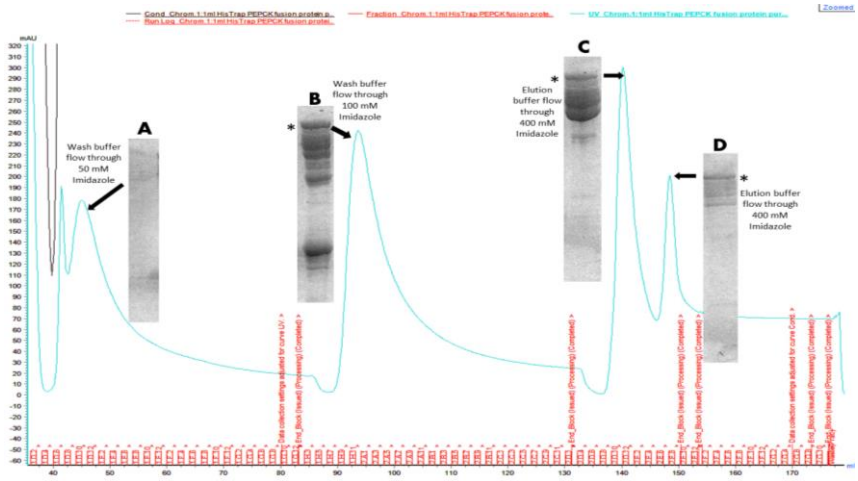

Fig E.1: Purification of fusion protein (PEPCK-NusA) by using Ni-NTA column (HisTrap™ HP) on an AKTA. The PEPCK was transformed into Rosetta host strains. The auto-induction medium containing 50 µg/ml ampicillin and 34 µg/ml chloramphenicol was incubated at 18°C for another 48 hours. The column was equilibrate with 10 column volume (CV) of binding buffer, 20 mM Tris-HCl, pH 7.4, 20 mM imidazole. The 35 ml of supernatant was then loaded into the column with the flow rate at 1ml per min **A;** No protein was detected from 50 mM imidazole

wash. **B;** Most of fusion protein eluted from the 100 mM imidazole wash. **C and D;** Remaining fusion protein eluted from the 400 mM imidazole wash.

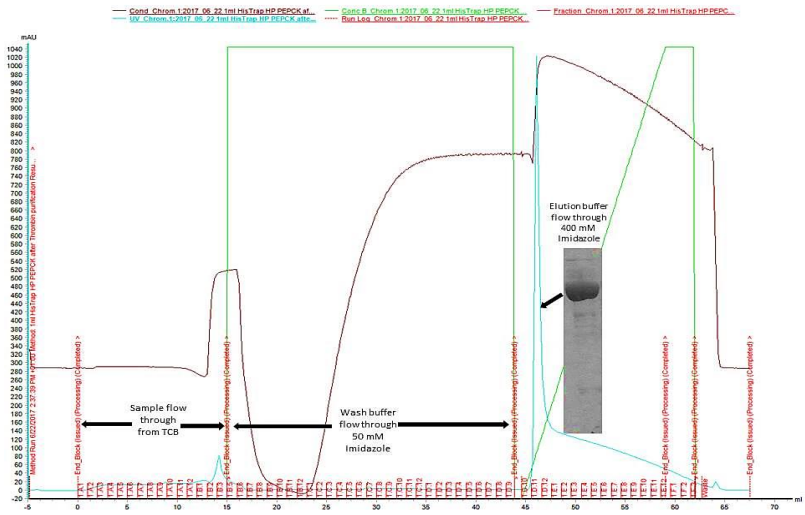

Fig E.2: Purification of PEPCK by using Ni-NTA column (HisTrap™ HP) on an AKTA after thrombin cleavage reaction at room temperature, 2 hours without agitation. The column was equilibrated with 10 column volume (CV) of TCB buffer, 25 mM Tris-HCl, pH 8. Non PEPCK was detected from 50 mM imidazole wash. The uncleaved protein was eluted with 15 CV of Elution buffer, 25 mM Tris-HCl, pH 7.4, 400 mM Imidazole.

Method C; No PEPCK after cleavage reaction of NusA-PEPCK with thrombin from induction in 2YT media

The fusion protein was purified from the 25 mM Tris-HCl buffer, pH 7.4 containing 400 mM imidazole but only one ml of the fraction containing target protein was eluted (Fig. 3.11 and 3.12). Thrombin cleavage reaction was performed on column, at 4°C for overnight. Then the cleaved PEPCK was purified by Ni-NTA column (Fig. 3.13), and SDS-PAGE analysis showed that there was no PEPCK (37 kDA) was detected from the purification (Fig. 3.14).

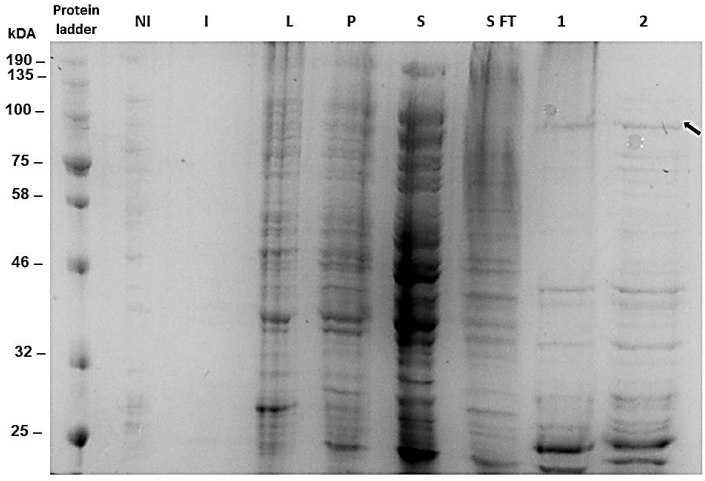

Fig E.3: SDS-PAGE analysis of PECK-NusA fusion protein purification by HisTrap™ HP column. The fusion protein was over-expressed in *Rosetta*, induced by 1 mM IPTG at 18°C for 24 hours in 2YT media. Lane NI; Non induced cell extract. Lane I; Induced protein with 1 mM IPTG. Lane L; Lysate after French press. Lane P: Cell Pellet. Lane S; Supernatant from centrifugation of the lysate. Lane S FT; Supernatant flow through. Lane 1; Fusion protein

eluted from 400 mM Imidazole from total 1 ml fraction. Lane 2; Solution mixture of fusion protein with thrombin in TCB before loaded into the column.

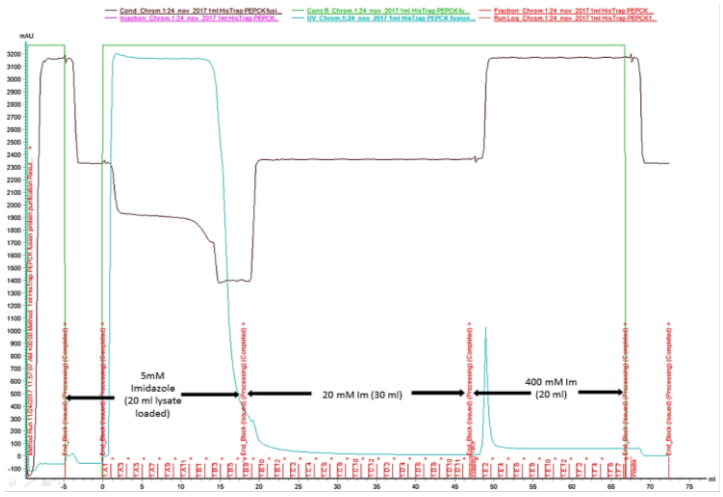

Fig E.4: Purification of fusion protein (PEPCK-NusA) by using Ni-NTA column (HisTrap™ HP) on an AKTA. The column was equilibrate with 10 column volume (CV) of binding buffer, 20 mM Tris-HCl, pH 7.4, 5 mM imidazole. A; The 20 ml of supernatant was then loaded into the column with the flow rate at 1ml per min B; The column was washed with 30 CV 20 mM imidazole buffer. C; Fusion protein was eluted from the 400 mM imidazole buffer.

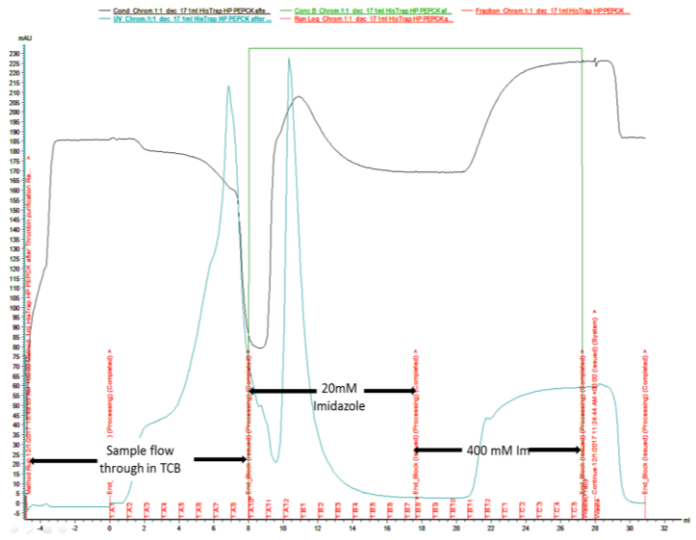

Fig E.5: Purification of PEPCK by using Ni-NTA column (HisTrap™ HP) on a AKTA after thrombin cleavage reaction takes overnight at 4°C on column. The column was equilibrate with 10 column volume (CV) of TCB buffer, 20 mM Tris-HCl, 100 mM NaOH, pH 8. Non protein was detected from 20 mM imidazole wash.

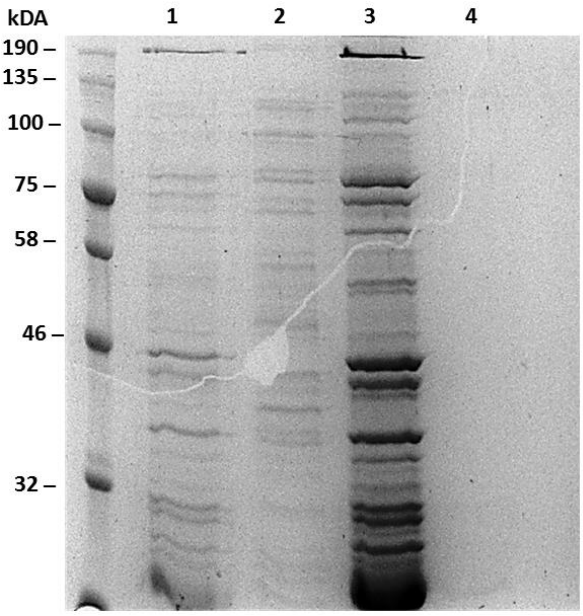

Fig E.6: SDS-PAGE analysis of PEPCK purification by HisTrap™ HP column after thrombin cleavage reaction. Three peaks from sample flow through, 20 mM imidazole and 400 mM imidazole wash did not show any presence of PEPCK band (37 kDA) from the SDS-Page gel image. Lane 1; Fusion protein with thrombin before loaded into the column. Lane 2; Sample flow through. Lane 3; Flow through from 20 mM Imidazole wash buffer. Lane 4; Flow through from 400 mM Imidazole buffer.

Method D: No PEPCK purified after cleavage reaction of PEPCK-NusA with thrombin from overexpression in auto-induction growth medium.

The fusion protein was purified from autoinduction medium but only one ml of fraction was eluted (Fig 3.15). Then thrombin digestion was performed on-column at 4°C for overnight, and an attempt to purified PEPCK was failed since no PEPCK band was detected in SDS-PAGE analysis (Fig 3.18). The low quantity of PEPCK-Nusa purified could be the reason there was no PEPCK was detected after the thrombin cleavage reaction.

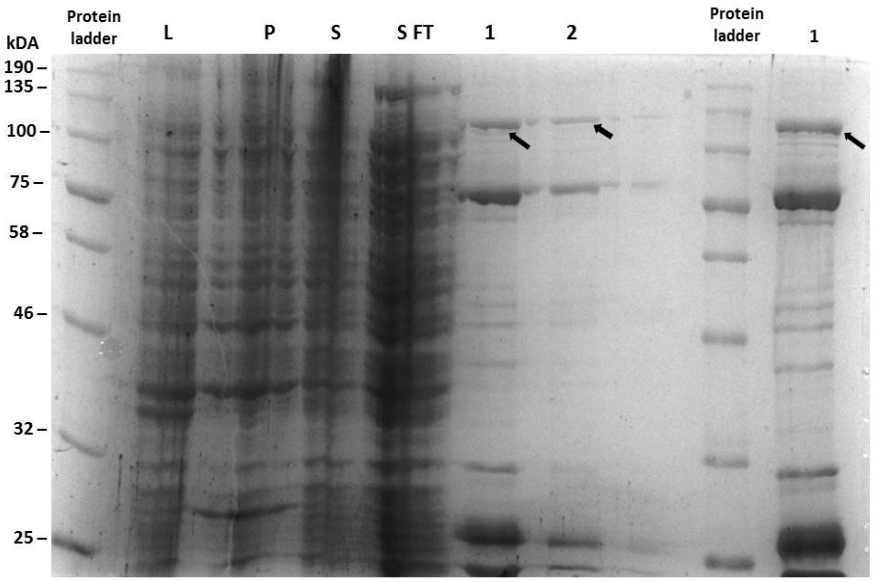

Fig E.7: SDS-PAGE analysis of PECK-NusA fusion protein purification by HisTrap™ HP column. The fusion protein was over-expressed in BL21 DE3 with 50 µg/ml of ampicillin in auto-induction medium with incubation at 18°C for 48 hours. Lane L; Lysate after French press. Lane P: Cell Pellet. Lane S; Supernatant from centrifugation of the lysate. Lane S FT; Supernatant flow through. Lane 1; Fusion protein eluted from 400 mM Imidazole from total 1 ml fraction. Lane 2; Solution mixture of fusion protein with thrombin in TCB before loaded into the column.

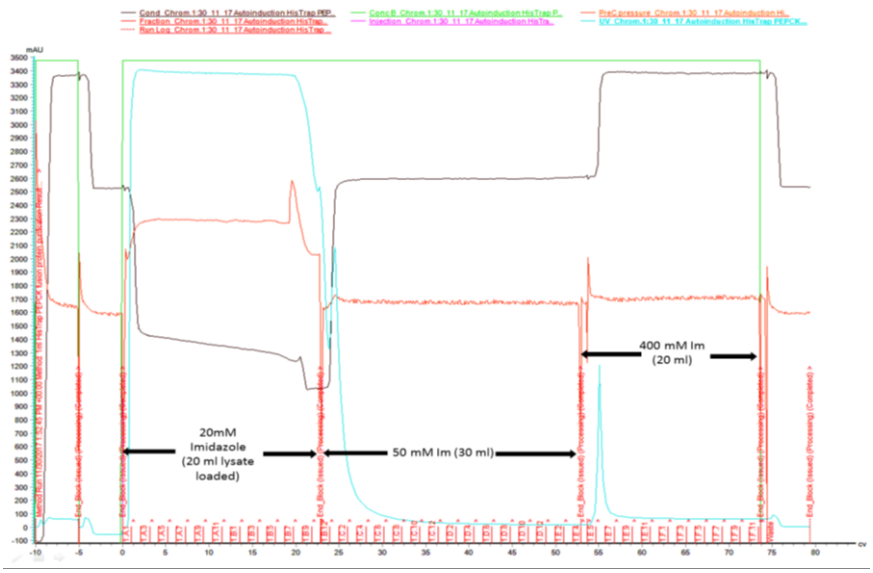

Fig E.8: Purification of fusion protein (PEPCK-NusA) by using Ni-NTA column (HisTrap™ HP) on an AKTA. The column was equilibrated with 10 column volume (CV) of binding buffer, 20 mM Tris-HCl, pH 7.4, 5 mM imidazole. **A;** The 20 ml of supernatant was then loaded into the column with the flow rate at 1ml per min **B;** The column was washed with 20 mM imidazole buffer. **C;** Fusion protein was eluted from the 400 mM imidazole buffer.

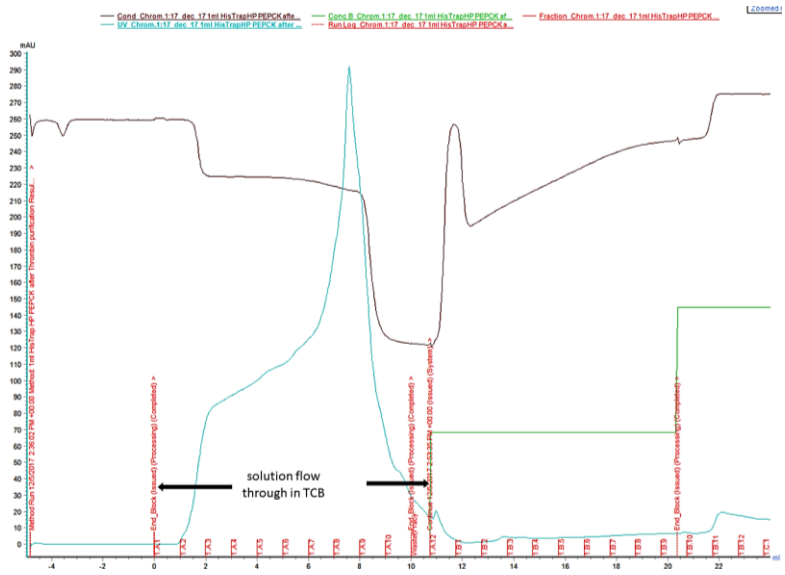

Fig E.9: Purification of PEPCK by using Ni-NTA column (HisTrap™ HP) on an AKTA after thrombin cleavage reaction takes overnight at 4°C on-column. The column was equilibrate with 10 column volume (CV) of TCB buffer, 20 mM Tris-HCl, 100 mM NaOH, pH 8. No protein was detected from 20 mM imidazole wash.

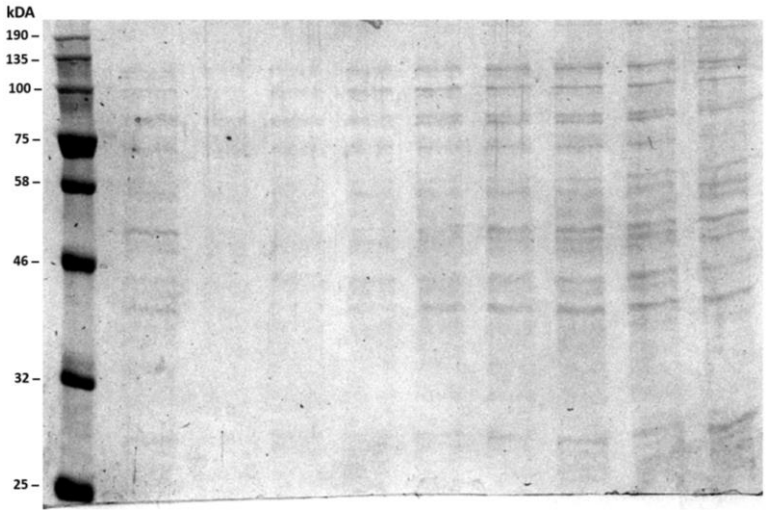

Fig E.10: SDS-PAGE analysis of PEPCK purification by HisTrap™ HP column after thrombin cleavage reaction. No presence of PEPCK band (37 kDA) was detected.

Method E and F; No fusion protein detected from LB, 0.5 mM IPTG, Rosetta, 18 hours

The fusion protein was over-expressed in *Rosetta* with 50 µg/ml of Ampicillin with 34 µg/ml chloramphenicol and induced by 0.5 mM IPTG at 18°C for 18 hours. There was no fusion protein purified from Ni-NTA column, although analysis from SDS-PAGE shows that it was overexpressed in the lysate of medium culture (arrow in Fig. 3.19; Fig. 3.20) from both trials.

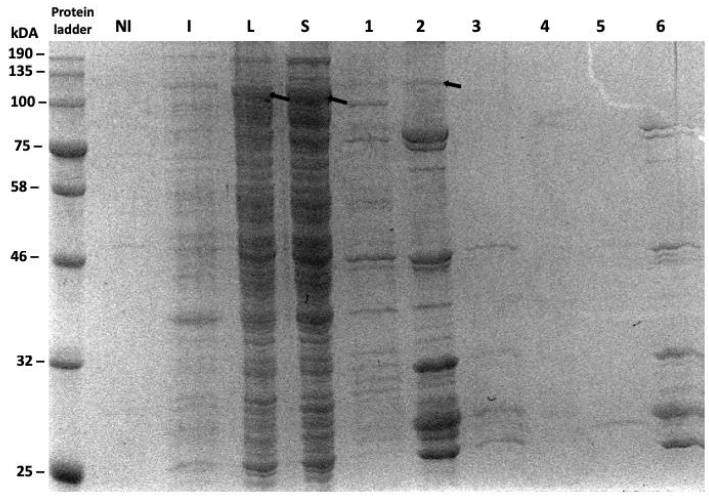

Fig E.11: SDS-PAGE analysis of PEPCK purification by HisTrap™ HP column. The fusion protein was over-expressed in *Rosetta* with 50 µg/ml of Ampicillin with 34 µg/ml chloramphenicol and induced by 0.5 mM IPTG at 18°C for 18 hours. NI: Non induced with IPTG. I: Induced with 0.5 mM IPTG for 18 hours at 18°C in LB medium. Lane L; Lysate after French press. Lane S; Supernatant from centrifugation of the lysate. Lane 1: 50 mM Imidazole. Lane 2: Fusion protein 400 mM Imidazole. Lane 3: Fusion protein with thrombin. Lane 4: Sample flow through from thrombin cleavage buffer. Lane 5: 20 mM imidazole (should have PEPCK here). Lane 6: Uncleaved fusion protein.

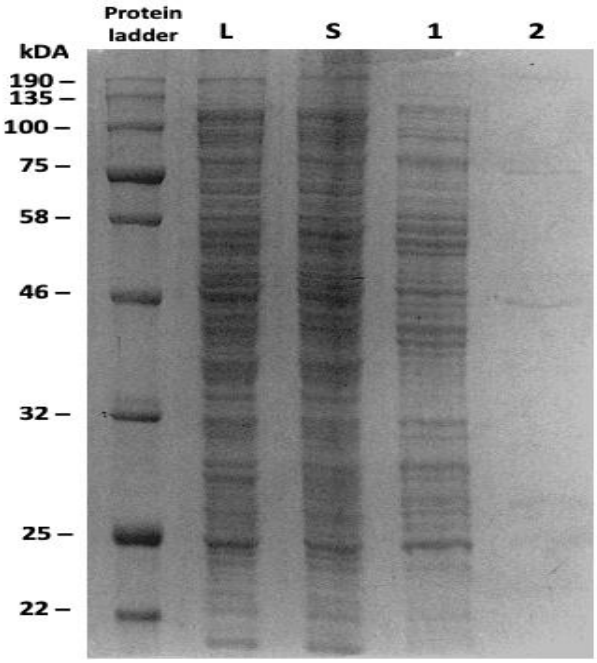

Fig E.12: SDS-PAGE analysis of PEPCK purification by HisTrap™ HP column. The fusion protein was over-expressed in *Rosetta* with 50 µg/ml of ampicillin with 34 µg/ml chloramphenicol and induced by 0.5 mM IPTG at 18°C for 18 hours. The column was equilibrated with 10 column volume (CV) of 20 mM Tris-HCl, 20 mM imidazole, pH 7.4. 70 ml of supernatant was loaded into the column followed by 20 CV of 50 mM imidazole and eluted at 400mM of imidazole (20 ml). Lane L; Lysate after French press. Lane S; Supernatant from centrifugation of the lysate. Total 13 ml fractions of fusion protein were eluted. Lane 1: 20 mM Imidazole. Lane 2: 400 mM Imidazole

Method G: No fusion protein (Nusa-PEPCK) detected from LB, 0.5 mM IPTG, BL21 DE3, 24 hours

In this method, instead transformed into Rosetta, the PEPCK plasmid was transformed into BL21-DE3. The protein was induced by 0.5 mM IPTG at 18°C for 24 hours. The period of incubation was increased up to 24 hours, in hope for PEPCK will be induced. None of fusion protein was purified from this method (Fig. 3.24; Fig. 3.25).

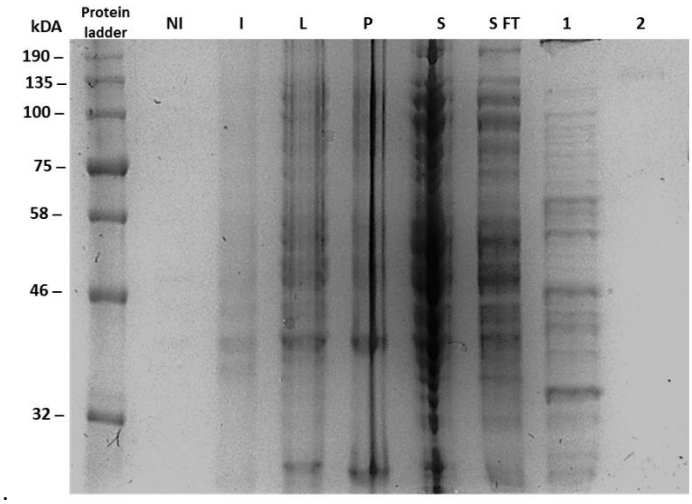

Fig E.13: SDS-PAGE analysis of PEPCK purification by HisTrap™ HP column. The fusion protein was over-expressed in *BL21 DE3* with 50µg/ml of Ampicillin and induced by 0.5 mM IPTG at 18°C for 24 hours. NI: Non induced with IPTG. I: Induced by 1 mM IPTG at 18°C for 22 hours in LB medium. Lane P: Cell Pellet. Lane L; Lysate after French press. Lane S; Supernatant from centrifugation of the lysate. Lane S FT; Supernatant flow through. Lane 1: 50mM Imidazole wash. Lane 2: 400 mM Imidazole

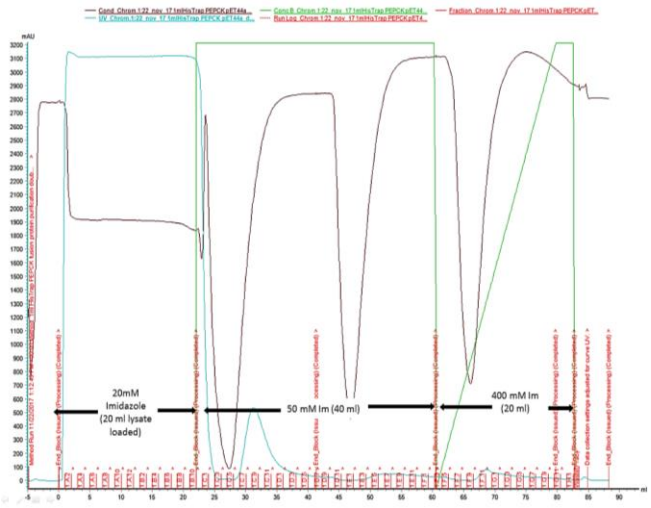

Fig E.14: Purification of fusion protein (PEPCK-NusA) by using Ni-NTA column (HisTrap™ HP) on an AKTA The column was equilibrated with 10 column volume (CV) of binding buffer, 20 mM Tris-HCl, pH 7.4,20 mM imidazole. A; The 20 ml of supernatant was then loaded into the column with the flow rate at 1ml per min B; The column was washed with 50 mM imidazole buffer. C; Fusion protein was eluted from the 400 mM imidazole buffer.

Overall, none PECK was recovered after thrombin cleavage reaction was performed followed by Ni-NTA purification step. Therefore, it was not possible to yield any purified PEPCK protein, despite the amounts of soluble recombinant proteins being initially detectable in the cell lysate, supernatant and pellet after IPTG induction.

PEPCK (without NusA) Induction in LB medium

	BL21-DE3(Ampicilin (50µg/ml))		Rosetta (Ampicilin (50µg/ml) + chloramphenicol (34 µg/ml))		
Time of incubation	18 hrs	24 hrs	18 hrs	24 hrs	
IPTG (mM)	0.5	1.0	0.5	0.5	1.0
	A	X	B	C	D

From the gel image, PEPCK at 37 kDA was induced from the 0.5 mM IPTG induction (arrow A) and available in lysate (arrow B), supernatant (arrow C). Target protein (arrow D) was detected in 100 mM imidazole elution but not as a major band and with contaminations.

F. Experiments of Purification of PEPCK without NusA

Experiment A1. Purification of PEPCK over-expressed in BL21-DE3 with 50µg/ml of ampicillin with 0.5 mM IPTG at 18°C for 18 hours

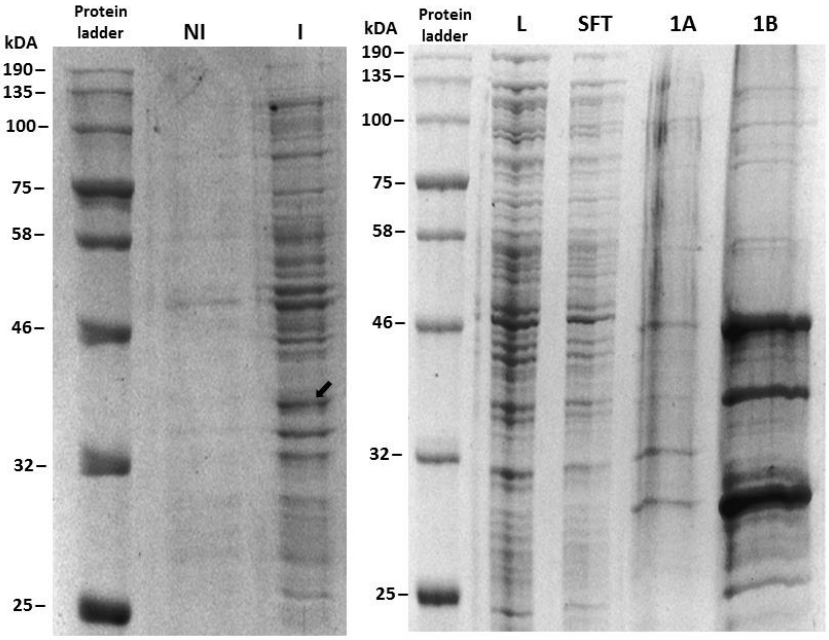

Figure F.1: SDS-gel electrophoresis of partially purified PEPCK protein over-expressed in BL21- DE3 induced with 0.5 mM IPTG at 18°C for 18 hours. Lane NI; Non induced. Lane I; Induced with 0.5 mM IPTG. Lane P: Cell Pellet. Lane L; Lysate after French press. Lane S; Supernatant from centrifugation of the lysate. Lane S FT; Supernatant flow through. Lane 1A; Fraction one from Wash buffer 20 mM Imidazole. Lane 1B: Fraction two from Wash buffer 20 mM Imidazole.

.

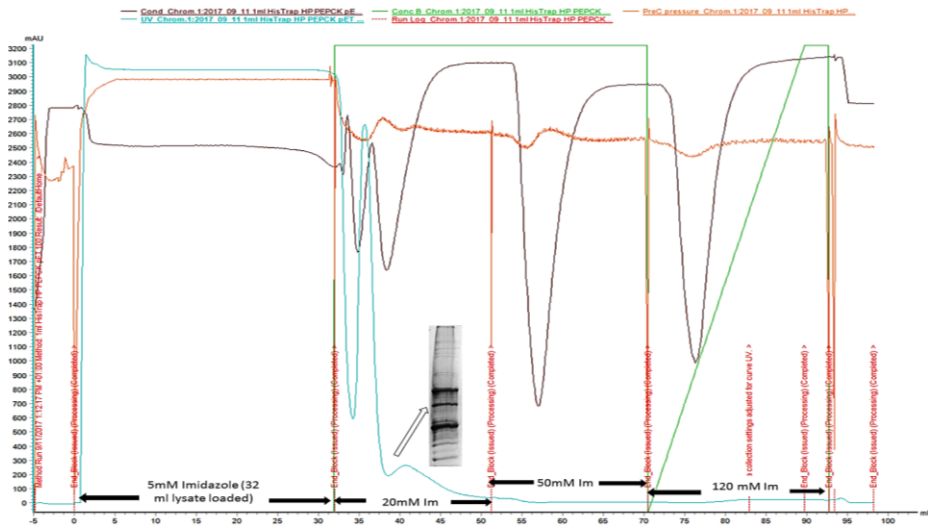

Figure F.2: Purification of PEPCK protein by using Ni-NTA column (HisTrap™ HP) on an AKTA. The column was equilibrate with 10 column volume (CV) of binding buffer, 20 mM Tris-HCl, pH 7.4, 20 mM imidazole. **A;** The 20 ml of supernatant was then loaded into the column with the flow rate at 1ml per min **B;** The column was washed with 50 mM imidazole buffer. **C;** None PEPCK protein was eluted from the 120 mM imidazole buffer.

Experiment A2. Purification of PEPCK over-expressed in BL21-DE3 with 50µg/ml of ampicillin, and induced by 0.5 mM IPTG at 18°C for 18 hours .

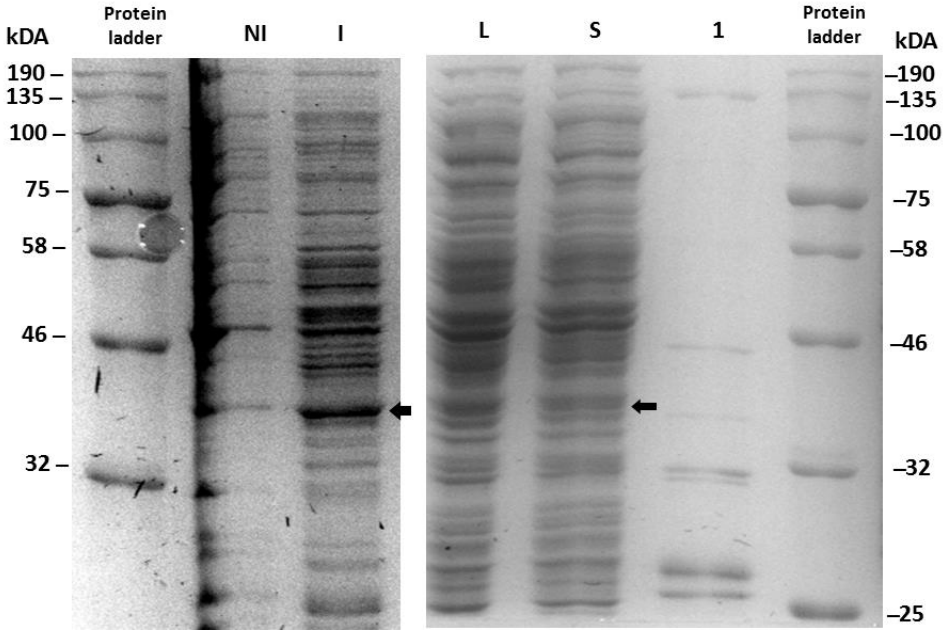

Figure F.3: SDS-gel electrophoresis of partially purified PEPCK protein over-expressed in BL21-DE3, induced with 0.5 mM IPTG at 18°C for 18 hours. Lane NI; Non induced. Lane I; Induced with 0.5 mM IPTG. Lane P: Cell Pellet. Lane L; Lysate after French press. Lane S; Supernatant from centrifugation of the lysate. Lane 1; Elution from 120 mM Imidazole.

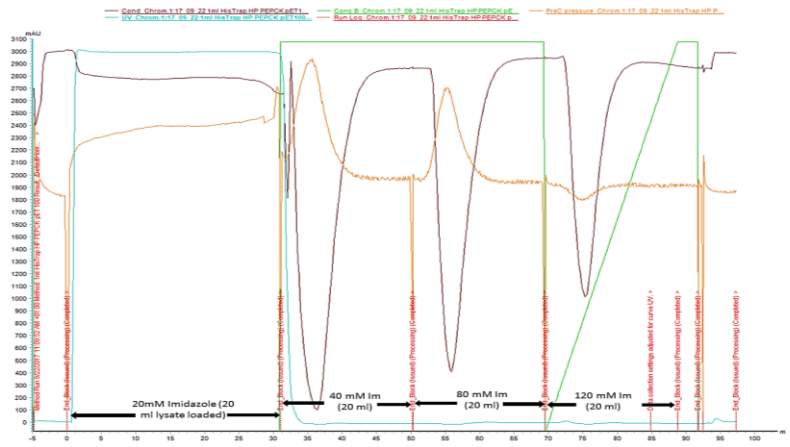

Figure F.4: Purification of PEPCK protein by using Ni-NTA column (HisTrap™ HP) on an AKTA. The column was equilibrate with 10 column volume (CV) of binding buffer, 20 mM Tris-HCl, pH 7.4, 5 mM imidazole. A; The 20 ml of supernatant was then loaded into the column with the flow rate at 1ml per min B; The column was washed with 20 mM imidazole buffer. C; Elution of protein was attempt by using 120 mM imidazole buffer. No peaks of target protein was detected (Fig 5) although PEPCK band was detected in induced cell growth (arrow A).

Experiment A3. Purification of PEPCK over-expressed in BL21-DE3 with 50µg/ml of ampicillin and induced by 0.5 mM IPTG at 18°C for 18 hours. A1 in different concentration of Imidazole.

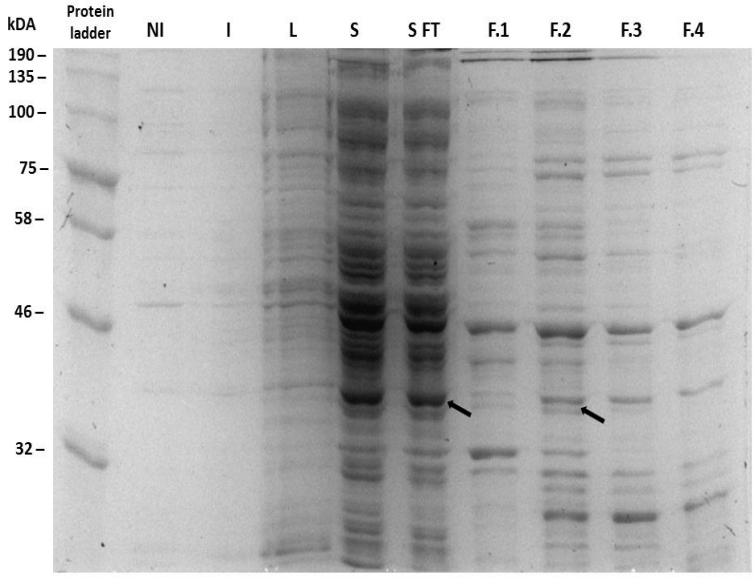

Figure F.5: SDS-gel electrophoresis of partially purified PEPCK protein over-expressed in BL21-DE3, induced with 0.5 mM IPTG at 18°C for 18 hours. Lane NI; Non induced. Lane I; Induced with 0.5 mM IPTG. Lane P: Cell Pellet. Lane L; Lysate after French press. Lane S; Supernatant from centrifugation of the lysate. Lane F.1,2,3,4: Sample flow through from 20 mM Imidazole buffer.

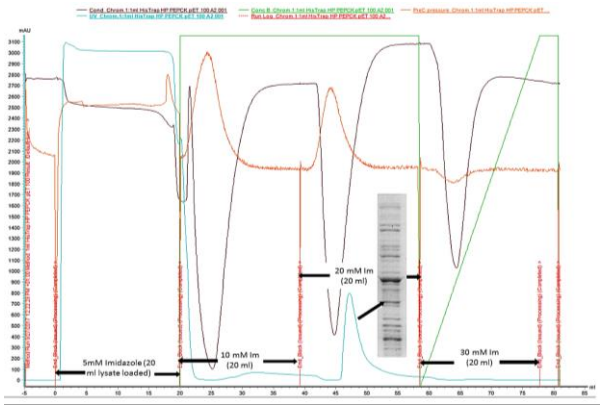

Figure F.6: Purification of PEPCK by HisTrap™ HP column, by using Ni-NTA column (HisTrap™ HP) on an AKTA. over-expressed in BL21-DE3 with 50µg/ml of ampicillin and induced by 0.5 mM IPTG at 18°C for 18 hours. The cell pellet was resuspended in 30 ml of binding buffer (25 mM tris-HCl, pH 7.4, 0.5 M NaCl, 5 mM imidazole,0.3 M glycerol) and French pressed twice. The clarified lysate was loaded onto the column equlibrated with 5 CVs of binding buffer. The column was washed with 20 CVs of 10 mM imidazole followed by another wash with 20 CVs of 20 mM imidazole. Elution was performed by 30 mM imidazole. Eluted fraction from 20 mM imidazole showed (arrow).12 ml fractions were pooled from 20 mM imidazole flow through. In Fig 6, SDS-PAGE gel image showed that majority of the target protein was detected in sample flow through (arrow A) and slightly in 20mM imidazole flow through (arrow B).

Experiment A4. Over-expressed in BL21-DE3 with 50µg/ml of ampicillin and induced by 0.5 mM IPTG at 18°C for 18 hours

The lysate was loaded into the column followed by 30 CV of 10 mM imidazole wash, 20 CV of 20 mM imidazole wash and then eluted at 20 CV of 100 mM imidazole and 20 CV of 400 mM imidazole.

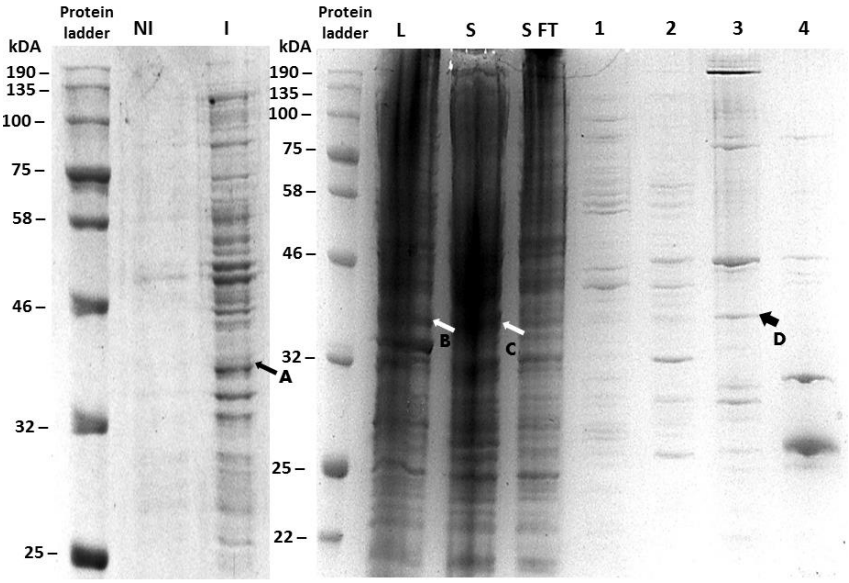

Figure F.7: SDS-gel electrophoresis of partially purified PEPCK protein over-expressed in BL21-DE3 with 50 µg/ml of ampicillin and induced by 0.5 mM IPTG at 18°C for 18 hours. Lane NI; Non-induced. I; Induced. Lane P: Cell Pellet. Lane L; Lysate after French press. Lane S; Supernatant from centrifugation of the lysate. Lane S FT; Supernatant flow through. Lane 1 and 2 : From 10 mM Imidazole. Lane 3; 100 mM Imidazole. Lane 4; 400 mM Imidazole wash. From the gel image, PEPCK at 37 kDA was induced from the 0.5 mM IPTG induction (arrow A) and available in lysate (arrow B), supernatant (arrow C). Target protein (arrow D) was detected in 100 mM imidazole elution but not as a major band and with contaminations.

Experiment B1: Purification of PEPCK over-expressed in Rosetta with 50 µg/ml of ampicillin, 34 µg/ml of chloramphenicol and induced by 0.5 mM IPTG at 18°C for 18 hours.

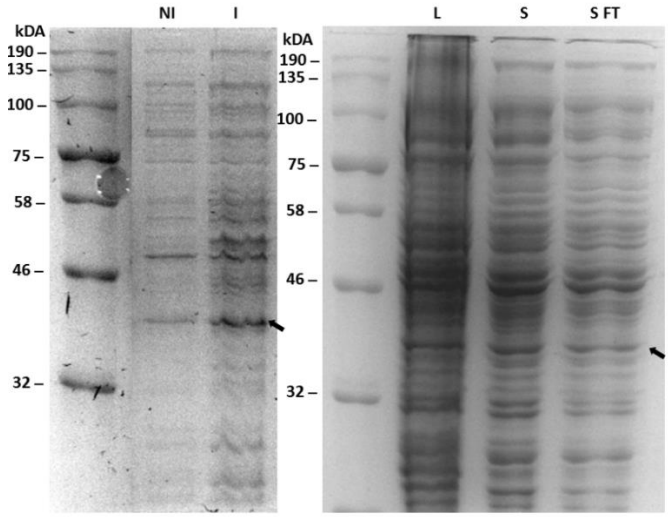

Figure F.8: SDS-gel electrophoresis of partially purified PEPCK protein over-expressed in Rosetta with 50 µg/ml of ampicillin, 34 µg/ml of chloramphenicol and induced by 0.5 mM IPTG at 18°C for 18 hours. Lane NI; Non induced. Lane I; Induced with 0.5 mM IPTG. Lane L; Lysate after French press. Lane S; Supernatant from centrifugation of the lysate. Lane S FT; Supernatant flow through. PEPCK was detected in cell induced growth (arrow), pellet and lysate

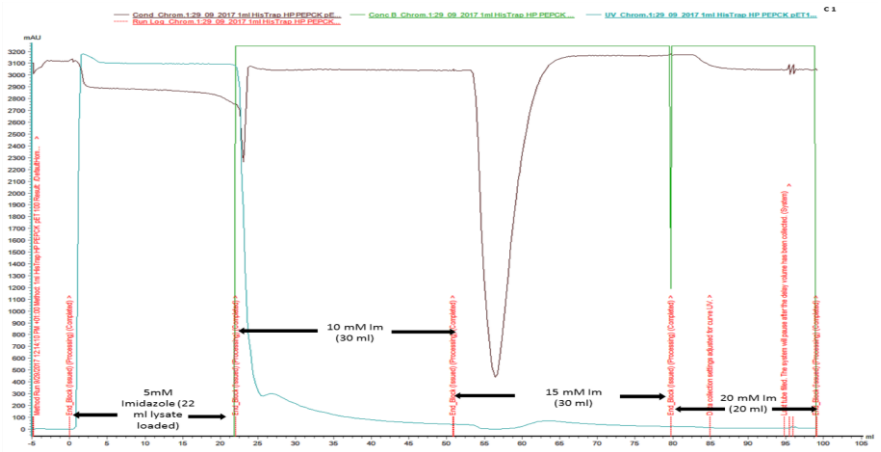

Figure F.9: Purification of PEPCK by HisTrap™ HP column, by using Ni-NTA column (HisTrap™ HP) on an AKTA; over-expressed in Rosetta with 50 µg/ml of ampicillin + 34 µg/ml of chloramphenicol and induced by 0.5 mM IPTG at 18°C for 18 hours. The column was equilibrate with 10 column volume (CV) of binding buffer, 20 mM Tris-HCl, pH 7.4, 5 mM imidazole. The 20 ml of supernatant was then loaded into the column with the flow rate at 1ml per min. The column was washed with 10 and 20 mM imidazole buffer. **C;** Fusion protein was eluted from the 30 mM imidazole buffer. No peaks were detected.

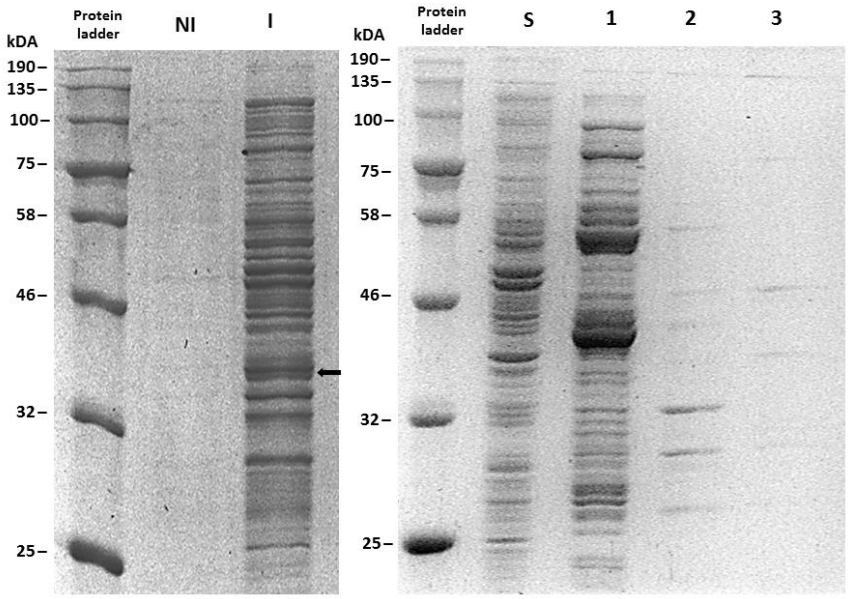

Figure F.10: SDS-gel electrophoresis of partially purified PEPCK protein over-expressed in Rosetta, induced with 0.5 mM IPTG at 18°C for 18 hours. The supernatant from the centrifugation was loaded into the column followed by 20 CV of 20 mM imidazole wash, then 20 CV of 40 mM imidazole and eluted at 120 mM of imidazole (20ml). N: Non-induced. I: Induced with 0.5 mM IPTG. S: Supernatant. Lane 1: Wash buffer 20 mM Imidazole. Lane 2: Wash buffer 40 mM Imidazole. Lane 3: 120 mM imidazole elution.

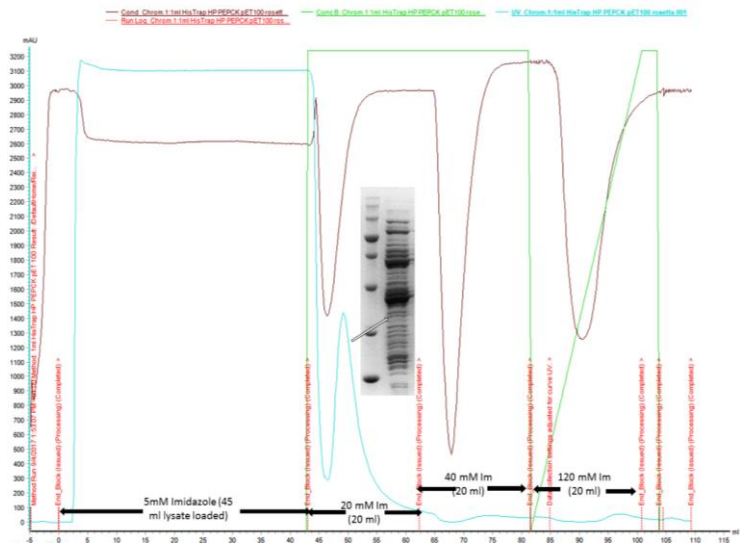

Figure F.11: Purification of PEPC protein by using Ni-NTA column (HisTrap™ HP) on an AKTA. The column was equilibrate with 10 column volume (CV) of binding buffer, 5 mM imidazole , 25 mM Tris-HCl, pH 7.4. **A;** The 20 ml of supernatant was then loaded into the column with the flow rate at 1ml per min **B;** The column was washed with 20 and 40 mM imidazole buffer. **C;** None PEPCK protein was eluted from the 400 mM imidazole buffer.

Experiment C1. Purification of PEPCK over-expressed in Rosetta with 50 µg/ml of ampicillin + 34 µg/ml of chloramphenicol and induced by 0.5 mM IPTG at 18°C for 24 hours.

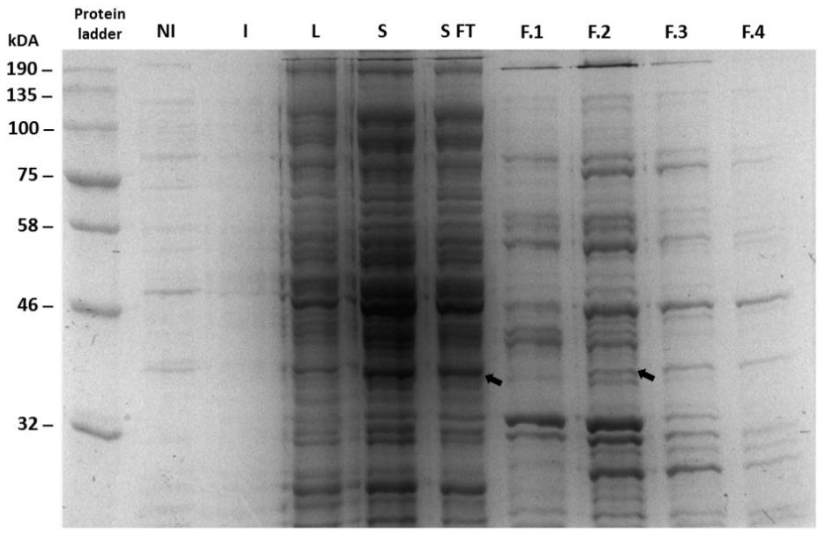

Figure F.12: SDS-gel electrophoresis of partially purified PEPCK protein over-expressed in Rosetta with 50 µg/ml of ampicillin + 34 µg/ml of chloramphenicol and induced by 0.5 mM IPTG at 18°C for 24 hours. Lane NI; Non induced. Lane I; Induced with 0.5 mM IPTG. Lane P: Cell Pellet. Lane L; Lysate after French press. Lane S; Supernatant from centrifugation of the lysate. Lane S FT; Supernatant flow through. Lane F.1,2,3,4: Sample flow through from 20 mM Imidazole buffer.

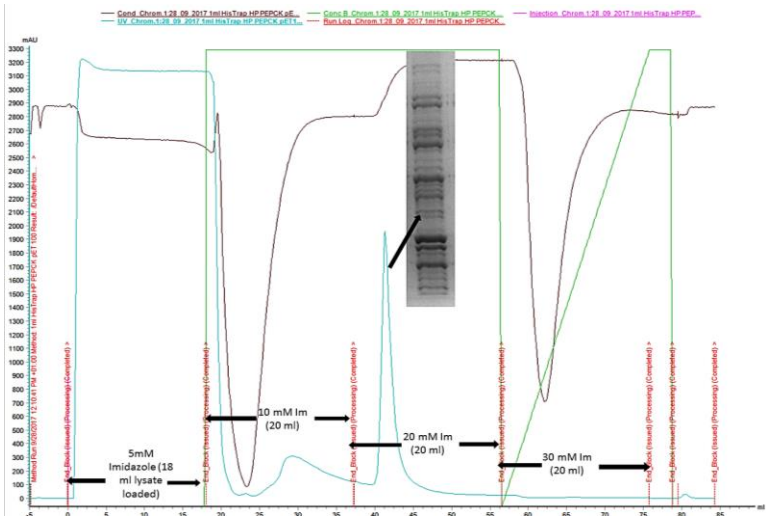

Figure F.13: Purification of PEPCK by HisTrap™ HP column, by using Ni-NTA column (HisTrap™ HP) on an AKTA; over-expressed in Rosetta with 50 µg/ml of ampicillin + 34 µg/ml of chloramphenicol and induced by 0.5 mM IPTG at 18°C for 24 hours. The column was equilibrate with 10 column volume (CV) of binding buffer, 20 mM Tris-HCl, pH 7.4, 10 mM imidazole. The 20 ml of supernatant was then loaded into the column with the flow rate at 1ml per min. The column was washed with 10 and 20 mM imidazole buffer. **C;** Fusion protein was eluted from the 30 mM imidazole buffer. Two major peaks were detected from 10 mM and 20 mM imidazole (arrow). 14 ml fractions were pooled from 10 mM imidazole wash flow through and 4 ml fractions were pooled from 20 mM imidazole flow through. In Fig 7, the results showed that the protein loss when loading the sample into the column (arrow **A**) and slightly detected in 20 mM imidazole flow through (arrow **B**) with multiple contaminant proteins.

Experiment C2. Over-expressed in Rosetta with 50µg/ml of ampicillin and induced by 0.5 mM IPTG at 18°C for 24 hours

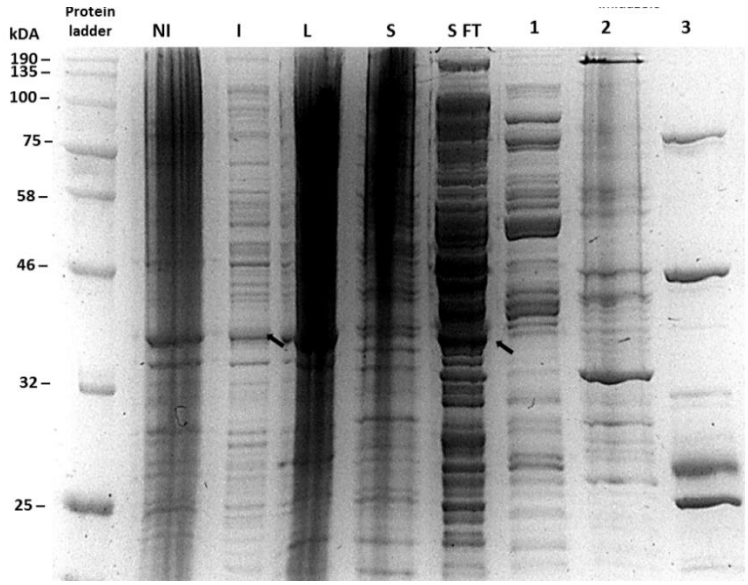

Figure F.14: SDS-gel electrophoresis of partially purified PEPCK protein over-expressed in Rosetta with 50 µg/ml of ampicillin, 34 µg/ml of chloramphenicol and induced by 1 mM IPTG at 18°C for 24 hours. Lysate was loaded into the column followed by 30 CV of 10 mM imidazole wash and then eluted at 15 CV of 100 mM imidazole and 15 CV of 200 mM imidazole. Lane NI; Non-induced. I; Induced. Lane P: Cell Pellet. Lane L; Lysate after French press. Lane S; Supernatant from centrifugation of the lysate. Lane S FT; Supernatant flow through. Lane 1,2,3: No PEPCK was detected.

From the gel image, PEPCK at 37 kDA were induced from the 1 mM IPTG induction (arrow) and available in supernatan (arrow Lane S FT). Target protein (arrow C) was detected from sample flow through showd that the target protein did not bind to the column. Although a peak was detected from 100 mM imidazole elution, SDS-Page gel image showed no PEPCK was detected.

Experiment D. Over-expressed in Rosetta with 50µg/ml of ampicillin and induced by 1 mM IPTG at 18°C for 24 hours

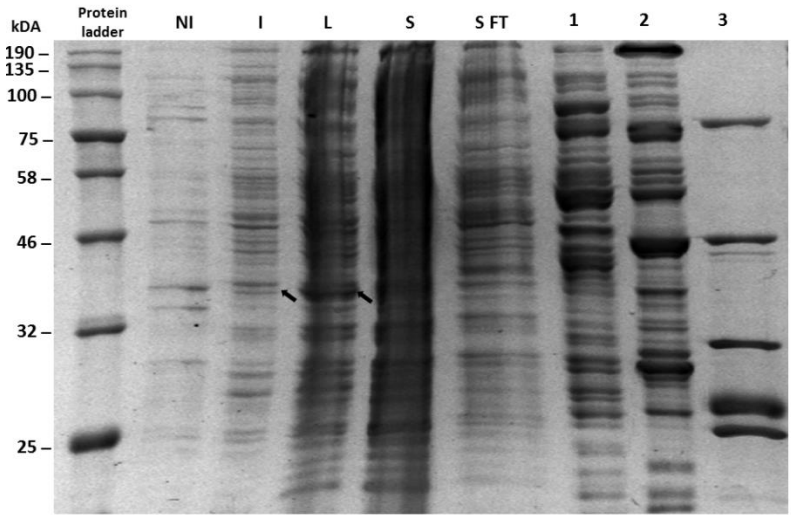

Figure F.15: SDS-gel electrophoresis of partially purified PEPCK protein over-expressed in BL21-DE3 with 50 µg/ml of ampicillin, 34 µg/ml of chloramphenicol and induced by 1 mM IPTG at 18°C for 24 hours. Lane NI; Non-induced. I; Induced. Lane P: Cell Pellet. Lane L; Lysate after French press. Lane S; Supernatant from centrifugation of the lysate. Lane S FT; Supernatant flow through. Lane 1; 10 mM Imidazole. Lane 2; 100mM Imidazole. Lane 3; 400 mM Imidazole. No PEPCK was detected.

G. Small scale of *in vitro* phosphorylation assay of PEPC *P. queenslandica* with Protein Kinase A (PKA) (1:0.5). Ruby stain

The reconstituted assay contained phosphorylation buffer (50 mM Tris-HCl pH 8, 20% glycerol), 5 mM $MgCl_2$, 50 µg/µl of PEPC Pqu, 25 Units of the catalytic subunit of PKA Catalytic Subunit from bovine heart (Sigma) and 1 mM ATP in a total volume 500 µl. The phosphorylation reaction was performed at 30°C from the beginning of adding ATP (1 min), 30 min, 1 hour, 2 hours, 3 hours and 4 hours. The phosphorylation reaction was initiated by the addition of 1 mM ATP and 20 µl aliquots were withdrawn at the specified times and the phosphorylation assay was terminated by adding with equal volume of SDS-sample buffer and heat up for 10 min at 75 °C. Each aliquots was analysed in 10% SDS-PAGE followed by the Coomassie blue staining (2.4.11) On the other 10% SDS-PAGE gel, the phosphorylated protein was determined by Pro-Q Diamond phosphoprotein stain and then Sypro Ruby staining for total protein determination. In each well of 10% SDS-PAGE gels, 50 µg of phosphorylated PEPC was loaded before run at 200 volts for 50 minutes.

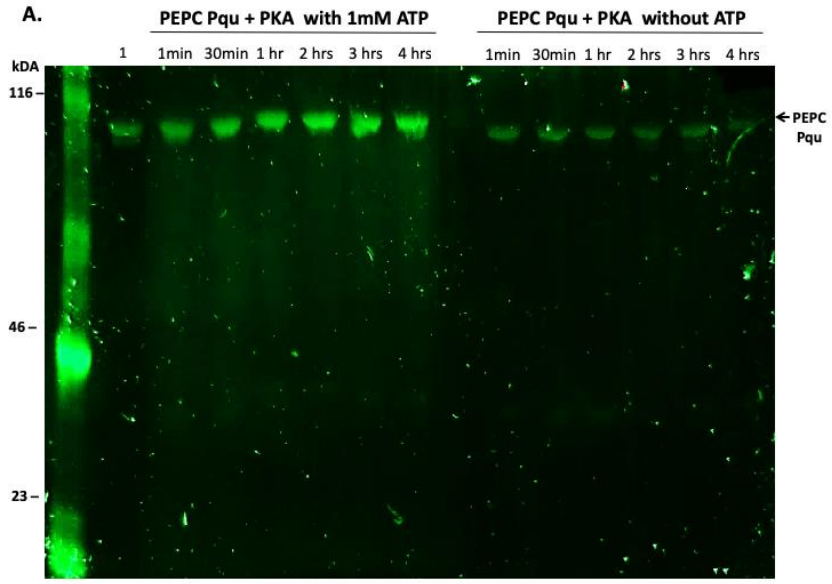

Figure G.1: The time course of PEPC Pqu phosphorylation with PK A for 1 min until 2 hours was analyzed by using SDS-PAGE followed by Pro-Q® Diamond stain. PEPC Pqu was incubated at 30C in the presence or absence of 1 mM ATP as indicated. Lane 1 is unphosphorylated PEPC Pqu.

Incubation in the absence of ATP produce less intensities of the bands, probably due to less phosphorylation occur or none at all. showed less phosphoprotein staining compared to eluents. Incubation with ATP (Fig. 2 A) show high intensitites of the band .

Peppermint Stick Molecular Weight Standards [PM] (0.025µg/µL) were added to each gel as a molecular weight standard and as a phosphoprotein control. Phosphorylated proteins in the PM were ovalbumin (45kDa) and β-casein (23.6kDa) while unphosphorylated protein (β-galactosidase at 116.25kDa) was not observed in this gel.

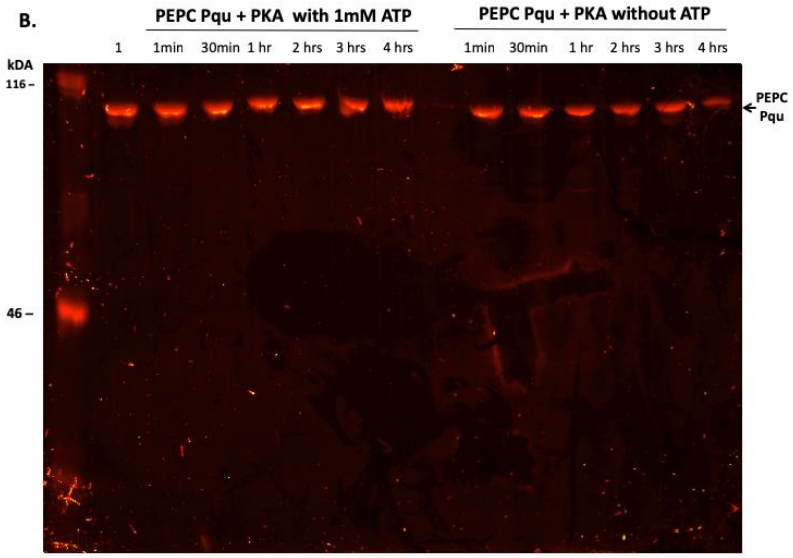

Figure G.2: The time course of PEPC Pqu phosphorylation with PK A for 1 min until 2 hours was analyzed by using SDS-PAGE followed by Pro-Q® Diamond stain. PEPC Pqu was incubated at 30°C in the presence or absence of 1 mM ATP as indicated. Lane 1 is unphosphorylated PEPC Pqu

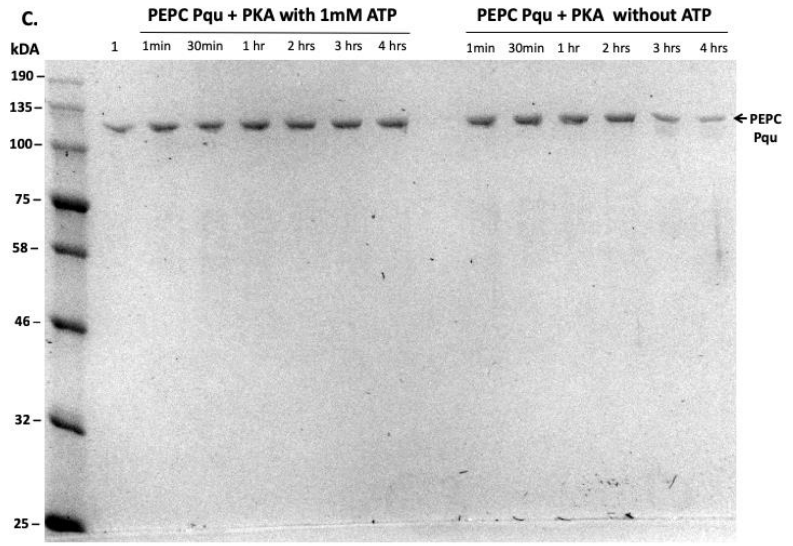

Figure G.3: The time course of PEPC Pqu phosphorylation with PK A for 1 min until 2 hours was analyzed by using SDS-PAGE followed by Comassie blue stain. PEPC Pqu was incubated at 30°C in the presence or absence of 1 mM ATP as indicated. Lane 1 is unphosphorylated PEPC Pqu.

H. i. Small scale *in vitro* phosphorylation assay of PEPC *P. queenslandicum* with PEPCK or Protein Kinase A

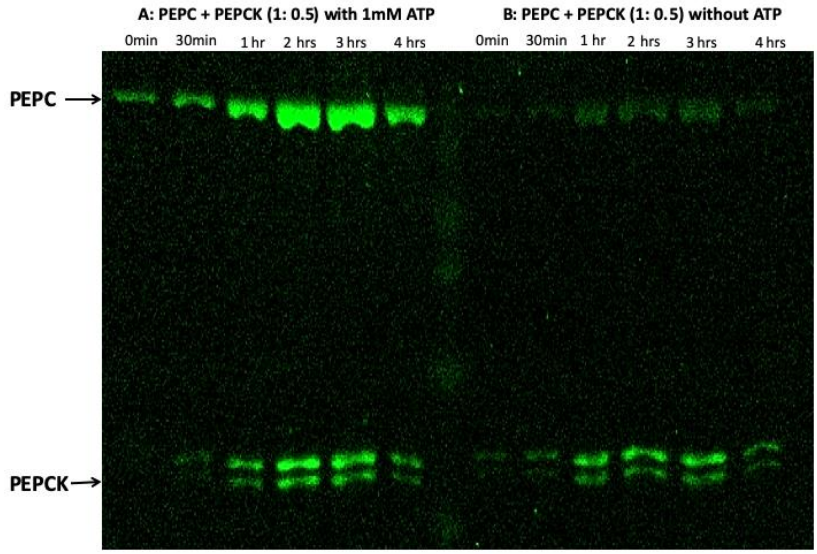

Fig. H.1: 10% SDS-PAGE analysis of *in vitro* phosphorylation of PEPC *P. queenslandicum* by PEPCK (1:0.5) from Pro-Q® Diamond stain. The gel shows two parts which is reaction with ATP (A) and without ATP as a control (B) in different time course as indicated. The phosphorylation reaction was performed at 30°C and 5 µl aliquots were withdrawn at the specified times (1 min, 30 min, 1 hour, 2 hrs, 3 hrs and 4 hrs) and the phosphorylation assay was terminated by adding with equal volume of SDS-sample buffer. Each aliquot was analysed in 10 % SDS-PAGE followed by Pro-Q® Diamond staining.

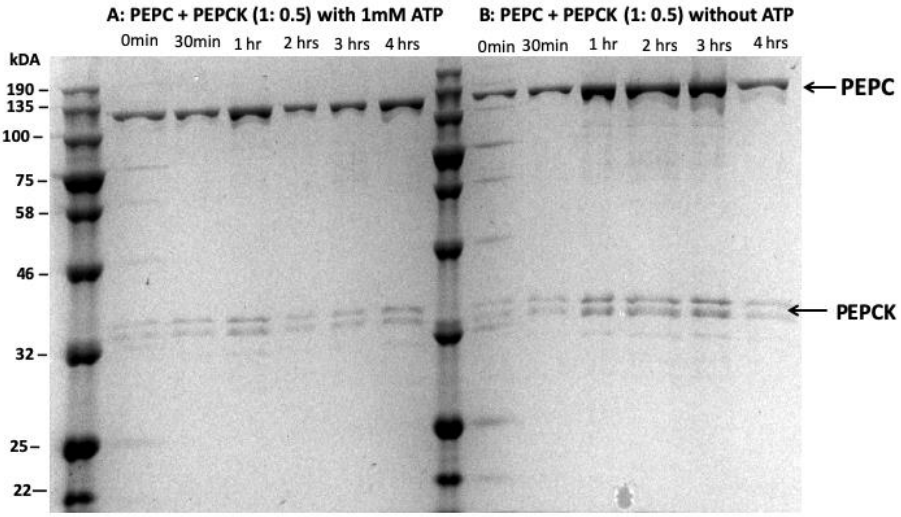

Fig. H.2: 10% SDS-PAGE analysis of *in vitro* phosphorylation of PEPC *P. queenslandicum* by PEPCK (1:0.5) from Coomassie blue staining. The gel shows two parts which is assay with ATP (A) and without ATP as a control (B) in different time course. The phosphorylation reaction was performed at 30°C and 5 µl aliquots were withdrawn at the specified times (1 min, 30 min, 1 hour, 2 hrs, 3 hrs and 4 hrs) and the phosphorylation assay was terminated by adding with equal volume of SDS-sample buffer. Each aliquot was analysed in 8 % SDS-PAGE followed by Coomassie blue staining.

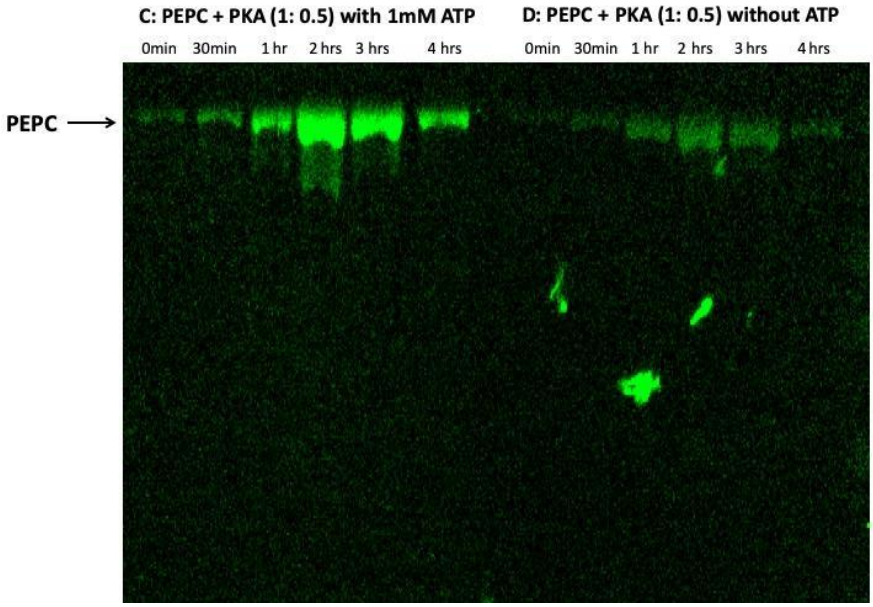

Fig. H.3: 10% SDS-PAGE analysis of *in vitro* phosphorylation of PEPC *P. queenslandicum* by PK A (1:0.5) from Pro-Q® Diamond stain. The gel shows two parts which is assay with ATP (C) and without ATP as a control (D) in different time course as indicated. The phosphorylation reaction was performed at 30°C and 5 µl aliquots were withdrawn at the specified times (1 min, 30 min, 1 hour, 2 hrs, 3 hrs and 4 hrs) and the phosphorylation assay was terminated by adding with equal volume of SDS-sample buffer. Each aliquot was analysed in 8 % SDS-PAGE followed by Pro-Q® Diamond staining.

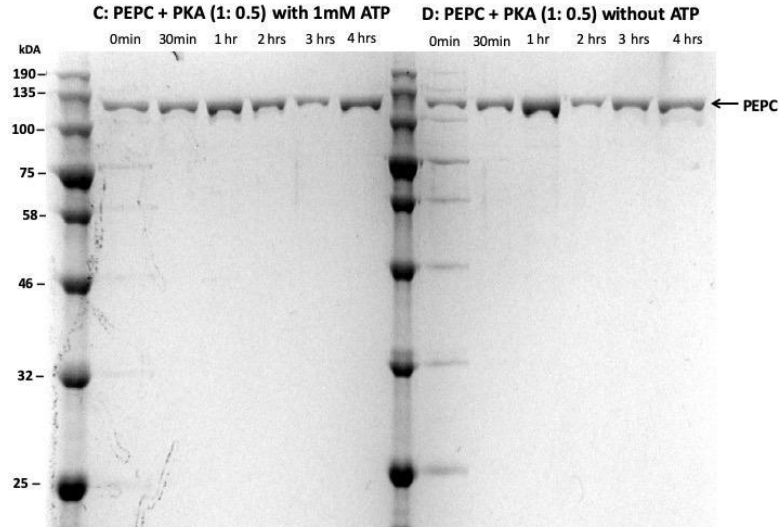

Fig. H.4: 10% SDS-PAGE analysis of *in vitro* phosphorylation of PEPC *P. queenslandicum* by PK A from Coomassie blue staining. The gel shows two parts which is assay with ATP (C) and without ATP as a control (D) in different time course as indicated. The phosphorylation reaction was performed at 30°C and 5 µl aliquots were withdrawn at the specified times (0 min, 30 min, 1 hour, 2 hrs, 3 hrs and 4 hrs) and the phosphorylation assay was terminated by adding with equal volume of SDS-sample buffer. Each aliquot was analysed in 8 % SDS-PAGE followed by Coomassie blue staining.

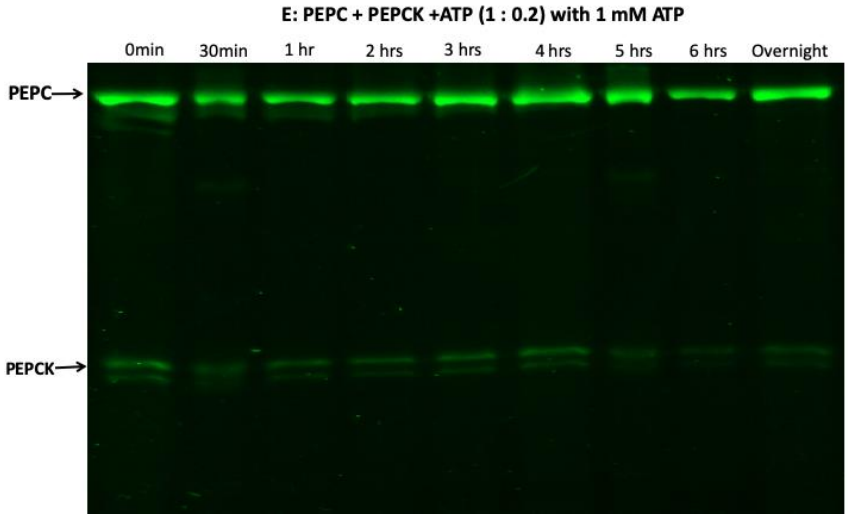

Fig. H.5: 10% SDS-PAGE analysis of *in vitro* phosphorylation of PEPC *P. queenslandicum* by PEPCK from Pro-Q® Diamond stain. The assay was added with 1 mM ATP in different time course as indicated. The phosphorylation reaction was performed at 30°C and 5 µl aliquots were withdrawn at the specified times (0 min, 30 min, 1 hour, 2 hrs, 3 hrs, 4 hrs, 5 hrs, 6 hrs and overnight) and the phosphorylation assay was terminated by adding with equal volume of SDS-sample buffer. Each aliquot was analysed in 10 % SDS-PAGE followed by Pro-Q® Diamond stain.

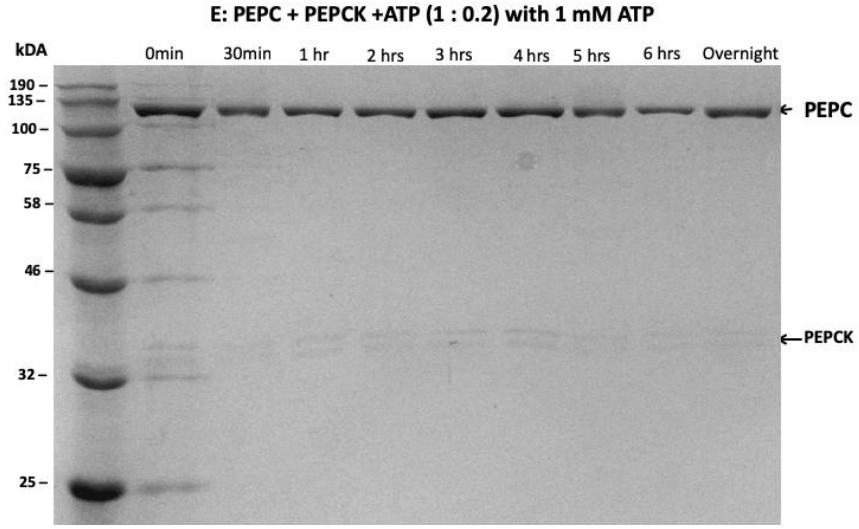

Fig. H.6: 10% SDS-PAGE analysis of *in vitro* phosphorylation of PEPC *P. queenslandicum* by PEPCK from Coomassie blue staining. The assay was added with 1 mM ATP in different time course as indicated. The phosphorylation reaction was performed at 30°C and 5 µl aliquots were withdrawn at the specified times (0 min, 30 min, 1 hour, 2 hrs, 3 hrs, 4 hrs, 5 hrs, 6 hrs and overnight) and the phosphorylation assay was terminated by adding with equal volume of SDS-sample buffer. Each aliquot was analysed in 10 % SDS-PAGE followed by Coomassie blue staining.

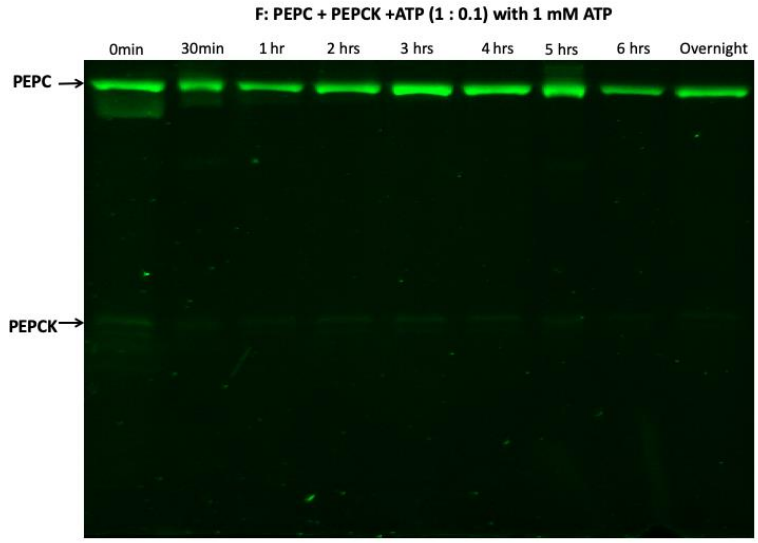

Fig. H.7: 10% SDS-PAGE analysis of *in vitro* phosphorylation of PEPC *P. queenslandicum* by PEPCK (1: 0.1) from Pro-Q® Diamond stain. The assay was added with 1 mM ATP in different time course as indicated. The phosphorylation reaction was performed at 30°C and 5 µl aliquots were withdrawn at the specified times (0 min, 30 min, 1 hour, 2 hrs, 3 hrs, 4 hrs, 5 hrs, 6 hrs and overnight) and the phosphorylation assay was terminated by adding with equal volume of SDS-sample buffer. Each aliquot was analysed in 10 % SDS-PAGE followed by Pro-Q® Diamond stain.

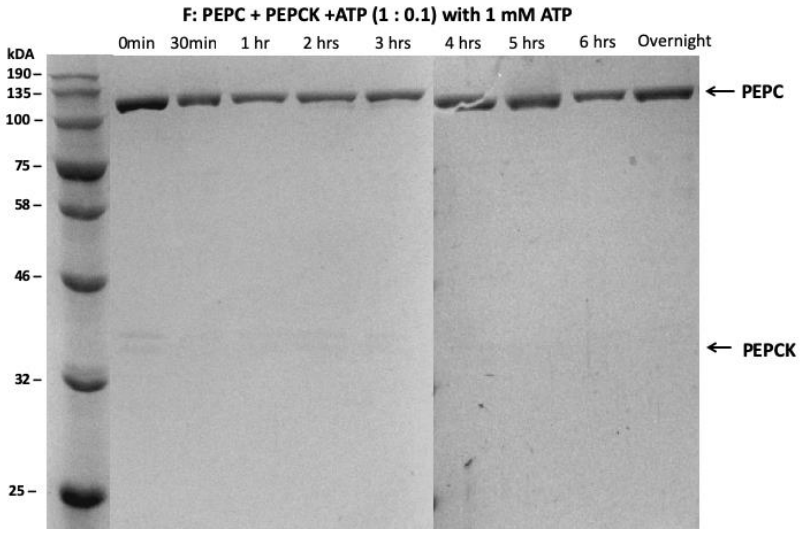

Fig. H.8: 10% SDS-PAGE analysis of *in vitro* phosphorylation of PEPC *P. queenslandicum* by PEPCK (1: 0.1) from Coomassie blue staining. The assay was added with 1 mM ATP in different time course as indicated. The phosphorylation reaction was performed at 30°C and 5 µl aliquots were withdrawn at the specified times (0 min, 30 min, 1 hour, 2 hrs, 3 hrs, 4 hrs, 5 hrs, 6 hrs and overnight) and the phosphorylation assay was terminated by adding with equal volume of SDS-sample buffer. Each aliquot was analysed in 10 % SDS-PAGE followed by Coomassie blue staining.

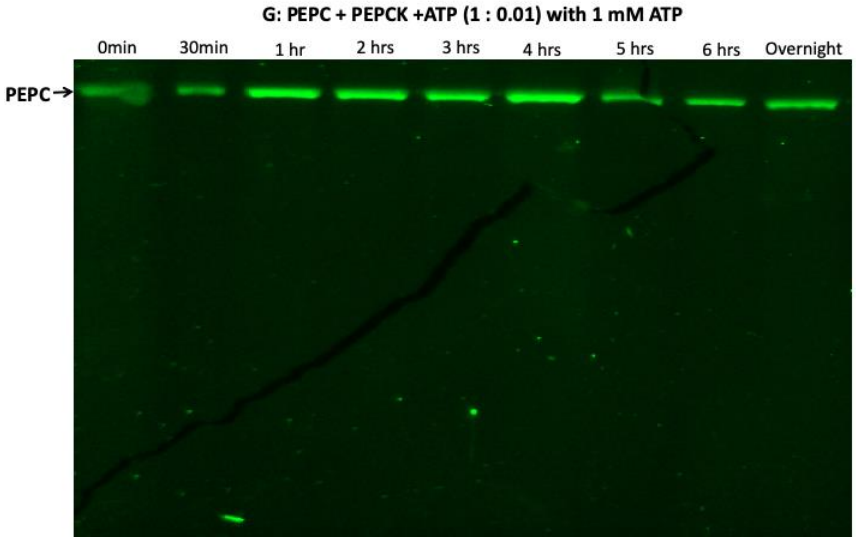

Fig. H.9: 10% SDS-PAGE analysis of *in vitro* phosphorylation of PEPC *P. queenslandicum* by PEPCK (1: 0.01) from Pro-Q® Diamond stain. The assay was added with 1 mM ATP in different time course as indicated. The phosphorylation reaction was performed at 30°C and 5 µl aliquots were withdrawn at the specified times (0 min, 30 min, 1 hour, 2 hrs, 3 hrs, 4 hrs, 5 hrs, 6 hrs and overnight) and the phosphorylation assay was terminated by adding with equal volume of SDS-sample buffer.

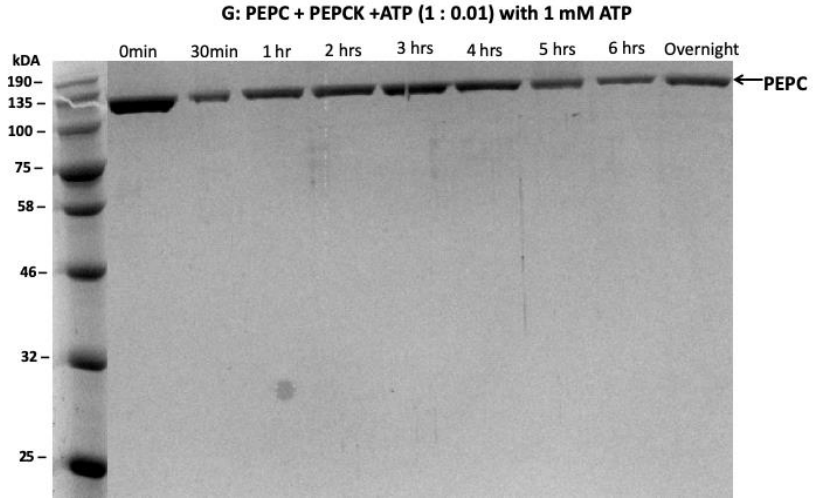

Fig. H.10: 10% SDS-PAGE analysis of *in vitro* phosphorylation of PEPC *P. queenslandicum* by PEPCK (1: 0.01) from Coomassie blue staining. The assay was added with 1 mM ATP in different time course as indicated. The phosphorylation reaction was performed at 30°C and 5 µl aliquots were withdrawn at the specified times (0 min, 30 min, 1 hour, 2 hrs, 3 hrs, 4 hrs, 5 hrs, 6 hrs and overnight) and the phosphorylation assay was terminated by adding with equal volume of SDS-sample buffer.

H. ii. Determination relative intensity of the Pro-Q® Diamond and SYPRO Ruby dye in SDS-PAGE gel in Chapter 4.

To discriminate between phosphorylated and unphosphorylated proteins, the 10 % SDS-PAGE gel was stained with Pro-Q® Diamond followed by SYPRO Ruby dye to determine total protein. The image of protein bands intensities were identified from the RBG Colour digital image by densitometry in ImageJ software (Schindelin, J., et. al., 2012). The relative intensity was calculated by dividing the densitometry of sample proteins with the respective densitometry of protein control.

Results of relative density

Table 1: Results of relative density from Figure 4.5 from Section 4.3 (Small scale in vitro phosphorylation assay of PEPC P. queenslandicum with PEPCK or Protein Kinase A (PKA).

Band	Area	Percent	Relative density
0 min (Control)	13523.74	7.069	1
30 min	13511.37	7.062	0.999
1 hr	13459.49	7.035	0.996
2 hrs	14723.93	7.696	1.093
3 hrs	14019.15	7.328	0.952
4 hrs	14063.2	7.351	1.003
5 hrs	13867.49	7.248	0.985
6 hrs	13665.49	7.143	0.985
overnight	13759.96	7.192	1.006

Table 2: Results of relative density from Figure 4.6 (Pro-Q® Diamond stain) from Section 4.4 (Large scale *in vitro* phosphorylation assay of PEPC *P. queenslandicum* with Protein Kinase A (PKA)).

Band	Area	Percent	Relative density
1(Control)	950.891	7.731	1
1 min	985.184	8.01	1.036
15 min	1147.891	9.332	1.207
30 min	1042.355	8.474	1.096
45 min	1110.77	9.031	1.168
60 min	3832.368	31.157	4.030138404
90 min	2328.154	18.928	2.448324926
120 min	902.477	7.337	0.949036347

Table 3: Results of relative density from Figure 4.6 (SYPRO Ruby stain) from Section 4.4 (Large scale *in vitro* phosphorylation assay of PEPC *P. queenslandicum* with Protein Kinase A (PKA)).

Band	Area	Percent	Relative density
1(Control)	3661.631	22.299	1
1 min	159.678	0.972	0.043
15 min	402.163	2.449	0.109
30 min	847.891	5.163	0.231
45 min	2204.811	13.427	0.602
60 min	3418.338	20.817	0.933
90 min	2090.518	12.731	0.570
120 min	3635.924	22.142	0.992

Table 4: Results of relative density from Figure 4.7 (Pro-Q® Diamond stain) with 1 mm ATP from Section 4.5 (Time course of *in vitro* phosphorylation assay of PEPC *P. pygmaeum* with Protein Kinase A (PKA).

Band	Area	Percent	Relative density
1(Control)	3169.882	15.71	1
2	3311.296	16.411	1.044
3	2871.589	14.231	0.905
4	3497.882	17.335	1.103
5	3868.711	19.173	1.220
6	3458.418	17.14	1.091

Table 5: Results of relative density from Figure 4.7 (Pro-Q® Diamond stain) without 1 mm ATP from Section 4.5 (Time course of *in vitro* phosphorylation assay of PEPC *P. pygmaeum* with Protein Kinase A (PKA).

Band	Area	Percent	Relative density
1 min(Control)	3169.882	15.71	1
30 min	3311.296	16.411	1.044
1 hr	2871.589	14.231	0.905
2 hr	3497.882	17.335	1.103
3 hr	3868.711	19.173	1.220
4 hr	3458.418	17.14	1.091

Table 6: Results of relative density from Figure 4.8 (from SYPRO Ruby stain) with 1 mm ATP from Section 4.5 (Time course of *in vitro* phosphorylation assay of PEPC *P. pygmaeum* with Protein Kinase A (PKA).

Band	Area	Percent	Relative density
1(Control)	3707.468	13.387	1
1 min	3797.054	13.711	1.024
30 min	3566.054	12.877	0.961
1 hr	3832.761	13.84	1.033
2 hr	3405.64	12.297	0.918
3 hr	2004.941	7.24	0.540
4 hr	3860.054	13.938	1.041

Table 7: Results of relative density from Figure 4.8 (from SYPRO Ruby stain) with 1 mm ATP from Section 4.5 (Time course of *in vitro* phosphorylation assay of PEPC *P. pygmaeum* with Protein Kinase A (PKA).

Band	Area	Percent	Relative density
1 min(Control)	1771.125	15.973	1
30 min	1588.296	14.324	0.896
1 hr	1915.246	17.272	1.081
2 hr	3740.388	33.732	2.111
3 hr	1633.311	13.154	0.823

Table 8: Results of relative density from Figure 4.10 (Pro-Q® Diamond stain) from Section 4.6 *In vitro* phosphorylation assay of PEPC *P. pygmaeum* with Protein Kinase A (PKA) with different ratio of PEPCK to PKA.

Band	Area	Percent	Relative density
A	31033.53	23.989	0.601
B(Control)	24194.73	18.702	1.00
C	25955.16	20.063	1.019
B	26169.92	20.229	0.224
D	22014.07	17.017	1.286

Table 9: Results of relative density from Figure 4.10 (SYPRO Ruby stain) from Section 4.6 (*In vitro* phosphorylation assay of PEPC *P. pygmaeum* with Protein Kinase A (PKA) with different ratio of PEPCK to PKA).

Band	Area	Percent	Relative density
A	66854.48	7.773	1.050
B(Control)	63655.53	7.401	1
C	65656.53	7.634	1.031
B	50933.34	5.922	0.800
D	59386.39	6.905	0.932

Table 10: Results of relative density from Figure 4.11 (Pro-Q® Diamond stain) from Section 4.6 *In vitro* phosphorylation assay of PEPC *P. pygmaeum* with Protein Kinase A (PKA) with different ratio of PEPCK to PKA.

Band	Area	Percent	Relative density
1 min (Control)	1697.184	11.078	1
15 min	1306.941	8.531	0.770
30 min	2738.912	17.878	1.613
45 min	654.506	4.272	0.385
60 min	2221.376	14.5	1.308
90 min	2803.669	18.301	1.652
120 min	3897.033	25.438	2.296

Table 11: Results of relative density from Figure 4.11 (SYPRO Ruby stain) from Section 4.6 *In vitro* phosphorylation assay of PEPC *P. pygmaeum* with Protein Kinase A (PKA) with different ratio of PEPCK to PKA.

Band	Area	Percent	Relative density
1 min (Control)	7573.598	13.336	1
15 min	6390.891	11.254	0.843
30 min	7457.305	13.132	0.984
45 min	9000.912	15.85	1.188
60 min	8695.569	15.312	1.148
90 min	8834.74	15.557	1.166
120 min	8836.154	15.56	1.166

I. Identification phosphorylation site of PEPC *P.pygmaeum* by protein digestion from solution.

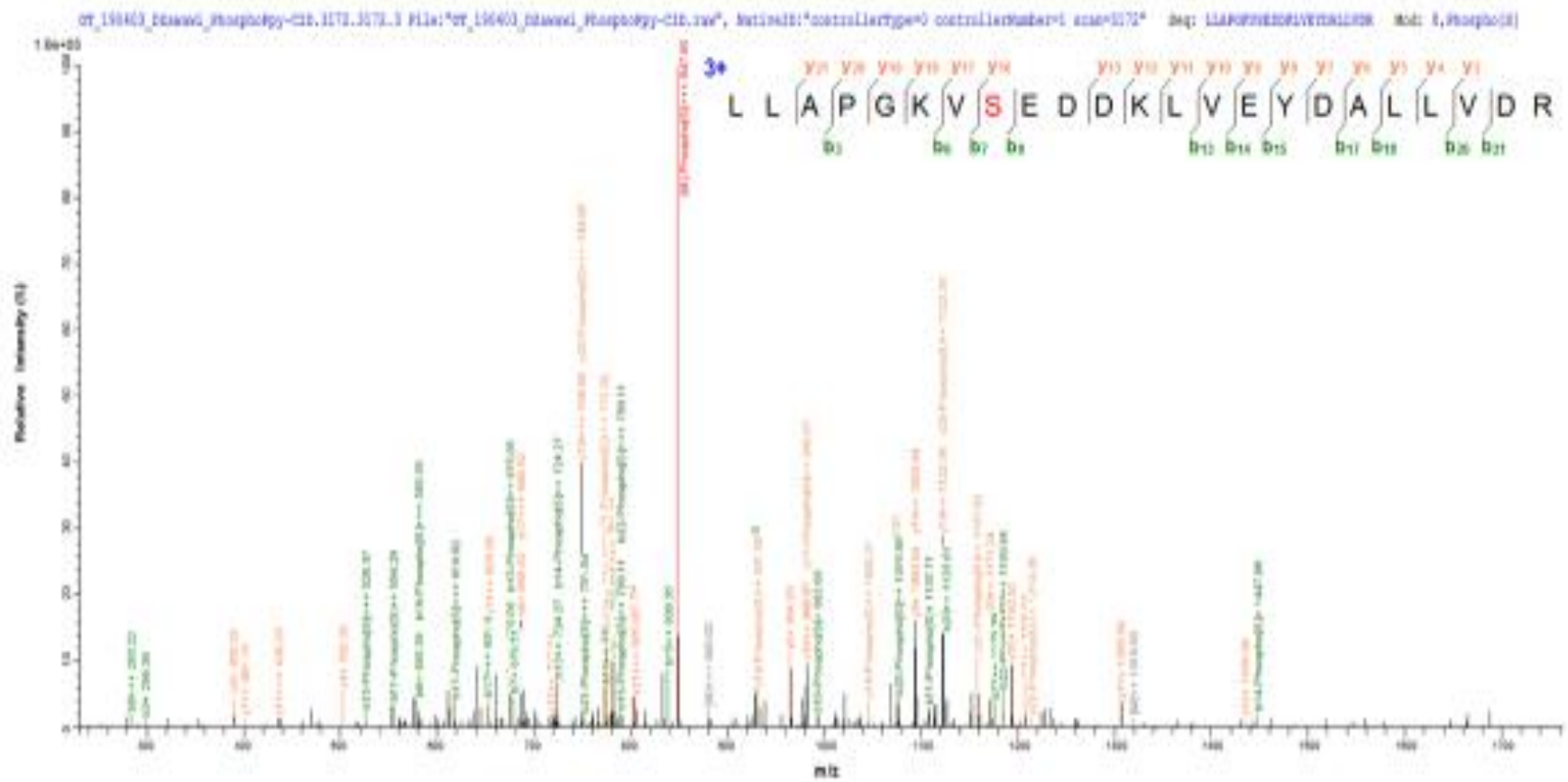

Fig. H.1: MS/MS spectrum of a triply charged of sequence LLAPGKVSEDDKLVEYDALLVDR K from PEPC *P. pygmaeum.* The phosphorylation site was localized to the serine (S) in the peptide. T

J. Normalisation graph, the competitive inhibition (K_{IC}) activity of PEPC *P. queenslandicum* (both non and phosphorylated) is more pronounced in the presence of inhibitors, malate and aspartate.

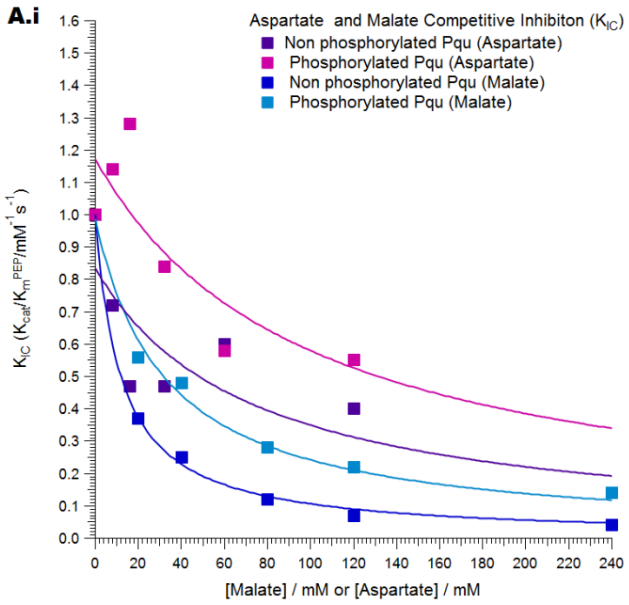

Fig. J. (A.i): From normalisation graph, the competitive inhibition (K_{IC}) activity of PEPC *P. queenslandicum* (both non and phosphorylated) is more pronounced in the presence of inhibitors, malate and aspartate.

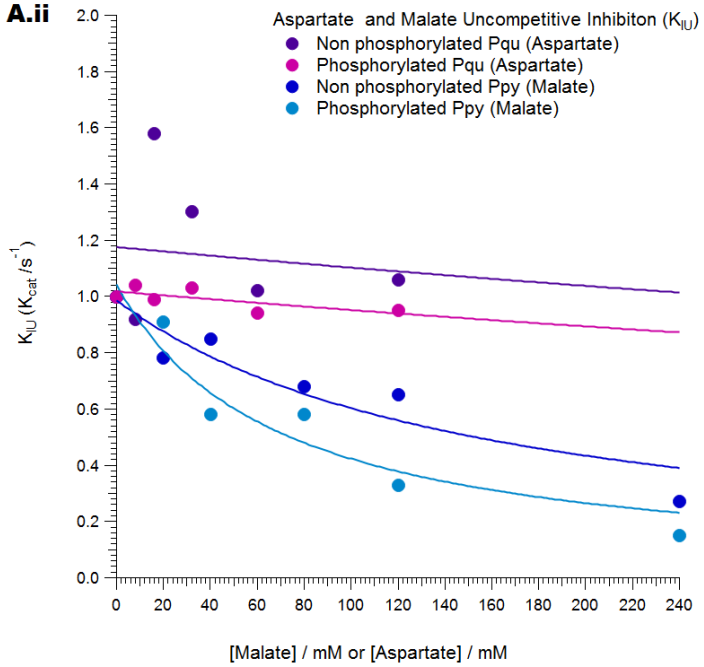

Fig. J. (A.ii): From normalisation graph, the uncompetitive inhibition (K_{IU}) activity of PEPC *P. queenslandicum* (both non and phosphorylated) is less pronounced in the presence of inhibitors, malate and aspartate.

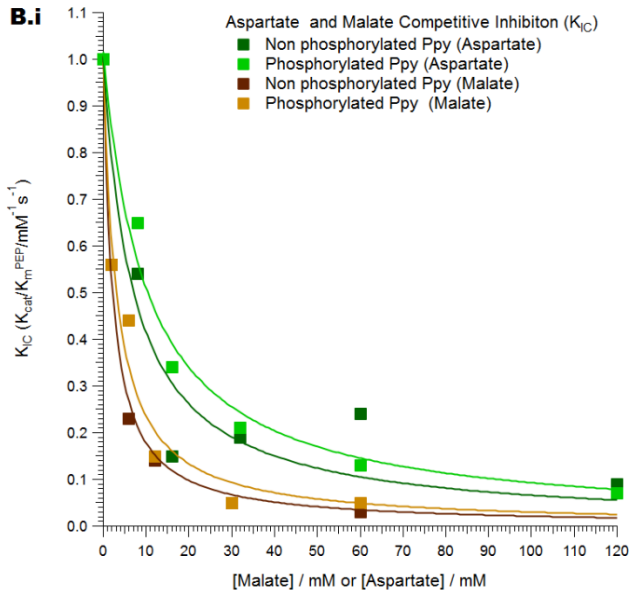

Fig. J. (B.i): From normalisation graph, the competitive inhibition (K_{IC}) activity of PEPC *P. pygmaeum* (both non and phosphorylated) is more pronounced in the presence of inhibitors, malate and aspartate.

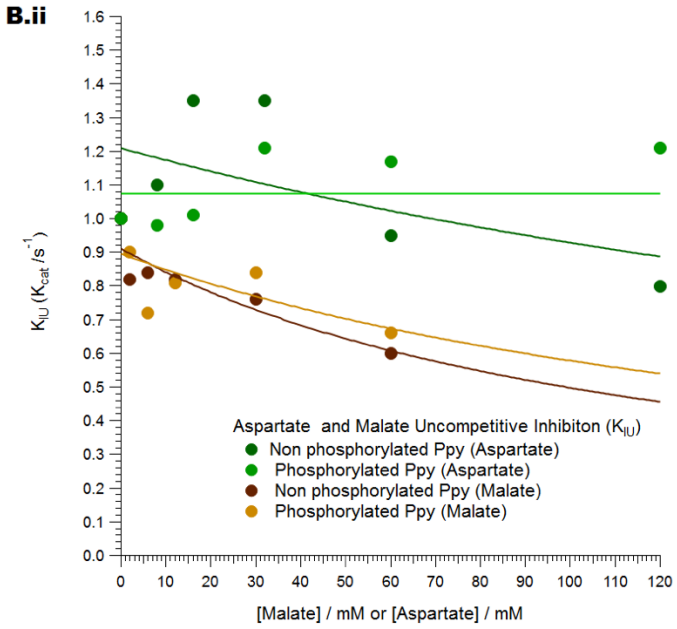

Fig. J. (B.ii): From normalisation graph, the uncompetitive inhibition (K_{IU}) activity of PEPC *P. pygmaeum* (both non and phosphorylated) is less pronounced in the presence of inhibitors, malate and aspartate.

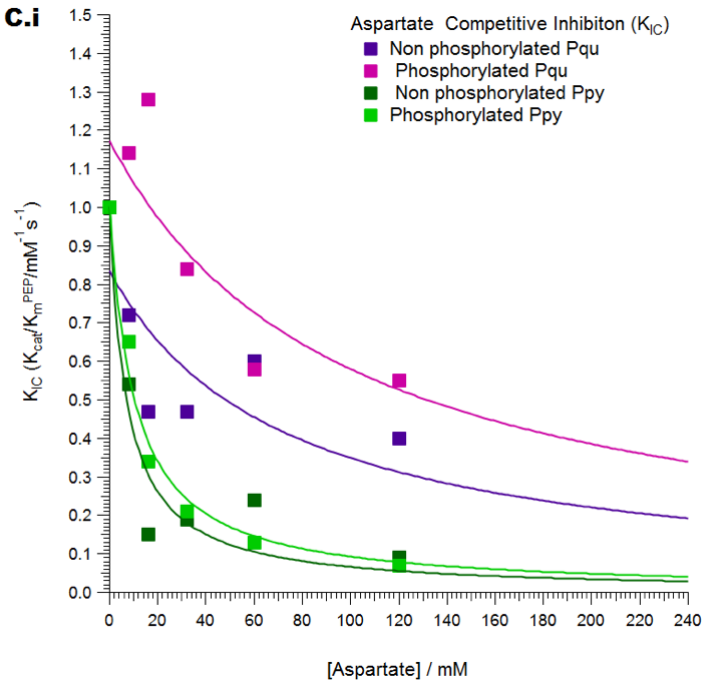

Fig. J. (C.i): From normalisation graph, the competitive inhibition (K_{IC}) activity of PEPC *P. queenslandicum* and *P. pygmaeum* (both non and phosphorylated) is more pronounced in the presence of inhibitor aspartate.

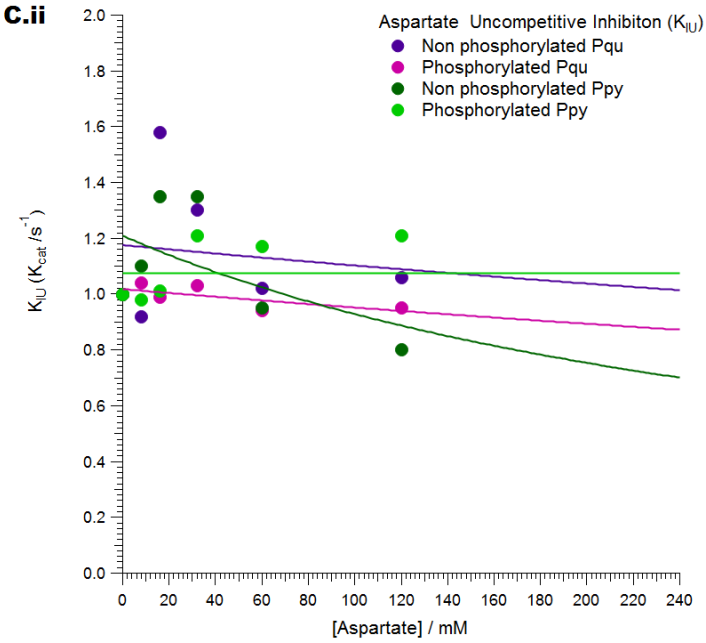

Fig. J. (C.ii): From normalisation graph, the uncompetitive inhibition (K_{IU}) activity of PEPC *P. queenslandicum* and *P. pygmaeum* (both non and phosphorylated) is less pronounced in the presence of inhibitor, aspartate.

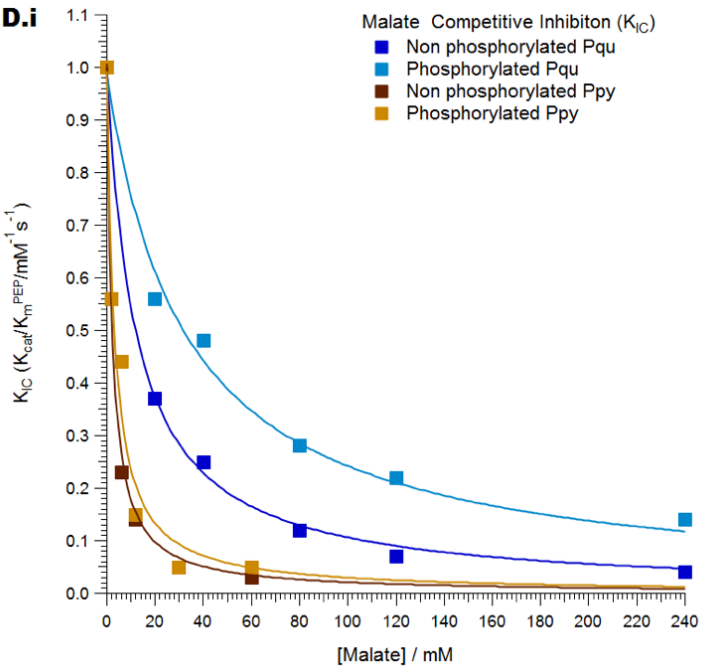

Fig. J. (D.i): From normalisation graph, the competitive inhibition (K_{IC}) activity of PEPC *P. queenslandicum* and *P. pygmaeum* (both non and phosphorylated) is more pronounced in the presence of inhibitor malate.

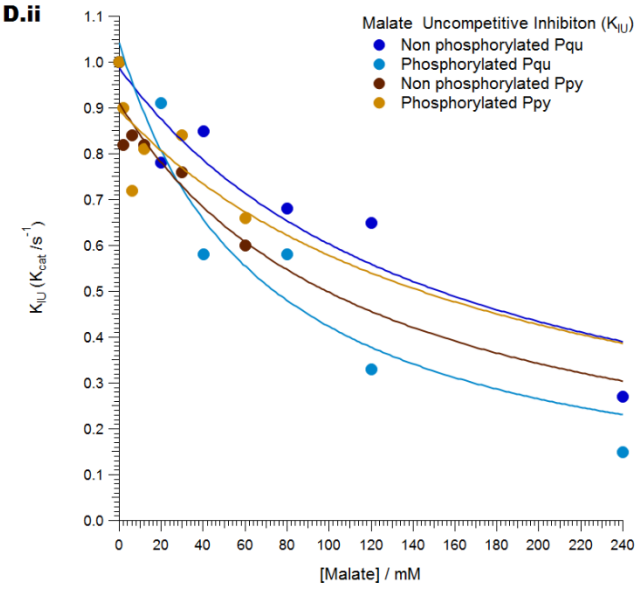

Fig. J. (D.ii): From normalisation graph, the uncompetitive inhibition (K_{IU}) activity of PEPC *P. queenslandicum* and *P. pygmaeum* (both non and phosphorylated) is more pronounced in the presence of inhibitor, malate.

K. Primary Plot Saturation curves for PEP from inhibition by malate from non-phosphorylated (A) and phosphorylated (B) *P. queenslandicum* PEPC.

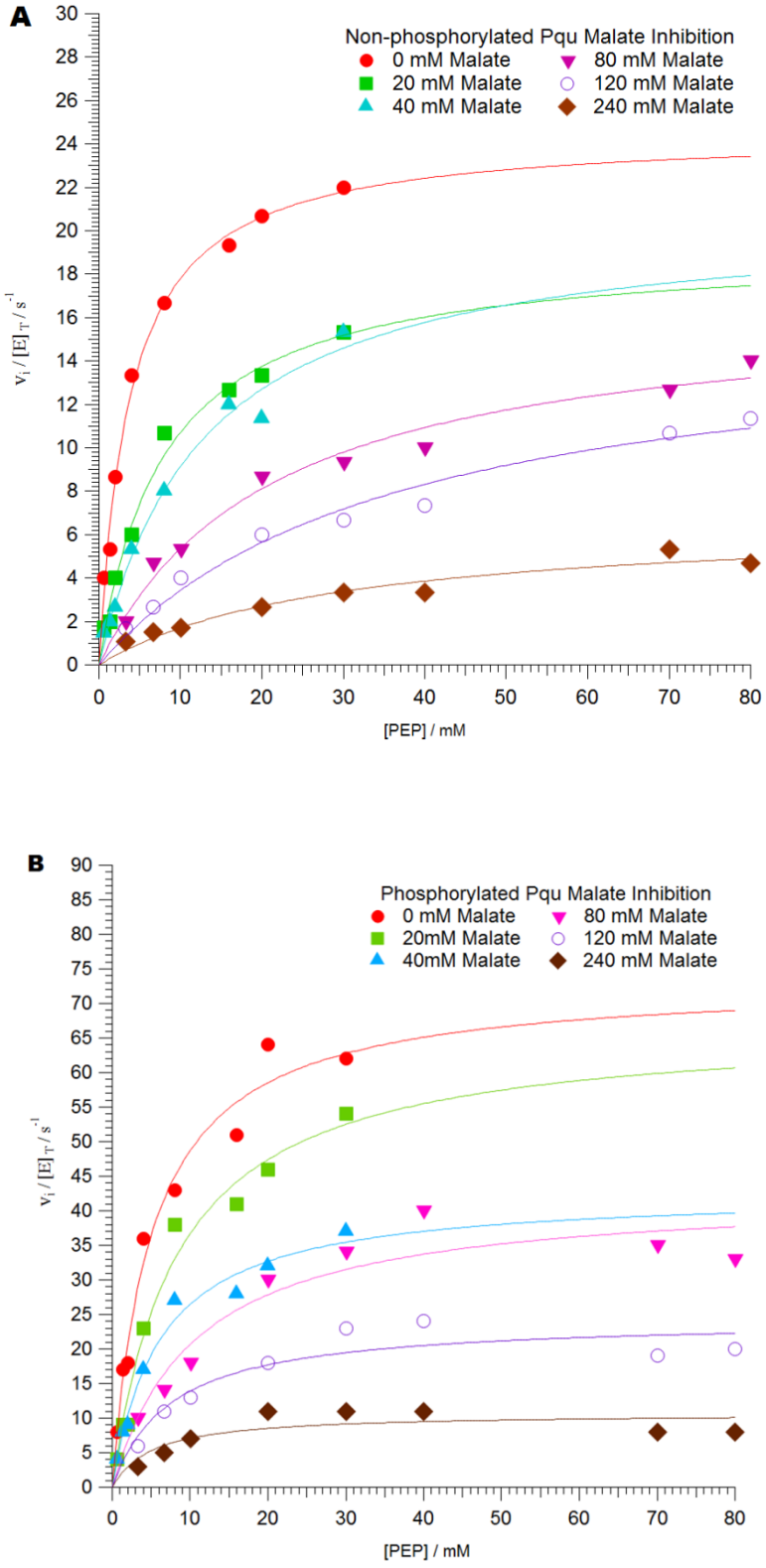

Fig. K. (A) & (B): Saturation curves for PEP from inhibition by malate from non-phosphorylated (A) and phosphorylated (B) *P. queenslandicum* PEPC. Dependence of PEPC reaction rate was determined on variable concentrations of PEP and L-malate (• 0 mM, ■ 20mM, ▲ 40mM, ▼ 80mM, ○ 120mM, ◆ 240 mM malate).

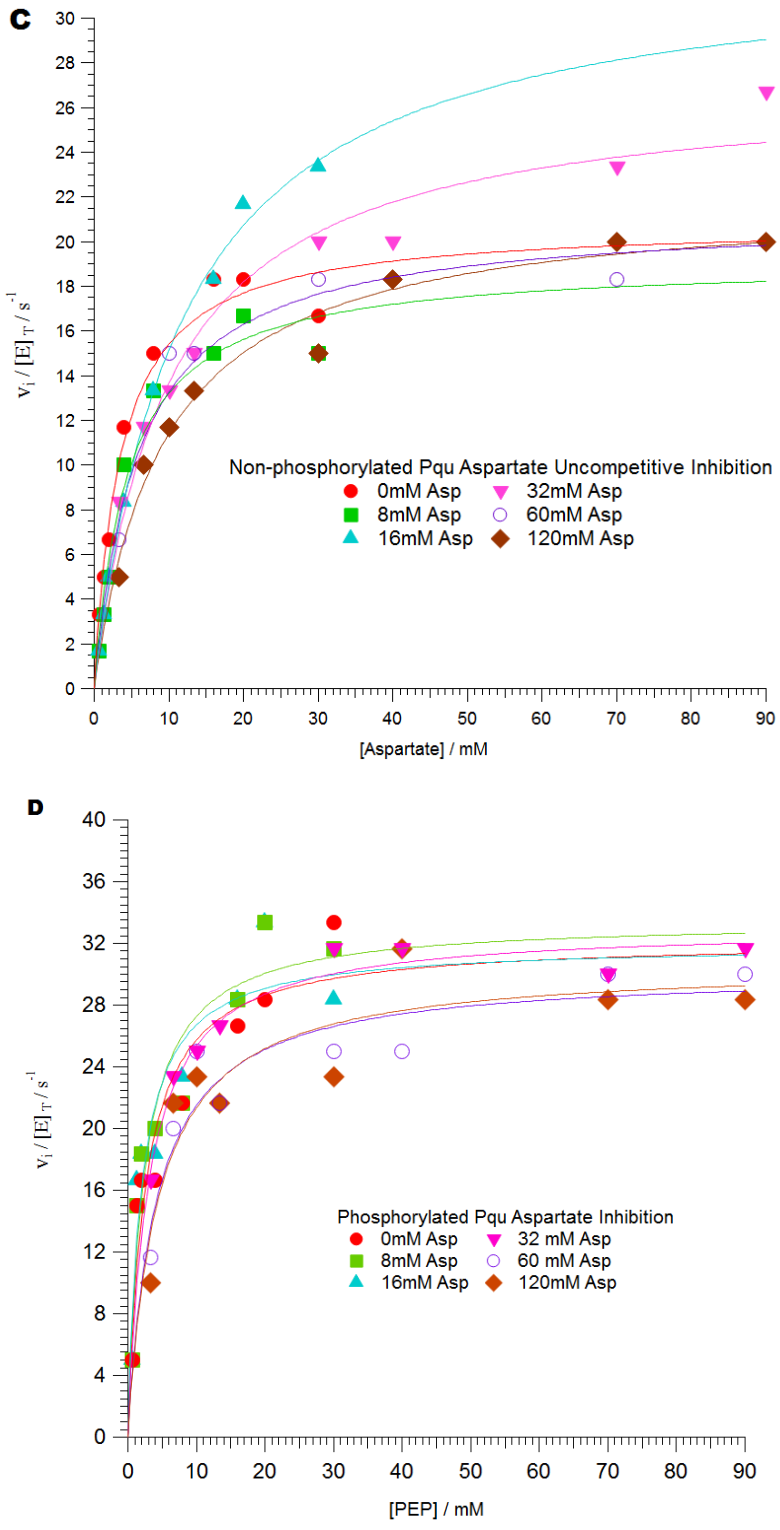

Fig. K. (C) & (D): Saturation curves for PEP from inhibition by aspartate from non-phosphorylated (C) and phosphorylated (D) *P. queenslandicum* PEPC. Dependence of PEPC reaction rate was determined on variable concentrations of PEP and aspartate (• 0mM, ■ 8mM, ▲ 16mM, ▼ 32mM, ○ 60mM, ◆ 120 mM of aspartate).

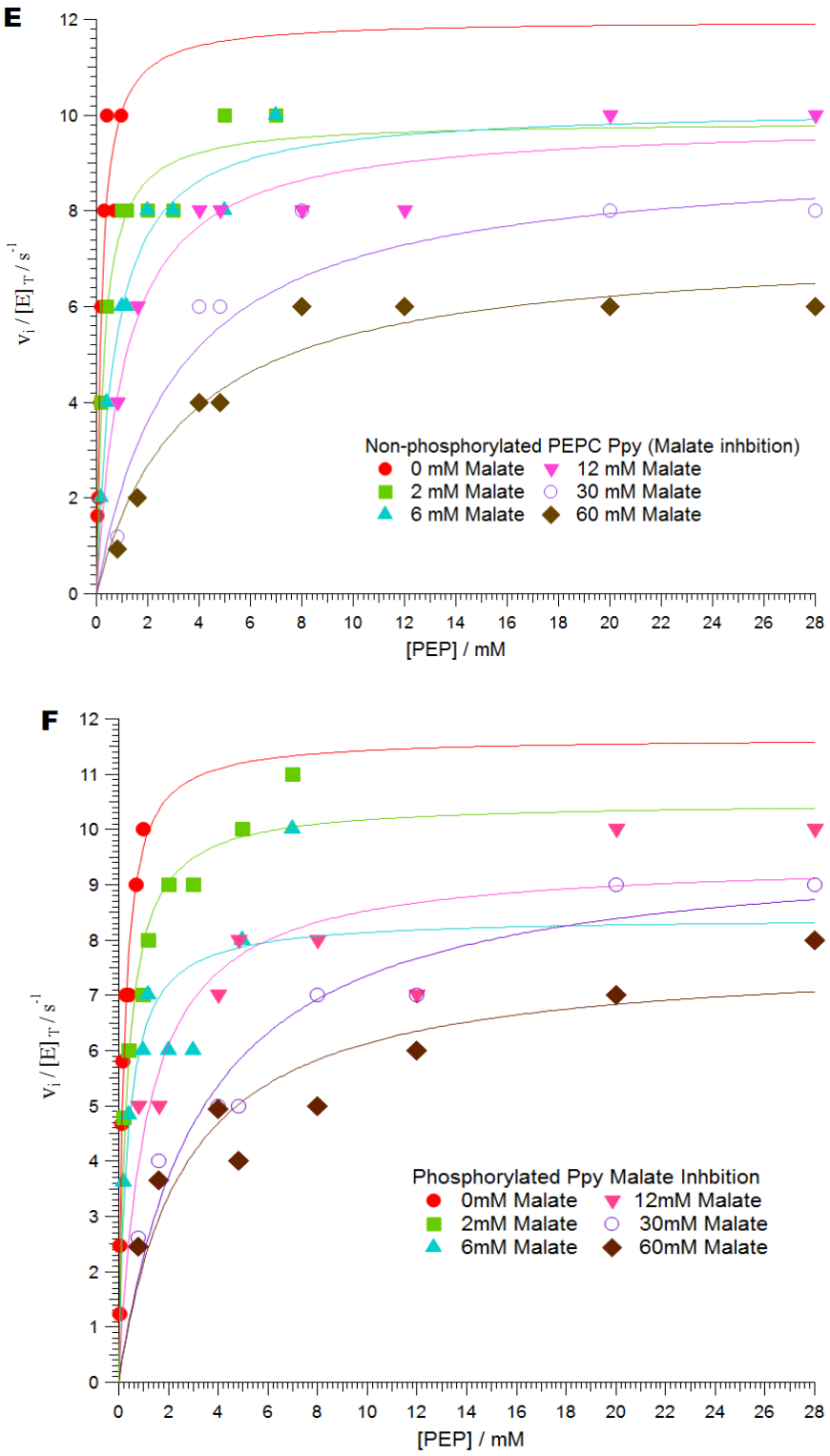

Fig. K. (E) & (F): Saturation curves for PEP from inhibition by malate from non-phosphorylated (E) and phosphorylated (F) *P. pygmaeum* PEPC. Dependence of PEPC reaction rate was determined on variable concentrations of PEP and malate (● 0 mM, ■ 2 mM, ▲ 6 mM, ▼ 12 mM, ○ 30 mM, ◆ 60 mM malate).

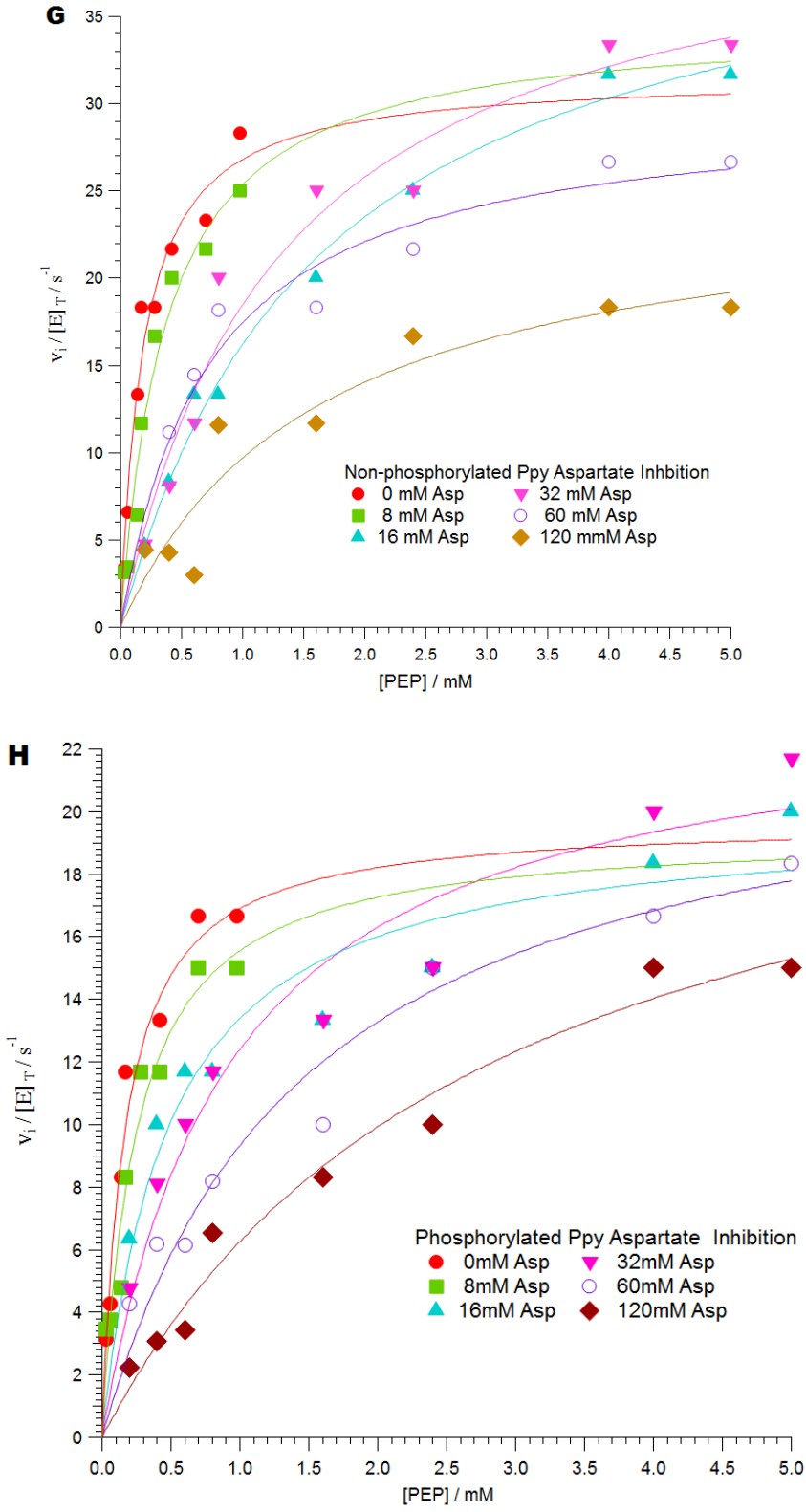

Fig. K. (G) & (H): Saturation curves for PEP from inhibition by aspartate from non-phosphorylated (G) and phosphorylated (H) *P. pygmaeum* PEPC. Dependence of PEPC reaction rate was determined on variable concentrations of PEP and aspartate (● 0 mM, ■ 2 mM, ▲ 6 mM, ▼ 12 mM, ○ 30 mM, ◆ 60 mM aspartate).

L. Determination of malate uncompetitive (K_{IU}) (A.i) and competitive inhibition (K_{IC}) (A.ii) for non-phosphorylated and phosphorylated of *P. queenslandicum* (10 nM)

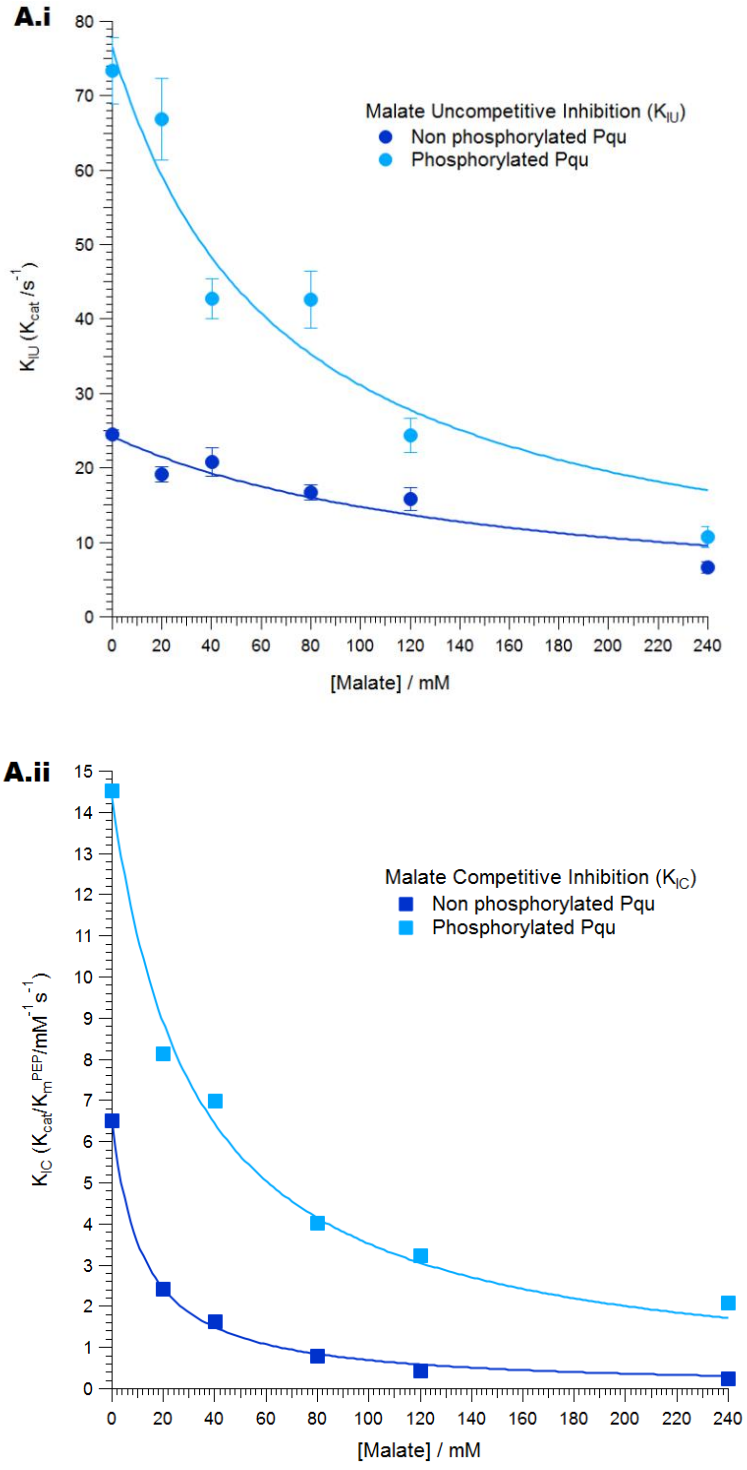

Fig. L. (A.i) & (A.ii): Determination of malate uncompetitive (K_{IU}) (A.i) and competitive inhibition (K_{IC}) (A.ii) for non-phosphorylated and phosphorylated of *P. queenslandicum* (10 nM). Activity was measured in the presence of 50 mM Tricine.KOH buffer, pH 8, 10 mM $MgCl_2$, 10 mM $KHCO_3$ and 0.15 mM NADH. The inhibition activity was determined with varying malate levels, as shown in the plot, as follows; 0 mM, 20mM, 40mM, 80mM, 120mM, 240 mM malate.

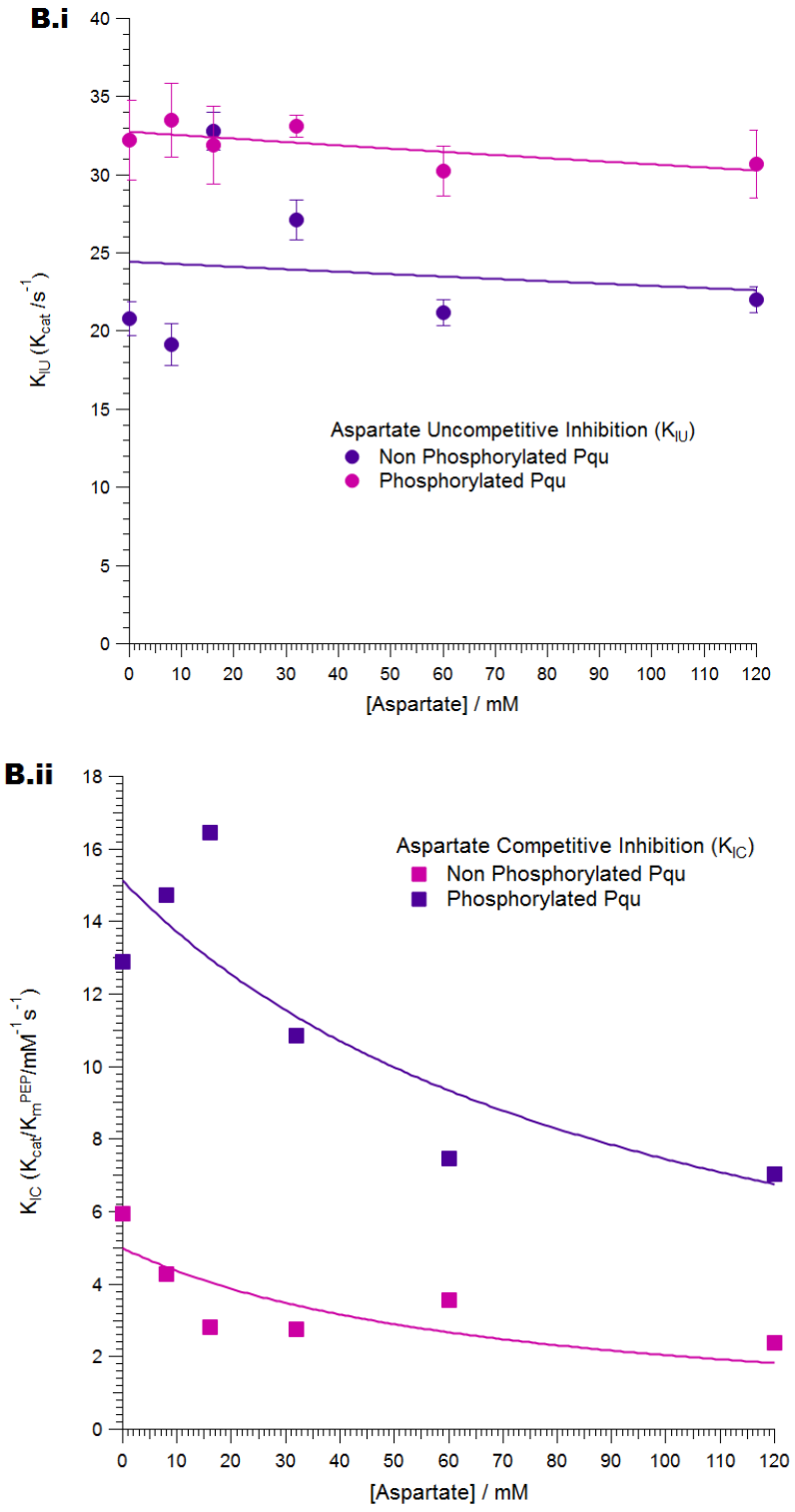

Fig. L. (B.i) & (B.ii): Determination of aspartate uncompetitive inhibition (K_{IU}) (B.i) and competitive inhibition (K_{IC}) (B.ii) for non-phosphorylated and phosphorylated of *P. queenslandicum* (10 nM). Activity was measured in the presence of 50 mM Tricine.KOH buffer, pH 8, 10 mM $MgCl_2$, 10 mM $KHCO_3$ and 0.15 mM NADH. The inhibition activity was determined with varying aspartate levels, as shown in the plot, as follows; 0 mM, 8 mM, 16 mM, 32 mM, 60 mM, 120 mM aspartate.

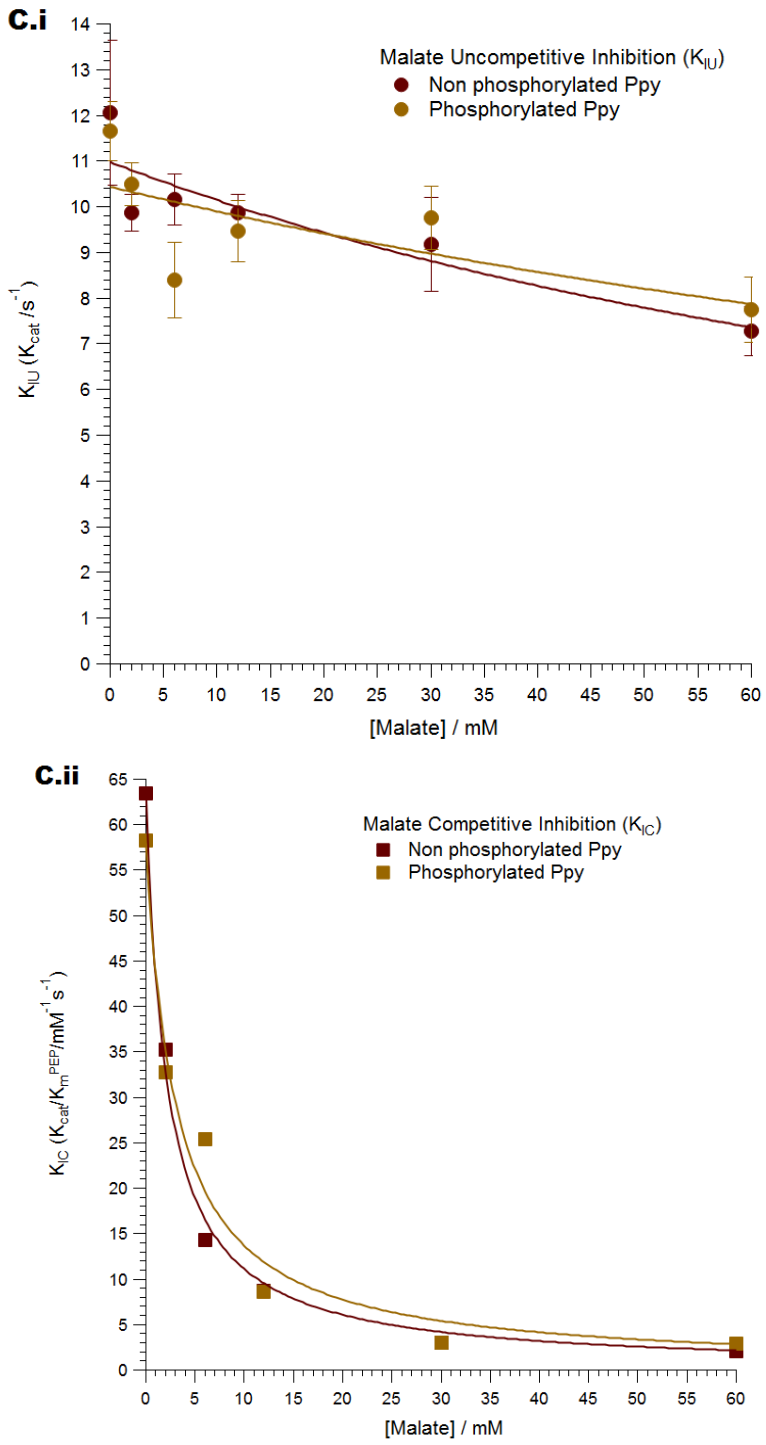

Fig. L. (C.i) & (C.ii): Determination of malate uncompetitive (K_{IU}) C.i) and competitive inhibition (K_{IC}) (C.ii) for non-phosphorylated and phosphorylated of PEPC *P. pygmaeum* (5 nM). Activity was measured in the presence of 50 mM Tricine.KOH buffer, pH 8, 10 mM $MgCl_2$, 10 mM $KHCO_3$ and 0.15 mM NADH. The inhibition activity was determined with varying malate levels, as shown in the plot, as follows; 0 mM, 20mM, 40mM, 80mM, 120mM, 240 mM malate.

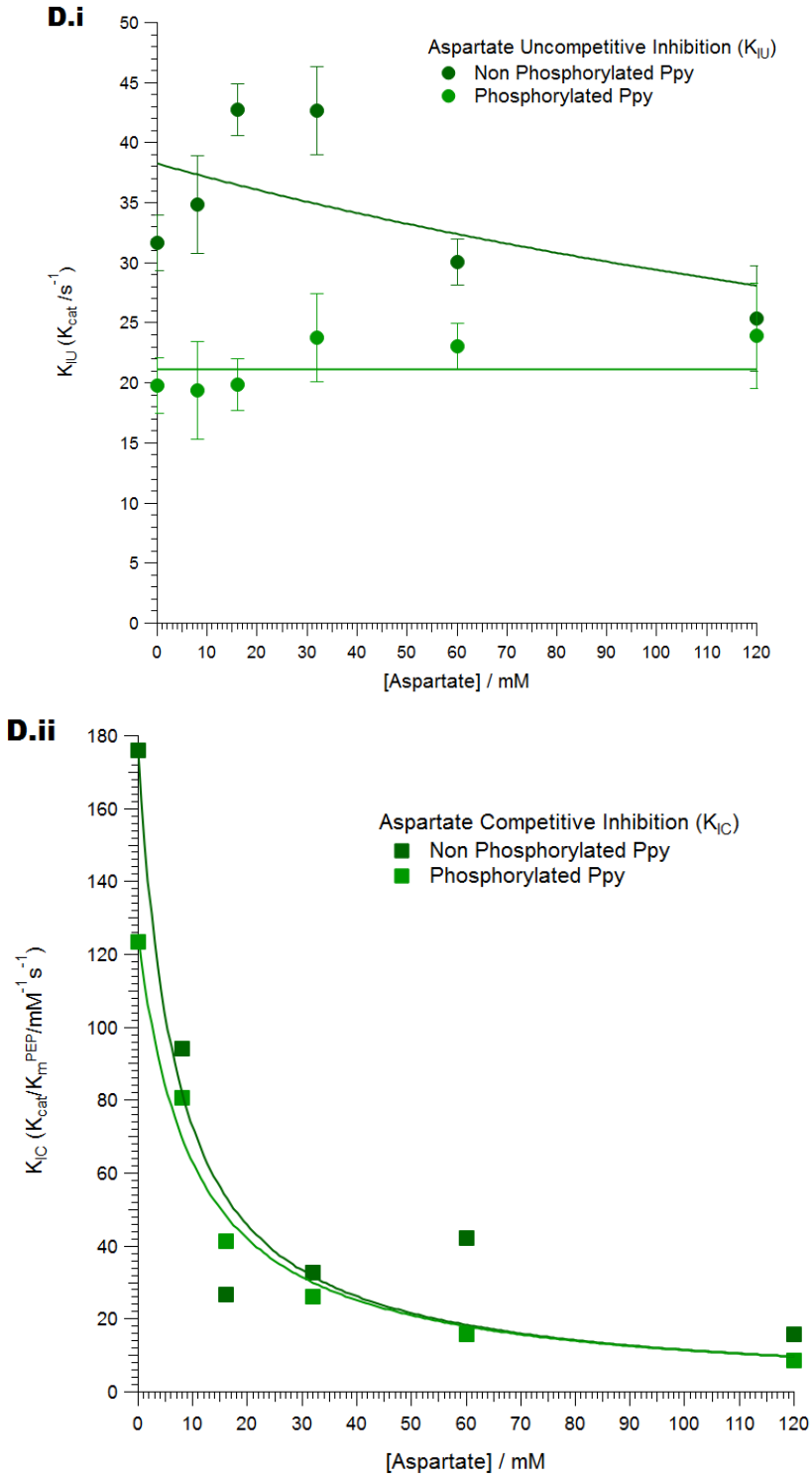

Fig. L. (D.i) & (D.ii): Determination of aspartate uncompetitive inhibition (K_{IU}) (D.i) and competitive inhibition (K_{IC}) (D.ii) for non-phosphorylated and phosphorylated of *P. pygmaeum* PEPC (5 nM). Activity was measured in the presence of 50 mM Tricine.KOH buffer, pH 8, 10 mM $MgCl_2$, 10 mM $KHCO_3$ and 0.15 mM NADH. The inhibition activity was determined with varying malate levels, as shown in the plot, as follows; 0 mM, 8 mM, 16 mM, 32 mM, 30 mM, 60 mM , 120 mM aspartate.

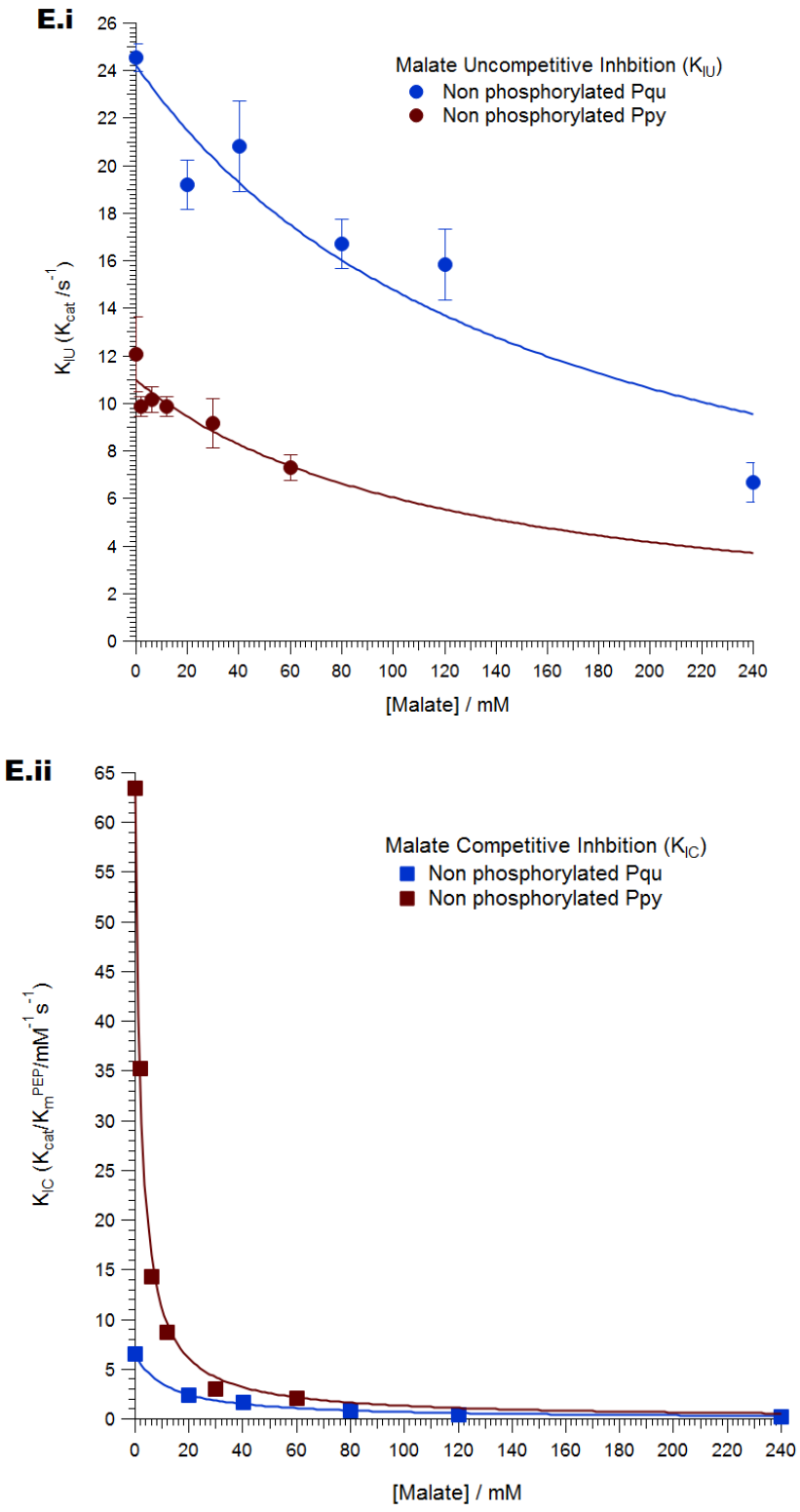

Fig. L. (E.i) & (E.ii): Determination of malate uncompetitive (K_{IU}) (E.i) and competitive inhibition (K_{IC}) (E.ii) for non-phosphorylated of *P. queenslandicum* (5 nM) and *P. pygmaeum* PEPC (5 nM). Activity was measured in the presence of 50 mM Tricine.KOH buffer, pH 8, 10 mM $MgCl_2$, 10 mM $KHCO_3$ and 0.15 mM NADH. The inhibition activity was determined with varying malate levels, as shown in the plot, at the different malate concentrations, as follows; 0 mM, 20mM, 40mM, 80mM, 120mM, 240 mM malate.

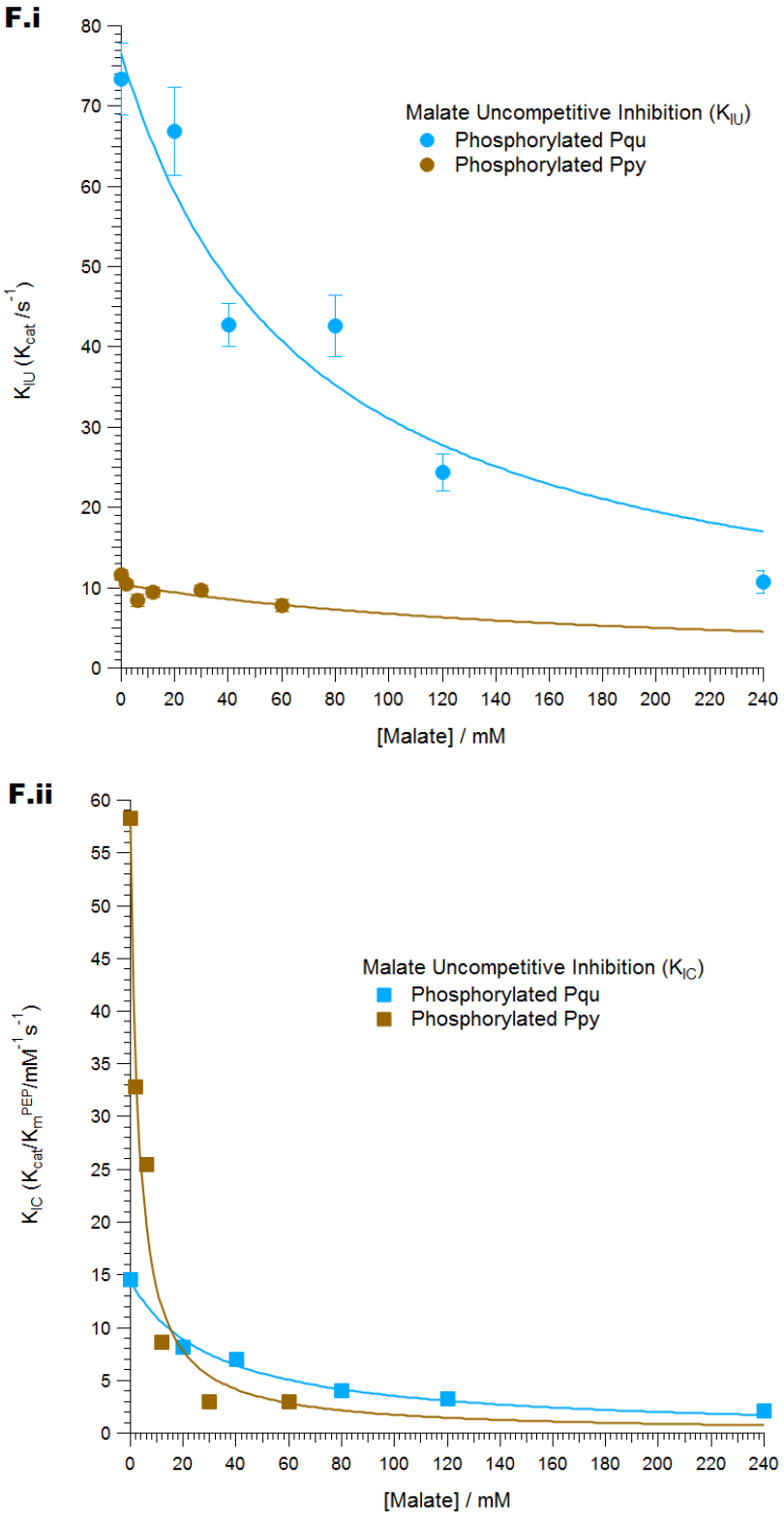

Fig. L. (F.i) & (F.ii): Determination of malate uncompetitive (K_{IU}) (F.i) and competitive inhibition (K_{IC}) (F.ii) for phosphorylated of *P. queenslandicum* (5 nM) and *P. pygmaeum* PEPC (5 nM). Activity was measured in the presence of 50 mM Tricine.KOH buffer, pH 8, 10 mM $MgCl_2$, 10 mM $KHCO_3$ and 0.15 mM NADH. The inhibition activity was determined with varying malate levels, as shown in the plot, at the different malate concentrations, as follows; 0 mM, 20mM, 40mM, 80mM, 120mM, 240 mM malate.

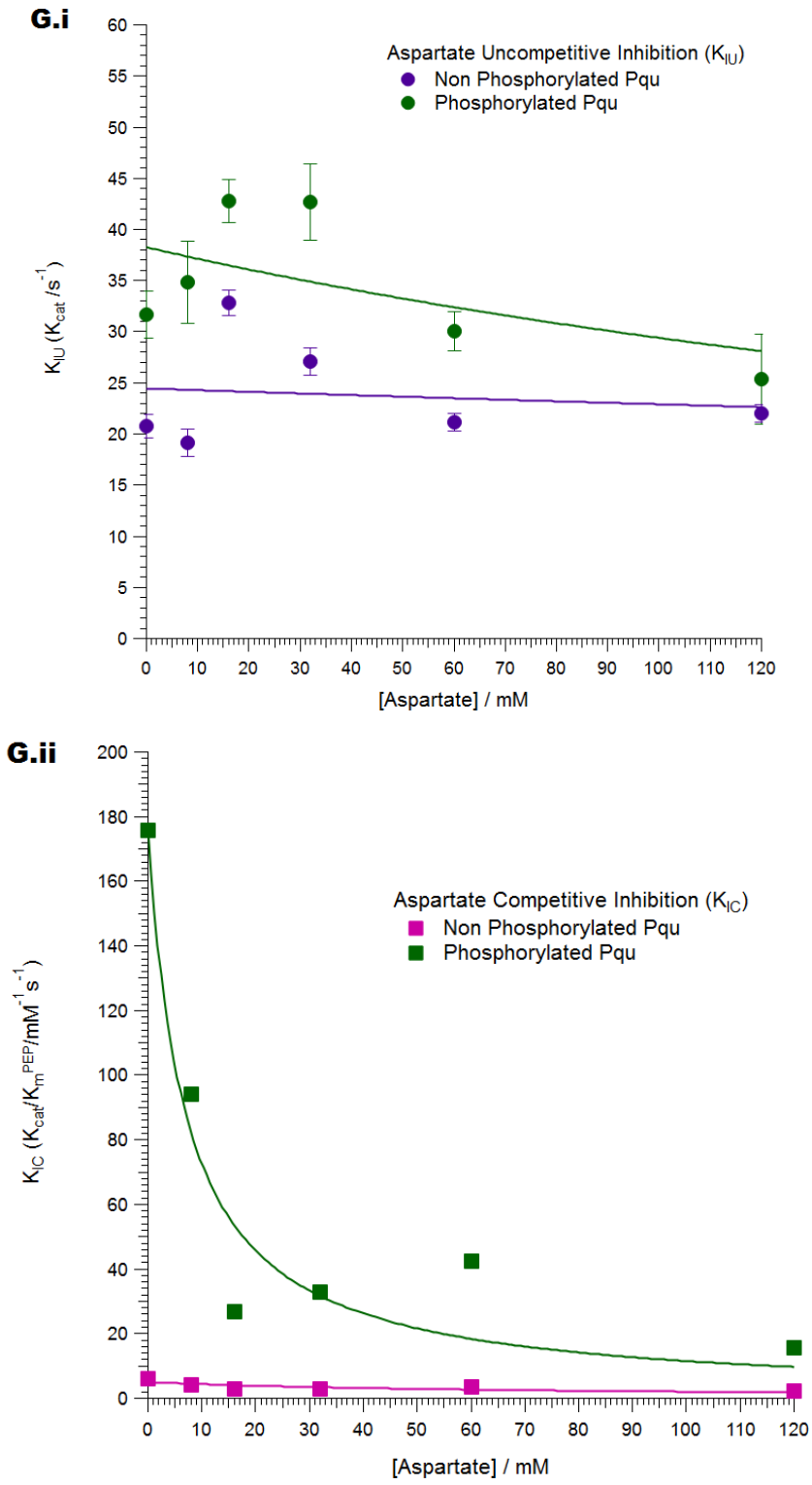

Fig. L. (G.i) & (G.ii): Determination of aspartate (K_{IU}) (G.i) and competitive inhibition (K_{IC}) (G.ii) for non-phosphorylated and phosphorylated of PEPC *P. queenslandicum* (5 nM). Activity was measured in the presence of 50 mM Tricine.KOH buffer, pH 8, 10 mM $MgCl_2$, 10 mM $KHCO_3$ and 0.15 mM NADH. The inhibition activity was determined with varying aspartate levels, as shown in the plot, as follows; 0 mM, 8 mM, 16 mM, 32 mM, 30 mM, 60 mM , 120 mM aspartate.

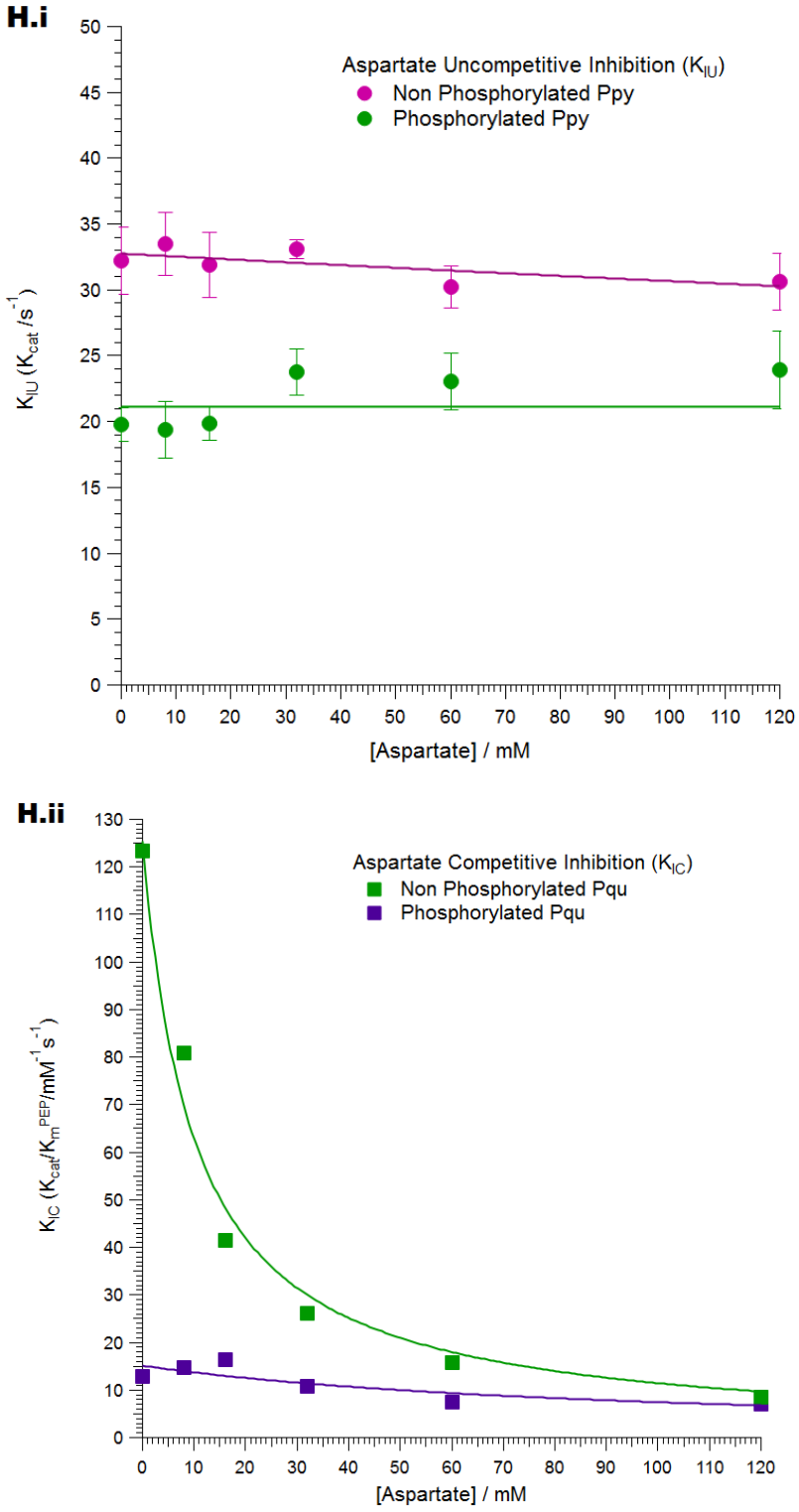

Fig. L. (H.i) & (H.ii): Determination of aspartate uncompetitive inhibition (K_{IU}) (H.i) and competitive inhibition (K_{IC}) (H.ii) for non-phosphorylated and phosphorylated of PEPC *P. queenslandicum* (5 nM). Activity was measured in the presence of 50 mM Tricine.KOH buffer, pH 8, 10 mM $MgCl_2$, 10 mM $KHCO_3$ and 0.15 mM NADH. The inhibition activity was determined with varying malate levels, as shown in the plot, as follows; 0 mM, 8 mM, 16 mM, 32 mM, 30 mM, 60 mM , 120 mM aspartate.

M. Screening for optimum ANS concentration in malate inhibition for non-phosphorylated PEPC P. queenslandicum.

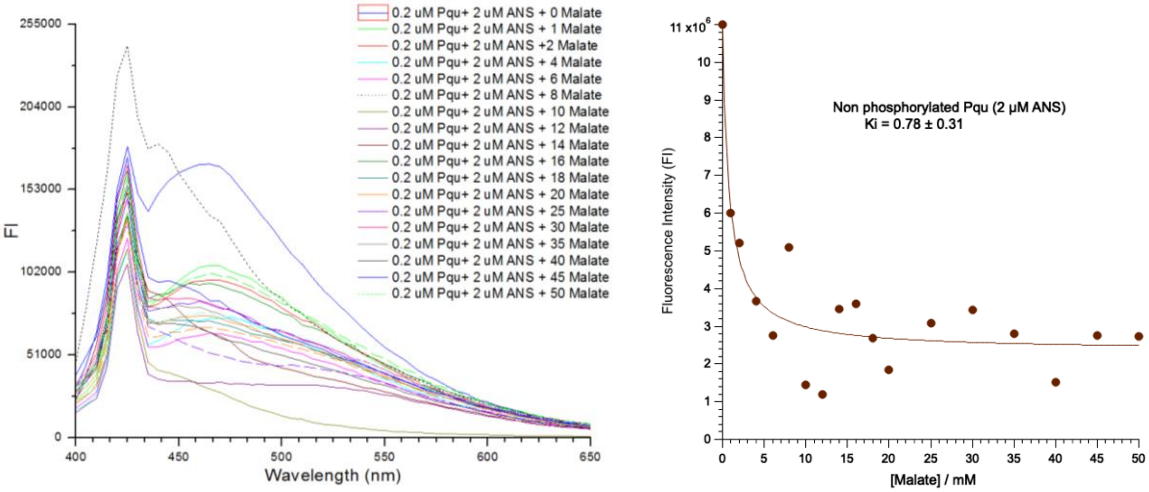

Fig. M.1 : (Left) The emission spectrum of the 2 µM of ANS-PEPC *P. queenslandicum* complex. The fluorescence assay mixture contained 50 mM tricine-KOH (pH 8), 10 mM $MgCl_2$, 0.2 µM PEPC, 2 µM of ANS and varying concentrations of malate from 0 to 50 mM, allowing to determination of dissociation constant (K_d); (Right) Determination of dissociation constant (K_d) for unphosphorylated of *P. queenslandicum* with K_d = 0.78 ± mM malate in 2 µM of ANS.

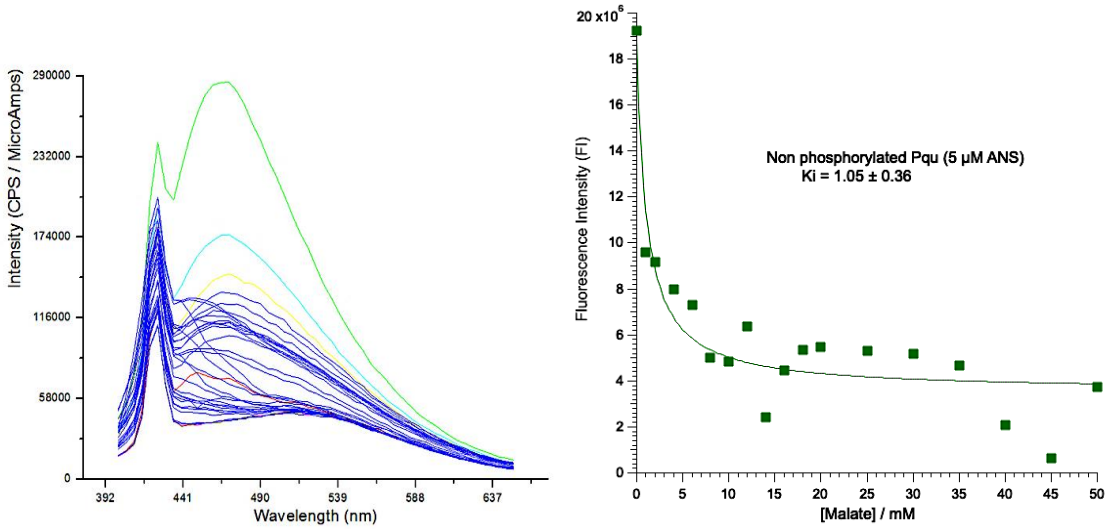

Fig. M.2: (Left) The emission spectrum of the ANS-PEPC *P. queenslandicum* complex. The fluorescence assay mixture contained 50 mM tricine-KOH (pH 8), 10 mM $MgCl_2$, 0.2 µM PEPC, 5.0 µM of ANS and varying concentrations of malate from 0 to 50 mM, allowing to determination of dissociation constant (K_d); (Right) Determination of dissociation constant (K_d) for unphosphorylated of *P. queenslandicum* with K_d = 1.05 ± 0.36 mM malate in 5 µM of ANS.

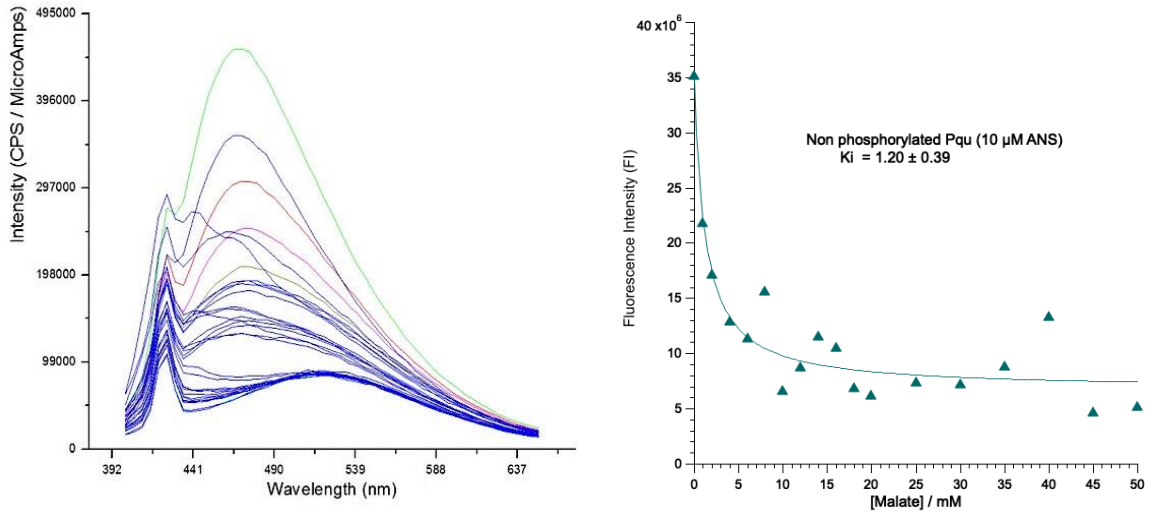

Fig. M.3: (Left) The emission spectrum of the 10 µM of ANS-PEPC *P. queenslandicum* complex. The fluorescence assay mixture contained 50 mM tricine-KOH (pH 8), 10 mM $MgCl_2$, 0.2 µM PEPC, 10.0 µM of ANS and varying concentrations of malate from 0 to 50 mM, allowing to determination of dissociation constant (K_d); (Right) Determination of dissociation constant (K_d) for unphosphorylated of *P. queenslandicum* with K_d = 1.20 ± mM malate in 10 µM of ANS.

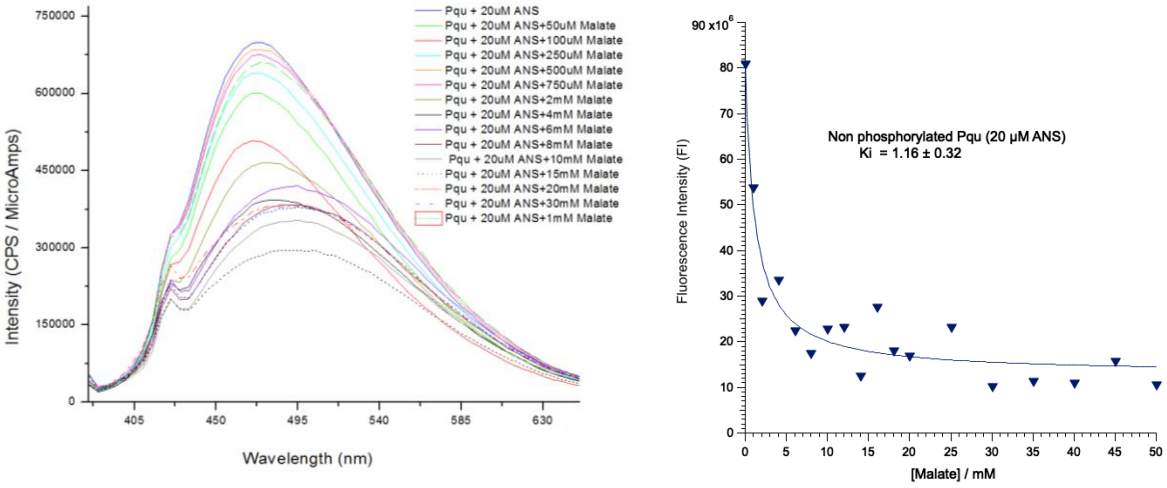

Fig. M.4: (Left) The emission spectrum of the ANS-PEPC *P. queenslandicum* complex. The fluorescence assay mixture contained 50 mM tricine-KOH (pH 8), 10 mM $MgCl_2$, 0.2 µM PEPC, 20.0 µM of ANS and varying concentrations of malate from 0 to 50 mM, allowing to determination of dissociation constant (K_d); (Right) Determination of dissociation constant (K_d) for unphosphorylated of *P. queenslandicum* with K_i= 1.16 ± mM malate in 20 µM of ANS.

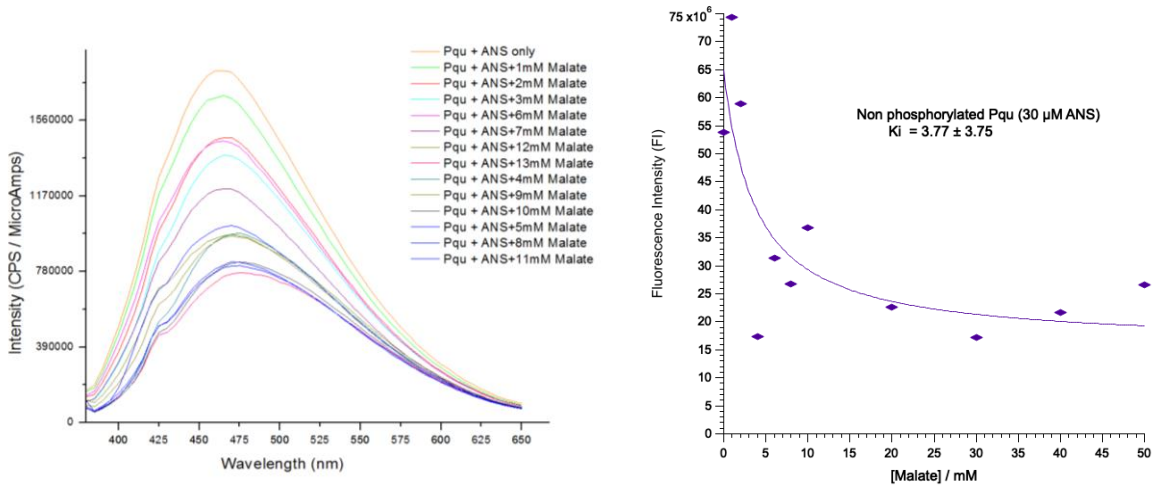

Fig. M.5: (Left) The emission spectrum of the ANS-PEPC *P. queenslandicum* complex. The fluorescence assay mixture contained 50 mM tricine-KOH (pH 8), 10 mM $MgCl_2$, 0.2 µM PEPC, 30 µM of ANS and varying concentrations of malate from 0 to 50 mM, allowing to determination of dissociation constant (K_d); (Right) Determination of dissociation constant (K_d) for unphosphorylated of *P. queenslandicum* with K_d = 3.77 ± 3.75 mM malate in 30 µM of ANS.

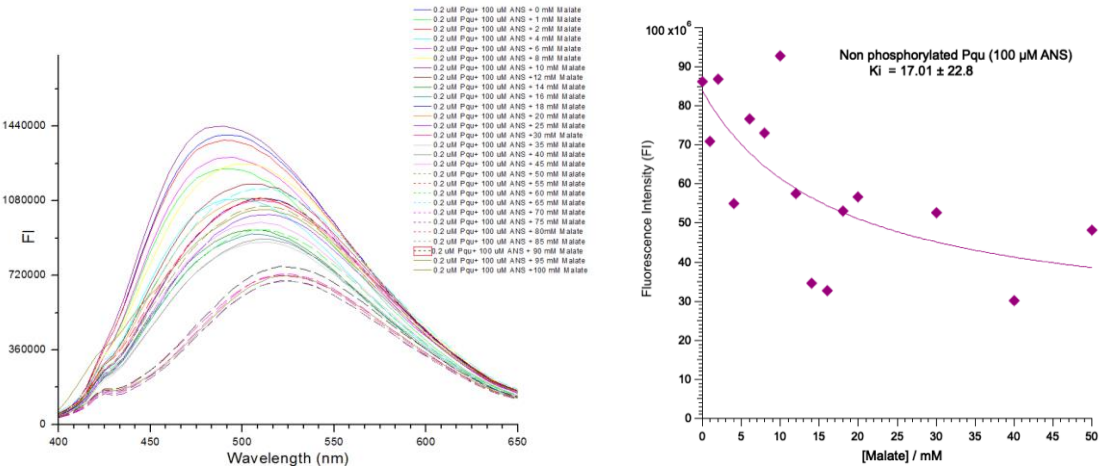

Fig. M.6: (Left) The emission spectrum of the ANS-PEPC *P. queenslandicum* complex. The fluorescence assay mixture contained 50 mM tricine-KOH (pH 8), 10 mM $MgCl_2$, 0.2 µM PEPC, 100 µM of ANS and varying concentrations of malate from 0 to 50 mM, allowing to determination of dissociation constant (K_d); (Right) Determination of dissociation constant (K_d) for unphosphorylated of *P. queenslandicum* with K_d = 17.01 ± 22.8 mM malate in 100 µM of ANS.

N. Screening for optimum ANS concentration in malate inhibition for non-phosphorylated and phosphorylated PEPC P. queenslandicum.

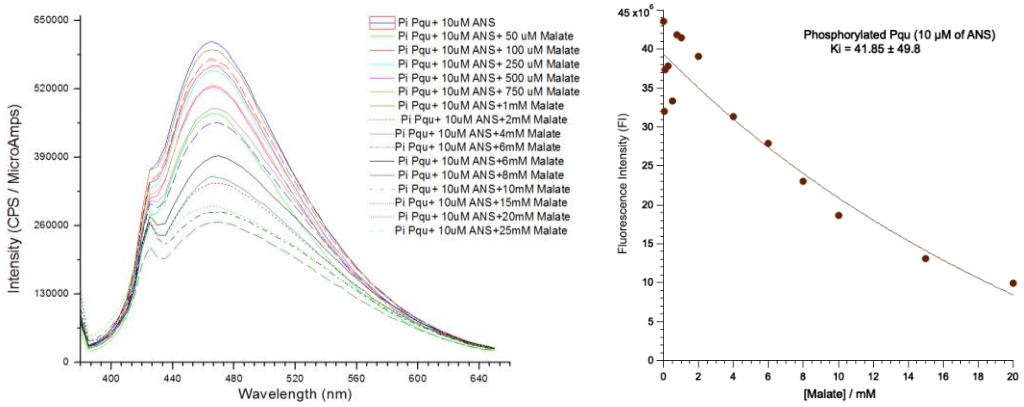

Fig. 5.18: (Left) The emission spectrum of the ANS-Phosphorylated PEPC *P. queenslandicum* complex. The fluorescence assay mixture contained 50 mM tricine-KOH (pH 8), 10 mM $MgCl_2$, 0.2 µM PEPC, 10 µM of ANS and varying concentrations of malate from 0 to 20 mM, allowing to determination of dissociation constant (K_d); (Right) Determination of dissociation constant (K_d) for phosphorylated of *P. queenslandicum* with K_d = 41.85 ± 49.8 mM Malate in 10 µM of ANS.

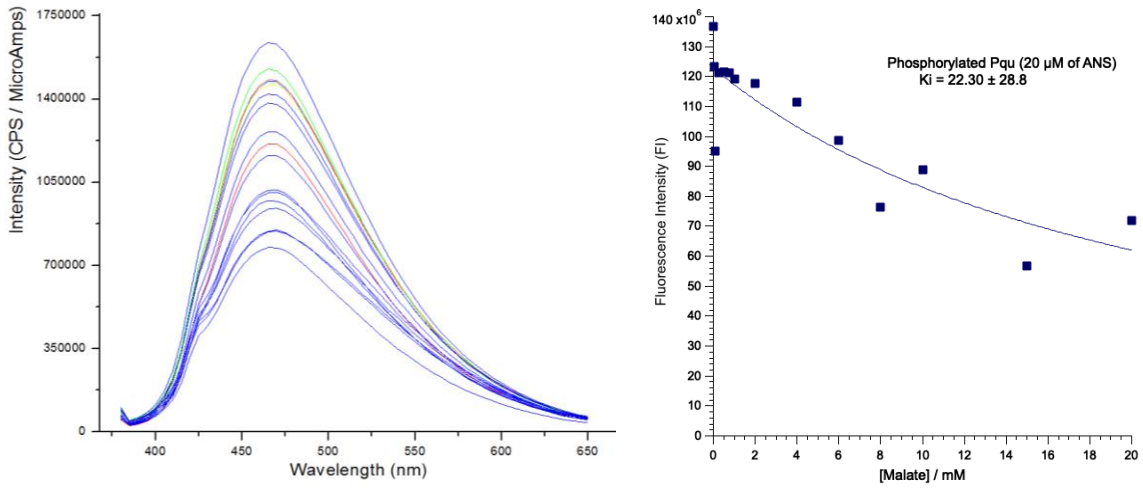

Fig. 5.19: (Left) The emission spectrum of the ANS-Phosphorylated PEPC *P. queenslandicum* complex. The fluorescence assay mixture contained 50 mM tricine-KOH (pH 8), 10 mM $MgCl_2$, 0.2 µM PEPC, 20 µM of ANS and varying concentrations of malate from 0 to 20 mM, allowing to determination of dissociation constant (K_d); (Right) Determination of dissociation constant (K_d) for phosphorylated of *P. queenslandicum* with K_d = 22.30 ± 28.8 mM malate in 100 µM of ANS.

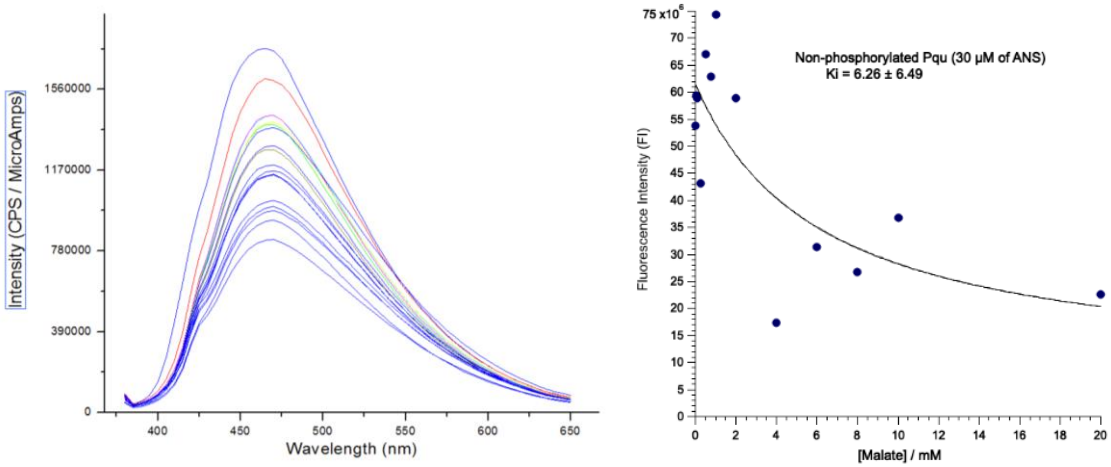

Fig. 5.20: (Left) The emission spectrum of the ANS-Phosphorylated PEPC *P. queenslandicum* complex. The fluorescence assay mixture contained 50 mM tricine-KOH (pH 8), 10 mM $MgCl_2$, 0.2 µM PEPC, 30 µM of ANS and varying concentrations of malate from 0 to 20 mM, allowing to determination of dissociation constant (K_d); (Right) Determination of dissociation constant (K_d) for unphosphorylated of *P. queenslandicum* with K_d = 6.26 ± 6.49 mM malate in 30 µM of ANS.

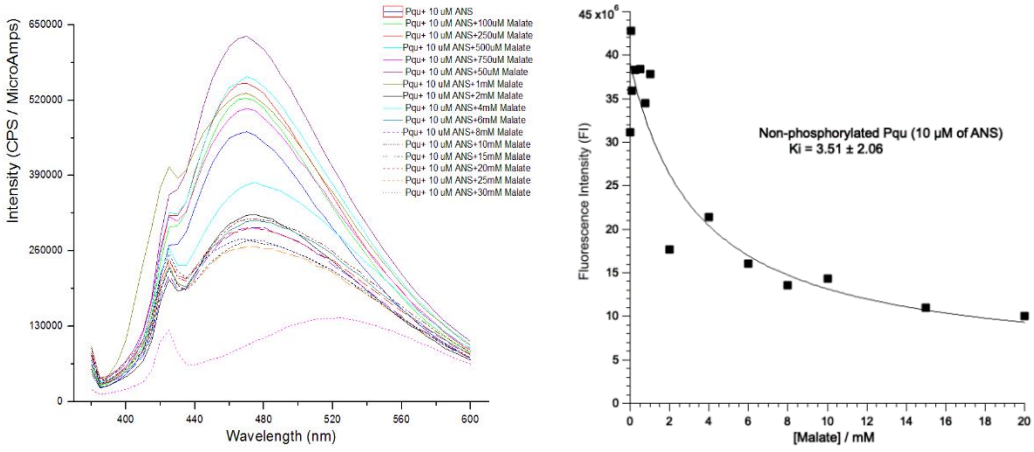

Fig. 5.22: (Left) The emission spectrum of the ANS-nonphosphorylated PEPC *P. queenslandicum* complex. The fluorescence assay mixture contained 50 mM tricine-KOH (pH 8), 10 mM $MgCl_2$, 0.2 µM PEPC, 10 µM of ANS and varying concentrations of malate from 0 to 20 mM, allowing to determination of dissociation constant (K_d); (Right) Determination of dissociation constant (K_d) for non-phosphorylated of *P. queenslandicum* with K_i= 3.51 ± 2.06 mM malate in 10 µM of ANS.

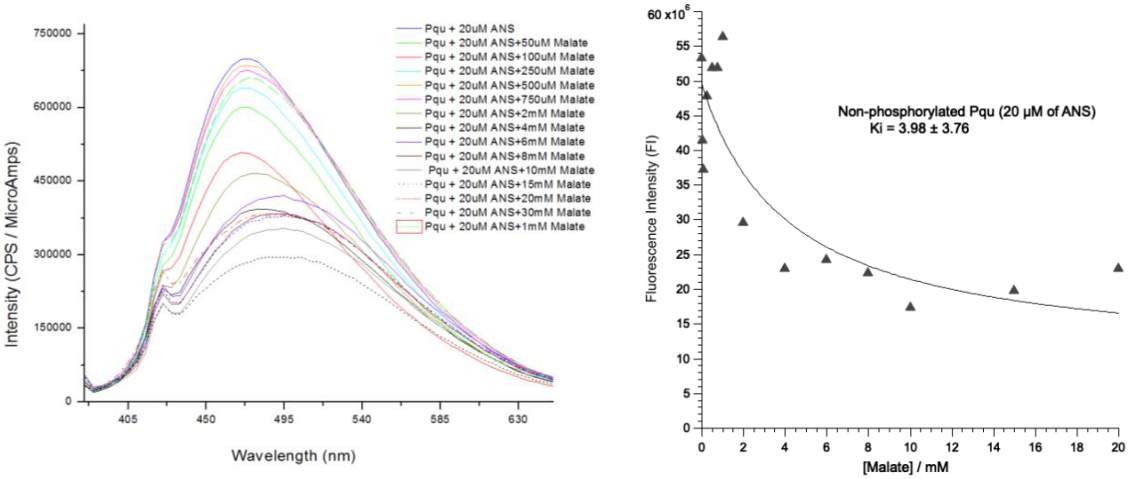

Fig. 5.23: (Left) The emission spectrum of the ANS-non-phosphorylated PEPC *P. queenslandicum* complex. The fluorescence assay mixture contained 50 mM tricine-KOH (pH 8), 10 mM $MgCl_2$, 0.2 µM PEPC, 20 µM of ANS and varying concentrations of malate from 0 to 20 mM, allowing to determination of dissociation constant (K_d); (B) Determination of dissociation constant (K_d) for nophosphorylated of *P. queenslandicum* with K_d= 3.96 ± 3.76 mM malate in 20 µM of ANS.

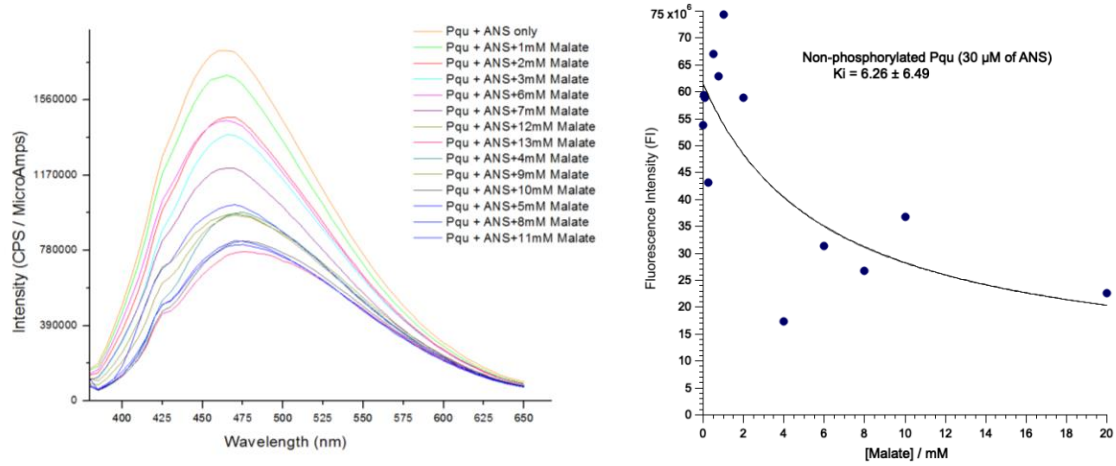

Fig. 5.24: (Left) The emission spectrum of the ANS-non-phosphorylated PEPC *P. queenslandicum* complex. The fluorescence assay mixture contained 50 mM tricine-KOH (pH 8), 10 mM $MgCl_2$, 0.2 µM PEPC, 30 µM of ANS and varying concentrations of malate from 0 to 20 mM, allowing to determination of dissociation constant (K_d); (Right) Determination of dissociation constant (K_d) for nophosphorylated of *P. queenslandicum* with K_d = 3.96 ± 3.76 mM malate in 30 µM of ANS.

O. ANS binding to non-phosphorylated and phosphorylated PEPC from *P. pygmaeum.*

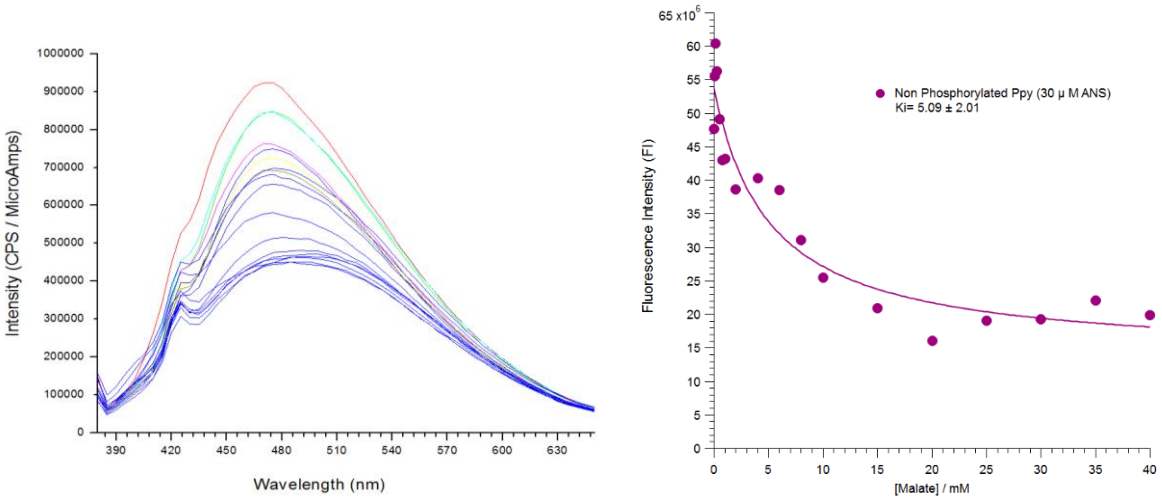

Fig. 5.27: (Left) The emission spectrum of the ANS-non-phosphorylated PEPC *P. pygmaeum* complex. The fluorescence assay mixture contained 50 mM tricine-KOH (pH 8), 10 mM $MgCl_2$, 0.2 µM PEPC, 30 µM of ANS and varying concentrations of malate from 0 to 40 mM, allowing to determination of dissociation constant (K_d); (Right) Determination of dissociation constant (K_d) for nophosphorylated of *P. pygmaeum* with K_d = 5.09 ± 2.01 mM malate in 30 µM of ANS.

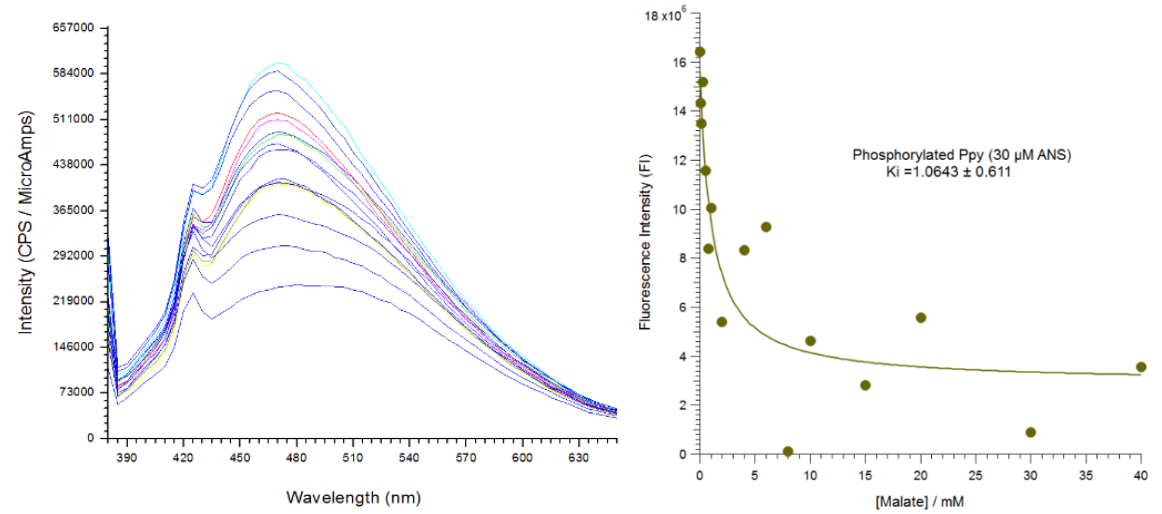

Fig. 5.28: (Left) The emission spectrum of the ANS-phosphorylated PEPC *P. pygmaeum* complex. The fluorescence assay mixture contained 50 mM tricine-KOH (pH 8), 10 mM $MgCl_2$, 0.2 µM PEPC, 30 µM of ANS and varying concentrations of malate from 0 to 40 mM, allowing to determination of dissociation constant (K_d); (Right) Determination of dissociation constant (K_d) for nophosphorylated of *P. pygmaeum* with K_d= 1.06 ± 0.61 mM malate in 30 µM of ANS.